

# ASPECTS OF CEREBRAL BLOOD FLOW IN HUMANS

MARC J. POULIN

A thesis submitted to the University of Oxford for the degree of D.Phil.

University Laboratory of Physiology  
University of Oxford

October, 1998

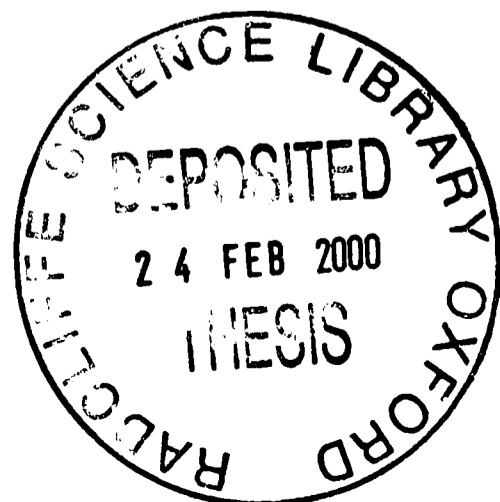


# TABLE OF CONTENTS

**GENERAL PREFACE**  
**DECLARATION**  
**ACKNOWLEDGEMENTS**  
**ABSTRACT**

## **1. GENERAL INTRODUCTION**

**1.1 HISTORICAL PERSPECTIVE**  
**1.2 GENERAL MECHANISMS**  
**1.3 TECHNIQUES FOR MEASURING CEREBRAL BLOOD FLOW IN HUMANS**  
**1.4 CEREBRAL BLOOD FLOW AND CARBON DIOXIDE**  
**1.5 CEREBRAL BLOOD FLOW AND HYPOXIA**  
**1.6 CEREBRAL BLOOD FLOW AND EXERCISE**  
**1.7 CEREBRAL BLOOD FLOW AND HYPOXIC VENTILATORY DEPRESSION**  
**1.8 REFERENCES**

## **2. INDEXES OF FLOW AND CROSS-SECTIONAL AREA OF THE MIDDLE CEREBRAL ARTERY USING DOPPLER ULTRASOUND DURING HYPOXIA AND HYPERCAPNIA IN HUMANS**

## **3. DYNAMICS OF THE CEREBRAL BLOOD FLOW RESPONSE TO STEP CHANGES IN END-TIDAL CO<sub>2</sub> AND O<sub>2</sub> IN HUMANS**

## **4. FAST AND SLOW COMPONENTS OF CEREBRAL BLOOD FLOW RESPONSE TO STEP DECREASES IN END-TIDAL PCO<sub>2</sub> IN HUMANS**

## **5. ASSESSMENTS OF FLOW BY TRANSCRANIAL DOPPLER ULTRASOUND IN THE MIDDLE CEREBRAL ARTERY DURING EXERCISE IN HUMANS**

## **6. INFLUENCE OF CEREBRAL BLOOD FLOW ON THE VENTILATORY RESPONSE TO HYPOXIA IN HUMANS**

## **7. GENERAL DISCUSSION**

**7.1 MAJOR FINDINGS**  
**7.2 FUTURE DIRECTIONS**  
**7.3 CONCLUDING COMMENTS**  
**7.4 REFERENCES**

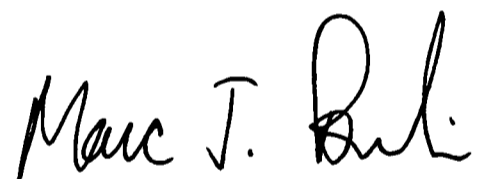
## **GENERAL PREFACE**

This Thesis consists of a General Introduction (Chapter 1), five Results chapters (Chapters 2-6), each based on a scientific paper, and a General Discussion (Chapter 7). Chapters 2 and 5 deal with the comparison of various indices that can be used with transcranial Doppler ultrasound, at rest (Chapter 2) and during exercise (Chapter 5). Chapters 3 and 4 use the techniques of Doppler ultrasound and dynamic end-tidal forcing to measure the dynamic aspects of the cerebral blood flow response to carbon dioxide and hypoxia. Chapter 6 attempts to predict the role of cerebral blood flow in the ventilatory response to acute isocapnic hypoxia in humans.

All of the papers included in this Thesis are joint- or multi-author studies. Thus, before the Results chapters I have included a Declaration of the extent of my own contribution to the study, as well as a Preface, to put the work in context.

## DECLARATION

The work described in this Thesis was undertaken in the University of Oxford Laboratory of Physiology. All the papers included in this Thesis are co- or multi-author studies. The extent of my own contribution to the work in each paper is described in detail in the Declaration accompanying each of the five Results chapters. No portion of the work included in this Thesis has been submitted in support of an application by me for another degree or qualification to this or any other University.

A handwritten signature in black ink, reading "Marc J. Poulin". The signature is written in a cursive style with a large, prominent initial 'M'.

Marc J. Poulin  
October, 1998

## ACKNOWLEDGEMENTS

It has been a privilege to undertake research work in the University Laboratory of Physiology in Oxford. For this opportunity, I am indebted to Professor Peter Robbins for his willingness to take me on board when I first contacted him from Canada, and to Professor Clive Ellory for providing me with laboratory space in the department.

I am also grateful to Professor Robbins for providing continuous support during my stay in Oxford, and for his generosity in sharing both time and ideas. It has been a rewarding experience to work in an environment that is both dynamic and stimulating, and where enthusiasm for science is contagious.

Thank you to my current colleagues, and to those who have come and gone, in the human and exercise physiology group, and in the University Laboratory of Physiology, since my arrival in 1993. I am grateful for having had the privilege and opportunity of working together.

Thank you to Mr. David O'Connor for providing continued and unfailing skillful technical assistance and many light-hearted discussions, and to all the volunteers who provided many hours of cheerful participation in the studies described in this Thesis. Without them, this work could not have been completed.

Finally, I am grateful for the funding that I have received to undertake this research work in Oxford. The research included in this Thesis has been funded by The Wellcome Trust. My personal support was provided by the Medical Research Council of Canada and the Heart and Stroke Foundation of Ontario. Travel grants to attend scientific meetings were provided by The Physiological Society of Great Britain and New College, Oxford.

# ASPECTS OF CEREBRAL BLOOD FLOW IN HUMANS

MARC J. POULIN  
NEW COLLEGE, OXFORD

A thesis submitted to the University of Oxford for the degree of D.Phil.

TRINITY TERM, 1998

## ABSTRACT

The technique of transcranial Doppler ultrasound (TCD) was used to assess cerebral blood flow (CBF) in humans. Studies were performed at rest and during dynamic submaximal exercise. In the resting experiments, TCD was combined with the technique of dynamic end-tidal forcing to study the dynamics of the CBF response to step changes in end-tidal (i.e. arterial)  $P_{CO_2}$  and  $P_{O_2}$ . In the resting and exercise experiments, the degree of consistency was examined between three indices of CBF that can be extracted from the TCD spectrum. Finally, the ventilatory and the CBF responses to acute isocapnic hypoxia were examined to try to quantify the possible reduction in ventilation that could be attributed to changes in CBF with hypoxia.

In the studies performed at rest, during either hypoxia and/or hypercapnia (Chapter 2), the three indices of CBF extracted from the TCD spectrum were all consistent. However, during submaximal exercise (Chapter 5), the indices were less consistent and results suggest that the increase in CBF with exercise that has been reported with TCD needs to be treated with caution.

The dynamic studies of the CBF response to step changes in end-tidal  $P_{CO_2}$  and  $P_{O_2}$  in humans revealed that the CBF response to hypercapnia (Chapter 3) is characterised by a significant asymmetry, with a slower on-transient than off-transient, and also by a degree of undershoot following the relief of hypercapnia. The CBF response to hypocapnia (Chapter 4) is also characterised by a significant asymmetry, with a faster on-transient than off-transient. Furthermore, there is a slow progressive adaptation throughout the hypocapnic period. These studies show that the CBF responses to hypercapnia and hypocapnia are much faster than previously been thought.

Finally, the work described in Chapter 6 attempts to quantify the possible reduction in ventilation that could be attributed to changes in CBF with hypoxia to determine whether it could be of sufficient magnitude to underlie hypoxic ventilatory decline (HVD). The results suggest that, in awake humans, changes in CBF during acute isocapnic hypoxia are quantitatively insufficient to underlie HVD.

## **CHAPTER 1**

### **GENERAL INTRODUCTION**

## 1 GENERAL INTRODUCTION

### 1.1 HISTORICAL PERSPECTIVE

The brain has long been recognised as an essential organ for sustaining human life. Some of the first anatomical records of the brain can be traced back to early Egyptian and Greek times (10,82,115,181). During the Renaissance period, accurate drawings and anatomical notebooks were provided by Leonardo da Vinci. The more recent human studies of cerebral blood flow and metabolism have evolved from the discoveries of Harvey and Willis in early Modern times. In *Circulation of the blood: men and ideas*, Seymour Kety (82) provides an extensive account of notable discoveries and contributions that have led to our modern day understanding of cerebral circulation in humans. A summary of those important contributions, as described by Kety and others (10,25,57,64,82,115,192), along with a short update since these publications, is provided in Table 1.1. More detailed reviews of various historical perspectives of the cerebral circulation including the anatomy and territories served by the cerebral arteries, cerebral blood flow and its regulation, oxygen consumption, and pharmacology are provided elsewhere (13,23,36,60,80-82,99,102,120,151,153,163,172,180,181,184).

William Harvey's description of cardiac function and blood circulation in *De Motu cordis et sanguinis*, published in 1628 (49), is considered one of the great publications in medicine. Harvey's work was succeeded by a number of important and notable discoveries, several of which are closely related to the contents of this Thesis.

**Table 1.1** Summary of notable historical events in human cerebral circulation.

<b>Era/Year</b>	<b>Contributor(s)</b>	<b>Contribution</b>
<i>Ancient Egyptian and early Greek Times</i>		
17 <sup>th</sup> century B.C.	Smith Papyrus	mention of pulsations of the brain during life
6 <sup>th</sup> century B.C.	Pythagoras	characterized the brain as organ of reasoning
ca. 500 B.C.	Alcmeon of Croton	recognized importance of blood in mental function
ca. 480 B.C. ca. 400 B.C.	Empedocles of Acragas, Diogenes of Apollonia	importance of Pneuma (air), blood for brain function Pneuma distributed by heart through vascular system
470-380 B.C.	Democritus	emotions and intellect related to air and blood
460-377 B.C.	Hippocrates of Cos	wrote treatise <i>On the sacred disease</i> (study of epilepsy; early account of anatomy of neck veins)
384-322 B.C.	Aristotle	denied ideas of Pythagoras; believed the brain functioned to cool and purify blood
ca. 300-250 B.C.	Herophylos of Chalcedon	described meninges, sinuses and <i>rete mirabile</i> ; re-established brain as seat of intelligence and consciousness; recognised pulsations in arteries
A.D. 130-201	Galen of Pergamon	doctrine of cerebral nutrition and function; demonstrated that arteries contained blood; described three essential ( <i>natural, vital, and animal</i> ) spirits
<i>The Renaissance Years</i>		
1270-1326	Mondino de' Luzzi	described choroid plexus & role in mental processes
ca. 1520	Berengario da Carpi	recognized a/v parts of choroid plexus; denied existence of <i>rete mirabile</i> (Galen's <i>animal spirit</i> ) in man
1452-1519	Leonardo da Vinci	anatomical notebooks and accurate drawings of vessels of the neck; realised that vessel compression could lead to unconsciousness in 1/100th part of hr (~36 sec); recognized the mental effects of wine
1514-1564	Andreas Vesalius	described the soporal (carotid) artery and absence of <i>rete mirabile</i> in man; provided detailed drawings of brain vessels in <i>De humani Corporis Fabrica</i>
1516-1580	Realdus Columbus	established that pulsations of the brain were synchronous with those of the heart and arteries
1523-1562	Gabriel Fallopius	published <i>Observationes Anatomicae</i> , description of cerebral blood vessels
1578-1657	William Harvey	discovery of the circulation of blood and published in <i>De motu cordis et sanguinis</i> ; revolutionized the physiological concepts of blood circulation

Table 1.1 Continued.

Era/Year	Contributor(s)	Contribution
1621-1675	Thomas Willis	published <i>Cerebri Anatome</i> , the first modern studies on the anatomy of the brain, nerves, and cerebral circulation; gave the most extensive description of the arteries at the base of the brain (Circle of Willis)
1632-1723	Christopher Wren	provided the anatomical drawings of the Circle of Willis published in <i>Cerebri Anatome</i>
1596-1650	René Descartes	accepted Galen's doctrine of the <i>animal spirit</i> (soul), thought it resided in pineal gland
1643-1679	John Mayow	linked the <i>animal spirit</i> with <i>spiritus nitroaerius</i> , Lavoisier's oxygen. Believed the brain depleted the blood of oxygen to produce the <i>animal spirit</i>
<i>The Modern Era</i>		
1708-1777	Albrecht Von Haller	observed variations in caliber of exposed pial vessels
1733-1817	Alexander Monro	doctrine of near incompressibility of the brain (constant blood vol. by continuous flow of blood)
1743-1794	Antoine Lavoisier	proved that phlogiston didn't exist; conducted extensive studies on breathing and respiration
1803-1853	Christian Doppler	Doppler principle
1849-1921	Charles Emile François-Franck	measured pressure in cerebral end of a cut internal carotid artery
1813-1878	Claude Bernard	established role of glucose in metabolism
1829-1910	Eduard Pflüger	showed that tissue cells governed oxygen uptake; introduced concept of R.Q.
1846	G. Burrows	observed that cerebrospinal fluid represented a volume which was variable
1818-1889	Frans Cornelius Donders	reported on ability of pial vessels to change their caliber in response to stimuli, including asphyxia
1829-1901	Adolf Fick	Fick principle
1858	T. Ackermann	modifications of the Donders technique allowing observations under relatively normal conditions
1867	H. Nothnagel	
1928	H.S. Forbes	
1936	H.G. Wolff	
1938	S. Cobb	

Table 1.1 Continued.

<b>Era/Year</b>	<b>Contributor(s)</b>	<b>Contribution</b>
1837-1897 1856-1952	Charles Roy Charles Sherrington	observed that the blood supply to the brain varies directly with systemic blood pressure; first to conclude that products of cerebral metabolism can cause variations in the calibre of cerebral arteries; first to suggest intrinsic local control of CBF with local variation in functional activity
1866-1952	Leonard Hill	refuted Roy and Sherrington's work; believed that cerebral circulation followed passively the changes in systemic blood pressure
1887	Gärtner and Wagner	made first attempts to make direct measurements of CBF in animals
1904	Paul Jensen	provided first values for CBF in the dog and rabbit
1933	F.A. Gibbs	devised a technique to measure directional changes in flow based on a heated thermocouple inserted into the internal jugular vein
1938	Forbes and Cobb	acknowledged the over-riding importance of the arterial blood pressure and reflexes and intrinsic factors from the cardiovascular centres of the CNS (esp. CO <sub>2</sub> )
1943	Dumke and Schmidt	made first quantitative measurements of CBF in living animal, macaque monkey
<i>Studies on the Human Cerebral Circulation</i>		
1881	Mosso	recorded changes in the volume of intracranial contents and inferred changes in CBF
1860-1936	J.S. Haldane	showed that CO <sub>2</sub> rather than oxygen was the main stimulus to breathing at sea level but appreciated the importance of oxygen deprivation: "Anoxia not only stops the machine, it wrecks the machinery".
1927	Myerson, Halloran and Hirsch	showed that cerebral venous blood could be obtained through a needle inserted into the superior bulb of the internal jugular vein
1932	Chorobski and Penfield	showed evidence of vasodilator innervation of cerebral vessels
1932, 1938	Lennox and Gibbs	used changes in the arteriovenous oxygen difference to infer changes in CBF under various conditions
1945	Kety and Schmidt	performed first measurement of CBF in man using the nitrous oxide technique (based on Fick principle)

Table 1.1 Continued.

Era/Year	Contributor(s)	Contribution
1947	Gibbs, Maxwell and Gibbs	applied the Stewart Principle of dye dilution to measurement of total intracranial blood flow
1955	Lassen and Munck	described whole brain method to measure CBF using inhalation gas (krypton-85)
1961	Ingvar and Lassen	first quantitative measurement of rCBF in humans
1967	Severinghaus and Lassen	used the a-vO <sub>2</sub> difference, saturation and PCO <sub>2</sub> to assess the time constant for the change in CBF with hypocapnia
1973	Sir Godfrey Hounsfield	first to use computers to analyze tomographic sections of the brain
1961, 1977	Louis Sokoloff	provided first studies showing coupling of regional blood flow to functional activity; measured metabolism using 2-DG-glucose, and later applied this with PET for clinical studies in humans.
1981	Rune Aaslid	demonstrated that Doppler ultrasound could be used to measure the blood flow velocity from the intracranial arteries in humans.

The Circle of Willis is an anatomical feature that describes the communicating network of cerebral arteries at the base of the brain. It was named after Thomas Willis, a Student of Christ Church College in 17<sup>th</sup> century Oxford. Willis (with the help of Christopher Wren) published the first acceptable illustration (Fig. 1.1) and description of the arteries that form the Circle of Willis. In addition, Willis hypothesised its physiological importance, and provided case studies showing its clinical relevance in medicine (65). To this day, a copy of Willis's famous 17<sup>th</sup> century manuscript, *Cerebri Anatome* (197) (Fig. 1.1, see end of section 1.1), remains under lock and key in the Sherrington room of the University Laboratory of Physiology, Oxford.

On 25 May 1842, an Austrian (Salzburg) - born physicist, Christian Doppler, presented a paper at the Royal Bohemian Society of Sciences in Prague in which he described a theory that is now applied to various techniques in medical research and in clinical settings. The 'Doppler' effect or the change in frequency produced by the scattering of waves by a moving object was described by Doppler in a paper entitled "*On the coloured light of the double stars and certain other stars of the heavens*" (31). In 1845, a Dutchman, C.H.D.B. Ballot, verified Doppler's theory experimentally (with sound). His set-up consisted of a locomotive and a flatcar, three teams of horn players, musically trained observers, and a few miles of track between Amsterdam and Utrecht. Details of these and other short accounts of Doppler's life are summarised elsewhere (31,32).

Roy and Sherrington were the first to recognise the close relationship between cerebral metabolism and blood flow. In an article published in the *Journal of*

*Physiology* (1890), they postulated that “the brain possesses an intrinsic mechanism by which its vascular supply can be varied locally in correspondence with local variations of functional activity”, (162).

In 1942, the first quantitative measurement of blood flow was made through the brain of a living and breathing animal, the macaque monkey (29). Quantitative measurements in humans, using the nitrous oxide method, soon followed (83,84,86). These experiments provided the first normative data for human cerebral blood flow and oxygen consumption of the brain, *ca.* 54 ml/100g/min (740 ml/min for brain of average weight) and 3.3ml O<sub>2</sub>/100g/min (46 ml/min for the whole brain) (86).

The past four decades of research in human cerebral circulation have been characterised by major technological advances. This has led to a better understanding of cerebral metabolism (23,173), quantification of the dynamic response of the cerebral circulation to alteration in arterial blood gases (167), a vast array of studies postulating various putative mechanisms of regulation (summarised in section 1.2), and to innovative techniques for brain imaging (44,133).

Finally, it was not until 1982, over one hundred years after Doppler’s publication, that Rune Aaslid and his colleagues demonstrated that Doppler ultrasound could be used to penetrate the skull to record the blood flow velocity from the intracranial arteries (2). The work presented in this Thesis used the technique of transcranial Doppler ultrasound to assess changes in cerebral blood flow in humans, at rest and during exercise. More details of this technique are provided in section 1.3, Chapters 2 and 3.



**Fig. 1.1 Top Panel:** Title page of *Cerebri Anatome*, 1664 (University Laboratory of Physiology Library, Oxford). **Bottom Panel:** Drawing of the base of a human brain, showing the Circle of Willis, as featured in *Cerebri Anatome*. Christopher Wren drew the original illustration.

Wharson 1739/40  
CEREBRI  
ANATOMIE:

CUI ACCESSIT

*Nervorum Descriptio*

ET USUS.

STUDIO

THOMÆ WILLIS,

Ex Æde Christi Oxon. M D. & in  
ista Celeberrima Academia Naturalis  
Philosophiæ Professoris *Sidleiani*.

LONDINI,

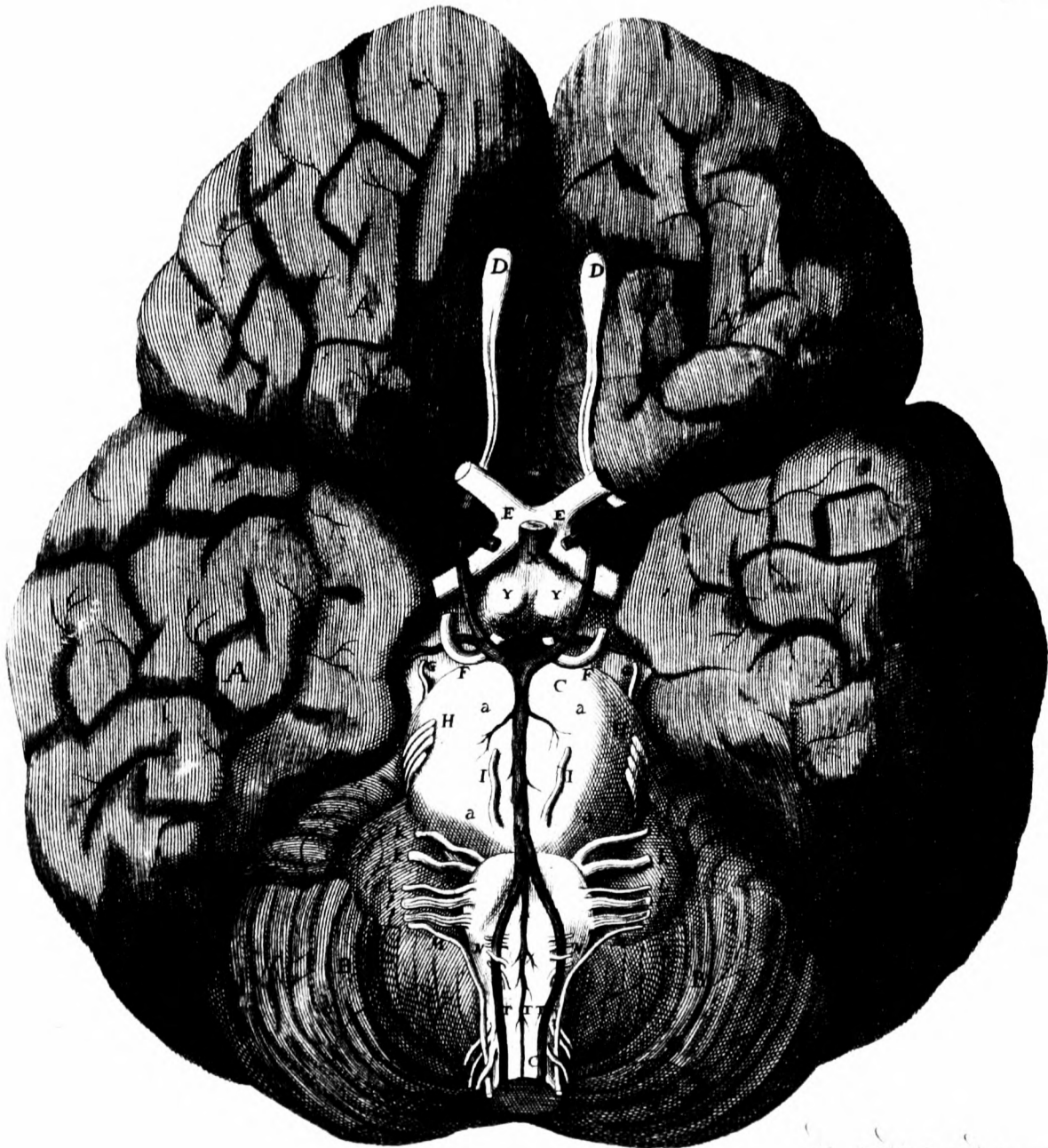
Typis Tho. Roycroft, Impensis Jo. Martij  
Ja. Allestry apud insigne Campanæ in  
Cœmeterio D. Pauli. M.DC.LXIV.

Imprimatur,

Jan. 20. THO. GRIGG R. in  
1663. Christo Pat. ac D<sup>no</sup>  
D. Humfr. Episc. Lon.  
à sac. Domesticis.

Figura 1<sup>a</sup>

pag. 21



STUDIO T. WILLIS

## 1.2 GENERAL MECHANISMS

This Thesis provides no direct evidence in support of any particular underlying mechanism of regulation of cerebral blood flow. However, it does provide useful information on the time course and form of the dynamic response of the cerebral circulation to changes in arterial hypoxia, hypercapnia and hypocapnia. Accordingly, putative mechanisms need to be consistent with the findings contained herein. An extensive review of the proposed mechanisms of regulation is beyond the scope of this Thesis. However, a brief review is presented and the reader is referred elsewhere for more extensive reviews (13,16,39,41,47,60,67,95,96,100-102,139,144,145,172, 179,188).

### 1.2.1 Mechanisms of control of cerebral blood flow

In normal, young, healthy humans, brain perfusion can be maintained constant within a large range of arterial pressure (*ca.* 60-150 mmHg). This characteristic of the cerebral circulation is known as autoregulation (see (18,139) for detailed reviews on Cerebral Autoregulation). In this range of perfusion pressures, variations in pial arteriolar tone mainly regulate cerebral blood flow in response to changes in the local chemical environment of the cerebral vessels, as pial vessels form the main resistance vessels (36,60,139). Chemical, endothelial, and neural factors (188) can modify arteriolar tone.

Despite the rich innervation of cerebral blood vessels, the physiological significance is poorly understood (33). If neural mechanisms play a role in the chemical regulation of the cerebral circulation, it appears to be a minor one (14). Innervation of cerebral arteries originates from various sources. First, there are sympathetic noradrenergic

nerves; they originate in the thoraco-lumbar outflow and ascend via the cervical sympathetic chains crossing the stellate ganglion (35,80,99). These fibres release constrictor transmitters, norepinephrine and neuropeptide Y (188) and decrease cerebral blood flow. Second, there are parasympathetic cholinergic nerves; they originate in the sphenopalatine, otic, and internal carotid ganglia. These fibres release dilator substances, acetylcholine and neuropeptides (vasoactive intestinal polypeptide [VIP]) (34,188) and increase cerebral blood flow. Third, there are fibres that originate in the trigeminal ganglion (54); they release dilator substances, including neuropeptides (substance P, calcitonin gene related peptide, neurokinin A) and they increase cerebral blood flow during cortical activation (188). There is also evidence for a fourth group, vasodilator fibres; they originate in the medulla and cross the facial greater superficial petrosal nerve, and act on pial vessels (19).

### **1.2.2 Carbon dioxide**

It is generally thought that the effects of CO<sub>2</sub> on the cerebral circulation operate via the direct effects of extracellular pH on the smooth muscle of cerebral pial vessels (6,7,51,60,95,100). Intracellular pH (pHi) is well regulated. No changes in pHi are detected in alkalinization-induced contractions (5) and hypercapnic (acidification)-induced relaxation (178) of vascular smooth muscle of rat cerebral arteries. In isolated human vessels, changes in pHi have been observed in response to hypercapnia and hypocapnia but the changes in pHi are smaller than the changes in extracellular pH (73).

The exact way by which it is thought that H<sup>+</sup> dilates cerebral vessels is still unclear. Several mechanisms have been postulated (reviews on the role of H<sup>+</sup> and pH in the regulation of cerebral blood flow are provided elsewhere (42,95,171)). First, the

underlying mechanism of regulation may include an effect of  $H^+$  on the intracellular calcium concentration, either by an effect on membrane fluxes of  $Ca^{2+}$  (96) or by effects on  $Ca^{2+}$  release from the sarcoplasmic reticulum stores (199). Second, nitric oxide is most likely involved. However, although nitric oxide appears to play a role in hypercapnia (38,39,66,67,191), its role in hypocapnia is unsettled (40,190). Possible sources of nitric oxide production during hypercapnia include the endothelial, smooth muscle, neural and glial cells (16,39,41,67,191). While a neuronal isoform of nitric oxide synthase appears more likely (16,191), the shear stress associated with blood flow (45) has also been proposed as a stimulus promoting nitric oxide synthesis from the endothelium, suggesting a role for an endothelial isoform of nitric oxide synthase. Third, three types of potassium channels might be involved; ATP-sensitive (38,41),  $Ca^{2+}$ -activated, and delayed-rectifier (16) potassium channels. A direct effect of nitric oxide on  $Ca^{2+}$ -activated potassium channels has been proposed (15). (Reviews of the physiological role and properties of potassium channels in smooth muscle and in cerebral circulation are provided elsewhere (41,125)). Fourth, glial cells might be involved. They are highly adapted for calcium signalling (187). Astrocytes have endfeet that terminate on pial surfaces and vessels and they have a high potassium conductance (129,140). Thus, glial cells are of considerable interest, as they appear well suited for regulating extracellular ion transport (130). Fifth, a role for prostanoids has been postulated in the hypercapnic response. This latter mechanism would appear to be an age and species specific process, involving a permissive role of prostacyclin from endothelial cells (and dependant on endothelial integrity) on smooth muscle cells via second messenger pathways (cAMP) (104).

The cerebral blood flow response to hypocapnia (and concomitant alkalosis) is of particular interest and a brief discussion on the postulated mechanisms is warranted.

Unlike the sustained nature of the cerebral blood flow response to hypercapnia, sustained hypocapnia is characterised by an initial decrease in cerebral blood flow (50,84,159,167,169) that is followed by some secondary recovery over time. This adaptation has been reported in the cerebral blood flow in response to hypocapnic exposures of two to six hours in humans (155), unanesthetized piglets (53) and goats (3). An adaptive process has also been observed in the vessel diameter of rabbit pial arterioles in response to 54 hours of hypocapnia (124).

The adaptation in cerebral blood flow with hypocapnia is associated with changes in extracellular pH; there is an initial increase in extracellular pH with the maximal value being reached from within 30 min (3,148) to a few hours (20,124,155) after the onset of hypocapnia. The initial increase is then followed by a decrease in extracellular pH toward normal values (3,20,124,148,155). Many studies in humans, dogs, rats, rabbits and goats have shown that the subsequent decrease in pH is associated with a decrease in extracellular bicarbonate concentration (20,147), perhaps secondary to a diminished secretion of bicarbonate by the choroid plexus (124), and to a progressive increase in brain lactate (3,26,79,92,107,143,146,147,155, 185,186,200). The decrease in bicarbonate (and buffering capacity) may play a role in the increased CO<sub>2</sub> sensitivity that is observed after sustained hypocapnia (79,108,124,154). While lactate is implicated, the time course over which the change in lactate occurs remains uncertain (3,79,143) and may involve species differences (143). It was initially thought that the increase in lactate with hypocapnia was secondary to an effect of hypoxia. However, studies of hypocapnia in dogs using various background levels of oxygen (euoxia, hypoxia and hyperoxia) all show an increase in brain lactate (148), and this casts doubt on the hypoxic theory for the increase in lactate with hypocapnia. More recent studies have suggested a theory

related to alkalosis. According to this theory, hypocapnia induces a state of alkalosis which, in turn, increases the rate of glycolysis (via the stimulation of phosphofructokinase [PFK], a pH-sensitive enzyme (114)). Accordingly, there is an increase in lactate through increased production of pyruvate (111,114,185).

The abundance of carbonic anhydrase in glial cells has led some to speculate on a possible role for these cells in the regulation of extracellular ion transport (and pH) during hypocapnia (16,130).

Finally, a whole array of mechanisms has been proposed to elucidate the intricate control of the cerebral circulation in response to alterations in carbon dioxide. This may suggest the existence of several parallel (and possibly permissive and/or redundant) mechanisms that operate to link changes in extracellular pH to changes in vascular tone. Thus, caution is required in the interpretation of *in vitro* and *in vivo* studies, in comparing different species, and in assessing pharmacological interventions and dosages used.

### **1.2.3 Hypoxia**

Many efforts have been made to elucidate how cerebral blood flow is modulated during hypoxia to ensure a constant oxygen delivery to the brain. Despite this, the exact mechanism(s) by which hypoxia acts to dilate cerebral pial arterioles remains unclear. Several mechanisms have been postulated. Detailed summaries of the putative mechanisms are provided in recent reviews (16,188).

First, a direct effect of a low  $P_{O_2}$  on the smooth muscle of the pial arterioles may be involved. This is supported by the finding of a decrease in tone and tension in isolated

smooth muscle cells from cat cerebral arteries when exposed to hypoxia (112). Second, it may involve an indirect affect from the release of vasodilators from the endothelium or from the release of vasodilator metabolites from the surrounding tissue. Adenosine has been suggested as a potential metabolite but its role remains controversial (157,198). Third, recent studies suggest the mechanism of action may involve shear stress and the production of nitric oxide (67,94,157). The activation of ATP-sensitive (41,89,152,157,158,175) and/or calcium-dependent (41) potassium channels may also be involved. Fourth, recent studies have showed an accumulation of lactate in the rat neocortex (142) and in the gerbil (4) with moderate hypoxia, thereby suggesting a possible role for lactate. The reason for an increase in lactate with hypoxia remains unclear although it is possible that lactate serves as a metabolic link between glial cells (in particular, astrocytes) and neurons (182). Finally, evidence for a neurogenic component, initiated by excitation of oxygen-sensitive neurons in the medulla (rostral ventrolateral reticular nucleus, RVL), has recently been advanced (47).

Recent studies in humans, lambs and other species have suggested that the mechanism of action may be one that is more closely linked to arterial oxygen content than directly to arterial  $P_{O_2}$ , hematocrit, viscosity, age, arterial  $PCO_2$  or blood pressure (17,123). Findings in awake humans (141) and in unanesthetized lambs (74) of increases in cerebral blood flow with exposure to carbon monoxide, or with hemodilution, lend support to such a mechanism. This is based on the fact that carbon monoxide and hemodilution serve to reduce the  $P_{50}$  (and the oxygen binding capacity of blood) without a concomitant decrease in arterial  $PO_2$ .

### 1.3 TECHNIQUES FOR MEASURING CEREBRAL BLOOD FLOW IN HUMANS

Since the introduction of the nitrous oxide technique by Kety and Schmidt in 1945 (83,86) several techniques have emerged for providing quantitative measurements of cerebral blood flow in humans. A summary of the different techniques, along with references that provide more extensive descriptions for each technique (including the main advantages and limitations), is provided in Table 1.2.

The older techniques such as nitrous oxide and xenon inhalation (or intravenous administration) were invasive and they placed major limitations on the investigators in terms of ease and repeatability of measurements. As such, experiments were restricted to steady-state measurements under various flow conditions. Over the past two decades, these techniques have given way to several non-invasive techniques such as Doppler ultrasound, Positron Emission Tomography (PET) scanning and functional magnetic resonance imaging (fMRI). The newer techniques have the advantage of offering outstanding temporal and spatial resolution, and make it possible to assess relative changes in flow in extremely small and specific regions of the brain. Additionally, cerebral blood flow can be assessed in many single cerebral vessels, including all of the vessels that form the Circle of Willis. Doppler ultrasound is currently the only technique that can provide the temporal resolution necessary to assess dynamic aspects of changes in cerebral blood flow. However, it is restricted to single vessel measurement and has the limitation of measuring only blood flow *velocity*, therefore providing only an indirect measure of cerebral blood flow. Conversely, while fMRI cannot (yet) provide the temporal resolution available with Doppler ultrasound, it has the advantage of providing detailed functional maps of the brain. It is clear that the door has now opened to a new era in the study of cerebral circulation. Hopefully, this will lead to a much greater understanding of functional

aspects of the cerebral circulation in humans in health and disease.

Table 1.2 Summary of the main techniques used to measure cerebral blood flow in humans.

Technique	Resolution Spatial Temporal	Invasiveness	Repeated	Continuous	Mapping	Reviews
Nitrous Oxide	global > 15 min	yes	yes	no	no	(48,55,83,86,153)
<sup>133</sup> Xe clearance (inhalation or intravenous)	regional > 15 min	yes	yes	no	no	(55,69,136,153)
Transcranial Doppler Ultrasound	single vessel 10 msec	no	yes	yes	no	(1,75,128,176)
Transcranial Color- Coded Sonography	single vessels beat-by-beat	no	yes	no	no	(8,116,117)
Near Infrared Spectroscopy	global > 4 sec	no	yes	no	no	(137)
Positron Emission Tomography	6 mm ~ 30 sec	yes	yes	no	yes	(11,44,48,153)
Single Photon Emission Tomography	20 mm ~2 min	yes	yes	no	yes	(11,48,133,196)
Functional Magnetic Resonance Imaging	1-3mm 5-8 sec	no	yes	no	yes	(28,44,87,88,119,132- 134,183)

## 1.4 CEREBRAL BLOOD FLOW AND CARBON DIOXIDE

In normal healthy humans, as in other species, the arterial  $P_{\text{CO}_2}$  is a potent physiological modulator of cerebral blood flow. The effects of alterations in  $P_{\text{aCO}_2}$  are consistent and reproducible. Cerebral blood flow is increased by hypercapnia and decreased by hypocapnia. In the physiological range, the cerebral blood flow response to alterations in  $P_{\text{aCO}_2}$  is more impressive and dramatic than the response to alterations in arterial  $P_{\text{O}_2}$ . The earliest evidence of this phenomenon was published in 1932. At that time, Lennox and Gibbs (105) estimated changes in cerebral blood flow in unanesthetized humans from the alterations in the cerebral arterial (brachial a.)-venous oxygen and carbon dioxide content of blood, measured with a thermo-electric blood flow recorder placed in the internal jugular vein. Their experiments, in which volunteers were subjected to 'violent hyperpneas' and to states of unconsciousness in one to two minutes by breathing nitrogen, would be hard-pressed to be approved by a modern day Ethics committee! Many studies have since been published (37,50,84,85,159,167,169,170) corroborating the early findings of Lennox and co-workers (105,106).

Lennox and Gibbs (105) must also be given credit for being the first to describe the nature of the relationship between cerebral blood flow and  $P_{\text{aCO}_2}$ . They observed that the decrease in cerebral blood flow with hyperpnea (per unit change in carbon dioxide content of arterial blood) was only 25-33% of the increase observed with carbon dioxide breathing. Many reports have since used various techniques to study the relationship between cerebral blood flow and  $P_{\text{aCO}_2}$ . In the eucapnic-hypercapnic range, there is general agreement on steady-state values of 3.9 to 4.4 percent increases in cerebral blood flow per mmHg increase in  $P_{\text{CO}_2}$ . In humans, regional differences in  $\text{CO}_2$  sensitivity have been reported in the eucapnic-hypercapnic range. The  $\text{CO}_2$

sensitivity in gray matter (insular cortex) has been shown to be three times greater than in white matter (centrum semiovale) (156). In the eucapnic-hypocapnic range, there is general agreement on steady-state values of 1.8 to 3.4 percent decreases in cerebral blood flow per mmHg decrease in  $P_{\text{CO}_2}$ . Regional differences in  $\text{CO}_2$  sensitivity have also been reported (in neonatal dogs) in the eucapnic-hypocapnic range, with the largest sensitivity being recorded in the hypothalamus, brainstem and spinal cord (200). The techniques used have included nitrous oxide inhalation (and tissue uptake based on the Fick principle) (84,85,167), Xenon<sup>133</sup> washout (136), transcranial Doppler (37,58,200) and positron emission tomography (9,156).

The reason for the difference in  $\text{CO}_2$  sensitivity between hypercapnia and hypocapnia is unclear. In humans, some studies have suggested a linear response across both a hypo- and hypercapnic range (56,58), but other studies have not (22,156), with some studies suggesting that the relationship is better described by an exponential (70,85,189) or sigmoid (159) function. In dogs (56), as in monkeys (159), the relationship has been described by a sigmoid function.

## 1.5 CEREBRAL BLOOD FLOW AND HYPOXIA

That cerebral blood flow is increased by hypoxia is a response that is common to various species. A striking feature of this response in dogs (118), rats and other species (36) is that cerebral blood flow remains essentially unchanged until the arterial  $PO_2$  falls to about 50-60 mmHg. Further decreases in  $PO_2$  below this so-called 'threshold' (93) result in a marked increase in cerebral blood flow.

In awake humans, the earliest studies on the cerebral blood flow response to hypoxia were published in the 1930s by Lennox and his colleagues (105)(106) using techniques described in the previous section (see section 1.4). Several studies have since been published, and all have consistently shown an increase in cerebral blood flow with hypoxia (21,24,37,72,85,97,168,193). However, while it is clear that cerebral blood flow is increased by hypoxia, there is a large variability of responses (21,24,37,72,85,97,168,193). Part of the variability can be explained by several factors. These include the different levels of hypoxia studied (range of  $PET_{O_2}$  from 35 to 82 mmHg), the inaccuracies associated with the different techniques, and the difficulties encountered in attempting to separate the effects of hypoxia from those caused by changes in  $PET_{CO_2}$ .

A summary of the main studies in humans, including the degree of hypoxia, the techniques used and the corresponding level of (or change from control in)  $PET_{CO_2}$  is provided in Table 1.3. The data from the human studies presented in Table 1.3 have been combined to generate a stimulus-response curve (Fig. 1.2). As illustrated in Fig. 1.2, the form of the response in humans appears to be similar to other species (36,118). In Fig. 1.2a, the relationship between cerebral blood flow and  $PO_2$  is characterised by a polynomial (inverse third order) function. However, when the

hypoxic sensitivity is expressed in terms of oxygen saturation, the relationship appears to be essentially linear (Fig. 1.2b, solid line).

In studies of acute responses, the vasodilatory effect of hypoxia on cerebral vessels is opposed by the vasoconstrictive influence of hypocapnia. This is evident in studies where the background level of carbon dioxide is left uncontrolled. Thus, the effect of decreases in arterial  $PCO_2$ , secondary to the hypoxia-mediated hyperventilation, is a blunting of the cerebral blood flow response to hypoxia. This effect is illustrated in Fig. 1.2b in which the data points that represent cerebral blood flow responses to 'hypocapnic-hypoxia' (i.e. when the end-tidal  $PCO_2$  was uncontrolled, **bold data** in Table 1.3) have been removed. The remaining data (those representing 'eucapnic-hypoxia') clearly show an increase in the slope of the response as well as an upward shift in the regression line that characterises the relationship between cerebral blood flow and oxygen saturation (Fig. 1.2b, dotted line). Thus, for a given oxygen saturation, 'eucapnia' results in a greater cerebral blood flow sensitivity to hypoxia. The extent of the vasoconstrictive influence of hypocapnia over longer-term periods of hypoxia (for example, > 8 hours) has not yet been established.

**Table 1.3** Chronological list of major studies describing the CBF response to acute hypoxia in humans (includes data published in this Thesis).

Study	Technique	Site of Measurement	PET <sub>O<sub>2</sub></sub> (mmHg)	PET <sub>CO<sub>2</sub></sub> (mmHg)	O <sub>2</sub> Sat <sup>1</sup>	CBF <sup>2</sup> (%)
Poulin <i>et al.</i> (unpublished)	TCD <sup>3</sup>	MCA <sup>4</sup>	60	40 (+1.5) <sup>5</sup>	91	104
			60	38 (0)	91	103
	TCD	MCA	50	42 (+1.5)	85	110
			45	42 (+1.5)	80	120
Clar <i>et al.</i> (21) (1997)	TCD <sup>2</sup>	MCA	300	39 (+1.5)	100	96
			100	39 (+1.5)	99	100
			56	39 (0)	89	106
			<b>57</b>	<b>35 (-4)</b>	<b>89</b>	<b>103</b>
Jensen <i>et al.</i> (72) (1996)	TCD	MCA	46	IH <sup>6</sup>	81	118
			37	IH	71	135
Ellingson <i>et al.</i> (37) (1987)	TCD	MCA	65	40	93	123
Shapiro <i>et al.</i> (168) (1970)	(a-v)O <sub>2</sub> diff	global	91	38 (0)	98	100
			<b>74</b>	<b>37 (-1)</b>	<b>95</b>	<b>99</b>
			<b>64</b>	<b>36 (-2)</b>	<b>92</b>	<b>105</b>
			<b>55</b>	<b>36 (-2)</b>	<b>88</b>	<b>105</b>
			<b>47</b>	<b>35 (-3)</b>	<b>82</b>	<b>115</b>
			<b>40</b>	<b>33 (-5)</b>	<b>74</b>	<b>135</b>
			41	36 (-2)	76	143
			95	38 (0)	98	100
			82	38 (0)	97	105
			68	39 (+1)	94	107
			49	39 (+1)	84	128
			<b>37</b>	<b>34 (-4)</b>	<b>70</b>	<b>143</b>
<b>42</b>	<b>27 (-11)</b>	<b>77</b>	<b>109</b>			
Cohen <i>et al.</i> (24) (1967)	Krypton & (a-v)O <sub>2</sub> diff	global	89	41	98	100
			35	39 (-2)	67	171
Wasserman <i>et al.</i> (193) (1964)	(a-v)O <sub>2</sub> diff	global	55		88	107
			45		80	123
			<b>40</b>	<b>- (-5)</b>	<b>74</b>	<b>139</b>
			40	- (-2)	74	148
Lambertsen <i>et al.</i> (97) (1953)	Nitrous Oxide & (a-v)O <sub>2</sub> diff	global	<b>~600</b>	<b>38 (-2)</b>	<b>100</b>	<b>85</b>
Kety & Schmidt (85) (1948)	Nitrous Oxide & (a-v)O <sub>2</sub> diff	global	600	42	100	86
			<b>10%</b> <sup>7</sup>	<b>36 (-4)</b>	-	<b>135</b>

**Abbreviations:** 1, O<sub>2</sub> sat is the percent oxygen saturation in the arterial blood calculated from the end-tidal PO<sub>2</sub> using the empirical relationship described by Severinghaus (166); 2, CBF is cerebral blood flow expressed as a percent change from air-breathing control (100%); 3, TCD is transcranial Doppler ultrasound; 4, MCA is middle cerebral artery; 5, end-tidal PCO<sub>2</sub> represents test value while number in parentheses represents difference from air-breathing value; 6, IH is isocapnic hypoxia; 7, data set not used in Fig. 1.2. Data in **bold font** represents situations when the end-tidal PCO<sub>2</sub> was uncontrolled.



**Fig. 1.2** Relationship between cerebral blood flow and arterial  $PO_2$  in humans. The stimulus-response curves were generated using both published data from previous studies and unpublished observations from the Oxford Laboratory. **Panel A:** the hypoxic sensitivity is expressed in terms of  $PET_{O_2}$  and the relationship is characterized by an inverse third order function (solid line). Cerebral blood flow remains essentially unchanged until the arterial  $PO_2$  falls below 50-60 mmHg. **Panel B:** the hypoxic sensitivity is expressed in terms of oxygen saturation and the relationship is essentially linear. The solid line represents a best-fit linear regression using all the data from Table 1.3. The dotted line represents a best-fit linear regression when the effects of hypocapnia (data in bold from Table 1.3) have been removed. Thus, for a given oxygen saturation, 'eucapnia' results in a greater cerebral blood flow sensitivity to hypoxia. *Symbols legend:* open squares and open triangles, Poulin *et al.* (unpublished); open circles, Clar *et al.*, (21); J, Jensen *et al.*, (72); E, Ellingsen *et al.*, (37); S, Shapiro *et al.*, (168); C, Cohen *et al.*, (24); W, Wasserman *et al.*, (193); L, Lambertsen *et al.*, (97); K, Kety and Schmidt, (85).



## 1.6 CEREBRAL BLOOD FLOW AND DYNAMIC EXERCISE

In humans, results of studies examining the response of cerebral blood flow during exercise remain equivocal. The conflicting reports and lack of agreement are related, in part, to whether global (34,83,91,164,201), cortical (63,77,78,177) or regional (or single vessel) (43,61,62,77,110,113,121,196) changes in cerebral blood flow are being measured. A summary of the major studies published since the first report in 1954, including the techniques used and the major findings, is provided in Table 1.4 (see end of section 1.6).

Studies measuring global changes in cerebral blood flow, using the nitrous oxide inhalation technique (based on the Fick principle) (90,91,98,164,165,201) or the  $^{133}\text{Xe}$ -inhalation technique (46,113), generally show no changes or slight decreases in cerebral blood flow during dynamic exercise. In contrast, studies measuring regional changes in cerebral blood flow, using the  $^{133}\text{Xe}$ -clearance technique (52,63,77,78,122,135), positron emission tomography (PET) scanning (43) or single photon emission computed tomography (SPECT) (196) report modest increases (i.e. 15-31%) in regional cerebral blood flow during exercise of light to moderate intensity (i.e.  $\leq 50\% \dot{V}_{O_2\text{max}}$ ). Studies measuring changes in single vessels, using transcranial or B-Mode Doppler ultrasound also show a modest increase with submaximal exercise (61,62,77,78,110,113,121,149).

The comparison of results from different studies is complicated by limitations associated with the various techniques used but also by the many different intensities of exercise that have been studied. This is an important consideration because exercise elicits several alterations in cardiovascular and respiratory function that may influence cerebral blood flow. These include exercise intensity-dependent changes in heart rate, blood pressure, alveolar ventilation and end-tidal (and possibly, arterial)  $\text{PCO}_2$  (27,161). Thus, although

studies have generally used light to moderate intensity exercise, the chosen intensities have elicited quite a wide range of cardiovascular and respiratory responses. Compared with resting values, the cardiovascular responses include increases in heart rate (range 24 to 136%) (46,62,113,135,150), increases in mean arterial pressure (range 12 to 40%) (46,58,63,113,135,150,177), small increases in hemoglobin concentration (range 6 to 9%) (98,113), and a small increase (9%) in arterial oxygen content of blood (98). The elicited respiratory responses include increases (7 to 25%) or no changes in end-tidal PCO<sub>2</sub> (63,77,78,121,177) and decreases (9%) or slight increases (4%) in arterial PCO<sub>2</sub> (46,63,77,78,110,113,135, 177).

Despite the various confounding factors, some general observations can be made. First, while it is not unreasonable to expect that global cerebral blood flow remains unchanged during exercise, recent studies using PET (43) and SPECT (196) provide convincing evidence showing relative increases in cerebral blood flow (~15%) in the motor sensory areas of the brain. Second, in line with studies showing increases in regional flow, studies using Doppler ultrasound to measure flow in single vessels have given fairly consistent results, suggesting modest increases of 10-42% in the flow velocity of the middle cerebral artery during light to moderate dynamic exercise (61,62,77,78,110,113,121,149). However, while some of the Doppler studies are consistent (61,68,77,78,110,113,150) with the results from studies using PET and SPECT, others are not, with some showing much larger increases in flow velocity (62,77,121,149).

The major complication underlying the Doppler-based studies is that most relate to beat averages of the velocities associated with the maximal frequencies of the Doppler shift. The use of this velocity as an index of cerebral blood flow requires first that the maximal

velocity is proportional to the mean velocity of the blood flow in the vessel, and secondly that the cross-sectional area of the blood vessel remains unchanged. During exercise, both heart rate and the pulsatility of arterial blood pressure increase markedly, and consequently the characteristics of cerebral blood flow may change. In this case, it is not clear that changes in the velocities associated with the maximal frequencies of the Doppler shift necessarily reflect changes in flow. This is the focus of the study in Chapter 5 of this Thesis.

**Table 1.4** Summary of the major studies on cerebral blood flow during exercise in humans.

Study	Exercise Modality	Intensity <sup>1</sup> (% or Watts)	CBF <sup>2</sup> (% change)	Site Measured
<i>Studies Using Transcranial Doppler Ultrasound</i>				
Imms <i>et al.</i> (68) (1998)	sustained contraction of right hand, supine	40%	17 (E) <sup>3</sup> NS (HV) <sup>3</sup>	MCA <sup>4</sup> MCA
Pott <i>et al.</i> (150) (1997)	rhythmic handgrip at 1 Hz, supine	20%	15 (contralateral) 8 (ipsilateral)	MCA MCA
Pott <i>et al.</i> (149) (1996)	rhythmic handgrip	20% MVC	21	MCA
	cycling, supine	moderate ~80%	21-29 31	MCA MCA
		≥80%	48	MCA
Hellström <i>et al.</i> (61) (1996)	dynamic, cycling supine	20%	13	MCA
		40%	16	MCA
		60%	14	MCA
		80%	11	MCA
Linkis <i>et al.</i> (110) (1995)	dynamic, cycling semi-supine,	136W	21, 19 21, 25	l/r MCA l/r ACA <sup>5</sup>
	right handgrip		19	left MCA
	right ankle flex./ext.		23	left ACA
Madsen <i>et al.</i> (113) (1993)	dynamic, cycling	50%	14 22 (CO <sub>2</sub> adj.)	MCA MCA
Hellström & Wahlgren (62), (1993)	dynamic, cycling	225W	51	MCA
Moraine <i>et al.</i> (121) (1993)	dynamic, cycling	57	42	MCA
Jørgensen <i>et al.</i> (76) (1993)	handgrip with regional anesthesia	r-hand	n/c, 20	r/l MCA
		l-hand	24, n/c	r/l MCA
Jørgensen <i>et al.</i> (77) (1992)	dynamic, cycling semi-supine	30W	10, -5	MCA, ACA
		60W	16, 2.5	MCA, ACA
		149W	28, 22	MCA, ACA
Jørgensen <i>et al.</i> (78) (1992)	dynamic, cycling	88W	15	MCA
		147W	17	MCA
	one-leg knee ext.	31%	7 (NS)	MCA

Table 1.4 Continued.

Study	Exercise Modality	Intensity <sup>1</sup> (% or Watts)	CBF <sup>2</sup> (% change)	Site Measured
<b>Study Using Duplex (B-mode, M-mode) Doppler Ultrasound</b>				
Hellström <i>et al.</i> (61) (1996)	dynamic, cycling supine	20%	10, 3	ICA <sup>6</sup> , CCA <sup>7</sup>
		40%	11, 18	ICA, CCA
		60%	17, 33	ICA, CCA
		80%	8, 42	ICA, CCA
<b>Study Using Single Photon Emission Computed Tomography (SPECT)</b>				
Williamson <i>et al.</i> (196) (1997)	active/passive cycling	1.5[ rest $\dot{V}O_2$ ]	17 9	SMPCG <sup>8</sup> left PIC <sup>9</sup>
<b>Study Using Positron Emission Tomography (PET)</b>				
Fink <i>et al.</i> (43) (1995)	flex./ext. of right knee	2.5[ rest $\dot{V}O_2$ ]	13 11	SMPCG SLPCG <sup>10</sup>
<b>Studies Using Inert Gas: <sup>133</sup>Xenon, intravenous</b>				
Madsen <i>et al.</i> (113) (1993)	dynamic, cycling	50%	-7 (NS) nc (CO <sub>2</sub> adj.)	global CBF global CBF
Jørgensen <i>et al.</i> (77) (1992a)	dynamic, cycling semi-supine	30W	15, 30 (ISI, F1) <sup>11</sup>	MCA area
		60W	25, 46	MCA area
		149W	42, 57	MCA area
Jørgensen <i>et al.</i> (78) (1992b)	dynamic, cycling	88W 147W	28, 34 (ISI, F1) 21, 45	MCA area MCA area
	one-leg static knee ext.	31%	-11 (ISI, NS)	MCA area
Thomas <i>et al.</i> (177) (1989)	dynamic, cycling semi-supine	30% 56%	23, 52 (ISI, F1) 36, 58	MCA area MCA area
Herholz <i>et al.</i> (63) (1987)	dynamic, cycling supine	25W 100W	12 (F1) 18	Pre-/Post- central regions
Olesen (135) (1971)	vigorous hand exercise (1 Hz)		54 (ISI) 61 (CO <sub>2</sub> adj.)	central region central region
<b>Studies Using Inert Gas: <sup>133</sup>Xenon, inhalation</b>				
Globus <i>et al.</i> (46) (1983)	dynamic, cycling supine	50%	-1.6 (ISI)	global
<b>Study Using Radioactively-labelled Erythrocytes</b>				
Hedlund <i>et al.</i> (59) (1962)	dynamic, cycling supine	~50W	19	global

Table 1.4 Continued.

Study	Exercise Modality	Intensity <sup>1</sup> (% or Watts)	CBF <sup>2</sup> (% change)	Site Measured
<i>Studies Using Inert Gas: Nitrous Oxide</i>				
Zobl <i>et al.</i> (201) (1965)	dynamic, cycling	>2[ rest $\dot{V}O_2$ ]	16 (NS)	global
Lambertsen <i>et al.</i> (98) (1959)	dynamic, cycling supine	~125W	2 (NS)	global
<i>Studies Using Inert Gas: Nitrous Oxide (continued)</i>				
Kleinerman & Sancetta, (90), (1955)	dynamic, cycling supine	~3W	-13	global
Scheinberg <i>et al.</i> (165) (1954)	treadmill walking	vigorous 5 (4%, 4.5mph)	(NS)	global

*Abbreviations and legend:* NS, non-significant; 1, exercise intensity is reported as a percent of maximal oxygen uptake (when reported) or otherwise as absolute work load in Watts; 2, CBF is cerebral blood flow reported as a percent change from values at rest; 3, E for eucapnic subjects and HV for hyperventilating subjects; 4, MCA is middle cerebral artery and unless stated,  $\bar{V}_P$  is reported; 5, ACA is anterior cerebral artery; 6, ICA is internal carotid artery; 7, CCA is common carotid artery; 8, SMPCG is superomedial precentral gyri (leg motor areas); 9, PIC is posterior insular cortex; 10, SLPCG is superolateral precentral gyri (volitional breathing areas); 11, ISI and F1 are cerebral (cortical) blood flow expressed as the initial slope index and as the first component flow, respectively.

## 1.7 CEREBRAL BLOOD FLOW AND HYPOXIC VENTILATORY DEPRESSION

The changes that occur in cerebral blood flow with alterations in arterial gas tensions are of considerable interest to respiratory physiologists because the changes in cerebral blood flow have implications for the resulting ventilatory responses. One example is the ventilatory response to hypoxia. While it is well known that cerebral blood flow is increased by hypoxia, the role of the alterations in cerebral blood flow in the development of hypoxic ventilatory depression (HVD) remains unclear.

In humans, the ventilatory response to isocapnic hypoxia is biphasic, characterised by a fast initial increase in ventilation followed by a slower decline (HVD) to a new value above the pre-hypoxic level (30,195). While the mechanisms underlying HVD still need to be elucidated, several broad conclusions can be drawn from the current state of knowledge. First, there appears to be an ontogenic component to HVD, with the response in neonates differing than the response in adults. Second, several mechanisms appear to operate at different degrees of hypoxia. Third, the mechanisms are dependent on the state of consciousness. Fourth, the mechanisms may differ between humans and other species such as cats and goats. Recent reviews are provided elsewhere (126,160,194).

Both central (126) and non-central (109,138) mechanisms have been proposed to underlie HVD. Among the central mechanisms that might underlie HVD is the notion that an increase in cerebral blood flow with hypoxia would increase carbon dioxide washout and thus lead to central hypocapnia (103,126). While it is well known that cerebral blood flow is increased by hypoxia (37,85,170), the role of the alterations in cerebral blood flow in the development of HVD remains unclear. In humans, the

changes in cerebral blood flow with hypoxia appear not to play a major role in the development of HVD (131,174). On the other hand, studies in anaesthetized cats suggest that the magnitude of HVD can be fully accounted for by hyperperfusion at the site of the central chemoreceptors due to an increase in cerebral blood flow (12,127). Inconsistent perhaps with the results of studies in cats, is the finding (again in cats) that changes in medullary extracellular  $\text{PCO}_2$  and pH do not change significantly with hypoxia (71). Thus, despite the fact that HVD has been the topic of extensive study, the role of the changes in cerebral blood flow in underlying HVD remains unclear.

## 1.8 REFERENCES (CHAPTER 1)

1. **Aaslid, R.** *Transcranial Doppler Sonography*. Wien: Springer-Verlag, 1986.
2. **Aaslid, R., T. Markwalder, and H. Nornes.** Noninvasive transcranial Doppler ultrasound recording of flow velocity in basal cerebral arteries. *J. Neurosurg.* 57:769-774, 1982.
3. **Albrecht, R. F., D. J. Miletich, and M. Ruttle.** Cerebral effects of extended hyperventilation in unanesthetized goats. *Stroke* 18:649-655, 1987.
4. **Allen, K., A. L. Busza, H. A. Crockard, and D. G. Gadian.** Brain metabolism and blood flow in acute cerebral hypoxia studied by NMR spectroscopy and hydrogen clearance. *NRM in Biomedicine* 5:48-52, 1992.
5. **Apkon, M. and W. F. Boron.** Extracellular and intracellular alkalization and the constriction of rat cerebral arterioles. *J. Physiol. (Lond.)* 484:743-753, 1995.
6. **Apkon, M., R. A. Weed, and W. F. Boron.** Motor responses of cultured rat cerebral vascular smooth muscle cells to intra- and extracellular pH changes. *Am. J. Physiol.* 273:H434-H445, 1997.
7. **Auer, L.** Pial arterial reactions to hyper- and hypocapnia: a dynamic experimental study in cats. *Eur. Neurol.* 17:351-362, 1978.
8. **Baumgartner, R. W., H. P. Mattle, and R. Aaslid.** Transcranial Color-Coded Duplex Sonography, Magnetic Resonance Angiography, and Computed Tomography Angiography: Methods, Applications, Advantages, and limitations. *J. Clin. Ultrasound* 23:89-111, 1995.
9. **Bednarczyk, E. M., W. F. Rutherford, G. P. Leisure, M. A. Munger, E. A. Panacek, F. D. Miraldi, and J. A. Green.** Hyperventilation-induced reduction in cerebral blood flow: assessment by positron emission tomography. *DICP* 24:456-460, 1990.
10. **Bell, B. A.** A history of the study of the cerebral circulation and the measurement of cerebral blood flow. *Neurosurgery* 14:238-246, 1984.
11. **Belliveau, J. W.** MRI techniques for functional mapping of the human brain: integration with PET, EEG/MEG and infrared spectroscopy. In: *Quantification of Brain Function: Tracer Kinetics and Image Analysis in Brain PET*. Edited by: K. Uemura, N. A. Lassen, T. Jones, and I. Kanno. Amsterdam: Elsevier Science Publishers, 1993, p. 639-659.
12. **Berkenbosch, A., C. N. Olievier, and J. DeGoede.** Respiratory responses to hypoxia: peripheral and central effects. In: *Modelling and Control of Ventilation*. Edited by: S. J. G. Semple, L. Adams, and B. J. Whipp. New York: Plenum Press, 1995, p. 251-256.
13. **Betz, E.** Cerebral blood flow: its measurement and regulation. *Physiol. Rev.* 52:595-630, 1972.
14. **Bevan, J. A. and R. D. Bevan.** Is innervation a prime regulator of cerebral blood flow? *NIPS* 8:149-153, 1993.
15. **Bolotina, V. M., S. Najibi, J. J. Palacino, P. J. Pagano, and R. A. Cohen.** Nitric oxide directly activates calcium-dependent potassium channels in vascular smooth muscle. *Nature* 368:850-853, 1994.
16. **Brian, J. E.** Carbon dioxide and the cerebral circulation. *Anesthesiology* 88:1365-1386, 1998.
17. **Brown, M. M., J. P. H. Wade, and J. Marshall.** Fundamental importance of arterial oxygen content in the regulation of cerebral blood flow in man. *Brain* 108:81-93, 1985.
18. **Busija, D. W.** Cerebral autoregulation. In: *The Regulation of Cerebral Blood Flow*. Edited by: J. W. Phillis. Florida: CRC Press, Inc. 1993, p. 45-61.

19. **Chorobski, J. and W. Penfield.** Cerebral vasodilator nerves and their pathway from the medulla oblongata. *Arch. Neurol. and Psychiat.* 28:1257-1289, 1932.
20. **Christensen, M. S.** Acid-base changes in cerebrospinal fluid and blood, and blood volume changes following prolonged hyperventilation in man. *Br. J. Anaesth.* 46:348-357, 1974.
21. **Clar, C., M. Pedersen, M. J. Poulin, J. G. Tansley, and P. A. Robbins.** Effects of 8 h of eucapnic and poikilocapnic hypoxia on middle cerebral artery velocity and heart rate in humans. *Experim. Physiol.* 82:791-802, 1997.
22. **Clark, J. M., B. E. Skolnick, R. Gelfand, R. E. Farber, M. Stierheim, W. C. Stevens, G. Beck, and C. J. Lambertsen.** Relationship of <sup>133</sup>Xe cerebral blood flow to middle cerebral arterial flow velocity in men at rest. *J. Cereb. Blood Flow Metab.* 16:1255-1262, 1996.
23. **Clarke, D. D. and L. Sokoloff.** Circulation and energy metabolism of the brain. In: *Basic Neurochemistry*. Edited by: G. J. Siegel, B. W. Agranoff, R. W. Albers, and P. B. Molinoff. New York: Raven Press, 1994, p. 645-680.
24. **Cohen, P. J., S. C. Alexander, T. C. Smith, M. Reivich, and H. Wollman.** Effects of hypoxia and normocarbina on cerebral blood flow and metabolism in conscious man. *J. Appl. Physiol.* 23:183-189, 1967.
25. **Cournand, A.** Air and Blood. In: *Circulation of the Blood: Men and Ideas*. Edited by: A. P. Fishman and D. W. Richards. Bethesda: American Physiological Society, 1982, p. 3-70.
26. **Dager, S. R., W. L. Strauss, K. I. Marro, T. L. Richards, G. D. Metzger, and A. A. Artru.** Proton magnetic resonance spectroscopy investigation of hyperventilation in subjects with panic disorder and comparison subjects. *Am. J. Psychiatry* 152:666-672, 1995.
27. **Dempsey, J. A., H. V. Forster, and D. M. Ainsworth.** Regulation of Hyperpnea, Hyperventilation, and Respiratory Muscle Recruitment During Exercise. In: *Regulation of Breathing*. Edited by: J. A. Dempsey and A. I. Pack. New York: Marcel Dekker, Inc. 1995, p. 1065-1134.
28. **DeYoe, E. A., P. Bandettini, J. Neitz, D. Miller, and P. Winans.** Functional magnetic resonance imaging (fMRI) of the human brain. *J. Neurosci. Methods* 54:171-187, 1994.
29. **Dumke, P. R. and C. F. Schmidt.** Quantitative measurements of cerebral blood flow in the macaque monkey. *Am. J. Physiol.* 138:421-431, 1943.
30. **Easton, P. A., L. J. Slykerman, and N. R. Anthonisen.** Ventilatory response to sustained hypoxia in normal adults. *J. Appl. Physiol.* 61:906-911, 1986.
31. **Eden, A.** The Beginnings of Doppler. In: *Transcranial Doppler Sonography*. Edited by: R. Aaslid. Wien: Springer-Verlag, 1986, p. 1-9.
32. **Eden A.** *The Search for Christian Doppler*. Vienna: Springer-Verlag, 1992.
33. **Edvinsson, L.** Sympathetic control of cerebral circulation. *TINS* 5:425-429, 1982.
34. **Edvinsson, L., H. Hara, and R. Uddman.** Retrograde tracing of nerve fibers to the rat middle cerebral artery with true blue: colocalization with different peptides. *J. Cereb. Blood Flow Metab.* 9:212-218, 1989.
35. **Edvinsson, L. and E. T. MacKenzie.** Amine mechanisms in the cerebral circulation. *Pharmacol. Rev.* 28:275-348, 1977.
36. **Edvinsson L, MacKenzie ET, and J. McCulloch.** *Cerebral Blood Flow and Metabolism*. New York: Raven Press, Ltd, 1993.

37. Ellingsen, I., A. Hauge, G. Nicolaysen, M. Thoresen, and L. Walloe. Changes in human cerebral blood flow due to step changes in  $PAO_2$  and  $PACO_2$ . *Acta Physiol. Scand.* 129:157-163, 1987.
38. Faraci, F. M., K. R. Breese, and D. D. Heistad. Cerebral vasodilation during hypercapnia. Role of glibenclamide-sensitive potassium channels and nitric oxide. *Stroke* 25:1679-1683, 1994.
39. Faraci, F. M. and J. E. J. Brian. Nitric oxide and the cerebral circulation. *Stroke* 25:692-703, 1994.
40. Faraci, F. M. and D. D. Heistad. Endothelium-derived relaxing factor inhibits constrictor responses of large cerebral arteries to serotonin. *J. Cereb. Blood Flow Metab.* 12:500-506, 1992.
41. Faraci, F. M. and D. D. Heistad. Regulation of cerebral circulation: role of endothelium and potassium channels. *Physiol. Rev.* 78:53-97, 1998.
42. Fencl, V. Acid-base balance in cerebral fluids. In: *Handbook of Physiology. Section 3: The Respiratory System. Vol. II. Control of Breathing, Part 1.* Edited by: N. S. Cherniack and J. G. Widdicombe. Baltimore: Waverly Press, 1986, p. 115-140.
43. Fink, G. R., L. Adams, J. D. G. Watson, J. A. Innes, B. Wuyam, I. Kobayashi, D. R. Corfield, K. Murphy, T. Jones, R. S. J. Frackowiak, and A. Guz. Hyperpnoea during and immediately after exercise in man: evidence of motor cortical involvement. *J. Physiol. (Lond.)* 489:663-675, 1995.
44. Frackowiak RSJ, Friston KJ, Frith CD, Dolan RJ, and J.C. Mazziotta. *Human Brain Function.* San Diego: Academic Press, 1997.
45. Gaw, A. J. and J. A. Bevar. Flow-induced relaxation of the rabbit middle cerebral artery is composed of both endothelium-dependent and -independent components. *Stroke* 24:105-110, 1993.
46. Globus, M., E. Melamed, A. Keren, D. Tzivoni, C. Granot, S. Lavy, and S. Stern. Effect of exercise on cerebral circulation. *J. Cereb. Blood Flow Metab.* 3:287-290, 1983.
47. Golanov, E. V. and D. J. Reis. Contribution of oxygen-sensitive neurons of the rostral ventrolateral medulla to hypoxic cerebral vasodilation in the rat. *J. Physiol. (Lond.)* 495:201-216, 1996.
48. Goldman, H. Techniques for the measurement of cerebral blood flow. In: *The Regulation of Cerebral Blood Flow.* Edited by: J. W. Phillis. Florida: CRC Press, Inc. 1993, p. 3-32.
49. Goodman, D. William Harvey. In: *Early Seventeenth Century Scientists.* Edited by: R. Harre. Oxford: Pergamon Press, 1965, p. 101-127.
50. Gotoh, F., J. S. Meyer, and Y. Takagi. Cerebral effects of hyperventilation in man. *Arch. Neurol.* 12:410-423, 1965.
51. Gotoh, F., Y. Tazaki, and J. S. Meyer. Transport of gases through brain and their extravascular vasomotor action. *Exp. Neurol.* 4:48-58, 1961.
52. Gunawardena, K. A., K. Houston, and A. P. Smith. Evaluation of the turbine pocket spirometer. *Thorax* 42:689-693, 1987.
53. Hansen, N. B., P. T. Nowicki, R. R. Miller, T. Malone, R. G. Bickers, and J. A. Menke. Alterations in cerebral blood flow and oxygen consumption during prolonged hypocarbia. *Pediatr. Res.* 20:147-150, 1986.
54. Hardeno, J. E. and N. Suzuki. Neural pathways to the cerebral circulation in humans. In: *The Human Brain Circulation: Functional Changes in Disease.* Edited by: R. D. Bevan and J. A. Bevan. Totowa: Humana, 1994, p. 37-46.

55. **Harper, A. M.** Measurement of cerebral blood flow. Anatomy and methods. In: *Cerebral blood flow and metabolism*. Edited by: A. M. Harper and S. Jennett. Manchester: Manchester University Press, 1990, p. 71-89.
56. **Harper, A. M. and H. I. Glass.** Effect of alterations in the arterial carbon dioxide tension on the blood flow through the cerebral cortex at normal and low arterial blood pressures. *J. Neurol. Neurosurg. Psychiatry* 28:449-452, 1965.
57. **Harre R.** *Early Seventeenth Century Scientists*. Oxford: Pergamon Press, 1965.
58. **Hauge, A., M. Thoresen, and L. Walloe.** Changes in cerebral blood flow during hyperventilation and CO<sub>2</sub>-breathing measured transcutaneously in humans by a bidirectional, pulsed, ultrasound Doppler blood velocimeter. *Acta Physiol. Scand.* 110:167-173, 1980.
59. **Hedlund, S., G. Nylin, and O. Regnstrom.** The behavior of the cerebral circulation during muscular exercise. *Acta Physiol. Scand.* 54:316-324, 1962.
60. **Heistad, D. D. and H. A. Kontos.** Cerebral circulation. In: *Handbook of Physiology, Section 2: The Cardiovascular System, Vol. III*. Edited by: J. T. Shepherd, F. M. Abbond, and J. R. Geiger. Bethesda, MD: Waverly Press, Inc., 1983, p. 137-182.
61. **Hellström, G., W. Fischer-Colbrie, N. G. Wahlgren, and T. Jogestrand.** Carotid artery blood flow and middle cerebral artery blood flow velocity during physical exercise. *J. Appl. Physiol.* 81:413-418, 1996.
62. **Hellström, G. and N. G. Wahlgren.** Physical exercise increases middle cerebral artery blood flow velocity. *Neurosurg. Rev.* 16:151-156, 1993.
63. **Herholz, K., W. Buskies, M. Rist, G. Pawlik, W. Hollmann, and W. D. Heiss.** Regional cerebral blood flow in man at rest and during exercise. *J. Neurol.* 234:9-13, 1987.
64. **Howard, J. H., P. A. Rechnitzer, D. A. Cunningham, and A. P. Donner.** Change in type A behaviour a year after retirement. *Gerontol.* 26:643-649, 1986.
65. **Hughes, J.T.** *Thomas Willis. 1621 - 1675: his life and work*. London: Royal Society of Medicine Services Limited, 1991.
66. **Iadecola, C.** Does nitric oxide mediate the increases in cerebral blood flow elicited by hypercapnia? *Proc. Natl. Acad. Sci.* 89:3913-3916, 1992.
67. **Iadecola, C., D. A. Pelligrino, M. A. Moskowitz, and N. A. Lassen.** Nitric oxide synthase inhibition and cerebrovascular regulation. *J. Cereb. Blood Flow Metab.* 14:175-192, 1994.
68. **Imms, F. J., F. Russo, V. I. Iyawe, and M. B. Segal.** Cerebral blood flow velocity during and after sustained isometric skeletal muscle contractions in man. *Clin. Sci.* 94:353-358, 1998.
69. **Ingvar, D. H. and N. A. Lassen.** Regional blood flow of the cerebral cortex determined by Krypton<sup>85</sup>. *Acta Physiol. Scand.* 54:325-338, 1962.
70. **James, I. M., R. A. Millar, and M. J. Purves.** Observations on the extrinsic neural control of cerebral blood flow in the baboon. *Circ. Res.* 25:77-93, 1969.
71. **Javaheri, S. and L. J. Teppema.** Ventral medullary extracellular fluid pH and PCO<sub>2</sub> during hypoxemia. *J. Appl. Physiol.* 63:1567-1571, 1987.
72. **Jensen, J. B., B. Sperling, J. W. Severinghaus, and N. A. Lassen.** Augmented hypoxic cerebral vasodilation in men during 5 days at 3,810 m altitude. *J. Appl. Physiol.* 80:1214-1218, 1996.
73. **Jensen, K. E., C. Thomsen, and O. Henriksen.** In vivo measurement of intracellular pH in human

- brain during different tensions of carbon dioxide in arterial blood. A  $^{31}\text{P}$ -NMR study. *Acta Physiol. Scand.* 134:295-298, 1988.
74. **Jones, M. D., R. J. Traystman, M. A. Simmons, and R. A. Molteni.** Effects of changes in arterial  $\text{O}_2$  content on cerebral blood flow in the lamb. *Am. J. Physiol.* 240:H209-H215, 1981.
75. **Jørgensen, L. G. Transcranial.** Doppler ultrasound for cerebral perfusion. *Acta Physiol. Scand.* 154 (Suppl. 625):1-44, 1995.
76. **Jørgensen, L. G., G. Perko, G. Payne, and N. H. Secher.** Effect of limb anesthesia on middle cerebral response to handgrip. *J. Am. Physiol.* 264:H553-H559, 1993.
77. **Jørgensen, L. G., G. Perko, and N. H. Secher.** Regional cerebral artery mean flow velocity and blood flow during dynamic exercise in humans. *J. Appl. Physiol.* 73:1825-1830, 1992.
78. **Jørgensen, L. G., M. Perko, B. Hanel, T. V. Schroeder, and N. H. Secher.** Middle cerebral artery flow velocity and blood flow during exercise and muscle ischemia in humans. *J. Appl. Physiol.* 72:1123-1132, 1992.
79. **Kazemi, H., L. M. Valenca, and D. C. Shannon.** Brain and cerebrospinal fluid lactate concentration in respiratory acidosis and alkalosis. *Respir. Physiol.* 6:178-186, 1969.
80. **Kety, S. S.** Circulation and metabolism of the human brain in health and disease. *Am. J. Med.* February:205-217, 1950.
81. **Kety, S. S.** Recent approaches to the measurement of cerebral blood flow and their underlying principles. *Res. Publ. Assoc. Res. Nerv. Ment. Dis.* 41:226-236, 1966.
82. **Kety, S. S.** The Cerebral Circulation. In: *Circulation of the Blood: Men and Ideas*. Edited by: A. P. Fishman and D. W. Richards. Bethesda: American Physiological Society, 1982, p. 703-742.
83. **Kety, S. S. and C. F. Schmidt.** The determination of cerebral blood flow in man by the use of nitrous oxide in low concentrations. *Am. J. Physiol.* 143:53-66, 1945.
84. **Kety, S. S. and C. F. Schmidt.** The effects of active and passive hyperventilation on cerebral blood flow, cerebral oxygen consumption, cardiac output, and blood pressure of normal young men. *J. Clin. Invest.* 25:107-119, 1946.
85. **Kety, S. S. and C. F. Schmidt.** The effects of altered arterial tensions of carbon dioxide and oxygen on cerebral blood flow and cerebral oxygen consumption of normal young men. *J. Clin. Invest.* 27:484-492, 1948.
86. **Kety, S. S. and C. F. Schmidt.** The nitrous oxide method for the quantitative determination of cerebral blood flow in man: theory, procedure and normal values. *J. Clin. Invest.* 27:476-483, 1948.
87. **Kim, S.-G.** Quantification of relative cerebral blood flow change by flow-sensitive alternating inversion recovery (FAIR) technique: application to functional mapping. *Magn. Reson. Med.* 34:293-301, 1995.
88. **Kim, S.-G., J. Ashe, A. P. Georgopoulos, H. Merkle, J. M. Ellermann, R. S. Menon, S. Ogawa, and K. Ugurbil.** Functional imaging of human cortex at high magnetic field. *J. Neurophysiol.* 69:297-302, 1993.
89. **Kitazono, T., F. M. Faraci, H. Taguchi, and D. D. Heistad.** Role of potassium channels in cerebral blood vessels. *Stroke* 26:1713-1723, 1995.
90. **Kleinerman, J. and S. M. Sancetta.** Effect of mild and steady state exercise on cerebral and general hemodynamics of normal untrained subjects. *J. Clin. Invest.* 34:945-946, 1955.

91. **Kleinerman, J. and L. Sokoloff.** Effects of exercise on cerebral blood flow and metabolism in man. *Fed. Proc.* 12:77, 1953.
92. **Kogure, K., R. Busto, A. Matsumoto, P. Scheinberg, and O. M. Reinmuth.** Effect of hyperventilation on dynamics of cerebral energy metabolism. *Am. J. Physiol.* 228:1862-1867, 1975.
93. **Kogure, K., P. Scheinberg, O. M. Reinmuth, M. Fujishima, and R. Busto.** Mechanism of cerebral vasodilation in hypoxia. *J. Appl. Physiol.* 29:223-229, 1970.
94. **Kuo, L., M. J. Davis, and W. M. Chilian.** Endothelial modulation of arterial tone. *NIPS* 7:5-10, 1992.
95. **Kuschinsky, W.** Role of Hydrogen Ions in Regulation of Cerebral Blood Flow and Other Regional Flows. In: *Ionic Regulation of the Microcirculation*. Edited by: B. M. Altura. Basel: Karger, 1982, p. 1-19.
96. **Kuschinsky, W. and M. Wahl.** Local chemical and neurogenic regulation of cerebral vascular resistance. *Physiol. Rev.* 58:656-689, 1978.
97. **Lambertsen, C. J., R. H. Kough, D. Y. Cooper, G. L. Emmel, H. H. Loeschcke, and C. F. Schmidt.** Oxygen toxicity. Effects in man of oxygen inhalation at 1 and 3.5 atmospheres upon blood gas transport, cerebral circulation and cerebral metabolism. *J. Appl. Physiol.* 5:471-486, 1953.
98. **Lambertsen, C. J., S. G. Owen, H. Wendel, M. W. Stroud, A. A. Lurie, W. Lochner, and G. F. Clark.** Respiratory and cerebral circulatory control during exercise at .21 and 2.0 atmospheres inspired  $PO_2$ . *J. Appl. Physiol.* 14:966-982, 1959.
99. **Lassen, N. A.** Cerebral blood flow and oxygen consumption in man. *Physiol. Rev.* 39:183-238, 1959.
100. **Lassen, N. A.** Brain extracellular pH: The main factor controlling cerebral blood flow. *Scand. J. Lab. Clin. Invest.* 22:247-251, 1968.
101. **Lassen, N. A.** Control of cerebral circulation in health and disease. *Circ. Res.* 34:749-760, 1974.
102. **Lassen, N. A. and M. S. Christensen.** Physiology of cerebral blood flow. *Br. J. Anaesth.* 48:719-734, 1976.
103. **Lee, L. and H. T. Milhorn.** Central ventilatory response to  $O_2$  and  $CO_2$  at three levels of carotid chemoreceptor stimulation. *Respir. Physiol.* 25:319-333, 1975.
104. **Leffler, C. W.** Prostanoids: intrinsic modulators of cerebral circulation. *NIPS* 12:72-76, 1997.
105. **Lennox, W. G. and E. L. Gibbs.** The blood flow in the brain and leg of man, and the changes induced by alteration of blood gases. *J. Clin. Invest.* 11:1155-1177, 1932.
106. **Lennox, W. G., F. A. Gibbs, and E. L. Gibbs.** Relationship of unconsciousness to cerebral blood flow and to anoxemia. *Arch. Neurol. and Psychiatry.* 34:1001-1013, 1935.
107. **Leusen, I. and G. Demeester.** Lactate and pyruvate in the brain of rats during hyperventilation. *Archives Internationales de Physiologie et de Biochimie* 74:25-34, 1966.
108. **Levasseur, J. E., E. P. Wei, H. A. Kontos, and J. L. Patterson.** Responses of pial arterioles after prolonged hypercapnia and hypoxia in the awake rabbit. *J. Appl. Physiol.* 46:89-95, 1979.
109. **Liang, P.-J., D. A. Bascom, and P. A. Robbins.** Extended models of the ventilatory response to sustained isocapnic hypoxia in humans. *J. Appl. Physiol.* 82:667-677, 1997.
110. **Linkis, P., L. G. Jorgensen, H. L. Olesen, P. L. Madsen, N. A. Lassen, and N. H. Secher.**

- Dynamic exercise enhances regional cerebral artery mean flow velocity. *J. Appl. Physiol.* 78:12-16, 1995.
111. **Macmillan, V. and B. K. Siesjo.** The influence of hypocapnia upon intracellular pH and upon some carbohydrate substrates, amino acids, and organic phosphates in the brain. *J. Neurochem.* 21:1283-1299, 1973.
112. **Madden, J. A., M. S. Vadula, and V. P. Kurup.** Effects of hypoxia and other vasoactive agents on pulmonary and cerebral artery smooth muscle cells. *Am. J. Physiol.* 263:L384-L393, 1992.
113. **Madsen, P. L., B. K. Sperling, T. Warming, J. F. Schmidt, N. H. Secher, G. Wildschiodtz, S. Holm, and N. A. Lassen.** Middle cerebral artery blood velocity and cerebral blood flow and O<sub>2</sub> uptake during dynamic exercise. *J. Appl. Physiol.* 74:245-250, 1993.
114. **Mansour, T. E.** Phosphofructokinase. In: *Current Topics in Cellular Regulation*. Edited by: B. L. Horecker and E. R. Stadtman. New York: Academic Press, 1972, p. 1-46.
115. **Marshall L.H. and H.W. Magoun.** *Discoveries in the Human Brain: Neuroscience Prehistory, Brain Structure, and Function*. Totowa: Humana Press, 1998.
116. **Martin, P. J., D. H. Evans, and A. R. Naylor.** Transcranial color-coded sonography of the basal cerebral circulation. *Stroke* 25:390-396, 1994.
117. **Martin, P. J., D. H. Evans, and A. R. Naylor.** Measurement of blood flow velocity in the basal cerebral circulation: advantages of Transcranial Color-Coded Sonography over conventional transcranial Doppler. *J. Clin. Ultrasound* 23:21-26, 1995.
118. **McDowall, D. G.** Interrelationships between blood oxygen tension and cerebral blood flow. In: *Oxygen Measurements in Blood and Tissues*. Edited by: J. P. Payne and D. W. Hill. London: Churchill, 1966, p. 205-214.
119. **Menon, R. S., S. Ogawa, S.-G. Kim, J. M. Ellermann, H. Merkle, D. W. Tank, and K. Ugurbil.** Functional brain mapping using magnetic resonance imaging: signal changes accompanying visual stimulation. *Invest. Radiol.* 27(Suppl.2):S47-S53, 1997.
120. **Milledge, J. S.** The great oxygen secretion controversy. *Lancet* 8469-70:1408-1411, 1985.
121. **Moraine, J. J., M. Lamotte, J. Berre, G. Niset, A. Leduc, and R. Naeije.** Relationship of middle cerebral artery blood flow velocity to intensity during dynamic exercise in normal subjects. *Eur. J. Appl. Physiol. Occup. Physiol.* 67:35-38, 1993.
122. **Morey, M. C., P. A. Cowper, J. R. Feussner, R. C. DiPasquale, G. M. Crowley, D. W. Kitzman, and R. J. Sullivan.** Evaluation of a supervised exercise program in a geriatric population. *J. Am. Geriatric Soc.* 37:348-354, 1989.
123. **Muizelaar, J. P., G. J. Bouma, J. E. Levasseur, and H. A. Kontos.** Effect of hematocrit variations on cerebral blood flow and basilar artery diameter in vivo. *Am. J. Physiol.* 262:H949-H954, 1992.
124. **Muizelaar, J. P., H. G. van der Poel, Z. Li, H. A. Kontos, and J. E. Levasseur.** Pial arteriolar vessel diameter and CO<sub>2</sub> reactivity during prolonged hyperventilation in the rabbit. *J. Neurosurg.* 69:923-927, 1988.
125. **Nelson, M. T. and J. M. Quayle.** Physiological roles and properties of potassium channels in arterial smooth muscle. *Am. J. Physiol.* 268:C799-C822, 1995.
126. **Neubauer, J. A., J. E. Melton, and N. H. Edelman.** Modulation of respiration during brain hypoxia. *J. Appl. Physiol.* 68:441-451, 1990.

127. **Neubauer, J. A., T. V. Santiago, M. A. Posner, and N. H. Edelman.** Ventral medullary pH and ventilatory responses to hyperperfusion and hypoxia. *J. Appl. Physiol.* 58:1659-1668, 1985.
128. **Newell, D. W. and R. Aaslid.** Transcranial Doppler: Clinical and Experimental Uses. *Cerebrovasc Brain Metab. Rev.* 4:122-143, 1992.
129. **Newman, E. A.** High potassium conductance in astrocyte endfeet. *Science* 233:453-454, 1986.
130. **Nicholson, C.** Extracellular space as the pathway for neuron-glia cell interaction. In: *Neuroglia*. Edited by: H. Kettenmann and B. R. Ransom. Oxford: Oxford University Press, 1995, p. 387-397.
131. **Nishimura, M., A. Suzuki, Y. Nishiura, H. Yamamoto, K. Miyamoto, F. Kishi, and Y. Kawakami.** Effect of brain blood flow on hypoxic ventilatory response in humans. *J. Appl. Physiol.* 63:1100-1106, 1987.
132. **Ogawa, S., T. M. Lee, A. R. Kay, and D. W. Tank.** Brain magnetic resonance imaging with contrast dependent on blood oxygenation. *Proc. Natl. Acad. Sci.* 87:9868-9872, 1990.
133. **Ogawa, S., R. S. Menon, S.-G. Kim, and K. Ugurbil.** On the characteristics of functional magnetic resonance imaging of the brain. *Ann. Rev. Biophys. Biomol. Struct.* 27:447-474, 1998.
134. **Ogawa, S., R. S. Menon, D. W. Tank, S.-G. Kim, H. Merkle, J. M. Ellermann, and K. Ugurbil.** Functional brain mapping by blood oxygenation level-dependent contrast magnetic resonance imaging. *Biophys. J.* 64:803-812, 1993.
135. **Olesen, J.** Contralateral focal increase of cerebral blood flow in man during arm work. *Brain* 94:635-646, 1971.
136. **Olesen, J., O. B. Paulson, and N. A. Lassen.** Regional cerebral blood flow in man determined by the initial slope of the clearance of intra-arterially injected  $^{133}\text{Xe}$ . *Stroke* 2:519-540, 1971.
137. **Owen-Reece, H., C. E. Elwell, W. Harkness, J. Goldstone, D. T. Delpy, J. S. Wyatt, and M. Smith.** Use of near infrared spectroscopy to estimate cerebral blood flow in conscious and anaesthetized adult subjects. *Br. J. Anaesth.* 76:43-48, 1996.
138. **Painter, R., S. Khamnei, and P. A. Robbins.** A mathematical model of the human ventilatory response to isocapnic hypoxia. *J. Appl. Physiol.* 74:2007-2015, 1993.
139. **Paulson, O. B.** Cerebral autoregulation. *Cerebrovasc Brain Metab. Rev.* 2:161-192, 1990.
140. **Paulson, O. B. and E. A. Newman.** Does the release of potassium from astrocyte endfeet regulate cerebral blood flow? *Science* 237:896-898, 1987.
141. **Paulson, O. B., H.-H. Parving, J. Olesen, and E. Skinhoj.** Influence of carbon monoxide and of hemodilution on cerebral blood flow and blood gases in man. *J. Appl. Physiol.* 35:111-116, 1973.
142. **Payen, J. F., E. LeBars, B. Wuyam, B. Tropini, J. L. Pepin, P. Levy, and M. Decorps.** Lactate accumulation during moderate hypoxic hypoxia in neocortical rat brain. *J. Cereb. Blood Flow Metab.* 16:1345-1352, 1996.
143. **Petroff, O. A. C., J. W. Prichard, K. L. Behar, D. L. Rothman, J. R. Alger, and R. G. Shulman.** Cerebral metabolism in hyper- and hypocarbia:  $^{31}\text{P}$  and  $^1\text{H}$  nuclear magnetic resonance studies. *Neurology* 35:1681-1688, 1985.
144. **Phillis, J. W.** Cerebral vascular responses to hypoxia, hyper- and hypocapnia, and hypotension. In: *The Regulation of Cerebral Blood Flow*. Edited by: J. W. Phillis. Florida: CRC Press, Inc. 1993, p. 249-265.
145. **Phillis, J.W.** *The Regulation of Cerebral Blood Flow*. Boca Raton, Florida: CRC Press, Inc. 1993.

146. **Plum, F. and J. B. Posner.** Selective CNS lactic acidosis in response to hypocapnia. *J. Clin. Invest.* 45:1057, 1966.
147. **Plum, F. and J. B. Posner.** Blood and cerebrospinal fluid lactate during hyperventilation. *Am. J. Physiol.* 212:864-870, 1967.
148. **Plum, F., J. B. Posner, and W. W. Smith.** Effect of hyperbaric-hyperoxic hyperventilation on blood, brain, and CSF lactate. *Am. J. Physiol.* 215:1240-1244, 1968.
149. **Pott, F., K. Jensen, N. J. Christensen, N. A. Lassen, and N. H. Secher.** Middle cerebral artery blood velocity and plasma catecholamines during exercise. *Acta Physiol. Scand.* 158:349-356, 1996.
150. **Pott, F., C. A. Ray, H. L. Olesen, K. Ide, and N. H. Secher.** Middle cerebral artery blood velocity, arterial diameter and muscle sympathetic nerve activity during post-exercise muscle ischaemia. *Acta Anaesth. Scand.* 160:43-47, 1997.
151. **Purves, M.J.** *The Physiology of the Cerebral Circulation.* London: Cambridge University Press, 1972.
152. **Quayle, J. M., M. T. Nelson, and N. B. Standen.** ATP-sensitive and inwardly rectifying potassium channels in smooth muscle. *Physiol. Rev.* 77:1165-1232, 1997.
153. **Raichle, M. E.** Circulatory and metabolic correlates of brain function in normal humans. In: *Handbook of Physiology, Section 1, The Nervous System.* Edited by: V. B. Mountcastle. American Physiological Society, 1987, p. 643-674.
154. **Raichle, M. E. and F. Plum.** Hyperventilation and cerebral blood flow. *Stroke* 3:566-575, 1972.
155. **Raichle, M. E., J. B. Posner, and F. Plum.** Cerebral blood flow during and after hyperventilation. *Arch. Neurol.* 23:394-403, 1970.
156. **Ramsay, S. C., K. Murphy, S. A. Shea, K. J. Friston, A. A. Lammertsma, J. C. Clark, L. Adams, A. Guz, and R. S. J. Frackowiak.** Changes in global cerebral blood flow in humans: effect on regional cerebral blood flow during a neural activation task. *J. Physiol. (Lond.).* 471:521-534, 1993.
157. **Reid, J. M., A. G. Davies, F. M. Ashcroft, and D. J. Paterson.** Effect of L-NMMA, cromakalim, and glibenclamide on cerebral blood flow in hypercapnia and hypoxia. *Am. J. Physiol.* 269:H916-H922, 1995.
158. **Reid, J. M., D. J. Paterson, F. M. Ashcroft, and D. H. Bergel.** The effect of tolbutamide on cerebral blood flow during hypoxia and hypercapnia in the anaesthetized rat. *Eur. J. Physiol.* 425:362-364, 1993.
159. **Reivich, M.** Arterial PCO<sub>2</sub> and cerebral hemodynamics. *Am. J. Physiol.* 206:25-35, 1964.
160. **Robbins, P. A.** Hypoxic ventilatory decline: site of action. *J. Appl. Physiol.* 79:373-374, 1995.
161. **Rowell, L.B.** *Human Cardiovascular Control.* New York: Oxford University Press, 1993.
162. **Roy, C. S. and C. S. Sherrington.** On the regulation of the blood-supply of the brain. *J. Physiol. (Lond.)* 11:85-108, 1890.
163. **Scheinberg, P.** The pharmacology of brain blood flow. *Res. Publ. Assoc. Res. Nerv. Ment. Dis.* 41:216-225, 1966.
164. **Scheinberg, P., I. Blackburn, M. Rich, and M. Saslaw.** Effects of vigorous physical exercise on cerebral circulation and metabolism. *Am. J. Med.* 16:549-554, 1953.

165. **Scheinberg, P., I. Blackburn, M. Rich, and M. Saslaw.** Effects of vigorous physical exercise on cerebral circulation and metabolism. *Am. J. Physiol.* 16:549-554, 1954.
166. **Severinghaus, J. W.** Proposed standard determination of ventilatory responses to hypoxia and hypercapnia in man. *Chest* 1(Suppl.):129-131, 1976.
167. **Severinghaus, J. W. and N. Lassen.** Step hypocapnia to separate arterial from tissue PCO<sub>2</sub> in the regulation of cerebral blood flow. *Circ. Res.* 20:272-278, 1967.
168. **Shapiro, W., A. J. Wasserman, J. P. Baker, and J. L. Patterson.** Cerebrovascular response to acute hypocapnic and eucapnic hypoxia in man. *J. Clin. Invest.* 49:2362-2368, 1970.
169. **Shapiro, W., A. J. Wasserman, and J. L. Patterson.** Mechanism and pattern of human cerebrovascular regulation after rapid changes in blood CO<sub>2</sub> tension. *J. Clin. Invest.* 45:913-922, 1966.
170. **Shapiro, W., A. J. Wasserman, and J. L. Patterson.** Human cerebrovascular response to combined hypoxia and hypercapnia. *Circ. Res.* 19:903-910, 1966.
171. **Siesjo, B. K.** The regulation of cerebrospinal fluid pH. *Kidney Int.* 1:360-374, 1972.
172. **Sokoloff, L.** The action of drugs on the cerebral circulation. *Pharmacol. Rev.* 11:1-85, 1959.
173. **Sokoloff, L., M. Reivich, C. Kennedy, M. H. Des Rosiers, C. S. Patlak, K. D. Pettigrew, O. Sakurada, and M. Shinohara.** The [14C]deoxyglucose method for the measurement of local cerebral glucose utilisation: theory, procedure, and normal values in the conscious and anesthetized albino rat. *J. Neurochem.* 28:897-916, 1977.
174. **Suzuki, A., M. Nishimura, H. Yamamoto, K. Miyamoto, F. Kishi, and Y. Kawakami.** No effect of brain blood flow on ventilatory depression during sustained hypoxia. *J. Appl. Physiol.* 66:1674-1678, 1989.
175. **Taguchi, H., D. D. Heistad, T. Kitazono, and F. M. Faraci.** ATP-sensitive K<sup>+</sup> channels mediate dilatation of cerebral arterioles during hypoxia. *Circ. Res.* 74:1005-1008, 1994.
176. **Tegeler, C.H., Babikian, V.L., and C.R. Gomez.** *Neurosonology*. St. Louis: Mosby, 1996.
177. **Thomas, S. N., T. Schroeder, N. H. Secher, and J. H. Mitchell.** Cerebral blood flow during submaximal and maximal dynamic exercise in humans. *J. Appl. Physiol.* 67:744-748, 1989.
178. **Tian, R., P. Vogel, N. A. Lassen, M. J. Mulvany, F. Andreassen, and C. Aalkjaer.** Role of extracellular and intracellular acidosis for hypercapnia-induced inhibition of tension of isolated rat cerebral arteries. *Circ. Res.* 76:269-275, 1995.
179. **Toole, J. F.** Applied Physiology of the Cerebral Circulation. In: *Cerebrovascular Disorders*. Edited by: J. F. Toole. New York: Raven Press, 1990, p. 28-49.
180. **Toole, J. F.** Applied Anatomy and Embryology of the Brain Arteries. In: *Cerebrovascular Disorders*. Edited by: J. F. Toole. New York: Raven Press, 1990, p. 1-27.
181. **Tower, D. B.** Cerebral circulation revisited: an historical essay. *Neurochem. Res.* 16:1085-1097, 1991.
182. **Tsacopoulos, M. and P. J. Magistretti.** Metabolic coupling between glia and neurons. *J. Neurosci.* 16:877-885, 1996.
183. **Ugurbil, K., M. Garwood, J. M. Ellermann, K. Hendrich, R. Hinke, X. Hu, S.-G. Kim, R. S. Menon, H. Merkle, S. Ogawa, and R. Salmi.** Imaging at high magnetic fields: initial experiences at 4 T. *Magn. Res. Quart.* 9:259-277, 1993.

184. **van der Zwan, A. and B. Hillen.** Review of the variability of the territories of the major cerebral arteries. *Stroke* 22:1078-1084, 1991.
185. **van Rijen, P. C., P. R. Luyten, J. W. Berkelbach van der Sprenkel, V. Kraaier, A. C. van Huffelen, C. A. F. Tulleken, and J. A. den Hollander.** <sup>1</sup>H and <sup>31</sup>P NMR measurement of cerebral lactate, high energy phosphate levels, and pH in humans during voluntary hyperventilation: associated EEG, capnographic, and Doppler findings. *Magn. Reson. Med.* 10:182-193, 1989.
186. **van Vaerenbergh, P. J. J., E. Lacroix, G. Demeester, and I. Leusen.** Lactate in cerebrospinal fluid during muscular exercise. *Archives Internationales de Physiologie et de Biochimie* 73:729-737, 1965.
187. **Verkhatsky, A., R. K. Orkand, and H. Kettenmann.** Glial calcium: Homeostasis and signaling function. *Physiol. Rev.* 78:99-141, 1998.
188. **Wahl, M. and L. Schilling.** Regulation of cerebral blood flow a brief review. *Acta Neurochir.* 59(Suppl):3-10, 1993.
189. **Waltz, A. G.** Effect of Pa<sub>CO2</sub> on blood flow and microvasculature of ischemic and nonischemic cerebral cortex. *Stroke* 1:27-37, 1970.
190. **Wang, Q., O. B. Paulson, and N. A. Lassen.** Effect of nitric oxide blockade by NG-nitro-L-arginine on cerebral blood flow response to changes in carbon dioxide tension. *J. Cereb. Blood Flow Metab.* 12:947-953, 1992.
191. **Wang, Q., D. A. Pelligrino, V. L. Baughman, H. M. Koenig, and R. F. Albrecht.** The role of neuronal nitric oxide synthase in regulation of cerebral blood flow in normocapnia and hypercapnia in rats. *J. Cereb. Blood Flow Metab.* 15:774-778, 1995.
192. **Ward, D. S. and J. W. Bellville.** Effect of intravenous dopamine on hypercapnic ventilation response in humans. *J. Appl. Physiol.* 55:1418-1425, 1983.
193. **Wasserman, A. J., W. Shapiro, and J. L. Patterson.** Human cerebrovascular effects of graded hypoxemia. *Circulation* 30:III-175, 1964.
194. **Weil, J. V.** Invited editorial on "Ventilatory responses to CO<sub>2</sub> and hypoxia after sustained hypoxia in awake cats". *J. Appl. Physiol.* 76:2251-2252, 1994.
195. **Weil, J. V. and C. Zwillich.** Assessment of ventilatory response to hypoxia. *Chest* 1:124-128, 1976.
196. **Williamson, J. W., A. C. L. Nobrega, R. McColl, D. Mathews, P. Winchester, L. Friberg, and J. H. Mitchell.** Activation of the insular cortex during dynamic exercise in humans. *J. Physiol. (Lond.)* 503:277-283, 1997.
197. **Willis T.** *Cerebri Anatome: cui accessit Nervorum descriptio et usus.* 1664.
198. **Winn, H. R., R. Rubio, and R. M. Berne.** Brain adenosine concentration during hypoxia in rats. *Am. J. Physiol.* 241:H235-H242, 1981.
199. **Wray, S.** The outside-in story of pH, Ca<sup>2+</sup> and vascular tone. *J. Physiol. (Lond.)* 503:235, 1997.
200. **Young, R. S. K. and S. K. Yagel.** Cerebral physiological and metabolic effects of hyperventilation in the neonatal dog. *Ann. Neurol.* 16:337-342, 1984.
201. **Zobl, E. G., F. N. Talmers, R. C. Christensen, and L. J. Baer.** Effect of exercise on cerebral circulation and metabolism. *J. Appl. Physiol.* 20:1289-1293, 1965.

## **CHAPTER 2**

### **INDEXES OF FLOW AND CROSS-SECTIONAL AREA OF THE MIDDLE CEREBRAL ARTERY USING DOPPLER ULTRASOUND DURING HYPOXIA AND HYPERCAPNIA IN HUMANS**

Poulin, M.J. and P.A. Robbins (1996)  
*Stroke* **27**:2244-2250

## PREFACE

In humans, cerebral blood flow (CBF) can be assessed using various techniques, including transcranial Doppler ultrasound. However, while transcranial Doppler ultrasound has been widely used, most studies have elected to use an index of CBF that relates to beat averages of the velocities associated with the maximal frequencies of the Doppler shift. It is not always clear, especially in conditions of non-steady state, that changes in this index necessarily reflect changes in real flow. There are other indices that can be extracted from the Doppler spectrum and what remains unclear is whether they are all consistent.

In this Chapter, we examined the degree of consistency among three indices of CBF that can be extracted from the whole transcranial Doppler spectrum. The experiments were performed at rest. Step changes in end-tidal  $P_{\text{CO}_2}$  and  $P_{\text{O}_2}$  were used to provide the necessary dynamic and steady-state variations in CBF.

## DECLARATION

The work presented in this chapter was carried out over a two year period in the University Laboratory of Physiology. This study was conceived by my supervisor, Professor Peter Robbins. It was designed and planned by Professor Robbins and myself. I carried out the experiments and the data analysis. Professor Robbins and I wrote the resulting paper. Results of this study were presented at the 6<sup>th</sup> Meeting of the Neurosonology Research Group of the World Federation of Neurology (Salzburg, Austria) and were published in abstract form in the *Journal of Neuroimaging* (5(Suppl.2):S87, 1995).

# Indexes of Flow and Cross-sectional Area of the Middle Cerebral Artery Using Doppler Ultrasound During Hypoxia and Hypercapnia in Humans

Marc J. Poulin, BPHE, MA, PhD; Peter A. Robbins, MA, DPhil, BM, BCh

**Background and Purpose** This study examined changes in cross-sectional area of the middle cerebral artery as assessed by changes in Doppler signal power during hypoxia and hypercapnia. In addition, it examined the degree of consistency among three indexes of cerebral blood flow and velocity: the velocity spectral outline ( $\bar{V}_p$ ), the intensity-weighted mean velocity ( $\bar{V}_{IWM}$ ), and an index of middle cerebral artery flow ( $P \cdot \bar{V}_{IWM}$ ).  $P \cdot \bar{V}_{IWM}$  was calculated as the product of  $\bar{V}_{IWM}$  multiplied by the total power signal. Power is proportional to cross-sectional area of the vessel; this calculation therefore allows for any changes in this variable.

**Methods** Four protocols were used, each repeated six times for six healthy adults aged  $20.8 \pm 1.7$  years (mean  $\pm$  SD). The first was a control protocol (A) with end-tidal  $PO_2$  ( $ETPO_2$ ) maintained at 100 mm Hg and  $ETPCO_2$  at 1 to 2 mm Hg above eucapnia throughout. The second was a hypoxic step protocol (B) with  $ETPO_2$  lowered from control values to 50 mm Hg for 20 minutes. The third was a hypercapnic step protocol (C) with  $ETPCO_2$  elevated from control by 7.5 mm Hg for 20 minutes. The fourth was a combined hypoxic and hypercapnic step protocol (D) lasting 20 minutes. A dynamic end-tidal forcing system was used to control  $ETPCO_2$  and  $ETPO_2$ . Doppler data were collected and stored every 10 milliseconds, and mean values were determined later on a beat-by-beat basis.  $\bar{V}_p$ ,  $\bar{V}_{IWM}$ , power, and  $P \cdot \bar{V}_{IWM}$  were

expressed as a percentage of the average value over a 3-minute period before the step.

**Results** In protocols A and B, there were no changes in power and there were no differences between  $\bar{V}_p$ ,  $\bar{V}_{IWM}$ , and  $P \cdot \bar{V}_{IWM}$ . In C, at the relief from hypercapnia, there was a transient nonsignificant increase in power and a transient nonsignificant decrease in both  $\bar{V}_p$  and  $\bar{V}_{IWM}$  compared with  $P \cdot \bar{V}_{IWM}$ . In D, during the stimulus period,  $\bar{V}_p$  was significantly higher than  $\bar{V}_{IWM}$  (paired *t* test,  $P < .05$ ), but both indexes were not different from  $P \cdot \bar{V}_{IWM}$ . In the period that followed relief from hypoxia and hypercapnia, the Doppler power signal was significantly increased by 3.8%. During this period,  $\bar{V}_p$  and  $\bar{V}_{IWM}$  were significantly lower than  $P \cdot \bar{V}_{IWM}$ .

**Conclusions** At the levels of either hypoxia or hypercapnia used in this study, there were no changes in cross-sectional area of the middle cerebral artery, and changes in both  $\bar{V}_p$  and  $\bar{V}_{IWM}$  accurately reflect changes in  $P \cdot \bar{V}_{IWM}$ . With combined hypoxia and hypercapnia, however, at the relief from the stimuli when there is a very large and rapid decrease in  $P \cdot \bar{V}_{IWM}$ , power is increased, suggesting an increase in the cross-sectional area. During this period, changes in  $\bar{V}_p$  and  $\bar{V}_{IWM}$  underestimate the changes in  $P \cdot \bar{V}_{IWM}$ . (*Stroke*. 1996;27:2244-2250.)

**Key Words** • cerebral blood flow • hypercapnia • hypoxia • ultrasonics

Transcranial Doppler ultrasound has been used to measure MCA blood flow velocities, which in turn may be used to provide some sort of index of MCA flow. The index that has most commonly been used has been the mean of the velocities associated with the maximal frequency of the Doppler shift ( $\bar{V}_p$ ), which, if the flow is laminar, will be proportional to the axial flow velocity (equal to the axial flow velocity if the angle of insonation is zero). Under conditions of laminar flow in a rigid tube, axial flow velocity is proportional to true flow. However, if the flow is complex, then the possibility exists that the relationship between  $\bar{V}_p$  and true flow may not be linear.

One way of circumventing the above problem is to use the entire velocity spectrum and calculate a  $\bar{V}_{IWM}$ . Because the intensity of the power spectrum at any velocity

should be related directly to the number of ultrasound scatterers (ie, red blood cells) moving at that velocity,<sup>1</sup> for flow in a rigid tube  $\bar{V}_{IWM}$  should provide a signal proportional to overall flow regardless of the complexity of the flow pattern.

A further problem relates to the fact that the MCA cannot be considered to be a rigid tube, but neither  $\bar{V}_p$  nor  $\bar{V}_{IWM}$  can be considered to remain proportional to blood flow if the area of the vessel is changing. To overcome this, it is possible to use the total power of the reflected Doppler signal as a measure of the total number of ultrasound scatterers. If the sample remains of constant depth and the power and position of the insonating beam are unchanged, then the Doppler power provides an index of cross-sectional area. An index of flow that takes variations in cross-sectional area into account may be calculated as the product of total power and the intensity-weighted mean velocity ( $P \cdot \bar{V}_{IWM}$ ).

The purpose of the present study was to examine changes in Doppler signal power (as an index of cross-sectional area of the MCA), as well as the degree of consistency among the three indexes for flow, namely,  $\bar{V}_p$ ,  $\bar{V}_{IWM}$ , and  $P \cdot \bar{V}_{IWM}$ . Data are taken from a previous study of the dynamics of the response of the cerebral circulation

Received June 5, 1996; final revision received August 13, 1996; accepted August 13, 1996.

From the University Laboratory of Physiology, University of Oxford (UK).

Correspondence to Peter A. Robbins, MA, DPhil, BM, BCh, University Laboratory of Physiology, Parks Rd, Oxford OX1 3PT, UK. E-mail peter.robbins@physiol.ox.ac.uk.

© 1996 American Heart Association, Inc.

**Selected Abbreviations and Acronyms**

MCA	= middle cerebral artery
$P \cdot \bar{V}_{IWM}$	= flow index (product of total power and intensity-weighted mean velocity)
ETPCO <sub>2</sub>	= end-tidal PCO <sub>2</sub>
ETPO <sub>2</sub>	= end-tidal PO <sub>2</sub>
$\bar{V}_{IWM}$	= intensity-weighted mean flow velocity
$\bar{V}_p$	= flow velocity spectral outline

to step changes in ETPCO<sub>2</sub> and ETPO<sub>2</sub>,<sup>2</sup> which provide the necessary variations in cerebral blood flow.

**Subjects and Methods**

This study involved six young adults. The study requirements were fully explained to all participants, with each giving informed consent before participation in the study. The research was approved by the Central Oxford Research Ethics Committee. Participants were not taking any medication, and none of the participants had a history of cardiovascular, cerebrovascular, or respiratory disease.

**Protocols**

Each participant visited the laboratory on six or seven occasions, each lasting 4 to 5 hours. On each visit, one repetition of each of four protocols was performed in a randomly assigned order, with each repetition lasting approximately 40 minutes. Before the experiments were started, room air measurements of resting Doppler signals and ETPCO<sub>2</sub> were collected. The subject's natural ETPCO<sub>2</sub> was measured using a nasal catheter, which disturbs quiet breathing less than a mouthpiece and nose clip arrangement.

The four protocols are shown in Fig 1 with the actual data obtained. For the control protocol (Fig 1A), ETPO<sub>2</sub> was maintained at 100 mm Hg and ETPCO<sub>2</sub> at 1 to 2 mm Hg above the subject's normal value for 30 minutes. Each of the test protocols started with a short 6- to 7-minute period during which ETPO<sub>2</sub>

was maintained at 100 mm Hg and ETPCO<sub>2</sub> at 1 to 2 mm Hg above the subject's natural value as determined that day. Then ETPO<sub>2</sub> and/or ETPCO<sub>2</sub> were altered rapidly (over one or two breaths) to a new set of desired levels, according to each protocol described below, and maintained constant for 20 minutes. Finally, ETPO<sub>2</sub> and/or ETPCO<sub>2</sub> were returned (again within one or two breaths) to their initial euoxic and near-eucapnic values and maintained constant for a further 10 minutes. For the hypoxic protocol (Fig 1B), ETPO<sub>2</sub> was lowered to 50 mm Hg while ETPCO<sub>2</sub> was continually maintained at 1 to 2 mm Hg above the subject's normal value. For the hypercapnic protocol (Fig 1C), ETPO<sub>2</sub> was continued at 100 mm Hg while ETPCO<sub>2</sub> was elevated by 7.5 mm Hg (ie, between 8.5 and 9.5 mm Hg above the subject's normal value). Finally, for the protocol combining hypoxia with hypercapnia (Fig 1D), ETPO<sub>2</sub> was lowered to 50 mm Hg and ETPCO<sub>2</sub> was elevated by 7.5 mm Hg.

This study used the technique of dynamic end-tidal forcing to regulate the end-tidal gas tensions accurately and to generate the desired rapid steps in end-tidal composition as required.<sup>3</sup> The apparatus and technique have been described previously.<sup>2,4,5</sup>

**Apparatus and Technique for Measurement of Cerebral Blood Flow**

A 2-MHz pulsed Doppler ultrasound system (PCDop 842, SciMed) was used to measure back-scattered Doppler signals from the right MCA. The Doppler system was adapted to make the Doppler signals (maximum and intensity-weighted mean Doppler frequency shifts and total power) available as analogue signals. These were updated each time a new spectrum was calculated (every 10 milliseconds). The signals were sampled every 10 milliseconds using a data acquisition package (DAQWare, National Instruments) running on another computer. These signals were saved for later analysis.

The MCA was identified by an insonation pathway through the right temporal window just above the zygomatic arch using standard search techniques that have been described previously.<sup>6,7</sup> Ultrasound gel was applied to the subject's skin and hair at the temporal window and to the probe before the experimenter pro-

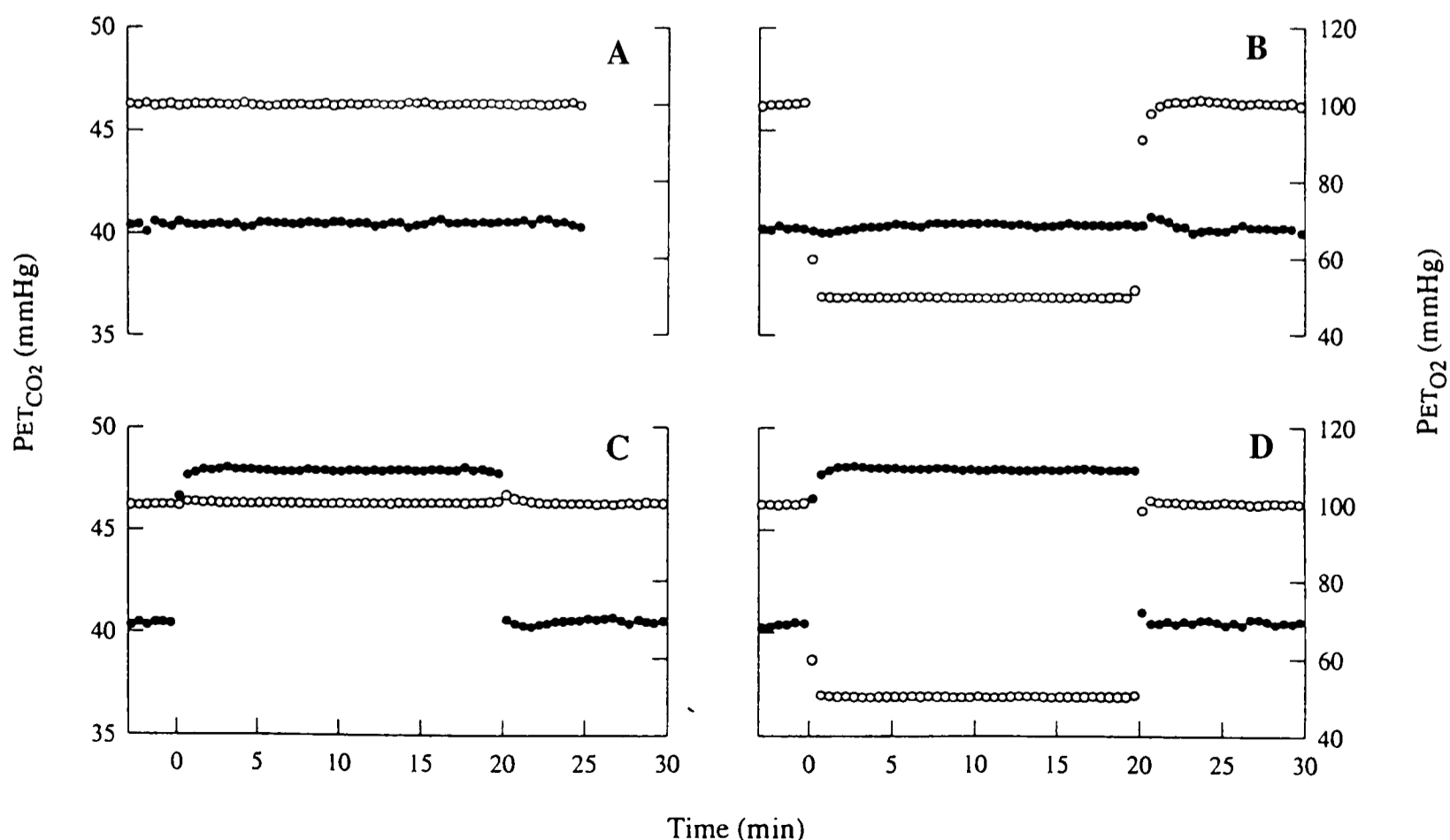


FIG 1. Ensemble averages for the group ( $n=6$  subjects) of the time-related changes in ETPO<sub>2</sub> (PETO<sub>2</sub>; ○) and ETPCO<sub>2</sub> (PETCO<sub>2</sub>; ●). Panels show protocols for control (A), hypoxia (B), hypercapnia (C), and combined hypoxia and hypercapnia (D). Each symbol represents a 30-second mean.

ceeded to locate and identify the main segment of the MCA. Optimization of the Doppler signals from the MCA was performed by varying the sample volume depth in incremental steps and at each depth varying the angle of insonation to obtain the best quality signals for the Doppler frequency shifts that corresponded to the maximum power signal. Ultrasound gel was then reapplied sparingly to both the insonation site and the probe before the probe was securely positioned in a headband device (Müller and Moll Fixation, Nicolet Instruments Ltd) to ensure optimal insonation position and angle for the duration of the experiment.

## Analysis

### Averaging Within Experimental Sessions

The data for MCA blood flow comprise one observation each for  $\bar{V}_P$ ,  $\bar{V}_{IWM}$ , and power every 10 milliseconds.  $P \cdot \bar{V}_{IWM}$  was calculated every 10 milliseconds as the product of  $\bar{V}_{IWM}$  and power, thus allowing for any systematic change in diameter throughout the cardiac cycle. The data for  $\bar{V}_P$ ,  $\bar{V}_{IWM}$ , power, and  $P \cdot \bar{V}_{IWM}$  were averaged over each heartbeat to give beat-by-beat values. The beat-by-beat data were further averaged to give one value every 15 seconds. Finally, for the statistical analysis, the 15-second data were averaged to give three 3-minute values for baseline (−3 to 0 minutes), stimulus (+17 to +20 minutes), and recovery (+27 to +30 minutes) periods.

In addition to the absolute values, normalized beat-by-beat values were calculated for  $\bar{V}_P$ ,  $\bar{V}_{IWM}$ , power, and  $P \cdot \bar{V}_{IWM}$ . The beat-by-beat data during the 3-minute period immediately before the onset of the stimulus were averaged, and this value was used as a baseline. The 3-minute baseline period was normalized to 100% and used to calculate the percent change over time in these variables (on a beat-by-beat basis) over the rest of the experimental record. The beat-by-beat normalized data were then further averaged to give one value every 15 seconds. Again, the 15-second data were averaged to give three 3-minute values for baseline, stimulus, and recovery periods.

### Statistics

To examine changes in Doppler signal power within each of the experimental protocols, the percent changes in Doppler power signal values obtained during the 3-minute stimulus and recovery periods were compared with the 3-minute baseline value (ie, 100%). Furthermore, to examine the degree of consistency among three indexes of cerebral blood flow, comparisons were made among the values obtained for  $\bar{V}_P$ ,  $\bar{V}_{IWM}$ , and  $P \cdot \bar{V}_{IWM}$  during the stimulus and recovery periods. Thus, paired *t* tests were used to (1) compare changes in Doppler power, (2) compare  $\bar{V}_P$  with  $\bar{V}_{IWM}$ , and (3) compare  $\bar{V}_P$  and  $\bar{V}_{IWM}$  with  $P \cdot \bar{V}_{IWM}$ . Because several pairwise comparisons were performed within each protocol, a Bonferroni correction was applied to make allowance for multiple comparisons. The overall level of statistical significance was taken as  $P < .05$ , which, with the Bonferroni correction, equates to a level of significance of  $P < .0083$  for each of the individual comparisons when six comparisons are made.

## Results

### Subjects

The average age of the six subjects was  $20.8 \pm 1.7$  years (mean  $\pm$  SD), average height was  $183.3 \pm 5.0$  cm, and average weight was  $74.2 \pm 10.0$  kg. None had a history of cardiovascular or respiratory disease, and all had normal systolic ( $116.3 \pm 6.3$  mm Hg), diastolic ( $79.0 \pm 4.0$  mm Hg), and mean arterial ( $91.4 \pm 3.7$  mm Hg) blood pressure. The average insonation depth (the distance from the probe to the start of the Doppler sample volume for detecting signals from the MCA) was  $5.02 \pm 0.03$  cm. Small variations in depth between subjects are attributed to differences in skull size.<sup>7</sup> The air-breathing data for each subject are listed in Table 1.

### Doppler Power Signal During Hypoxia and Hypercapnia

Ensemble averages for the group means for the normalized Doppler power signal are shown in Fig 2. The data in Fig 2 were obtained by first ensemble averaging all repetitions of each protocol in a single subject over the 15-second periods and then ensemble averaging the responses of all six subjects. The group means for the 3-minute averages for the normalized Doppler power are shown in Table 2. In the control and hypoxic protocols, no changes were apparent in the Doppler power signal from the baseline value of 100% (Fig 2A and 2B). This was confirmed on the three averages by *t* tests. In hypercapnia, at the relief from the stimulus, there appeared to be a small increase in the power signal (Fig 2C), but this was not significant as assessed by *t* test. In combined hypoxia and hypercapnia, during the recovery period from the stimuli, the Doppler power signal increased by 3.8% (Fig 2D), and this increase was significant ( $P < .001$ , *t* test).

### Comparison of $\bar{V}_P$ With $\bar{V}_{IWM}$

Ensemble averages for the group means for the normalized velocities are shown in Fig 2. The data in Fig 2 were obtained by first ensemble averaging all repetitions of each protocol in a single subject over 15-second periods and then ensemble averaging the responses among the six subjects. The group means for the 3-minute averages are presented as absolute values for the 3-minute means of  $\bar{V}_P$  and  $\bar{V}_{IWM}$  (ie, in centimeters per second) in Table 2 and as normalized responses in Table 3. In general, the group responses show that the temporal profiles for  $\bar{V}_P$  and  $\bar{V}_{IWM}$  appear to be very similar. One exception is noted in combined hypoxia and hypercapnia:  $\bar{V}_P$  and  $\bar{V}_{IWM}$  appeared to be different during the stimulus period (Fig 2D). When this difference was assessed statistically (paired *t* test), it was significant ( $P < .001$ ).

### Comparison of $\bar{V}_P$ and $\bar{V}_{IWM}$ With $P \cdot \bar{V}_{IWM}$

Ensemble averages for the group means for the normalized flow index ( $P \cdot \bar{V}_{IWM}$ ) are shown in Fig 2. The data for  $P \cdot \bar{V}_{IWM}$  were obtained by first ensemble averaging all repetitions of each protocol in a single subject over 15-second periods and then ensemble averaging the responses among the six subjects. The group means for the 3-minute averages are presented in Table 3. In general, the group responses show that the temporal profiles for  $\bar{V}_P$  and  $\bar{V}_{IWM}$  appear to be very similar to those for  $P \cdot \bar{V}_{IWM}$ . Exceptions are noted in hypercapnia and in combined hypoxia and hypercapnia: during the periods of recovery,  $\bar{V}_P$  and  $\bar{V}_{IWM}$  appear to underestimate  $P \cdot \bar{V}_{IWM}$  (Fig 2C and 2D). These differences correspond to the changes in power that have been noted above. In hypercapnia, these differences among  $\bar{V}_P$ ,  $\bar{V}_{IWM}$ , and  $P \cdot \bar{V}_{IWM}$  were not significant as assessed from the 3-minute means (Table 3). However, in combined hypoxia and hypercapnia, the 3-minute means for  $\bar{V}_P$  and  $\bar{V}_{IWM}$  were significantly lower than for  $P \cdot \bar{V}_{IWM}$  (Table 3).

To highlight further the effects of changes in Doppler power on the Doppler velocities, we calculated the ratios between the normalized velocities and  $P \cdot \bar{V}_{IWM}$  (ie,  $\bar{V}_P / P \cdot \bar{V}_{IWM}$  and  $\bar{V}_{IWM} / P \cdot \bar{V}_{IWM}$ ). If the changes in the various indexes of MCA flow match, then the value of this index should be one; this index provides a useful graphic illustration of variations among the indexes throughout the ex-

TABLE 1. Air Breathing Data for Each Subject

n	Subject	$\bar{V}_P$ , cm/s	$\bar{V}_{IWM}$ , cm/s	ETPCO <sub>2</sub> , mm Hg	ETPO <sub>2</sub> , mm Hg	Heart Rate, beats/min
24	940	56.4±3.5	35.3±2.2	41.2±0.7	99.6±0.7	59.3±6.7
21	959	49.5±5.7	31.7±4.1	40.1±0.8	99.4±0.9	68.3±6.0
24	964	59.0±3.5	35.5±3.0	42.3±1.1	100.1±0.4	65.1±5.6
24	966	64.0±3.5	40.3±3.0	40.7±1.0	100.0±0.5	62.0±5.0
24	967	63.3±6.1	45.9±5.0	39.5±1.0	100.2±0.5	76.5±8.1
24	971	50.7±4.6	35.2±3.4	38.1±1.1	100.0±0.6	64.2±8.4
141	Mean±SD	57.3±7.2	37.4±5.7	40.3±1.7	99.9±0.6	65.9±8.6

perimental periods, including the transients. Ensemble averages for the group means for these ratios are shown in Fig 2. In the control and hypoxic protocols, there were no apparent changes in  $\bar{V}_P/P \cdot \bar{V}_{IWM}$  and  $\bar{V}_{IWM}/P \cdot \bar{V}_{IWM}$  (Fig 2A and 2B). In hypercapnia, at the relief from the stimulus, transient decreases in  $\bar{V}_P/P \cdot \bar{V}_{IWM}$  and  $\bar{V}_{IWM}/P \cdot \bar{V}_{IWM}$  are observed (Fig 2C). In combined hypoxia and hypercapnia, in the recovery period when Doppler power was signifi-

cantly increased,  $\bar{V}_P/P \cdot \bar{V}_{IWM}$  and  $\bar{V}_{IWM}/P \cdot \bar{V}_{IWM}$  are lower than unity (Fig 2D).

### Discussion

#### Major Findings

This study used the technique of transcranial Doppler ultrasound to detect changes in cross-sectional area of the

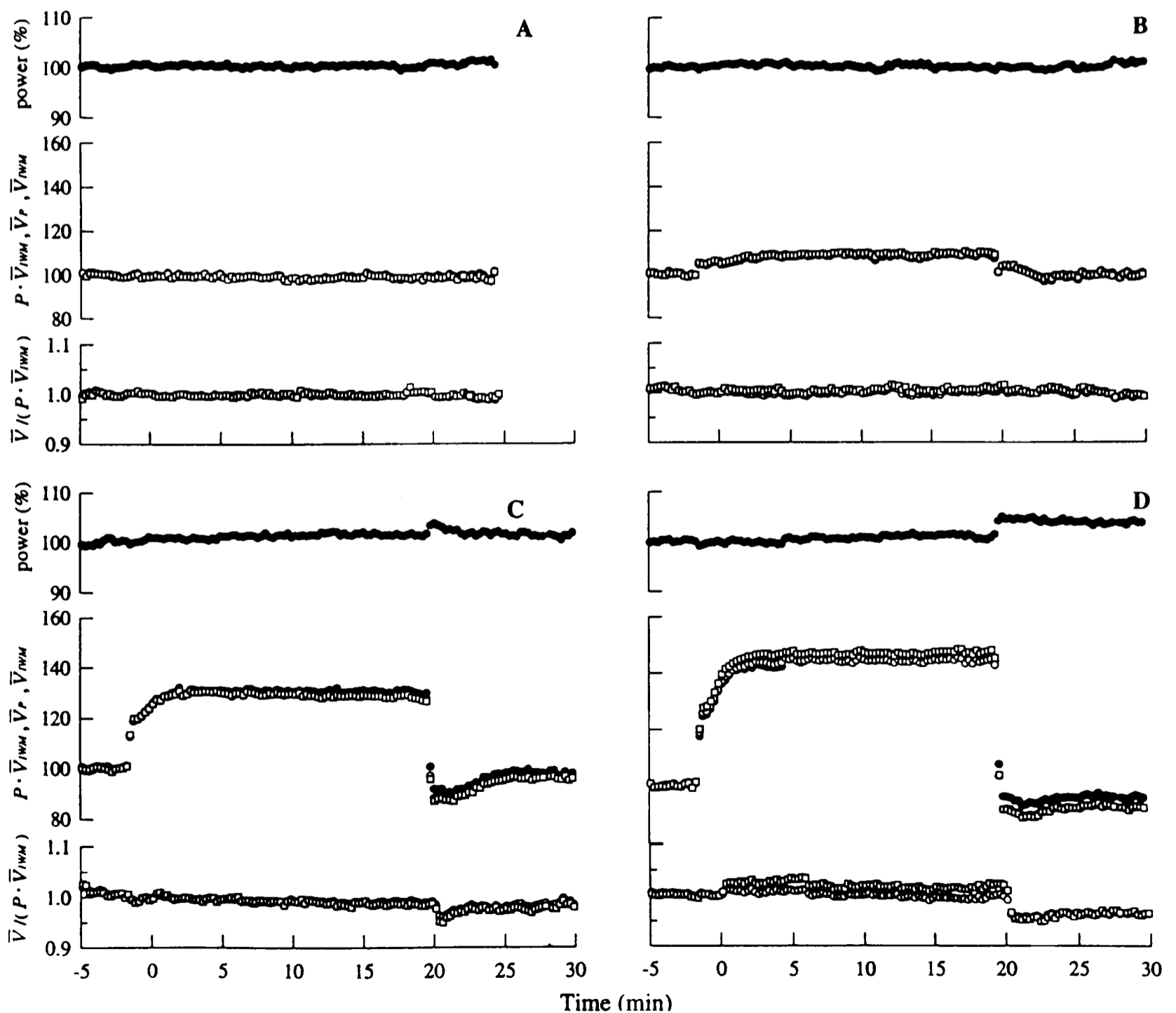


FIG 2. Ensemble averages for the group (n=6 subjects) for power, MCA flow index, velocities and ratio between the flow index, and velocities during control (A), hypoxia (B), hypercapnia (C), and combined hypoxia and hypercapnia (D). For each panel, the top graph shows results for power; the middle graph shows the results for  $P \cdot \bar{V}_{IWM}$  (●),  $\bar{V}_P$  (□), and  $\bar{V}_{IWM}$  (○). The bottom graph shows the ratios  $\bar{V}_P/P \cdot \bar{V}_{IWM}$  (□) and  $\bar{V}_{IWM}/P \cdot \bar{V}_{IWM}$  (○). Data are expressed as a percentage of the average value for the 3-minute period preceding time zero. Each symbol represents a 15-second mean.

TABLE 2. Changes in Velocities and Power During Hypoxia and Hypercapnia

Subject Group	$\bar{V}_p$ , cm/s			$\bar{V}_{IWM}$ , cm/s			Power, % Change		
	Baseline	Peak	Recovery	Baseline	Peak	Recovery	Baseline	Peak	Recovery
Control (n=35)	58.0±7.7	57.3±7.6	57.1±7.5*	38.1±6.3	37.6±6.3	37.4±6.2*	100.0±0.2	100.2±4.4	100.8±4.3
Hypoxia (n=35)	56.9±6.8	62.3±7.8*	56.7±6.7	37.3±5.3	40.6±6.0*	37.1±5.1	100.0±0.1	99.9±3.7	100.3±3.7
Hypercapnia (n=35)	57.6±8.2	73.8±10.7*	55.1±7.9*	37.7±6.5	48.3±7.7*	36.2±5.8*	100.0±0.1	101.1±6.3	101.4±6.8
Hypoxia and hypercapnia (n=36)	56.7±6.0	83.6±12.8*	52.7±7.2*	36.6±4.8	52.8±9.2*	33.9±5.2*	100.0±0.2	101.0±6.1	103.8±5.6*

Baseline indicates -3 to 0; Peak, 17 to 20; and Recovery, 27 to 30. Values are mean±SD.

\*Significantly different from baseline value at  $P<.05$ .

MCA, as assessed by changes in Doppler power, during hypoxia and hypercapnia in humans. Additionally, this study assessed the degree of consistency among three indexes of cerebral blood flow obtained with transcranial Doppler ultrasound during hypoxia and hypercapnia. Two new findings are reported. First, at the levels of either hypoxia or hypercapnia alone used in this study, there was very little change in MCA cross-sectional area. However, in the combined hypoxic and hypercapnic protocol, at the relief of the stimuli when there was a very large and rapid decrease in cerebral blood flow, Doppler signal power was increased by 3.8%, suggesting an increase in the cross-sectional area of the MCA. Second, at the levels of stimulation associated with either hypoxia or hypercapnia alone, changes in  $\bar{V}_p$  and  $\bar{V}_{IWM}$  (and  $P \cdot \bar{V}_{IWM}$ ) were all very similar. However, in the combined hypoxic and hypercapnic protocol, the change in  $\bar{V}_p$  was significantly greater than the change in  $\bar{V}_{IWM}$ . Additionally, at the relief of the stimuli when Doppler signal power was increased, the changes in  $\bar{V}_p$  and  $\bar{V}_{IWM}$  significantly underestimated the change in  $P \cdot \bar{V}_{IWM}$ .

### Comparison With Other Measures of Cross-sectional Area Change

Evidence is now available from several studies in humans to suggest that various interventions that result in steady-state changes in cerebral hemodynamics are associated with only small changes in the caliber of the larger cerebral vessels.

Studies using transcranial Doppler ultrasound have generally taken one of two approaches to address the issue of whether, with various interventions, there are changes in caliber of large cerebral vessels such as the MCA. First, studies have correlated changes in  $\bar{V}_p$  with more direct

indexes of changes in cerebral blood flow. Results from these studies show good agreement between changes in  $\bar{V}_p$  in the MCA and the change in  $\bar{V}_p$  in the internal carotid artery (combined with B-mode measurements of the diameter of the internal carotid artery)<sup>8</sup> and between changes in  $\bar{V}_p$  in the MCA and changes in cerebral blood flow seen using techniques such as xenon washout,<sup>9</sup> single-photon emission CT,<sup>10</sup> and electromagnetic flowmeters<sup>11</sup> during hypercapnia, blood pressure variations, or acetazolamide injections.<sup>8,11,12</sup> Studies using the second approach have assessed changes in cross-sectional area as reflected by changes in Doppler power. Small changes in Doppler power have been reported in response to hypercapnia and hypocapnia,<sup>13</sup> step decreases in arterial blood pressure,<sup>14,15</sup> orthostasis,<sup>16</sup> and anesthetic agents.<sup>17</sup>

The present study is the first to provide continuous beat-by-beat measurements of Doppler power during periods of sustained hypoxia and hypercapnia. Our results show no changes in Doppler power during "pure" hypoxia and hypercapnia and only small changes in Doppler power during combined hypoxia and hypercapnia. Thus, our findings are consistent with the suggestion that the caliber of the larger cerebral vessels changes very little when cerebral blood flow is moderately increased. Our result of an unchanged Doppler power during hypercapnia is different from that of Müller and Casty,<sup>13</sup> who reported a 20% increase in Doppler power during hypercapnia (using a rebreathing technique). However, Müller and Casty also reported a large standard deviation in Doppler power ( $\pm 18\%$  versus  $\pm 6\%$  in the present study; Table 2), and it is unclear whether any attempts were made to deal with some of the potential difficulties associated with the use of Doppler power (ie, the need for several repetitions to ensure a high signal-to-noise ratio).

TABLE 3. Percent Changes in Velocities and Flow Index During Hypoxia and Hypercapnia

Subject Group	$\bar{V}_p$ , % Change			$\bar{V}_{IWM}$ , % Change			$P \cdot \bar{V}_{IWM}$ , % Change		
	Baseline	Peak	Recovery	Baseline	Peak	Recovery	Baseline	Peak	Recovery
Control (n=35)	100.0±0.1	98.9±3.0	98.6±3.3*	100.0±0.1	98.8±3.5	98.4±4.0*	100.0±0.3	99.0±5.3	99.3±6.3
Hypoxia (n=35)	100.0±0.1	109.5±5.4*	99.7±4.1	100.0±0.1	108.8±5.6*	99.5±5.2	100.0±0.1	108.7±7.2*	99.9±6.7
Hypercapnia (n=35)	100.0±0.1	128.4±10.8*	95.8±7.4*	100.0±0.1	128.9±12.8*	96.4±8.6*	100.0±0.1	130.1±14.3*	97.9±11.5
Hypoxia and hypercapnia (n=36)	100.1±0.2	147.4±14.0*†	93.0±8.0*‡	100.1±0.3	144.2±13.9*	92.8±9.2*‡	100.1±0.4	145.0±15.0*	96.3±10.6*

Baseline indicates -3 to 0; Peak, 17 to 20; and Recovery, 27 to 30. Values are mean±SD.

\*Significantly different from baseline value at  $P<.05$ .

†Significantly different from peak value for  $\bar{V}_{IWM}$  at  $P<.05$ .

‡Significantly different from recovery value for  $P \cdot \bar{V}_{IWM}$  at  $P<.05$ .

The findings from the above studies generally agree with those of more invasive approaches that have been used to assess changes in cross-sectional area of the large cerebral vessels. Giller et al<sup>18</sup> measured the diameters of human cerebral arteries during craniotomies under moderate changes in mean blood pressure and ETPCO<sub>2</sub> and reported small diameter changes (3% to 4%) in the large cerebral arteries (including the main branch of the MCA). In another study, Huber and Handa<sup>19</sup> used contrast-agent angiography and found a 3.8% increase in vessel diameter in response to hypercapnia.

Thus, the general consensus from the studies so far published is that although changes in the vessel caliber of large cerebral vessels have been reported, the changes appear to be quite small. Our results are in agreement with this and therefore provide some reassurance that studies reporting the changes in velocities using transcranial Doppler ultrasound provide indexes of changes in underlying flow that are not distorted through changes in cross-sectional area of the vessel.

#### $\bar{V}_P$ , $\bar{V}_{IWM}$ , and $P \cdot \bar{V}_{IWM}$ as Measures of Cerebral Blood Flow

The results from this study indicate that there is very little difference among these indexes when assessing cerebral blood flow responses to modest stimuli. Given this, the use of either  $\bar{V}_P$  or  $\bar{V}_{IWM}$  has considerable advantages over the use of  $P \cdot \bar{V}_{IWM}$ . First, an absolute value can be ascribed to the velocities, whereas the reflected power depends entirely on the power and other properties of the insonating beam. The only caveat to this statement is that the values for velocities will always be somewhat lower than the true values because the insonating beam will not be completely axial. However, the effect of this is likely to be small (eg, an angle of insonation of 30° difference gives an error of <13%, and in general the true value for this angle is likely to be substantially less than this). Second, the position and fixation of the probe are far less critical for successful measurement of velocities than for power.

There are some additional disadvantages associated with the use of  $P \cdot \bar{V}_{IWM}$  as a flow index. First, small movements of the probe (and therefore sample volume) can cause some changes in the reflected power signal, which would then be wrongly interpreted as changes in flow. In the present study, this potential problem was avoided by always taking extreme care to identify accurately the center of the insonated vessel by maximizing the Doppler power signal and to secure firmly the probe and headpiece to minimize any noise in the power signal due to probe movements. Second, each protocol was repeated several times, and the results for each protocol were averaged, thereby minimizing any effect due to noise artifact, as well as the random error associated with the measurement of blood flow using Doppler ultrasound.<sup>20</sup> Third, the use of  $P \cdot \bar{V}_{IWM}$  requires the need to optimize and maximize both the reflected Doppler power signal and  $\bar{V}_P$  (or  $\bar{V}_{IWM}$ ), and this can add a significant amount of time to assessments of cerebral hemodynamics with transcranial Doppler ultrasound. Despite these difficulties in measuring power, it can provide a useful check on whether there are changes in cross-sectional area in situations in which this might be suspected. In such conditions, the use of  $P \cdot \bar{V}_{IWM}$  is preferable because this index should result in a constant estimation of flow.<sup>14</sup>

Turning to the two measurements for velocity,  $\bar{V}_P$  has been used much more widely than  $\bar{V}_{IWM}$ . The resting absolute values for  $\bar{V}_P$  in this study (Table 2) are very similar to those published elsewhere,<sup>6,21,22</sup> but for  $\bar{V}_{IWM}$  we have not managed to find published data for comparison. Most of the studies using transcranial Doppler ultrasound have elected to use  $\bar{V}_P$  instead of  $\bar{V}_{IWM}$  or  $P \cdot \bar{V}_{IWM}$  as an index for flow because it has been suggested that  $\bar{V}_P$  is easier to measure accurately than  $\bar{V}_{IWM}$ .<sup>9</sup> Indeed, to our knowledge, this is the first study to assess the relationship between  $\bar{V}_P$  and  $\bar{V}_{IWM}$  when cerebral blood flow is increased moderately during "pure" hypoxia or hypercapnia. Our results show that under such conditions both indexes accurately reflect changes in  $P \cdot \bar{V}_{IWM}$ . However, in combined hypoxia and hypercapnia, the change in  $\bar{V}_P$  was significantly larger than the change in  $\bar{V}_{IWM}$ .

Despite the widespread use of  $\bar{V}_P$ ,  $\bar{V}_{IWM}$  does involve fewer assumptions about the nature of the flow; furthermore, differences between the two indexes were detected experimentally in the combined stimulus protocol. Given the complex nature of the flow, it is difficult to say exactly why  $\bar{V}_P$  should change more than  $\bar{V}_{IWM}$ , but theoretically the change in  $\bar{V}_{IWM}$  is more likely to represent the true changes in flow. For established steady laminar flow in a rigid cylindrical tube, the ratio of  $\bar{V}_{IWM}$  to  $\bar{V}_P$  ( $\bar{V}_{IWM}/\bar{V}_P$ ) is 0.5. Our results in combined hypoxia and hypercapnia give a value for this ratio of 0.63. Assuming an MCA diameter in the region of 0.3 cm,<sup>23</sup> we can calculate Reynolds numbers in the region of 291 to 420 and 451 to 665 for  $\bar{V}_{IWM}$  and  $\bar{V}_P$ , respectively. Thus, the deviation from a ratio of 0.5 is likely to be due to bending of the flow at junctions, elastic walls, and nonsteady flow rather than any turbulence induced through a high Reynolds number (critical Reynolds number for turbulent flow is approximately 2000).

#### Summary

Results from the present study suggest that the caliber of the MCA does not change significantly under conditions of moderate hypoxia or hypercapnia alone; therefore,  $\bar{V}_P$  and  $\bar{V}_{IWM}$  appear to be acceptable as indexes of changes in cerebral blood flow. Further investigations are needed to evaluate the relationships between  $\bar{V}_P$ ,  $\bar{V}_{IWM}$ , and  $P \cdot \bar{V}_{IWM}$  to determine whether these results apply to other interventions. The use of the Doppler power signal will be useful in future investigations to assess conditions in which there are alterations in the caliber of the MCA.

#### Acknowledgments

This study was approved by the Central Oxford Research Ethics Committee. It was supported by the Wellcome Trust and by an MRC (Canada) postdoctoral research fellowship (Dr Poulin). We wish to acknowledge the skilled technical assistance from David O'Connor and the volunteers for their participation in the study.

#### References

1. Arts MGJ, Roevros JMIG. On the instantaneous measurement of blood flow by ultrasonic means. *Med Biol Eng.* 1972;10:23-34.
2. Poulin MJ, Liang P-J, Robbins PA. Dynamics of the cerebral blood flow response to step changes in end-tidal PCO<sub>2</sub> and PO<sub>2</sub> in humans. *J Appl Physiol.* 1996;81:1084-1095.
3. Swanson GD, Bellville JW. Step changes in end tidal CO<sub>2</sub>: methods and implications. *J Appl Physiol.* 1975;39:377-385.
4. Howson MG, Khamnei S, McIntyre ME, O'Connor DF, Robbins PA. A rapid computer controlled binary gas mixing system for studies in respiratory control. *J Physiol (Lond).* 1987;403:103P. Abstract.

5. Robbins PA, Swanson GD, Howson MG. A prediction correction scheme for forcing alveolar gases along certain time courses. *J Appl Physiol.* 1982;52:1353-1357.
6. Aaslid R, Markwalder T, Nornes H. Noninvasive transcranial Doppler ultrasound recording of flow velocity in basal cerebral arteries. *J Neurosurg.* 1982;57:769-774.
7. Padayachee TS, Kirkham FJ, Lewis RR, Gillard J, Hutchinson MCE, Gosling RG. Transcranial measurement of blood velocities in the basal cerebral arteries using pulsed Doppler ultrasound: a method of assessing the circle of Willis. *Ultrasound Med Biol.* 1986;12:5-14.
8. Kleiser B, Scholl D, Widder B. Doppler CO<sub>2</sub> and diamox test: decreased reliability by changes of the vessel diameter? *Cerebrovasc Dis.* 1995;5:397-402.
9. Sorteberg W, Lindegaard KF, Rootwelt K, Dahl A, Russell D, Nyberg-Hansen R, Nornes H. Blood velocity and regional blood flow in defined cerebral artery systems. *Acta Neurochir (Wien).* 1989;97:47-52.
10. Dahl A, Lindegaard KF, Russell D, Nyberg-Hansen R, Rootwelt K, Sorteberg W, Nornes H. A comparison of transcranial Doppler and cerebral blood flow studies to assess cerebral vasoreactivity. *Stroke.* 1992;23:15-19.
11. Lindegaard KF, Lundar T, Wiberg J, Sojberg D, Aaslid R, Nornes H. Variations in middle cerebral artery blood flow investigated with non-invasive transcranial blood velocity measurements. *Stroke.* 1987;18:1025-1030.
12. Bishop CC, Powell S, Rutt D, Browse NL. Transcranial Doppler measurement of middle cerebral artery blood flow velocity: a validation study. *Stroke.* 1986;17:913-915.
13. Müller HR, Casty M. CO<sub>2</sub> reactivity of middle cerebral artery truncal caliber. *J Ultrasound Med.* 1991;10:S47. Abstract.
14. Aaslid R, Newell DW, Stooss R, Sorteberg W, Lindegaard KF. Assessment of cerebral autoregulation dynamics from simultaneous arterial and venous transcranial Doppler recordings in humans. *Stroke.* 1991;22:1148-1154.
15. Aaslid R, Lindegaard KF, Sorteberg W, Nornes H. Cerebral autoregulation dynamics in humans. *Stroke.* 1989;20:45-52.
16. Müller HR, Casty M, Moll R, Zehnder R. Response of middle cerebral artery volume flow to orthostasis. *Cerebrovasc Dis.* 1991;1:82-89.
17. Schregel W, Schaefermeyer H, Sihle-Wissel M, Klein R. Transcranial Doppler sonography during isoflurane/N<sub>2</sub>O anaesthesia and surgery: flow velocity, "vessel area" and "volume flow." *Can J Anaesth.* 1994;41:607-612.
18. Giller CA, Bowman G, Dyer H, Mootz L, Krippner W. Cerebral arterial diameters during changes in blood pressure and carbon dioxide during craniotomy. *Neurosurgery.* 1993;32:737-742.
19. Huber P, Handa J. Effect of contrast material, hypercapnia, hyperventilation, hypertonic glucose and papaverine on the diameter of the cerebral arteries: angiographic determination in man. *Invest Radiol.* 1967;2:17-32.
20. Gill RW. Measurement of blood flow by ultrasound: accuracy and sources of error. *Ultrasound Med Biol.* 1985;11:625-641.
21. Martin PJ, Evans DH, Naylor AR. Measurement of blood flow velocity in the basal cerebral circulation: advantages of transcranial color-coded sonography over conventional transcranial Doppler. *J Clin Ultrasound.* 1995;23:21-26.
22. Lindegaard KF, Bakke SJ, Grolimund P, Aaslid R, Huber P, Nornes H. Assessment of intracranial hemodynamics in carotid artery disease by transcranial Doppler ultrasound. *J Neurosurg.* 1985;63:890-898.
23. du Boulay GH, Symon L. The anaesthetist's effect upon the cerebral arteries. *Proc R Soc Med.* 1971;64:77-80.

## **CHAPTER 3**

### **DYNAMICS OF THE CEREBRAL BLOOD FLOW RESPONSE TO STEP CHANGES IN END-TIDAL CO<sub>2</sub> AND O<sub>2</sub> IN HUMANS**

Poulin, M.J., P.-J. Liang and P.A. Robbins (1996)  
*J. Appl. Physiol.* **81**:1084-1095

## PREFACE

Previous studies in humans have established that cerebral blood flow is increased by hypoxia and hypercapnia. However, an accurate description of the dynamics of the alterations in cerebral blood flow to changes in arterial CO<sub>2</sub> and O<sub>2</sub> has not yet been provided. This has been due, in large part, to limitations with existing techniques. This Chapter describes how we combined two techniques, to overcome the existing limitations, and to examine the dynamic response of the cerebral vasculature to hypoxia and hypercapnia. Transcranial Doppler ultrasound was used to provide a suitable time resolution for assessing cerebral blood flow, while the technique of dynamic end-tidal forcing was used to provide accurate and continuous control over arterial (end-tidal) P<sub>CO2</sub> and P<sub>O2</sub>. In order to quantify the dynamics of the response, a model was fit to the data to provide gain terms and time-constants for the responses to the onset and relief of hypoxia and hypercapnia.

## DECLARATION

The work presented in this chapter was carried out over a two-year period in the University Laboratory of Physiology. This study was conceived by Professor Peter Robbins and was designed and planned by Professor Robbins and myself. I carried out the experiments and the data analysis. Dr. Pei-Ji Liang helped with the mathematical modelling. Professor Robbins and I wrote the resulting paper. Results of this study were presented at The Physiological Society Meetings (Oxford, England) and were published in abstract form in the *Journal of Physiology* (487:176P, 1995).

# Dynamics of the cerebral blood flow response to step changes in end-tidal $\text{PCO}_2$ and $\text{PO}_2$ in humans

M. J. POULIN, P.-J. LIANG, AND P. A. ROBBINS

*University Laboratory of Physiology, Oxford OX1 3PT, United Kingdom*

**Poulin, M. J., P.-J. Liang, and P. A. Robbins.** Dynamics of the cerebral blood flow response to step changes in end-tidal  $\text{PCO}_2$  and  $\text{PO}_2$  in humans. *J. Appl. Physiol.* 81(3): 1084–1095, 1996.—This study examined the dynamics of the cerebral blood flow response to hypoxia and hypercapnia in humans. Middle cerebral artery blood flow (MCAF) was assessed continuously using transcranial Doppler ultrasound. MCAF was calculated on a beat-by-beat basis as the product of the intensity-weighted mean velocity and the total power of the reflected signal. End-tidal  $\text{PCO}_2$  ( $\text{PET}_{\text{CO}_2}$ ) and  $\text{PO}_2$  ( $\text{PET}_{\text{O}_2}$ ) were controlled using a dynamic end-tidal forcing system. Six repeats of each of four protocols were administered to six subjects. The first was a control protocol with  $\text{PET}_{\text{O}_2}$  held at 100 Torr and  $\text{PET}_{\text{CO}_2}$  held 1–2 Torr above eucapnia throughout. The second was a hypoxic step protocol with  $\text{PET}_{\text{O}_2}$  lowered from control values to 50 Torr for 20 min. The third was a hypercapnic step protocol with  $\text{PET}_{\text{CO}_2}$  elevated from control by 7.5 Torr for 20 min. The fourth was a hypoxic-and-hypercapnic step protocol lasting 20 min. The total power of the Doppler signal remained relatively constant, suggesting that the cross-sectional area of the vessel changed little. After the initial transient in MCAF at the onset of the stimulus, no adaptation or progressive increase was observed over the remaining 20 min. A simple model consisting of a single pure delay, gain terms, time constants, and offsets for the on and off transients was fitted to the hypoxic and hypercapnic protocols. For hypercapnia, all the parameters for the onset were significantly different from the relief of the stimulus. The asymmetry was characterized by a slower on transient than off transient and also by a degree of undershoot after the relief of hypercapnia. Finally, the results from this study show that the cerebral blood flow response to hypoxia and hypercapnia in humans is much faster than has previously been thought.

transcranial Doppler; hypoxia; hypercapnia; modeling

---

ALTHOUGH IT IS WELL KNOWN that cerebral blood flow is increased by hypoxia and hypercapnia (7, 16, 30), the dynamics of the alterations in cerebral blood flow to changes in arterial  $\text{CO}_2$  and  $\text{O}_2$  have yet to be accurately described. Previous attempts to study dynamic responses to alterations in cerebral blood flow have been mostly of limited success because of problems with the techniques used to measure cerebral blood flow and to control end-tidal (i.e., arterial) gases.

To study the dynamic response of the cerebral vasculature to hypoxia and hypercapnia, a method for assessing cerebral blood flow with a suitable time resolution has to be employed and a method for controlling the arterial  $\text{PCO}_2$  and  $\text{PO}_2$  accurately and continuously has to be used.

One method that has the potential to provide a continuous measurement of blood flow with the required time resolution is transcranial Doppler ultrasound. However, previous studies using transcranial

Doppler ultrasound to assess changes in cerebral blood flow in response to hypoxia and hypercapnia have measured the maximum velocity or the intensity-weighted mean velocity of the Doppler signal. These indexes are proportional to flow only if the cross-sectional area of the vessel remains constant (18). A more suitable index of cerebral blood flow may be the intensity-weighted mean of the velocity signal multiplied by the overall intensity (power) of the signal (18). This is because the total power of the signal is proportional to cross-sectional area (3), and so the proposed index allows for any changes that occur in the cross-sectional area of the vessel. The current study uses the power signal as a measure of cross-sectional area.

To gain the necessary control over arterial (end-tidal)  $\text{PCO}_2$  and  $\text{PO}_2$ , the technique of dynamic end-tidal forcing was employed (13, 26). This technique was originally designed for studying respiratory control, and its important features are as follows: 1) it regulates the end-tidal gases in such a way that the effect of the ensuing changes in pulmonary ventilation on the end-tidal values are minimized, and 2) the end-tidal  $\text{PCO}_2$  ( $\text{PET}_{\text{CO}_2}$ ) is regulated accurately during alterations in end-tidal  $\text{PO}_2$  ( $\text{PET}_{\text{O}_2}$ ) and vice versa.

In the current study, the changes in middle cerebral artery blood flow (MCAF) were determined in response to 1) 20 min of acute isocapnic hypoxia, 2) 20 min of acute euoxic hypercapnia, and 3) 20 min of hypoxia and hypercapnia. To quantify the dynamics of the response, one simple model was fit to the data to provide gain terms and time constants for the responses to the onset and relief of hypoxia and hypercapnia.

## METHODS

### Subjects

Six healthy young students volunteered to take part in the study; the requirements were fully explained in written and verbal forms to all participants, and each gave informed consent before participating in the study. The research was approved by the Central Oxford Research Ethics Committee. On the first session each participant was given a brief examination, which included measurements of heart rate, blood pressure, height, and weight. Participants were not on any medication, and none had a history of cardiovascular, cerebrovascular, or respiratory disease.

### Protocols

Each participant visited the laboratory at the same time of day on six or seven occasions, each lasting 4–5 h. Subjects were requested not to eat or drink caffeine-containing beverages within 4 h before their scheduled testing sessions in the laboratory. On each visit one repetition of each of four protocols was performed in a randomly assigned order; each repetition lasted ~40 min.

Before the experiments were started, room air measurements of resting Doppler signals and PET<sub>CO<sub>2</sub></sub> were collected. The subject's natural PET<sub>CO<sub>2</sub></sub> was measured using a nasal catheter, which disturbs quiet breathing less than a mouthpiece-and-noseclip arrangement.

For the control protocol (*protocol I*), PET<sub>O<sub>2</sub></sub> was held at 100 Torr and PET<sub>CO<sub>2</sub></sub> was held 1–2 Torr above the subject's normal value for 30 min. Each of the test protocols started with a short 6- to 7-min period when PET<sub>O<sub>2</sub></sub> was held at 100 Torr and PET<sub>CO<sub>2</sub></sub> was held 1–2 Torr above the subject's normal value as determined on that day. Then PET<sub>O<sub>2</sub></sub> and/or PET<sub>CO<sub>2</sub></sub> was altered rapidly (over 1 or 2 breaths) to a new set of desired levels, according to each protocol described below, and maintained constant for 20 min. Finally, PET<sub>O<sub>2</sub></sub> and/or PET<sub>CO<sub>2</sub></sub> was returned (again within 1 or 2 breaths) to initial euoxic and near-eucapnic values and maintained constant for a further 10 min. For the hypoxic protocol (*protocol II*), PET<sub>O<sub>2</sub></sub> was lowered to 50 Torr while PET<sub>CO<sub>2</sub></sub> continued to be held 1–2 Torr above the subject's normal value. For the hypercapnic protocol (*protocol III*), PET<sub>O<sub>2</sub></sub> continued to be held at 100 Torr while PET<sub>CO<sub>2</sub></sub> was elevated by 7.5 Torr (i.e., 8.5–9.5 Torr above the subject's normal value). Finally, for the protocol combining hypoxia with hypercapnia (*protocol IV*), PET<sub>O<sub>2</sub></sub> was lowered to 50 Torr and PET<sub>CO<sub>2</sub></sub> was elevated by 7.5 Torr.

#### *Apparatus and Technique for Dynamic End-Tidal Forcings*

Accurate control of the end-tidal gases was achieved using the technique of dynamic end-tidal forcing (13, 26). Subjects sat quietly in a chair and breathed through a mouthpiece with the nose occluded. Respiratory volumes were measured with a turbine volume transducer (SensorMedics VMM Series, CardioKinetics, Salford, UK). Respiratory flows and timing information were obtained using a pneumotachograph (Fleisch) and differential pressure transducer (Morgan, Gillingham, UK). Gas was sampled continuously at the mouth at a rate of 20 ml/min and analyzed by mass spectrometer (model MGA3000, Airspec, Biggin Hill, UK) for fractional concentrations of O<sub>2</sub>, CO<sub>2</sub>, and N<sub>2</sub>. Two microcomputers were used: one as a data acquisition computer and the other as a controlling computer. The data acquisition computer sampled the experimental variables every 20 ms, logged each occurrence of a QRS complex from an electrocardiogram attached to the subject, detected the end-tidal gas tensions, passed the end-tidal tensions to the controlling computer as they were found, and stored the data obtained for later analysis. Before the start of the actual experiment, the desired end-tidal partial pressures were entered into the controlling computer. Also entered into the controlling computer were the inspired partial pressures that were predicted to achieve these desired end-tidal partial pressures. At the start of the experiment, the computer generated the predicted inspired partial pressures by use of a fast gas-mixing system. The controlling computer received feedback of the measured end-tidal partial pressures on a breath-by-breath basis as the experiment progressed. These measured end-tidal values were compared with the desired values, and the computer then adjusted the initial predicted inspired gas mixture by use of an integral proportional feedback algorithm based on the deviations of the measured end-tidal values from the desired end-tidal values. Thus a new inspiratory mixture was delivered with each breath. This experimental system regulated the end-tidal gas tensions accurately in the face of a constantly changing ventilation and generated accurate rapid steps in end-tidal composition as required (31).

#### *Apparatus and Technique for Measurement of Cerebral Blood Flow*

A 2-MHz pulsed Doppler ultrasound system (PCDop 842, SciMed, Bristol, UK) was used to measure backscattered Doppler signals from the right middle cerebral artery. The Doppler system was adapted to make the Doppler signals (maximum and intensity-weighted mean Doppler frequency shifts and total power) available as analogue signals. These were updated each time a new spectrum was calculated every 10 ms. The signals were sampled every 10 ms by use of a data acquisition package (DAQWare, National Instruments, United Kingdom, Newbury, UK) running on another computer. These signals were saved for later analysis.

The middle cerebral artery was identified by an insonation pathway through the right temporal window just above the zygomatic arch by use of standard search techniques, which have been described previously (1, 22). Ultrasound gel was applied to the skin and hair of the temporal window as well as to the probe before the experimenter proceeded to locate and identify the main segment of the middle cerebral artery. Optimization of the Doppler signals from the middle cerebral artery was performed by varying the sample volume depth in incremental steps and, at each depth, varying the angle of insonance to obtain the best quality signals for the Doppler frequency shifts that corresponded with the maximum power signal. Ultrasound gel was then reapplied to the insonation site and the probe before the probe was securely positioned in a headband device (Müller and Moll Fixation, Nicolet Instruments, Warwick, UK) to ensure optimal insonation position and angle for the duration of the experiment.

#### *Calculation of MCAF*

MCAF was calculated using two different approaches. With *method 1*, for each 10-ms sample, the product for the intensity-weighted mean velocity and power was calculated, and the sum of the products for each sample over each heartbeat interval was divided by the number of samples in the interval. With *method 2*, the average values for the intensity-weighted mean velocity and power were calculated separately for each heartbeat interval, and the two values were subsequently multiplied together. Both methods provided nearly identical results, and in this study we present the data derived using *method 1*, because this method allows for any systematic change in diameter throughout the cardiac cycle.

#### *Modeling the Cerebral Blood Flow Responses to Hypoxia and Hypercapnia*

If we assume that the rate of change of cerebral blood flow is proportional to the deviation of cerebral blood flow from the value it would obtain in the steady state, then a simple dynamic model may be written in the form

$$d(\text{MCAF})/dt = 1/\tau[g \cdot u(t - T_d) + \text{MCAF}^* - \text{MCAF}] \quad (1)$$

where  $\tau$  is a time constant,  $g$  is a gain term,  $u(t - T_d)$  is the input function,  $T_d$  is a pure delay, and  $\text{MCAF}^*$  is the steady-state value for MCAF when  $u(t - T_d)$  is zero. Such a dynamic model will give an exponential output for a step input.

For hypoxia we assume that the increase in steady-state cerebral blood flow is proportional to the degree of desaturation of the blood, and thus

$$u(t - T_d) = [1 - S(t - T_d)] \quad (2)$$

The saturation ( $S$ ) may be calculated from the PET<sub>O<sub>2</sub></sub> by use of

the empirical relationship described by Severinghaus (27)

$$S = 1 - 1.89 \exp(-0.05 \text{PET}_{\text{O}_2}) \quad (3)$$

For hypercapnia we assume that the increase in steady-state cerebral blood flow is proportional to the increase in  $\text{PET}_{\text{CO}_2}$  above control, and thus

$$u(t - T_d) = [\text{PET}_{\text{CO}_2}(t - T_d) - \text{PET}_{\text{CO}_2}^*] \quad (4)$$

where  $\text{PET}_{\text{CO}_2}^*$  is the control  $\text{PET}_{\text{CO}_2}$  for the subject.

The differential Eq. 1 may be solved to provide a difference equation that supplies a series of values for cerebral blood flow on a beat-by-beat basis, provided that we assume that the input function can be regarded as constant over any single heartbeat. For the  $n$ th beat at time  $t_n$  we may write

$$K_n = g \cdot u(t_n - T_d) + \text{MCAF}^* \quad (5)$$

where  $K_n$  is a constant for this beat. The differential Eq. 1 becomes

$$d(\text{MCAF})/dt = 1/\tau(K_n - \text{MCAF}) \quad (6)$$

This may be solved by separation of variables and direct integration

$$\int_{\text{MCAF}_n}^{\text{MCAF}_{n+1}} d(\text{MCAF})/(K_n - \text{MCAF}) = \int_{t_n}^{t_{n+1}} dt/\tau \quad (7)$$

which yields

$$[-\ln(K_n - \text{MCAF})]_{\text{MCAF}_n}^{\text{MCAF}_{n+1}} = [t/\tau]_{t_n}^{t_{n+1}} \quad (8)$$

On rearranging, this gives

$$\text{MCAF}_{n+1} = K_n - (K_n - \text{MCAF}_n) \exp^{-((t_{n+1} - t_n)/\tau)} \quad (9)$$

and  $\text{MCAF}$  for the  $n + 1$  beat may be calculated from the  $\text{MCAF}$  for the  $n$ th beat together with the value for  $K_n$  for this beat.

#### Parameter Estimation Process

To allow for asymmetry between the on and off transients, separate parameter values were estimated for the on and off transients. The switch between the on and off parameters was undertaken in the middle of the 20-min period of hypoxia and/or hypercapnia. This resulted in seven parameters for estimation, namely, gain terms for the on and off transients ( $g_{\text{on}}$ ,  $g_{\text{off}}$ ), time constants for the on and off transients ( $\tau_{\text{on}}$ ,  $\tau_{\text{off}}$ ), baseline terms for the on and off transients ( $\text{MCAF}_{\text{on}}^*$ ,  $\text{MCAF}_{\text{off}}^*$ ), and a single pure time delay ( $T_d$ ).

Six of the parameters ( $g_{\text{on}}$ ,  $g_{\text{off}}$ ,  $\tau_{\text{on}}$ ,  $\tau_{\text{off}}$ ,  $\text{MCAF}_{\text{on}}^*$ ,  $\text{MCAF}_{\text{off}}^*$ ) were estimated using a routine for minimizing a sum of squares. The seventh parameter ( $T_d$ ) was determined on a "grid search" basis by minimizing the sum of squares for the other six parameters over a range of fixed pure delays of 0–20 s (in 1-s steps) and choosing the pure delay associated with the lowest minimum found.

The model input was the breath-by-breath  $\text{PET}_{\text{CO}_2}$  or  $\text{PET}_{\text{O}_2}$  (from which a saturation was calculated). Values at times between breaths were obtained by linear interpolation. The model output was compared with the data on a beat-by-beat basis to determine the residuals; no averaging was employed. A single set of parameter values was determined for all repetitions combined of a given protocol for a single subject by minimizing the total sum of squared residuals across all repetitions. This totaled ~11,000–15,000 residuals (1 for each heartbeat). For each repetition, the data employed for

parameter estimation included a 2-min prehypoxic or prehypocapnic period, the 20-min hypoxic or hypercapnic period, and the 10-min recovery period.

The particular routine employed for the minimization was taken from the Numerical Algorithms Group (Oxford, UK) FORTRAN library subroutine E04FDF. This routine is designed to minimize a nonlinear function of a number of variables when that function takes the special form of a sum of squares. All parameters in the cost function were constrained to be positive. The routine required initial guesses to be made for the parameters of the model. The guesses were based on visual inspection of the data combined with a knowledge of the range of likely values based on known physiology. A number of such starting points was employed in each case in an attempt to determine whether there were multiple minima. In every case, only a single minimum was detected.

## RESULTS

### General

The average age, height, and weight of the six subjects who undertook the study were  $20.8 \pm 1.7$  (SD) yr,  $183.3 \pm 5.0$  cm, and  $74.2 \pm 10.0$  kg, respectively. None had a history of cardiovascular or respiratory disease, and all had normal systolic ( $116.3 \pm 6.3$  mmHg) and diastolic ( $79.0 \pm 4.0$  mmHg) blood pressure.

Each subject attended the laboratory on at least six occasions. On a few occasions, repetitions were spoiled by, e.g., electrical power failures or fire alarms, and those repetitions were repeated during extra visits. *Subject 959* was a visiting student from abroad who returned home at the end of the academic term, and his results for *protocols I–III* represent an average of five repetitions only.

Table 1 lists the individual values and the group mean for the depth of the Doppler sample volume at which the main segment of the middle cerebral artery was insonated. Small variations in depth between subjects are attributed to differences in skull size (22). Small variations in depth within each subject represent day-to-day differences in the experimenter's determination of the best quality Doppler signals, because the optimization of signals was performed on each visit without reference to results from previous visits.

### Quality of Input Stimuli

Figure 1 shows typical responses for one repetition of each protocol for *subject 967*. Figure 1 illustrates the

Table 1. Distance (depth) from probe to start of Doppler sample volume for detecting signals from the MCA

Subj No.	MCA Depth, cm
940	$5.02 \pm 0.10$
959	$5.05 \pm 0.15$
964	$5.11 \pm 0.09$
966	$4.86 \pm 0.11$
967	$5.03 \pm 0.14$
971	$5.07 \pm 0.15$
Mean	$5.02 \pm 0.03$

Values are means  $\pm$  SD. MCA, middle cerebral artery.

high quality of control exerted over PET<sub>O<sub>2</sub></sub> and PET<sub>CO<sub>2</sub></sub> that is achieved by using a dynamic end-tidal forcing technique.

Figure 2 shows ensemble averages of the time-related changes in PET<sub>O<sub>2</sub></sub> and PET<sub>CO<sub>2</sub></sub> for each subject and for each protocol. Each profile represents an average of six repetitions, except for *subject 959* whose results for *protocols I-III* represent an average of five repetitions. There are some minor imperfections in the

desired PET<sub>CO<sub>2</sub></sub> and PET<sub>O<sub>2</sub></sub>, and these may be noted particularly at the onset and relief of hypoxia and/or hypercapnia. However, the overall quality of input stimulation was good.

#### General Features of Cerebrovascular Responses

Figure 1 shows the responses for middle cerebral artery velocity (MCAV), power, and MCAF for one

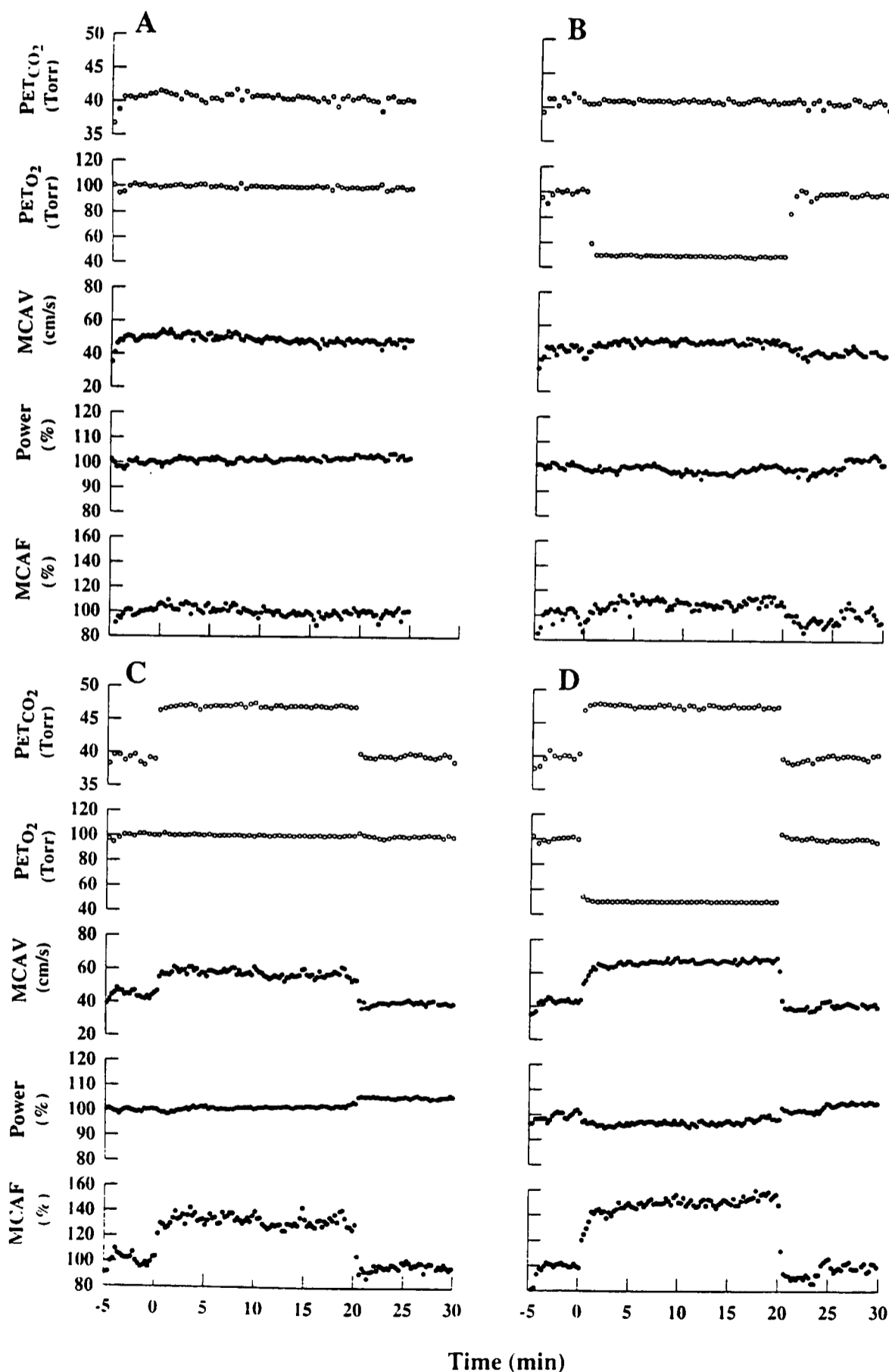


Fig. 1. Typical results for one repetition of each protocol for *subject 967*. Power and middle cerebral artery flow (MCAF) are expressed as percentage of average value for 3-min period preceding *time 0*. A: control; B: hypoxia; C: hypercapnia; D: hypoxia and hypercapnia. Data for end-tidal PO<sub>2</sub> and PCO<sub>2</sub> (PET<sub>O<sub>2</sub></sub> and PET<sub>CO<sub>2</sub></sub>) are averaged over 30-s periods; data for middle cerebral artery velocity (MCAV), power, and MCAF are averaged over 15-s periods.

repetition of each protocol in one subject. Power and MCAF have been expressed as a percentage of a 3-min baseline immediately preceding *time 0* for each protocol. The responses to stimulation were readily discernible events within a single experimental protocol before any averaging.

Figure 3 shows ensemble averages of the responses for MCAV, power, and MCAF for each subject and for each protocol. Power and MCAF have been expressed as a percentage of a 3-min baseline immediately preceding *time 0*. In general, the temporal profiles for MCAV and MCAF appear quite similar. The profiles for the power signals appear not to change much from baseline

values of 100%. Exceptions are noted where there appears to be a slight drift in power over time (*subject 940*) and where there appears to be a slight increase in power in all but the control protocol (*subject 959*). In other subjects there appears to be a small increase in the power signal at the off transients, most often noted in *protocol IV* (hypercapnia and hypoxia; *subjects 964* and *971*) but also seen in *protocol III* (hypercapnia; *subject 967*).

The magnitude of the changes in MCAF resulting from the different stimuli is fairly similar in all subjects, with the largest increase in MCAF resulting from the combination of hypoxia and hypercapnia. In all

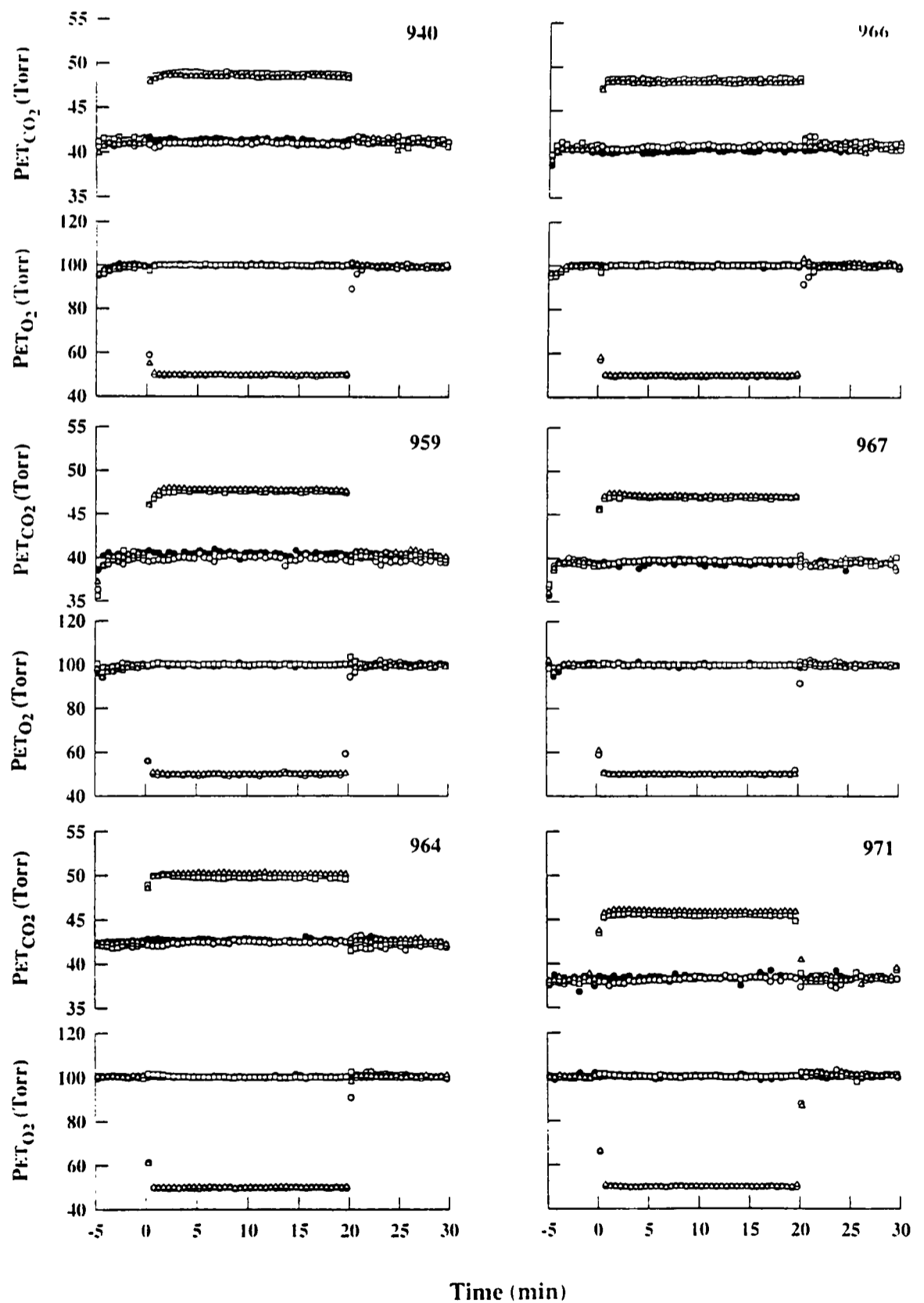


Fig. 2. Ensemble averages of time-related changes in PETO<sub>2</sub> and PETCO<sub>2</sub> for each subject. ●, Control protocols; ○, hypoxia; □, hypercapnia; △, hypoxia and hypercapnia. Each symbol represents a 30-s mean.

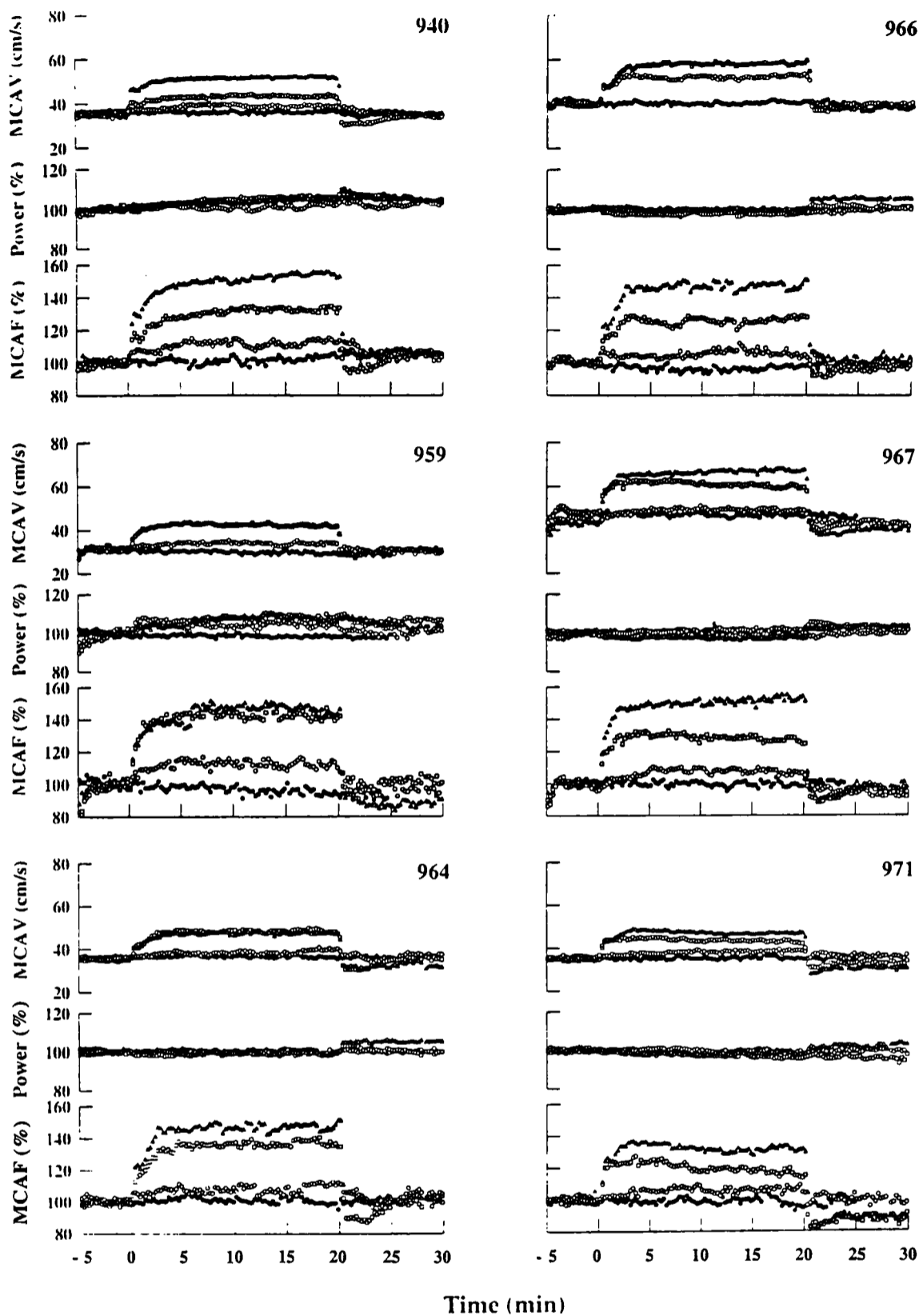


Fig. 3. Ensemble averages of MCAV, power, and MCAF responses for each subject. ●, Control; ○, hypoxia; □, hypercapnia; △, hypoxia and hypercapnia. Each symbol represents a 15-s mean.

subjects, the magnitude of the increase in MCAF resulting from hypercapnia was larger than the increase resulting from hypoxia. In *subjects 959 and 964*, the increase in MCAF resulting from the combined stimuli was very similar to that seen in hypercapnia.

The individual MCAF- $P_{ETCO_2}$  response lines in euoxia and hypoxia are shown in Fig. 4. The slope of the response in hypoxia is greater than the slope in euoxia in *subjects 940, 966, 967, and 971*, but in *subjects 959 and 964* the MCAF response slope is less in hypoxia than in euoxia. Thus overall there is no significant difference between the group mean for the MCAF- $P_{ETCO_2}$  response slope in euoxia [ $4.07 \pm 0.51\%/Torr$  (SE)] and in hypoxia ( $4.82 \pm 0.51\%/Torr$ ).

#### Dynamics of MCAF Responses to Hypoxia

The fitted model output, along with the experimental data and residuals, is shown for each subject in Fig. 5. The individual values and group means for the estimated model parameters are listed in Table 2. The time delay after which the MCAF responses to hypoxia start was estimated at 5.2 s. The time constant for the on response is almost three times slower than the time constant for the off response, although this difference is not significant. The gain term for the on response is slightly smaller than the gain term for the off response, although again this difference is not significant. Once the initial transient is over, there does not appear to be

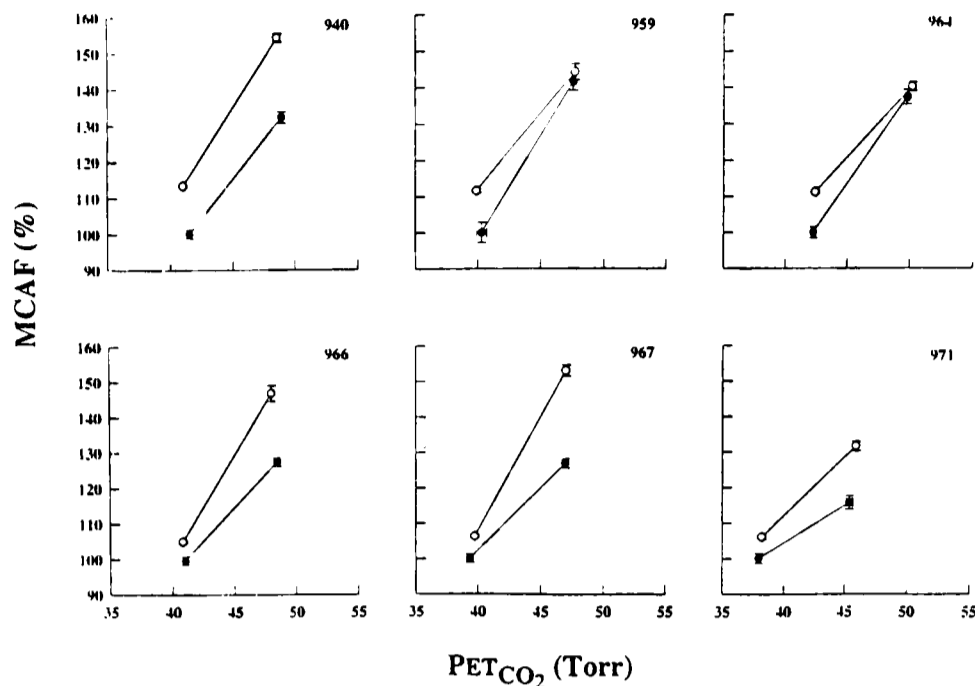


Fig. 4. Steady-state MCAF- $PET_{CO_2}$  responses in euoxia (●) and hypoxia (○) for each subject. Euoxic means were calculated from hypercapnic protocol; eucapnic mean represents 3-min prehypercapnic period; hypercapnic mean represents last 3-min exposure in hypercapnia (*minutes 17–20*). Means in hypoxia were calculated from 2 protocols; eucapnic mean represents last 3-min exposure of hypoxia (*minutes 17–20*) from hypoxic protocol. Hypercapnic mean represents last 3-min exposure of hypoxia and hypercapnia (*minutes 17–20*) from hypoxic-hypercapnic protocol.

any further increase or decrease in MCAF after the remainder of the 20-min hypoxia exposure.

#### *Dynamics of MCAF Responses to Hypercapnia*

The fitted model output, along with the experimental data and residuals, is shown for each subject in Fig. 6, whereas the individual values and group means for the estimated model parameters are listed in Table 2. The MCAF responses to hypercapnia start after an estimated delay of 6.0 s, which is similar to that observed with hypoxia. The time constant for the on response is more than seven times slower than the time constant for the off response, and this difference is significant. The gain term is significantly smaller for the on response than for the off response, and the baseline is significantly greater before than after the off response. As with hypoxia, there does not appear to be an appreciable trend over the remainder of the 20-min period once the transient is over. There are indications that the single-exponential model is an oversimplification for the on and off transients. There appear to be two components to the on transient in four of the six subjects (940, 964, 966, 967), and there appears to be an undershoot in the response during the relief of hypercapnia in five subjects (940, 959, 964, 966, 967). The latter feature may explain the significant differences between the gain and baseline terms for the on and off responses.

## DISCUSSION

### *Major Findings*

This is the first study to provide continuous beat-by-beat measurements of an index of MCAF during sustained hypoxia and hypercapnia in humans. The major findings of this study are as follows: 1) with sustained

hypoxia or hypercapnia over 20 min there is no adaptation or progressive increase in MCAF after the initial transient at the onset of the stimulus is over; 2) there is little change in the total power of the Doppler signal with the levels of hypoxic and hypercapnic stimuli used in this study, suggesting that the cross-sectional area of the middle cerebral artery changes little; 3) there is significant asymmetry of the response to hypercapnia characterized by a slower on than off transient and also by a degree of undershoot after the relief of hypercapnia; and 4) the cerebral blood flow response to hypoxia and hypercapnia in humans is much faster than has been previously reported.

### *Use of Transcranial Doppler*

Several techniques are available to measure cerebral blood flow in humans, but most do not provide the time resolution necessary to assess dynamic changes in cerebral blood flow. Transcranial Doppler ultrasound provides a near-continuous measurement of blood flow velocity, giving the required time resolution, but the use of velocity signals alone as an indication of true flow will be inaccurate when there are changes in cross-sectional area, such as may occur during rapid changes in cerebral blood flow (18). A more accurate index of flow is one that combines the measurements of average blood flow velocity with measurements of total Doppler signal power as an index of cross-sectional area (18). Although this index has been used in studies of cerebral autoregulation dynamics (2), it has not to the authors' knowledge been used to examine the dynamics of the cerebral vascular response to changes in arterial  $PCO_2$  and  $PO_2$ .

The current study used the product of the intensity-weighted mean velocity signal and the total power of the reflected signal as an index of flow (MCAF) to

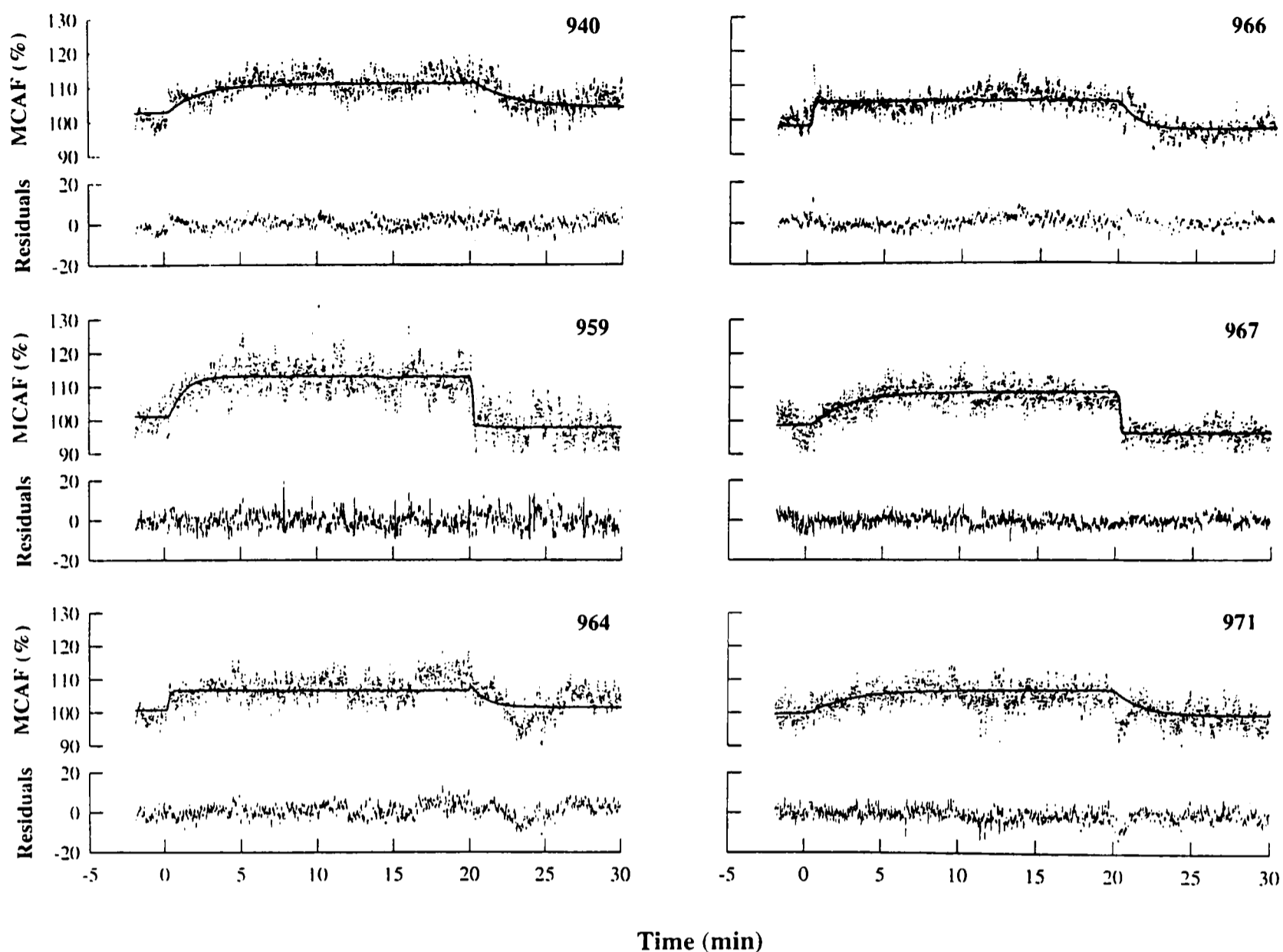


Fig. 5. MCAF responses to hypoxia (●), model fit (solid line), and residuals for each subject. Each data set represents an ensemble average of data from all repetitions for each subject. Beat-by-beat data are interpolated over 0.5-s intervals.

account for changes in the caliber of the middle cerebral artery. One disadvantage of using this index is that small movements of the probe (and therefore sample volume) can cause some changes in the reflected power signal, which would then be wrongly interpreted as changes in flow. To avoid this potential problem, extreme care was always taken to identify accurately the center of the insonated vessel by maximizing the Doppler power signal and to secure firmly the probe and headpiece in order to minimize any noise in the power signal due to probe movements. Additionally, each protocol was repeated several times, and the results for each protocol were averaged, thereby minimizing any effect due to noise artifact. Within the ranges of cerebral blood flow associated with the pure hypoxic or pure hypercapnic stimuli studied, there appeared to be very little change in the cross-sectional area of the middle cerebral artery. This suggests that percent changes in cerebral blood flow velocity reported previously under these conditions (7) are likely to be a reasonably accurate reflection of the underlying changes in blood flow.

#### Control of End-Tidal Gases

Studies of the dynamic response of the cerebral vasculature to hypoxia and hypercapnia require precise control continuously over end-tidal (i.e., in healthy subjects, arterial) PO<sub>2</sub> and PCO<sub>2</sub>. In earlier studies of the cerebral blood flow response to hypoxia or hypercapnia, it was often not possible to achieve such accurate control over end-tidal gases because of limitations in the techniques used to administer the changes in the PO<sub>2</sub> and PCO<sub>2</sub>. Most studies simply switched between different fixed inspired gas mixtures to obtain the hypoxic and hypercapnic responses (16, 28, 29). This technique is inadequate on its own for the study of dynamic responses, because it can require several minutes for the stimuli to reach the desired steady hypoxic and hypercapnic levels, and furthermore the precise form of the dynamic stimuli depends on the ventilatory response of the subject. In a more recent study, Ellingsen et al. (7) attempted to administer step changes in PETO<sub>2</sub> and PETCO<sub>2</sub> by adjusting the flow of the inspired gas mixtures at the beginning of the steps, but

Table 2. *Estimated model parameters for cerebral blood flow response to hypoxia and hypercapnia*

Subj No.	MCAF* <sub>on</sub>	MCAF* <sub>off</sub>	g <sub>on</sub>	g <sub>off</sub>	τ <sub>on</sub>	τ <sub>off</sub>	T <sub>d</sub>
<i>Hypoxia</i>							
940	102.3	102.9	54.8	61.6	119.9	153.6	2.0
959	100.1	96.6	82.5	101.2	53.8	0.5	8.0
964	100.2	100.9	40.6	56.2	0.8	55.6	5.0
966	97.8	96.3	47.4	61.6	0.2	61.2	7.0
967	98.0	95.1	66.0	76.4	137.9	0.6	8.0
971	99.2	99.8	49.1	40.0	165.3	101.7	1.0
Mean	99.6	98.4	56.7	66.0	79.6	28.9	5.2
± SE	± 0.7	± 1.2	± 6.2	± 8.6	± 29.2	± 12.6	± 1.3
<i>Hypercapnia</i>							
940	102.3	101.4	3.7	4.2	92.6	6.1	6.0
959	99.5	99.7	5.9	6.0	22.8	5.8	7.0
964	101.5	95.9	4.5	5.6	78.3	8.3	5.0
966	100.7	97.1	3.3	4.0	37.4	5.4	7.0
967	100.5	91.4	3.8	4.7	31.6	4.6	8.0
971	97.1	84.5	3.2	4.3	8.8	6.7	3.0
Mean	100.3	95.1	4.1	4.8	45.3	6.1	6.0
± SE	± 0.7	± 2.5*	± 0.4	± 0.3*	± 13.4	± 0.5*	± 0.7
P		0.04		0.007		0.03	

MCAF\*<sub>on</sub> and MCAF\*<sub>off</sub>, pre- and post-MCAF baselines (%); g<sub>on</sub> and g<sub>off</sub>, gain terms for on- and off-responses (%/unit desaturation for hypoxia and %/Torr for hypercapnia); τ<sub>on</sub> and τ<sub>off</sub>, time constants for on and off responses (s); T<sub>d</sub>, time delay (s). \*Significantly different from on response, P ≤ 0.05.

the steps were somewhat slow to reach the new steady-state levels and, therefore, not ideal for accurate determination of dynamic cerebral blood flow responses. In the current study, a dynamic end-tidal forcing system was used. This system uses prediction and feedback correction (via the end-tidal gas values) to adjust the inspired gas composition on a breath-by-breath basis to hold the subjects' PET<sub>CO<sub>2</sub></sub> and PET<sub>O<sub>2</sub></sub> at the desired level despite changes in ventilation. The use of this apparatus provided better control over the stimuli than can be achieved by the methods previously employed to study cerebral blood flow responses.

### Modeling

The dynamic models used in this study to describe the responses to hypoxia and hypercapnia were selected on the basis of simplicity; the model structure is such that for a perfect step input the result is a perfect exponential output. Cerebral blood flow is linearly related to arterial oxygen content during steady hypoxia (4, 28), and therefore saturation was used as the input in the model for the hypoxic response. In steady hypercapnia, cerebral blood flow is linearly related to arterial PCO<sub>2</sub> (17, 21, 25), and therefore PCO<sub>2</sub> was used as the input in the model of the hypercapnic response. A particular feature of the estimation procedure for the model parameters is that the actual breath-by-breath Po<sub>2</sub> and PCO<sub>2</sub> were used in the input functions; this avoids making any assumptions about the input, such as assuming that the input was a perfect step change.

The results of model fitting for the MCAF responses to hypoxia and hypercapnia show that the "single-exponential" model describes the MCAF responses fairly

well, provided that different parameters are used for the on and off transients. A close examination of the data, model fit, and residuals in Figs. 5 and 6, however, indicates that the single-exponential model may be an oversimplified model. This is more obvious in hypercapnia than in hypoxia, where there appear to be two phases to the on transient and an undershoot in the off transient.

In this study, each model was fitted simultaneously to all repetitions for the protocol for each subject, and the result was that one set of parameter values was obtained that best described each subject's response. One disadvantage of this method, however, is that the fitting procedure does not allow for the subjects' responses being different from day to day (23), although visual observation of the data, as well as previous findings (11, 29), suggests that such variability may be small.

### Sensitivities to Hypercapnia and Hypoxia

The parameter values estimated for the gains were 4.1%/Torr for hypercapnia and 56.7%/unit desaturation for hypoxia. The results in hypercapnia compare well with the steady-state values of 3.9–4.4%/Torr reported previously in the eucapnic-hypercapnic range with use of several techniques, including nitrous oxide inhalation (and tissue uptake based on the Fick principle) (16), <sup>133</sup>Xe washout (21), and transcranial Doppler (7, 11). The hypoxic sensitivities are lower than the steady-state responses of previous studies (5, 7, 16, 28), which themselves show a large degree of variability (range 98.5–389.8%/unit desaturation).

The large variability of responses between studies may be explained in part by several factors, including the different hypoxic levels at which responses were obtained (PET<sub>O<sub>2</sub></sub> = 35–65 Torr), the inaccuracies associated with the different techniques, and the difficulties encountered in attempting to separate the effects of hypoxia from those caused by changes in PET<sub>CO<sub>2</sub></sub>.

### Hypoxia-and-Hypercapnia Protocol

Very little has been reported on the simultaneous effects of hypoxia and hypercapnia on cerebral blood flow in humans. Shapiro et al. (30) used the N<sub>2</sub>O inhalation technique to examine cerebral blood flow during hypoxia (arterial Po<sub>2</sub> = 62 Torr) and hypercapnia (arterial PCO<sub>2</sub> = 7 Torr above resting values) in six subjects. They concluded that hypoxia and hypercapnia had additive dilator effects on the cerebral vasculature and that the increase in cerebral blood flow was the sum of the individual responses. Results from the present study (presented in Fig. 4) suggest considerable variability between subjects. In four subjects, the response to combined hypoxia and hypercapnia appeared greater than the sum of the responses to hypercapnia and hypoxia alone. In two subjects, however, the response appeared less than the sum of the responses to hypercapnia and hypoxia alone.

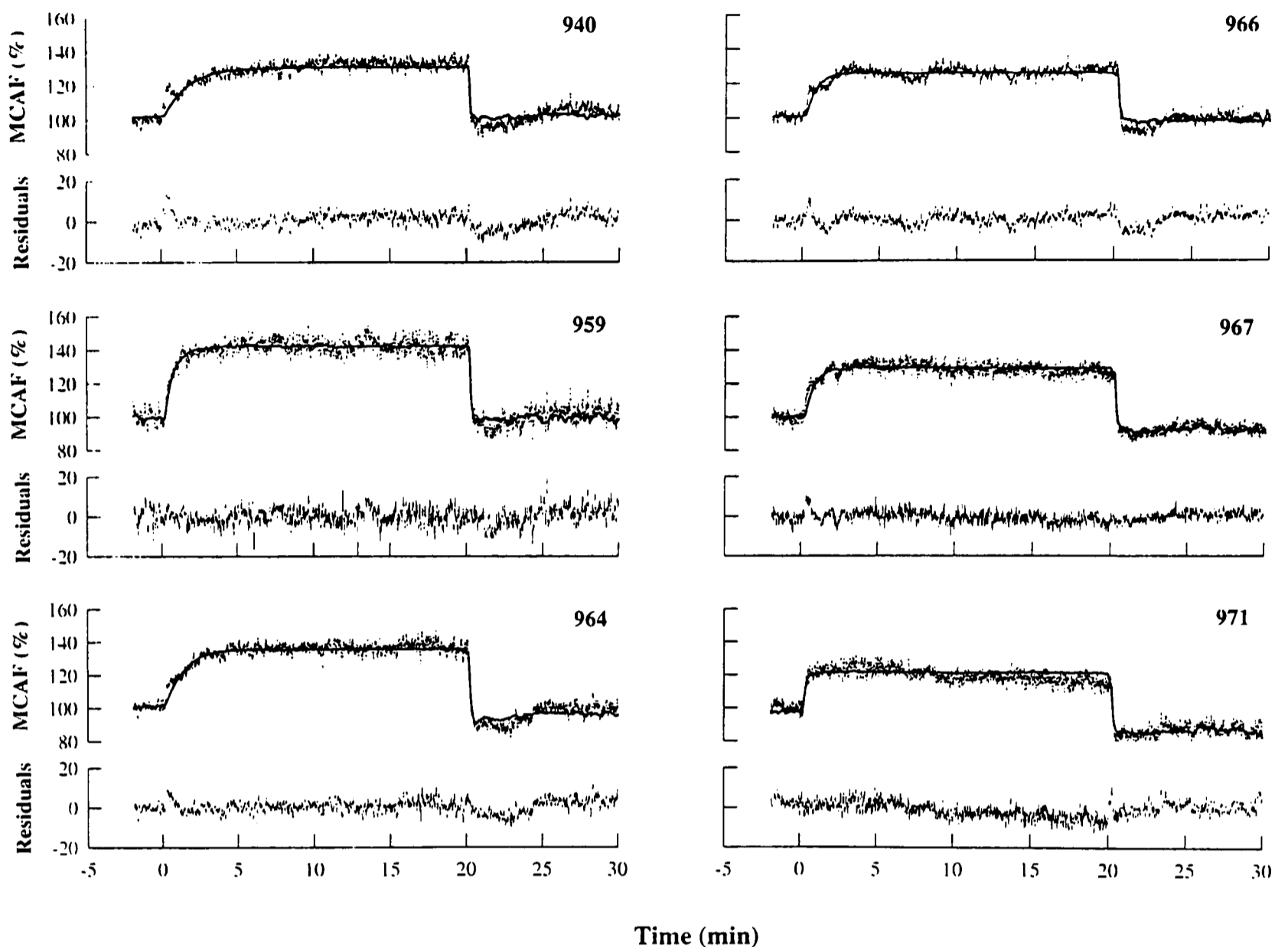


Fig. 6. MCAF responses to hypercapnia (●), model fit (solid line), and residuals for each subject. Each data set represents an ensemble average of data from all repetitions for each subject. Beat-by-beat data are interpolated over 0.5-s intervals.

#### *Sustained Nature of the Cerebral Blood Flow Response*

We observed no adaptation or progressive increase in the cerebral blood flow response to hypoxia or hypercapnia after the initial transient. Ellingsen et al. (7), however, showed an adaptation in the blood flow velocity in the carotid artery in response to hypercapnia. They reported that the blood flow velocity started to return toward control values shortly after a step increase in the level of hypercapnia (10 Torr above resting  $PET_{CO_2}$ ). In our study, no adaptation in MCAF was observed over the 20-min period of hypercapnia (8.5–9.0 Torr above resting  $PET_{CO_2}$ ; Fig. 6). The reasons for this difference are unclear, but there are some important technical differences between the two studies. In the study by Ellingsen et al., there was no measure of cross-sectional area, and only measurements of blood velocity were made. Consequently, if there were small increases in the diameter of the carotid artery, then this could explain the observed decreases in velocity despite an unchanged flow. Additionally, measurements were made in different arteries (carotid vs. middle cerebral),

and different techniques were used to control end-tidal  $PET_{CO_2}$  and  $PET_{O_2}$ .

#### *Asymmetry and Speed of Response*

*Hypoxia.* In subjects 959 and 967 the speed of the increase in cerebral blood flow at the onset of hypoxia appears slower than the speed of the decrease in blood flow at the relief of hypoxia. In these two subjects, the time constant is slower for the on transient than for the off transient. They also had the two greatest increases in cerebral blood flow in response to hypoxia and what would appear to be the best signal-to-noise ratio for determining the response. In the other four subjects, any asymmetry in response is less apparent. However, in these four subjects the response to hypoxia was smaller, and the signal-to-noise ratio appeared to be poor. In addition, the residuals do not appear to be white, and these two components of a poor signal-to-noise ratio and nonwhite residuals make the assessment of the dynamics of the response to hypoxia much more difficult. It is possible that these four subjects

might also show clear asymmetric responses with more intense levels of hypoxia when the signal-to-noise ratio is improved.

The estimated pure delay between the changes in end-tidal composition and the vascular response is very fast (5 s). The calculation of the pure delay is dependent on the conventions used for fixing the time of a gas composition measurement within the respiratory cycle and for fixing the time of a flow measurement with the cardiac cycle. The delay would be increased by as much as a breath and a heartbeat (~2.5–4 s) with different assumptions.

The response times of the cerebral vasculature to hypoxia (on response time constant = 80 s; off response time constant = 29 s) reported in this study are much faster than those suggested by previous investigators (7, 28). Shapiro et al. (28) suggested that 6–7 min were required for the cerebral blood flow response to hypoxia to reach its maximal response. Ellingsen et al. (7) suggested time constants of 360 s for the on response and 65 s for the off response. The most likely explanation is that this reflects the greater length of time taken in the previous studies to generate the change in alveolar gas composition. In the current study, step changes in PET<sub>O<sub>2</sub></sub> were completed rapidly, normally after the first or second breath (~5–8 s) after the step. Ellingsen et al. observed that the on response was slower than the off response, but it was not quite clear whether the asymmetry observed in hypoxia arose as an intrinsic part of the cerebral vasculature's response or whether it was due to the rather sluggish changes in PET<sub>O<sub>2</sub></sub> that resulted in the relief of hypoxia (a nonlinear function of PO<sub>2</sub>) being substantially faster than the onset of hypoxia.

The speed of response of the cerebral circulation to hypoxia has been estimated in species other than humans. Van Beek et al. (33) measured vertebral artery flow response to isocapnic hypoxia (PET<sub>O<sub>2</sub></sub> = 55 Torr) in anesthetized cats. A first-order model was fitted to the time course of the blood flow response. After an initial time delay of 3 s, cerebral blood flow increased with a time constant of 44 ± 37 (SD) s, whereas the time constant for the off response was ~2.5 times faster (19 ± 18 s). Doblzar et al. (6) measured the internal maxillary artery blood flow in response to sinusoidal hypoxia (mean arterial saturation = 85%) in anesthetized and paralyzed goats. They reported a circulatory delay between the lung and the brain of 8 s followed by a time constant of 36 s for the response in cerebral blood flow. Jennett et al. (15) examined the time course of intracranial pressure changes associated with the inhalation of hypoxic gas mixtures in anesthetized dogs, cats, and rabbits. Intracranial pressure, an indirect indicator of vasodilatation and vasoconstriction, was measured at the onset and at the relief of brief periods of hypoxia. Intracranial pressure increased within seconds (~9 s) of the start of inhalational hypoxia and dropped very quickly (~6 s) at the relief of hypoxia. These findings generally are in accord with the pure delay, the speed of response, and the possible asymme-

try of the response to hypoxia that we observe in our conscious human subjects.

*Hypercapnia.* For all the subjects in this study the rate of increase in cerebral blood flow at the onset of hypercapnia was slower than the rate of decrease in blood flow at the relief of hypercapnia. The pure delay between end-tidal and vascular response (6 s) was comparable with that seen in hypoxia. The average value for the time constant for the on response (45 s) was 7.5 times slower than that for the off response (6 s).

The response times of the cerebral vasculature to hypercapnia reported in this study are much faster than those reported by previous investigators. Shapiro et al. (29) reported that the cerebral blood flow response started within 30 s of the beginning of CO<sub>2</sub> inhalation and reached peak values at 156 and 61 s for the on and off responses, respectively. Ellingsen et al. (7) reported that cerebral blood flow took ~2 min to reach peak values. However, in this study, the step increases in hypercapnia were somewhat sluggish, and it appears that the time required for the full response to develop may have been longer because of the difficulties in reaching the correct PET<sub>CO<sub>2</sub></sub> and maintaining constant PO<sub>2</sub>. Thus the longer time constants reported in previous studies may be explained by differences in the actual CO<sub>2</sub> time course in the alveolar gas.

Estimates of the speed of response of the cerebral circulation to hypercapnia have also been reported in other species. Vis and Folgering (34) measured vertebral artery flow response to step increases and step decreases in PET<sub>CO<sub>2</sub></sub> in anesthetized cats. A first-order model was fitted to the time course of the blood flow response. After an initial time delay of 5 s, cerebral blood flow increased with a time constant of 339 ± 145 (SD) s, whereas the time constant for the off response was 8.3 times faster (41 ± 18 s). These findings generally are in accord with the pure delay and the asymmetry of the response to hypercapnia that we observe in our conscious human subjects.

#### *Mechanisms of Control of Cerebral Blood Flow*

This study provides no direct evidence in support of any particular underlying mechanism of regulation of MCAF. Mostly, this regulation is accomplished by variations in pial arteriolar tone, inasmuch as the pial arteries form the main resistance vessels (12). However, our study provides useful information on the time course and form of the dynamic response of the cerebral circulation. Putative mechanisms need to be consistent with these findings.

*Hypoxia.* The exact mechanism by which hypoxia acts to dilate cerebral pial arterioles remains unclear, but it may involve a direct effect of a low PO<sub>2</sub> on the smooth muscle of the pial arterioles and an indirect effect causing the release of vasodilator metabolites. Adenosine has been suggested as a potential metabolite, but its role remains controversial (24, 35). Recent studies suggest that the mechanism of action may involve shear stress and the production of nitric oxide (19) and the activation of ATP-sensitive (24, 32) potassium channels.

**Hypercapnia.** It is generally thought that the effects of CO<sub>2</sub> on the cerebral circulation operate via the direct effects of extracellular pH on the smooth muscle of cerebral pial vessels (12). The exact way by which H<sup>+</sup> is thought to dilate cerebral vessels is still unclear, although underlying mechanisms of regulation may include an effect of H<sup>+</sup> on membrane fluxes of Ca<sup>2+</sup> (20), the production of nitric oxide (14), and the activation of ATP-sensitive potassium channels (8). Possible sources of nitric oxide production during hypercapnia include the endothelial, neural, and glial cells (9). It has also been proposed that stimuli promoting nitric oxide synthesis from the endothelium may be the shear forces associated with blood flow (10).

We acknowledge the skilled technical assistance from David O'Connor and the volunteers for their participation in the study.

This study was supported by the Wellcome Trust. M. J. Poulin was supported by a Medical Research Council (Canada) postdoctoral research fellowship.

Address for reprint requests: P. A. Robbins, University Laboratory of Physiology, Parks Rd., Oxford OX1 3PT, UK.

Received 29 November 1995; accepted in final form 9 April 1996.

#### REFERENCES

- Aaslid, R., T. Markwalder, and H. Nornes. Noninvasive transcranial Doppler ultrasound recording of flow velocity in basal cerebral arteries. *J. Neurosurg.* 57: 769–774, 1982.
- Aaslid, R., D. W. Newell, R. Stooss, W. Sorteberg, and K. F. Lindegaard. Assessment of cerebral autoregulation dynamics from simultaneous arterial and venous transcranial Doppler recordings in humans. *Stroke* 22: 1148–1154, 1991.
- Arts, M. G. J., and J. M. J. G. Roevros. On the instantaneous measurement of blood flow by ultrasonic means. *Med. Biol. Eng.* 10: 23–34, 1972.
- Borgstrom, L., H. Johannsson, and B. K. Siesjo. The relationship between arterial PO<sub>2</sub> and cerebral blood flow in hypoxic hypoxia. *Acta Physiol. Scand.* 93: 423–432, 1975.
- Cohen, P. J., S. C. Alexander, T. C. Smith, M. Reivich, and H. Wollman. Effects of hypoxia and normocarbina on cerebral blood flow and metabolism in conscious man. *J. Appl. Physiol.* 23: 183–189, 1967.
- Doblar, D. D., B. G. Min, R. W. Chapman, E. R. Harbach, W. Welkowitz, and N. H. Edelman. Dynamic characteristics of cerebral blood flow response to sinusoidal hypoxia. *J. Appl. Physiol.* 46: 721–729, 1979.
- Ellingsen, I., A. Hauge, G. Nicolaysen, M. Thoresen, and L. Walloe. Changes in human cerebral blood flow due to step changes in PAO<sub>2</sub> and PACO<sub>2</sub>. *Acta Physiol. Scand.* 129: 157–163, 1987.
- Faraci, F. M., K. R. Breese, and D. D. Heistad. Cerebral vasodilation during hypercapnia. Role of glibenclamide-sensitive potassium channels and nitric oxide. *Stroke* 25: 1679–1683, 1994.
- Faraci, F. M., and J. E. J. Brian. Nitric oxide and the cerebral circulation. *Stroke* 25: 692–703, 1994.
- Gaw, A. J., and J. A. Bevar. Flow-induced relaxation of the rabbit middle cerebral artery is composed of both endothelium-dependent and -independent components. *Stroke* 24: 105–110, 1993.
- Hauge, A., M. Thoresen, and L. Walloe. Changes in cerebral blood flow during hyperventilation and CO<sub>2</sub>-breathing measured transcutaneously in humans by a bidirectional, pulsed, ultrasound Doppler blood velocimeter. *Acta Physiol. Scand.* 110: 167–173, 1980.
- Heistad, D. D., and H. A. Kontos. Cerebral circulation. In: *Handbook of Physiology. The Cardiovascular System. Peripheral Circulation and Organ Blood Flow.* Bethesda, MD: Am. Physiol. Soc., 1983, sect. 2, vol. III, p. 137–182.
- Howson, M. G., S. Khamnei, M. E. McIntyre, D. F. O'Connor, and P. A. Robbins. A rapid computer controlled binary gas mixing system for studies in respiratory control (Abstract). *J. Physiol. Lond.* 403: 103P, 1987.
- Iadecola, C. Does nitric oxide mediate the increases in cerebral blood flow elicited by hypercapnia? *Proc. Natl. Acad. Sci. USA* 89: 3913–3916, 1992.
- Jennett, S., L. H. Pitts, and J. B. North. Rapid cerebral vasodilation in brief hypoxia in anaesthetized animals. *Q. J. Exp. Physiol.* 66: 447–463, 1981.
- Kety, S. S., and C. F. Schmidt. The effects of altered arterial tensions of carbon dioxide and oxygen on cerebral blood flow and cerebral oxygen consumption of normal young men. *J. Clin. Invest.* 27: 484–492, 1948.
- Kirkham, F. J., T. S. Padayachee, S. Parsons, L. S. Seargeant, F. R. House, and R. G. Gosling. Transcranial measurement of blood velocities in the basal cerebral arteries using pulsed Doppler ultrasound: velocity as an index of flow. *Ultrasound Med. Biol.* 12: 15–21, 1986.
- Kontos, H. A. Validity of cerebral arterial blood flow calculations from velocity measurements. *Stroke* 20: 1–3, 1989.
- Kuo, L., M. J. Davis, and W. M. Chilian. Endothelial modulation of arterial tone. *News Physiol. Sci.* 7: 5–10, 1992.
- Kuschinsky, W., and M. Wahl. Local chemical and neurogenic regulation of cerebral vascular resistance. *Physiol. Rev.* 58: 656–689, 1978.
- Olesen, J., O. B. Paulson, and N. A. Lassen. Regional cerebral blood flow in man determined by the initial slope of the clearance of intra-arterially injected <sup>133</sup>Xe. *Stroke* 2: 519–540, 1971.
- Padayachee, T. S., F. J. Kirkham, R. R. Lewis, J. Gillard, M. C. E. Hutchinson, and R. G. Gosling. Transcranial measurement of blood velocities in the basal cerebral arteries using pulsed Doppler ultrasound: a method of assessing the circle of Willis. *Ultrasound Med. Biol.* 12: 5–14, 1986.
- Painter, R., S. Khamnei, and P. A. Robbins. A mathematical model of the human ventilatory response to isocapnic hypoxia. *J. Appl. Physiol.* 74: 2007–2015, 1993.
- Reid, J. M., A. G. Davies, F. M. Ashcroft, and D. J. Paterson. Effect of L-NMMA, cromakalim, and glibenclamide on cerebral blood flow in hypercapnia and hypoxia. *Am. J. Physiol.* 269 (Heart Circ. Physiol. 38): H916–H922, 1995.
- Reivich, M. Arterial PCO<sub>2</sub> and cerebral hemodynamics. *Am. J. Physiol.* 206: 25–35, 1964.
- Robbins, P. A., G. D. Swanson, and M. G. Howson. A prediction correction scheme for forcing alveolar gases along certain time courses. *J. Appl. Physiol.* 52: 1353–1357, 1982.
- Severinghaus, J. W. Proposed standard determination of ventilatory responses to hypoxia and hypercapnia in man. *Chest* 1, Suppl.: 129–131, 1976.
- Shapiro, W., A. J. Wasserman, J. P. Baker, and J. L. Patterson. Cerebrovascular response to acute hypocapnic and eucapnic hypoxia in man. *J. Clin. Invest.* 49: 2362–2368, 1970.
- Shapiro, W., A. J. Wasserman, and J. L. Patterson. Human cerebrovascular response time to elevation of arterial carbon dioxide tension. *Arch. Neurol.* 13: 130–138, 1965.
- Shapiro, W., A. J. Wasserman, and J. L. Patterson. Human cerebrovascular response to combined hypoxia and hypercapnia. *Circ. Res.* 19: 903–910, 1966.
- Swanson, G. D., and J. W. Bellville. Step changes in end-tidal CO<sub>2</sub>: methods and implications. *J. Appl. Physiol.* 39: 377–385, 1975.
- Taguchi, H., D. D. Heistad, T. Kitazono, and F. M. Faraci. ATP-sensitive K<sup>+</sup> channels mediate dilatation of cerebral arterioles during hypoxia. *Circ. Res.* 74: 1005–1008, 1994.
- Van Beek, J. H. G. M., A. Berkenbosch, J. DeGoede, and C. N. Olievier. Response of vertebral and carotid blood flow to isocapnic changes in end-tidal oxygen tension. *Respir. Physiol.* 63: 65–77, 1986.
- Vis, A., and H. Folgering. The dynamic effect of PETCO<sub>2</sub> on vertebral blood flow in cats. *Respir. Physiol.* 42: 131–143, 1980.
- Winn, H. R., R. Rubio, and R. M. Berne. Brain adenosine concentration during hypoxia in rats. *Am. J. Physiol.* 241 (Heart Circ. Physiol. 10): H235–H242, 1981.

## **CHAPTER 4**

### **FAST AND SLOW COMPONENTS OF CEREBRAL BLOOD FLOW RESPONSE TO STEP DECREASES IN END-TIDAL PCO<sub>2</sub> IN HUMANS**

Poulin, M.J., P.-J. Liang and P.A. Robbins (1998)  
*J. Appl. Physiol.* **85**:388-397

## PREFACE

The previous Chapter described the dynamics of the cerebral blood flow response to hypoxia and hypercapnia. While it has become fairly straightforward to use the technique of dynamic end-tidal forcing to administer hypercapnic and hypoxic steps, the question of administering step decreases in carbon dioxide (i.e. hypocapnia) is not quite as simple. This came to our attention while writing up the studies described in Chapters 2 and 3 and realising that the existing literature was void of any accurate description of the dynamics of the cerebral blood flow response to hypocapnia. In order to address this question, we again combined the two techniques described in Chapters 2 and 3. However in order to obtain a stable level of hypocapnia, it was necessary to add a technique of controlled voluntary hyperventilation.

This Chapter describes the dynamics of cerebral blood flow in response to sustained euoxic hypocapnia. The first few experiments revealed the presence of some secondary recovery of cerebral blood flow over time. Thus, a model was fit to the data to provide gain terms, time-constants, and a delay for the response to the onset and relief of hypocapnia as well as a gain term and a time-constant for a second slower component.

## DECLARATION

The work presented in this chapter was carried out over a two-year period in the University Laboratory of Physiology. This study was conceived, designed and planned by Professor Peter Robbins and myself. I carried out the experiments and the data analysis. Dr. John G. Tansley helped with some of the data collection. Dr. Pei-Ji Liang helped with the mathematical modelling. Professor Robbins and I wrote the resulting paper. Results of this study were presented in part at the 10<sup>th</sup> International Symposium on Cerebral Hemodynamics in Association with the 1<sup>st</sup> Meeting of the European Society of Neurosonology and Cerebral Hemodynamics (Munich, Germany) and at the Canadian Conference on Modelling and Control of Ventilation (VII<sup>TH</sup> Oxford Conference, Huntsville, Canada). Results were published in abstract form in *Cerebrovascular Diseases* (6(suppl 3):31, 1996) and in *Advances in Modeling and Control of Ventilation* (in press). A book chapter also emerged from this study (In: *New Trends in Cerebral Hemodynamics and Neurology*, Eds: J. Klingelhöfer et al., Elsevier Science, pp. 563-569, 1997).

# Fast and slow components of cerebral blood flow response to step decreases in end-tidal PCO<sub>2</sub> in humans

MARC J. POULIN, PEI-JI LIANG, AND PETER A. ROBBINS

University Laboratory of Physiology, Parks Road, Oxford OX1 3PT, United Kingdom

**Poulin, Marc J., Pei-Ji Liang, and Peter A. Robbins.** Fast and slow components of cerebral blood flow response to step decreases in end-tidal PCO<sub>2</sub> in humans. *J. Appl. Physiol.* 85(2): 388–397, 1998.—This study examined the dynamics of the middle cerebral artery (MCA) blood flow response to hypocapnia in humans ( $n = 6$ ) by using transcranial Doppler ultrasound. In a control protocol, end-tidal PCO<sub>2</sub> (PETCO<sub>2</sub>) was held near eucapnia (1.5 Torr above resting) for 40 min. In a hypocapnic protocol, PETCO<sub>2</sub> was held near eucapnia for 10 min, then at 15 Torr below eucapnia for 20 min, and then near eucapnia for 10 min. During both protocols, subjects hyperventilated throughout and PETCO<sub>2</sub> and end-tidal PO<sub>2</sub> were controlled by using the dynamic end-tidal forcing technique. Beat-by-beat values were calculated for the intensity-weighted mean velocity ( $\bar{V}_{IWM}$ ), signal power ( $\bar{P}$ ), and their instantaneous product ( $\bar{P} \cdot \bar{V}_{IWM}$ ). A simple model consisting of a delay, gain terms, time constants ( $\tau_{f,on}$ ,  $\tau_{f,off}$ ) and baseline levels of flow for the on- and off-transients, and a gain term ( $g_s$ ) and time constant ( $\tau_s$ ) for a second slower component was fitted to the hypocapnic protocol. The cerebral blood flow response to hypocapnia was characterized by a significant ( $P < 0.001$ ) slow progressive adaptation in  $\bar{P} \cdot \bar{V}_{IWM}$ , with  $g_s = 1.26$  %/Torr and  $\tau_s = 427$  s, that persisted throughout the hypocapnic period. Finally, the responses at the onset and relief of hypocapnia were asymmetric ( $P < 0.001$ ), with  $\tau_{f,on}$  (6.8 s) faster than  $\tau_{f,off}$  (14.3 s).

transcranial Doppler; hypocapnia; modeling

response to 20 min of euoxic hypocapnia, in particular to determine the time course of any adaptation in cerebral blood flow over time. To quantify the dynamics of the response, a simple model was fit to the data to provide gain terms, time constants, and a pure time delay for the response to the onset and relief of hypocapnia as well as a gain term and a time constant for a second slower component.

## METHODS

### Glossary

$V_P$	Instantaneous (10-ms) value for the velocity associated with the maximum frequency of the Doppler shift
$V_{IWM}$	Instantaneous (10-ms) value for the velocity associated with the intensity-weighted mean frequency of the Doppler spectrum
$P$	Instantaneous (10-ms) value for the total power (arbitrary units) of the Doppler spectrum
$P \cdot V_{IWM}$	Instantaneous (10-ms) product of $V_{IWM}$ and $P$
$\bar{V}_P$	Mean for $V_P$ averaged over the cardiac cycle
$\bar{V}_{IWM}$	Mean for $V_{IWM}$ , averaged over the cardiac cycle
$\bar{P}$	Mean for $P$ , averaged over the cardiac cycle
$\bar{P} \cdot \bar{V}_{IWM}$	Mean for $P \cdot V_{IWM}$ , averaged over the cardiac cycle

### Subjects

Six healthy young adults volunteered to take part in this study. The study requirements were fully explained in written and verbal forms to all participants, and each gave informed consent before participation in the study. The research was approved by the Central Oxford Research Ethics Committee. At the first session, each participant was given a brief examination that included measurements of heart rate, blood pressure, height, and weight. Participants were not on any medication, all were normotensive, and none had a history of cardiovascular, cerebrovascular, or respiratory disease. At the completion of each experimental test, subjects were asked to complete a questionnaire on symptoms associated with hypocapnia (7).

### Protocols

Each participant visited the laboratory, at the same time of day, on four or five occasions, each lasting 3–4 h. Subjects were requested not to eat or drink caffeine-containing beverages within 4 h before their scheduled testing sessions in the laboratory. On each day, before the experiments began, room air measurements of resting Doppler signals and end-tidal PCO<sub>2</sub> (PETCO<sub>2</sub>) were collected. For these measurements, the subjects' natural PETCO<sub>2</sub> was measured by using a nasal catheter.

Two protocols were employed: the control protocol (*protocol I*) and the hypocapnic protocol (*protocol II*). On each day, either one or two repeats of each protocol were undertaken. During both protocols, subjects hyperventilated throughout, and PETCO<sub>2</sub> and end-tidal PO<sub>2</sub> (PETO<sub>2</sub>) were controlled by using the dynamic end-tidal forcing technique.

IT IS WELL KNOWN THAT cerebral blood flow decreases with hypocapnia (11, 20, 32, 34, 35). However, measurements of cerebral blood flow a few hours after the induction of hypocapnia suggest that there is some secondary recovery of cerebral blood flow over time. The time course associated with this is uncertain. One report suggests that there is an adaptation of carotid artery flow to both hyper- and hypocapnia over 20 min (10), but in a previous study we were unable to reproduce that finding for hypercapnia in the middle cerebral artery, where blood flow remained constant after the initial rise (27).

To address the question of the time course of adaptation over time with sustained hypocapnia, two particular methodological problems have to be addressed. First, a stable level of hypocapnia has to be obtained, and, second, a continuous measure of cerebral blood flow has to be employed. In this study, the technique of combining hyperventilation with dynamic end-tidal forcing (16, 33) has been employed to address the first issue. To obtain continuous measurements of cerebral blood flow, transcranial Doppler ultrasound has been employed, suitably modified to allow for any changes in cross-sectional area that might occur (27, 28).

Thus the purpose of the present study is to examine the dynamics of the middle cerebral artery blood flow in

In *protocol I*,  $PET_{O_2}$  was held at 100 Torr and  $PET_{CO_2}$  was held 1.5 Torr above the subject's normal value for 40 min. *Protocol II* started with an 11-min period when  $PET_{O_2}$  was held at 100 Torr and  $PET_{CO_2}$  was held 1.5 Torr above the subject's natural value as determined on that day. Then,  $PET_{CO_2}$  was decreased rapidly (over a few breaths) by 15.0 Torr (i.e., by 13.5 Torr below the subject's normal value), while  $PET_{O_2}$  continued to be held at 100 Torr and maintained constant for 20 min. Finally,  $PET_{CO_2}$  was returned (within 1 or 2 breaths) to its initial near-eucapnic value and maintained constant for a further 10 min.

#### *Hyperventilation and Control of $PET_{CO_2}$*

Throughout each protocol, subjects sat in a chair and hyperventilated in a controlled manner through their mouth with their nose occluded. Respiratory volumes were measured with a turbine volume transducer, (17) and respiratory gas composition was measured by mass spectrometry. The level of hyperventilation necessary to ensure that rapid reductions in  $PET_{CO_2}$  could be achieved at the onset of hypocapnia was determined in preliminary experiments. It was found to be  $\sim 30$  l/min and was achieved with a breathing frequency of 24 breaths/min and a tidal volume of 1.25 l/breath. The desired breathing frequency was achieved by use of auditory cues from a metronome, whereas the desired tidal volume was achieved by use of visual feedback from an oscilloscope, calibrated to display the volume of each inspiration.

Accurate control of the end-tidal gases was achieved by using the technique of dynamic end-tidal forcing (16, 33). At the start of the experiment, a controlling computer generated the inspired partial pressures predicted to give the desired end-tidal partial pressures by using a fast gas-mixing system (16). The controlling computer receives feedback of the measured end-tidal partial pressures on a breath-by-breath basis as the experiment progresses. These measured end-tidal values are compared with the desired values, and the computer then adjusts the initial predicted inspired gas mixture by using an integral proportional feedback algorithm based on the deviations of the measured end-tidal values from the desired end-tidal values.

#### *Measurement of Cerebral Blood Flow*

A 2-MHz pulsed Doppler ultrasound system (PCDop 842, SciMed) was used to measure backscattered Doppler signals from the right middle cerebral artery. The Doppler system was adapted to make the Doppler signals (maximum and intensity-weighted mean Doppler frequency shifts and total power) available as analog signals. These were updated each time a new spectrum was calculated every 10 ms. The signals were sampled every 10 ms by using a data-acquisition package (DAQWare, National Instruments) running on another computer. These signals, along with the occurrence of each QRS complex from an electrocardiogram attached to the subject, were logged to the computer and saved for later analysis.

The middle cerebral artery was identified by an insonation pathway through the right temporal window just above the zygomatic arch by using search techniques described previously (1, 24). Optimization of the Doppler signals from the middle cerebral artery was performed by varying the sample volume depth in incremental steps and, at each depth, varying the angle of insonance to obtain the best-quality signals for the Doppler frequency shifts that corresponded with the maximum power signal. The probe was secured in a headband device (Müller and Moll Fixation, Nicolet Instru-

ments) to ensure optimal insonation position and angle for the duration of the experiment.

For each cardiac cycle, mean values for the velocity associated with the maximum frequency of the Doppler shift ( $\bar{V}_p$ ), the intensity-weighted mean velocity ( $\bar{V}_{IWM}$ ), signal power ( $\bar{P}$ ), and the product of the 10-ms values for these variables ( $\bar{P} \cdot \bar{V}_{IWM}$ ) were calculated. The total power of the signal is proportional to cross-sectional area (3), and so the proposed index ( $\bar{P} \cdot \bar{V}_{IWM}$ ) allows for any changes that occur in the cross-sectional area of the vessel. Additionally, taking the product of the 10-ms values to obtain the index ( $\bar{P} \cdot \bar{V}_{IWM}$ ) allows for any systematic change in diameter throughout the cardiac cycle.

#### *Modeling Cerebral Blood Flow Responses to Hypocapnia*

In a previous study (27), we developed a simple one-compartment model for the cerebrovascular response to hypercapnia that can be written as

$$d\dot{Q}_f/dt = 1/\tau_f [g_f [PET_{CO_2}(t - T_d) - PET_{CO_2}^*] - \dot{Q}_f] \quad (1)$$

and

$$MCAF = \dot{Q}_f + MCAF^* \quad (2)$$

where in *Eq. 1*  $\dot{Q}_f$  is the fast component of the response in middle cerebral artery flow to changes in  $PET_{CO_2}$ ,  $\tau_f$  is a time constant,  $g_f$  is a gain term,  $PET_{CO_2}(t - T_d)$  is the input function for  $PET_{CO_2}$ ,  $T_d$  is a pure delay, and  $PET_{CO_2}^*$  is the control  $PET_{CO_2}$  for the subject. In *Eq. 2*, MCAF is middle cerebral artery flow and MCAF\* is the middle cerebral artery flow when  $PET_{CO_2} = PET_{CO_2}^*$  (the control  $PET_{CO_2}$  for the subject). This model has been rewritten slightly compared that in with our previous study (27) by replacing MCAF in the original differential equation with MCAF\* +  $\dot{Q}_f$  and defining MCAF in a separate equation (*Eq. 2*). The model gives an exponential output for a step input.

The differential equation (*Eq. 1*) may be solved to provide a difference equation that supplies a series of values for  $\dot{Q}_f$  on a beat-by-beat basis, provided that we assume that the input function can be regarded as constant over any single heart-beat.  $\dot{Q}_f$  for the  $n + 1$  beat may be calculated from  $\dot{Q}_f$  for the  $n$ th beat, together with the value for the input function for this beat, and we may write

$$\begin{aligned} \dot{Q}_{f,n+1} = & g_f [PET_{CO_2}(t_{n+1} - T_d) - PET_{CO_2}^*] \\ & - [g_f [PET_{CO_2}(t_n - T_d) - PET_{CO_2}^*] - \dot{Q}_{f,n}] \exp^{-(t_{n+1} - t_n)/\tau_f} \end{aligned} \quad (3)$$

and

$$MCAF_n = \dot{Q}_{f,n} + MCAF^* \quad (4)$$

In the present study the data suggest that a second compartment is required in the model (see RESULTS). This equation can be written as

$$d\dot{Q}_s/dt = 1/\tau_s [g_s [PET_{CO_2}(t - T_d) - PET_{CO_2}^*] - \dot{Q}_s] \quad (5)$$

where  $\dot{Q}_s$  is the slow component of the middle cerebral artery flow in response to changes in  $PET_{CO_2}$ ,  $\tau_s$  is a time constant, and  $g_s$  is a gain term. The total flow is given by

$$MCAF = \dot{Q}_f + \dot{Q}_s + MCAF^* \quad (6)$$

The differential equation (*Eq. 5*) may be solved to provide a difference equation that supplies a series of values for  $\dot{Q}_s$  on a

beat-by-beat basis and we may write

$$\begin{aligned} \dot{Q}_{s,n+1} = & g_s[\text{PET}_{\text{CO}_2}(t_{n+1} - T_d) - \text{PET}_{\text{CO}_2}^*] \\ & - [g_s[\text{PET}_{\text{CO}_2}(t_{n+1} - T_d) - \text{PET}_{\text{CO}_2}^*] - \dot{Q}_{s,n}] \exp^{-(t_{n+1}-t_n)/\tau_s} \end{aligned} \quad (7)$$

Finally, middle cerebral artery flow for the  $n + 1$  beat may be calculated as

$$\text{MCAF}_n = \text{MCAF}^* + \dot{Q}_{f,n} + \dot{Q}_{s,n} \quad (8)$$

#### Parameter Estimation Process

To allow for the asymmetry between the on- and off-transients (27), separate parameter values were estimated for the fast component of the on- and off-transients. The switch between the on- and off-parameters was undertaken in the middle of the 20-min period of hypocapnia. This resulted in nine parameters for estimation, namely, gain terms for the on- and off-transients ( $g_{f,\text{on}}$ ,  $g_{f,\text{off}}$ ); time constants for the on- and off-transients ( $\tau_{f,\text{on}}$ ,  $\tau_{f,\text{off}}$ ); baseline terms for the on- and off-transients ( $\text{MCAF}_{\text{on}}^*$ ,  $\text{MCAF}_{\text{off}}^*$ ); a single pure time delay ( $T_d$ ); and a slow component describing the adaptation of cerebral blood flow during hypocapnia that was composed of a gain term ( $g_s$ ) and a time constant ( $\tau_s$ ).

Eight of the parameters ( $g_{f,\text{on}}$ ,  $g_{f,\text{off}}$ ,  $g_s$ ,  $\tau_{f,\text{on}}$ ,  $\tau_{f,\text{off}}$ ,  $\tau_s$ ,  $\text{MCAF}_{\text{on}}^*$ , and  $\text{MCAF}_{\text{off}}^*$ ) were estimated by using a routine for minimizing a sum of squares. The ninth parameter ( $T_d$ ) was determined by minimizing the sum of squares for the other eight parameters for a set of fixed pure delays ranging between 0 and 20 s in steps of 1 s. The estimated pure delay is the value that is associated with the lowest value for the sum of squares from these minimization procedures.

The model input was the breath-by-breath  $\text{PET}_{\text{CO}_2}$ . Values at times between breaths were obtained by linear interpolation. The model output was compared with the data on a beat-by-beat basis to determine the residuals, and no averaging was employed. A single set of parameter values was determined for each repetition for a single subject by minimizing the sum of squared residuals for each repetition. For each repetition, this totaled between ~2,000 and 3,000 residuals (1 for each heartbeat). The data employed for parameter estimation included a 2-min prehypocapnic period, the 20-min hypocapnic period, and the 10-min recovery period.

The particular routine employed for the minimization was taken from the Numerical Algorithms Group (Oxford, UK) FORTRAN library, subroutine E04FDF. This routine is designed to minimize a nonlinear function of a number of variables when that function takes the special form of a sum of squares. All parameters (except the gain of the slow component) in the cost function were constrained to be positive. The routine required initial guesses to be made for the parameters of the model. The guesses were based partly on visual inspection of the data and partly on a knowledge of the range of likely values where previous information was available. A number of such starting points was employed in each case to try to determine whether there were multiple minima. In every case, only a single minimum was detected.

## RESULTS

### General

The six subjects who undertook the study had an average age of  $23.0 \pm 4.9$  (SD) yr, an average height of  $181.6 \pm 4.1$  cm, and an average weight of  $69.9 \pm 4.1$  kg. None had a history of cardiovascular or respiratory

disease, and all had normal systolic ( $115.3 \pm 7.7$  mmHg) and diastolic ( $75.7 \pm 6.6$  mmHg) blood pressure. Each subject attended the laboratory on at least four or five occasions. On a few occasions, repetitions were spoiled and were therefore repeated during extra visits.

After each experimental test, subjects completed a short questionnaire on symptoms associated with hypocapnia. Symptoms, rated on a six-point scale (from 0 = absent to 5 = severe), included sweating, chest pains, tingling fingers/toes, tingling lips, muscle cramps, light-headedness, dizziness, headache, warmth, cold, effort of breathing, irritability, and drowsiness. On the six-point scale, two symptoms, tingling fingers/toes and light-headedness, were rated significantly higher during hypocapnia (1.6 and 2.5, respectively) than during eucapnia (0.1 and 0.0, respectively), with paired  $t$ -tests.

Table 1 lists the individual values and the group mean for the depth of the Doppler sample volume at which the main segment of the middle cerebral artery was insonated. Small variations in depth among subjects are attributable to differences in skull size (24). Small variations in depth within each subject represent day-to-day differences in the experimenter's determination of the best-quality Doppler signals because the optimization of signals was performed on each visit without any reference to results from previous visits. The test-to-test individual variations in  $\bar{V}_P$  and  $\bar{V}_{\text{TWM}}$ , together with the associated  $\text{PET}_{\text{CO}_2}$ , are listed in Table 2.

### Quality of Input Stimuli

Figure 1 shows responses for one repetition of each protocol in one subject (*subject 951*). This figure illustrates the quality of control exerted over  $\text{PET}_{\text{O}_2}$  and  $\text{PET}_{\text{CO}_2}$  that can be achieved by using the dynamic end-tidal forcing technique in combination with voluntary hyperventilation. Both the onset of hypocapnia and the recovery from hypocapnia were rapid, and the level of hypocapnia was well controlled throughout the hypocapnic period.

Figure 2 shows ensemble averages of the time-related changes in  $\text{PET}_{\text{O}_2}$  and  $\text{PET}_{\text{CO}_2}$  for each subject and for each protocol. Each profile represents an average of six repetitions. Figure 2 shows that good control over the end-tidal gases was achieved, although some

Table 1. Distance (depth) from probe to start of Doppler sample volume for detecting signals from middle cerebral artery for each subject

Subject No.	MCA Depth, cm
951	$4.94 \pm 0.15$
964	$4.87 \pm 0.25$
966	$4.87 \pm 0.06$
967	$4.99 \pm 0.04$
971	$4.92 \pm 0.02$
1009	$4.64 \pm 0.27$
Group mean	$4.87 \pm 0.12$

Values are means  $\pm$  SD. MCA, middle cerebral artery.

Table 2. Test-to-test variability in middle cerebral blood flow velocities together with associated  $PET_{CO_2}$  of each repetition, for each subject

Repetition No.	$PET_{CO_2}$ , Torr	$\bar{V}_P$ , cm/s	$\bar{V}_{IWM}$ , cm/s	$PET_{CO_2}$ , Torr	$\bar{V}_P$ , cm/s	$\bar{V}_{IWM}$ , cm/s	$PET_{CO_2}$ , Torr	$\bar{V}_P$ , cm/s	$\bar{V}_{IWM}$ , cm/s	$PET_{CO_2}$ , Torr	$\bar{V}_P$ , cm/s	$\bar{V}_{IWM}$ , cm/s	$PET_{CO_2}$ , Torr	$\bar{V}_P$ , cm/s	$\bar{V}_{IWM}$ , cm/s	$PET_{CO_2}$ , Torr	$\bar{V}_P$ , cm/s	$\bar{V}_{IWM}$ , cm/s
	Subject 951			Subject 964			Subject 966			Subject 967			Subject 971			Subject 1009		
1	40.0	44.0	28.7	43.5	59.1	39.3	42.0	62.6	34.6	38.6	73.9	50.2	37.1	48.4	32.7	44.0	52.3	37.3
2	40.0	44.7	27.5	43.6	58.9	39.5	42.0	60.6	34.0	38.6	68.7	45.8	37.0	44.7	31.2	42.0	44.9	31.0
3	40.1	49.5	33.5	43.6	58.3	39.0	42.0	61.8	35.2	39.5	69.1	46.6	38.0	57.2	39.8	42.0	43.2	27.3
4	40.0	43.9	29.1	43.5	54.4	34.2	41.0	74.3	43.7	39.7	65.0	46.0	38.0	57.6	39.7	42.1	44.3	26.1
5	40.0	47.0	27.9	43.5	54.1	31.7	41.1	74.0	45.6	40.5	71.2	47.9	37.7	48.8	33.2	41.0	45.2	29.0
6	40.0	47.8	31.2	43.6	55.6	26.3	41.5	71.0	41.3	40.5	65.4	45.1	36.4	49.8	34.2	41.1	53.6	34.4
7	40.0	50.6	33.6	43.5	48.9	30.4	41.5	71.0	44.5	40.5	63.7	43.7	36.5	50.7	35.4	41.0	39.1	26.4
8	40.0	61.2	41.8	43.4	51.9	32.2	40.0	68.4	41.2	39.5	68.7	44.6	37.1	52.6	34.5	41.0	41.5	27.7
9	40.0	59.7	40.7	43.4	54.4	33.6	40.0	67.2	40.4	39.0	66.6	43.9	36.5	52.4	34.0	40.9	41.4	28.0
10	40.0	50.9	33.6	43.5	48.8	30.1	40.0	63.5	37.8	39.1	66.8	42.0	35.5	50.1	35.2	41.0	41.6	28.2
11	40.0	50.0	33.3	43.5	48.9	30.1	41.5	65.1	40.7	40.5	72.2	51.9	35.5	50.5	34.9	42.0	42.8	28.1
12	40.2	49.6	32.8	43.5	50.3	30.9	41.0	70.3	42.7	40.6	67.8	49.2	37.0	47.3	32.7	42.0	49.8	30.4
Mean	40.0	49.9	32.8	43.5	53.6	33.1	41.1	67.5	40.1	39.7	68.2	46.4	36.9	50.9	34.8	41.7	45.0	29.5
CV, %	0.2	11.1	13.9	0.1	7.3	12.7	1.9	7.0	9.8	2.0	4.5	6.3	2.3	7.4	7.5	2.1	10.2	11.4

Values for each repetition are 5-min means of beat-by-beat data.  $PET_{CO_2}$ , end-tidal  $PCO_2$ ;  $\bar{V}_P$ , mean for instantaneous (10-ms) value for velocity associated with maximum frequency of Doppler shift ( $V_P$ ) averaged over cardiac cycle;  $\bar{V}_{IWM}$ , mean for instantaneous (10-ms) value for velocity associated with intensity-weighted mean frequency of Doppler spectrum ( $V_{IWM}$ ) averaged over cardiac cycle; CV, coefficient of variation.

minor imperfections in the desired  $PET_{O_2}$  and  $PET_{CO_2}$  can be detected at the onset and relief of hypocapnia.

General Features of Cerebrovascular Responses

Figure 1 shows the responses for  $\bar{V}_{IWM}$ ,  $\bar{P}$ , and  $\bar{P} \cdot \bar{V}_{IWM}$  for one repetition of each protocol in one subject.  $\bar{P}$  and

$\bar{P} \cdot \bar{V}_{IWM}$  have been expressed as a percentage of a 5-min baseline immediately preceding *time 0* for each protocol. The control data illustrate the general level of stability that was achieved from the output of the Doppler system in a single experiment. The data from *protocol II* show that the responses to stimulation were

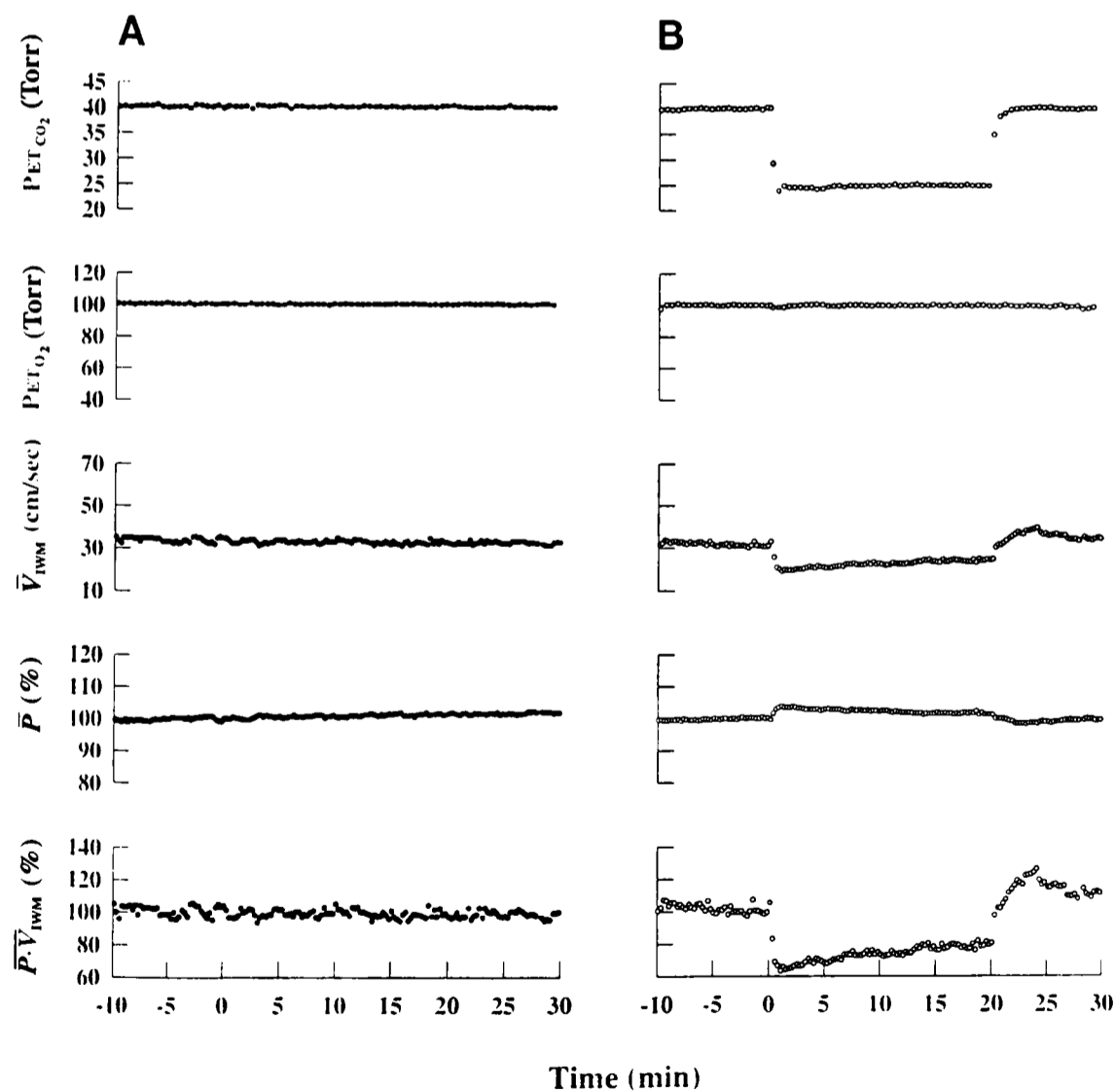


Fig. 1. Typical results for 1 repetition of each protocol for 1 subject (*subject 951*). A: control (●). B: hypocapnia (○).  $PET_{CO_2}$ , end-tidal  $PCO_2$ ;  $PET_{O_2}$ , end-tidal  $PO_2$ ;  $\bar{V}_{IWM}$ , middle cerebral artery velocity;  $\bar{P} \cdot \bar{V}_{IWM}$ , middle cerebral artery flow. Power ( $\bar{P}$ ) and  $\bar{P} \cdot \bar{V}_{IWM}$  are expressed as percentage of average value for 5-min period preceding *time 0*. Data for  $PET_{CO_2}$ ,  $PET_{O_2}$ ,  $\bar{V}_{IWM}$ ,  $\bar{P}$ , and  $\bar{P} \cdot \bar{V}_{IWM}$  are averaged over 15-s periods.

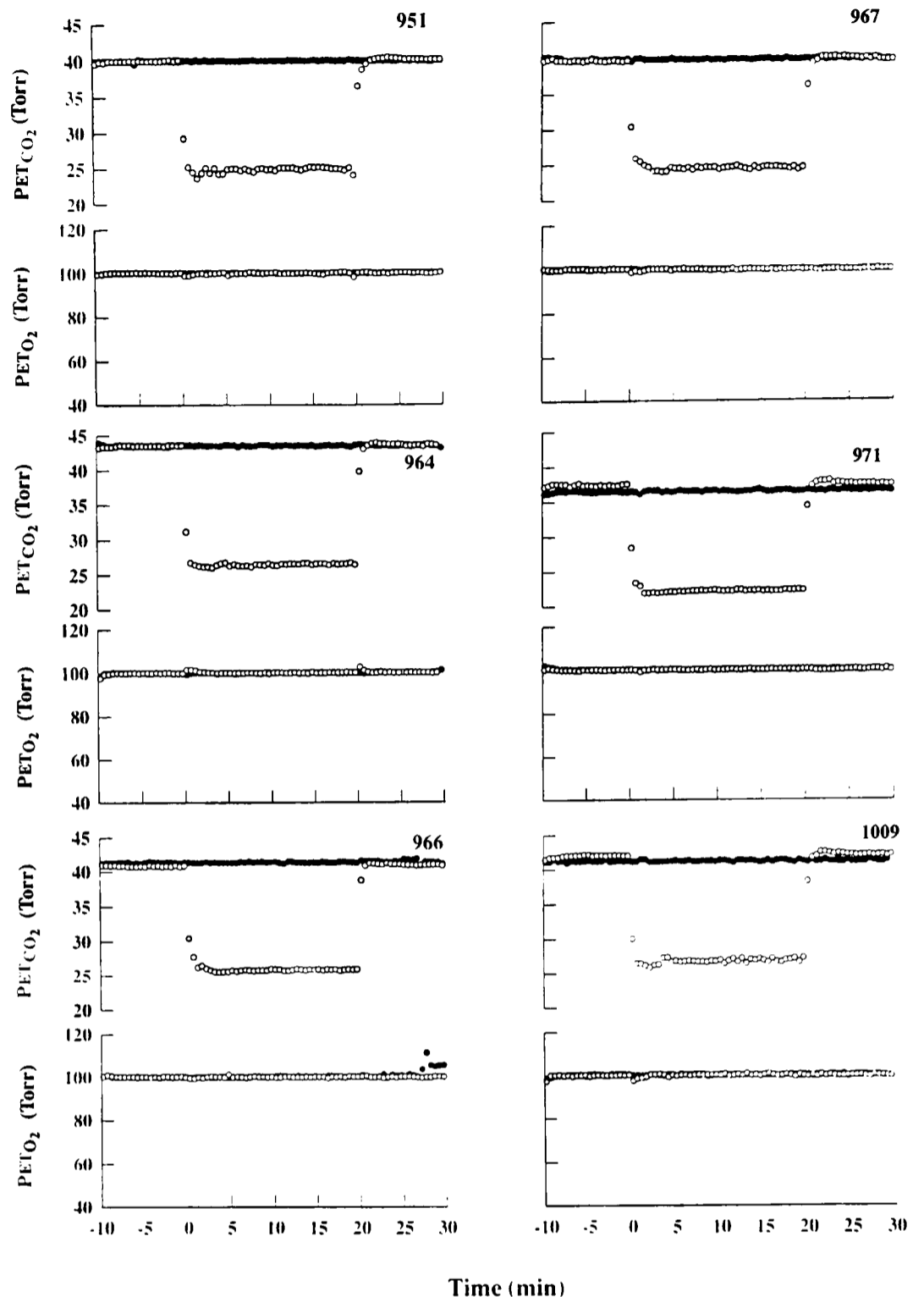


Fig. 2. Ensemble averages of time-related changes in  $PET_{O_2}$  and  $PET_{CO_2}$  for each subject (subjects 951, 964, 966, 967, 971, and 1009). ●, Control; ○, hypocapnia. Each symbol represents a 30-s mean.

readily discernible events within a single experimental protocol before any averaging. The response suggests the presence of some adaptation after the rapid responses at the onset and relief of hypocapnia.

Figure 3 shows ensemble averages of the responses for  $\bar{V}_{IWM}$ ,  $\bar{P}$ , and  $\bar{P} \cdot \bar{V}_{IWM}$  for each subject and for each protocol.  $\bar{P}$  and  $\bar{P} \cdot \bar{V}_{IWM}$  have been expressed as a percentage of a 5-min baseline immediately preceding *time 0*. First, the eupapnic control data show relatively stable values for  $\bar{V}_{IWM}$ ,  $\bar{P}$ , and  $\bar{P} \cdot \bar{V}_{IWM}$  throughout the experimental period. For the hypocapnic data, the profiles for the power signal appear to not change much from baseline values of 100%, although in general there appear to be slight increases in the power associated with initial period of hypocapnia. The most striking observation is that there are marked changes in  $\bar{V}_{IWM}$  and  $\bar{P} \cdot \bar{V}_{IWM}$  associated with the hypocapnia, the changes in

$\bar{V}_{IWM}$  and  $\bar{P} \cdot \bar{V}_{IWM}$  being similar against the background of relatively constant values for  $\bar{P}$ . Apart from the rapid and consistent changes at the onset and relief of hypocapnia, there appears to be adaptation throughout the period of hypocapnia, which is a consistent finding across all subjects. This adaptation process also appears to be present in the period after the relief of hypocapnia.

Average values for a range of variables obtained from the Doppler signals (both as absolute and as normalized values) are given in Table 3 for the 5 min preceding the induction of hypocapnia, the first 2 min of hypocapnia, the last 2 min of hypocapnia, and the last 2 min of the recovery period, together with the matching values for the eupapnic control data. For the eupapnic control data, there is little variation over these time periods. For the hypocapnic data, apart from the obvious fall in velocity with the induction of hypocapnia, there is a

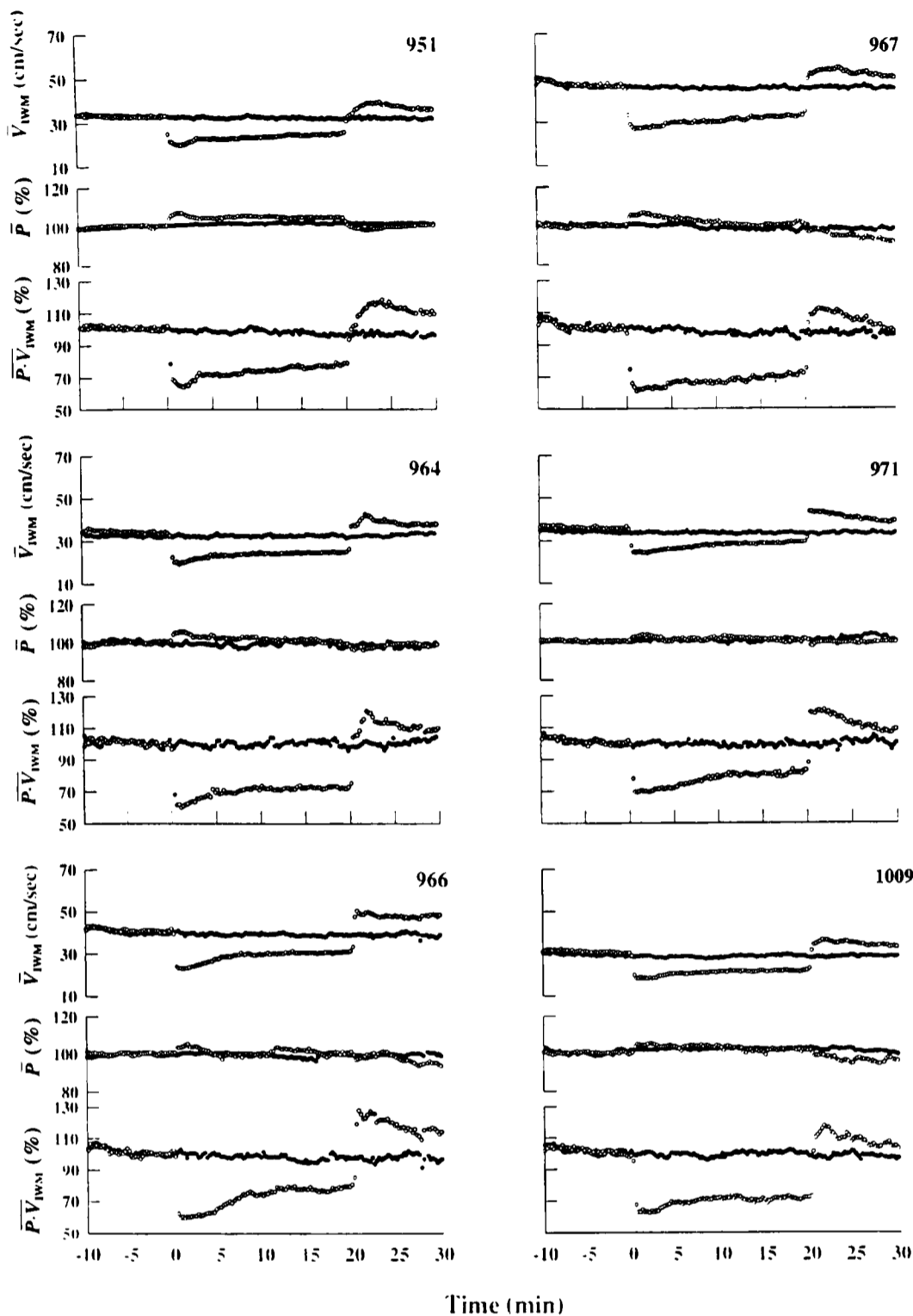


Fig. 3. Ensemble averages of  $\bar{V}_{IWM}$ ,  $\bar{P}$ , and  $\bar{P} \cdot \bar{V}_{IWM}$  responses for each subject. Symbols and subjects are defined as in Fig. 2. Each symbol represents a 15-s mean.

small rise in power that is nevertheless significant ( $P < 0.001$ , ANOVA). Similarly, after the relief of hypocapnia, there is a persistent, small reduction in power compared with control, which again is significant ( $P < 0.001$ , ANOVA).

The small change in power at the onset of hypocapnia is reflected in small but significant ( $P < 0.001$ , paired  $t$ -test) differences in the percent reductions in  $\bar{V}_{IWM}$  and  $\bar{V}_P$  compared with  $\bar{P} \cdot \bar{V}_{IWM}$ . No differences in the percent reductions between  $\bar{V}_{IWM}$  and  $\bar{V}_P$  were detected.

#### Dynamics of MCAF Responses to Hypocapnia

The fitted model output, averaged across individual repeats of the hypocapnic protocol within a subject, along with the averaged experimental data and the 95% confidence intervals for the ensemble-averaged

residuals, is shown for each subject in Fig. 4. The two-compartment model used to describe the data was devised following the observation that, in addition to the rapid responses at the onset and relief of hypocapnia, there also appeared to be a second, slower component to the response. This consistent feature in all subjects, is observed in Fig. 4.

The individual values and group means for the estimated model parameters are listed in Table 4. The  $\bar{P} \cdot \bar{V}_{IWM}$  responses to hypocapnia start after an estimated delay of 3.9 s. The time constant for the on-response is more than two times faster than the time constant for the off-response, and this difference is significant. The gain term for the on-response is significantly smaller than the gain term for the off-response, and this difference is significant. The baseline before

Table 3. Changes in velocities, flow index, and power during protocols

Variable	Baseline (minutes -5 to 0)	Stimulus 1 (minutes 0 to 2)	Stimulus 2 (minutes 18 to 20)	Recovery (minutes 28 to 30)
<i>Control (n = 6)</i>				
$\bar{V}_p$ , cm/s	55.3 ± 10.1	55.1 ± 10.4	54.2 ± 9.9	54.1 ± 10.0
$\bar{V}_{IWM}$ , cm/s	35.6 ± 6.3	35.5 ± 6.4	34.9 ± 6.1	34.8 ± 6.1
$\bar{P}$ , %	100.0 ± 0.0	100.2 ± 0.8	99.7 ± 1.7	99.7 ± 1.0
$\bar{V}_p$ , %	100.0 ± 0.0	99.5 ± 1.0	98.1 ± 1.7	97.8 ± 2.9
$\bar{V}_{IWM}$ , %	100.0 ± 0.0	99.5 ± 1.1	98.2 ± 2.0	98.0 ± 3.1
$\bar{P} \cdot \bar{V}_{IWM}$ , %	100.0 ± 0.0	99.8 ± 0.6	97.9 ± 1.8	97.7 ± 2.6
<i>Hypocapnia (n = 6)</i>				
$\bar{V}_p$ , cm/s	56.4 ± 9.4	37.2 ± 5.5	41.5 ± 6.9	62.8 ± 12.3
$\bar{V}_{IWM}$ , cm/s	36.7 ± 6.0	24.2 ± 3.8	27.1 ± 4.5	40.5 ± 7.1
$\bar{P}$ , %	100.0 ± 0.0	104.0 ± 1.0*	101.2 ± 1.4	96.7 ± 3.1*
$\bar{V}_p$ , %	100.0 ± 0.0	66.5 ± 3.7†	74.2 ± 3.8	111.2 ± 4.8
$\bar{V}_{IWM}$ , %	100.0 ± 0.0	66.4 ± 3.5†	74.7 ± 4.5	110.9 ± 5.1
$\bar{P} \cdot \bar{V}_{IWM}$ , %	100.0 ± 0.0	68.8 ± 3.4	75.6 ± 4.5	107.4 ± 5.1

Values are means ± SD. *n*, No. of subjects;  $\bar{P}$ , mean for instantaneous (10-ms) value for total power of Doppler spectrum (*P*) averaged over cardiac cycle;  $\bar{P} \cdot \bar{V}_{IWM}$ , mean for instantaneous (10-ms) product of  $\bar{V}_{IWM}$  and *P* ( $\bar{P} \cdot \bar{V}_{IWM}$ ) averaged over cardiac cycle; *stimulus 1*, initial 2-min period of hypocapnia; *stimulus 2*, final 2-min period of hypocapnia. \*Significantly different from baseline value,  $P < 0.001$ . †Significantly different from  $\bar{P} \cdot \bar{V}_{IWM}$  during same time period,  $P < 0.001$ .

the response is significantly smaller than that after the off-response, and this difference is significant. Once the initial transient is over, there appears to be a slow increase in  $\bar{P} \cdot \bar{V}_{IWM}$  that persists for the remainder of the 20-min hypocapnic exposure. This slow adaptation in  $\bar{P} \cdot \bar{V}_{IWM}$  has a gain of 1.26%/Torr and a time constant of 426.9 s; the gain is significantly different from zero (Table 4).

## DISCUSSION

### Major Findings

This study provides a continuous beat-by-beat measurement of middle cerebral artery flow during 20 min of sustained euoxic hypocapnia in humans. The major findings are that 1) after the rapid fall in  $\bar{P} \cdot \bar{V}_{IWM}$  at the onset of hypocapnia, there is a subsequent slow adaptation (i.e., a progressive increase) in  $\bar{P} \cdot \bar{V}_{IWM}$  that continues throughout the 20-min period of hypocapnia; 2) there is significant asymmetry of the response to hypocapnia, characterized by a faster on-transient than off-transient; and 3) there are small changes in the total power of the Doppler signal associated with hypocapnia, suggesting small changes in the cross-sectional area of the middle cerebral artery.

### Adaptive Nature of Cerebral Blood Flow Response

We observed a significant adaptation in the response of cerebral blood flow to hypocapnia after the initial transient. This slow adaptation was consistent in all our subjects, but the time constant appeared to be somewhat variable among subjects. The constant values for cerebral blood flow throughout the control protocol show that this adaptation is an effect of hypocapnia rather than a mechanical effect of hyperventilation.

In a previous study, Ellingsen et al. (10) measured blood flow velocity in the internal carotid artery (by using Doppler ultrasound) in response to both step increases and step decreases in alveolar  $PCO_2$  and reported progressive changes in cerebral blood flow over 20 min for both types of experiments. However, in a previous study (27) we were unable to reproduce the

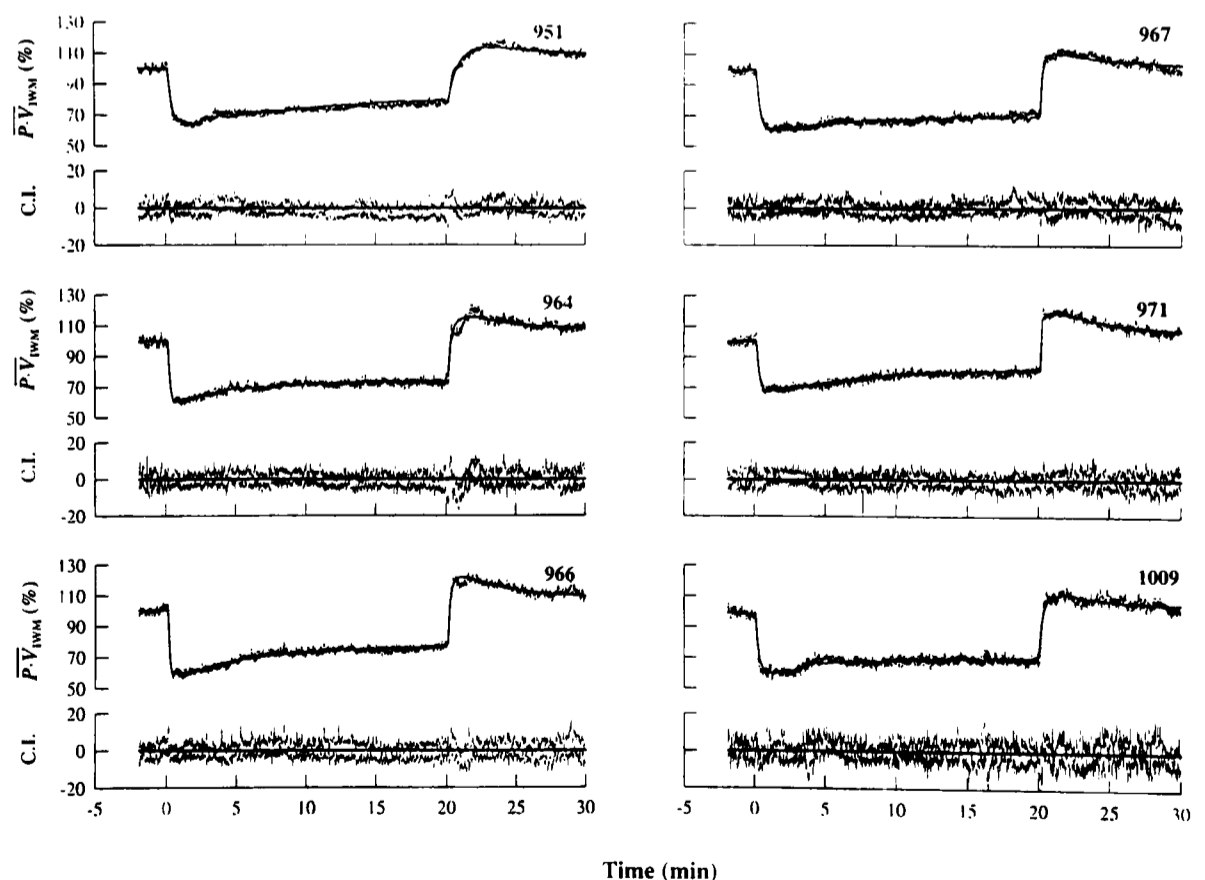


Fig. 4.  $\bar{P} \cdot \bar{V}_{IWM}$  responses to hypocapnia (●), model fit (solid horizontal line), and 95% confidence intervals (CI) for associated residuals for each subject. Subjects are same as in Fig. 2. Each data set represents an ensemble average of data from all repetitions for each subject. Beat-by-beat data are interpolated over 0.5-s intervals.

Table 4. Estimated model parameters for cerebral blood flow response to hypocapnia

Subject No.	MCAF <sub>on</sub> *	MCAF <sub>off</sub> *	g <sub>f,on</sub>	g <sub>s</sub>	g <sub>f,off</sub>	τ <sub>f,on</sub>	τ <sub>s</sub>	τ <sub>f,off</sub>	T <sub>d</sub>
951	100.3 ± 1.4	101.3 ± 3.3	2.55 ± 0.43	-1.58 ± 0.25	2.74 ± 0.44	12.70 ± 6.31	756.8 ± 443.8	35.30 ± 12.46	2.7 ± 0.4
964	99.8 ± 1.3	104.8 ± 7.5	2.44 ± 0.28	-1.00 ± 0.26	2.79 ± 0.48	4.38 ± 1.33	402.5 ± 316.0	14.35 ± 10.54	4.5 ± 0.8
966	100.5 ± 0.8	104.1 ± 3.0	3.11 ± 0.49	-1.71 ± 1.00	3.41 ± 0.45	2.97 ± 0.95	338.6 ± 309.7	11.53 ± 7.09	5.0 ± 1.3
967	99.6 ± 1.5	100.4 ± 5.2	2.91 ± 0.34	-0.92 ± 0.26	2.87 ± 0.19	7.73 ± 2.00	329.2 ± 189.4	8.08 ± 3.08	3.5 ± 1.5
971	100.2 ± 1.5	102.7 ± 5.5	2.43 ± 0.25	-1.38 ± 0.38	2.66 ± 0.37	3.99 ± 2.18	443.4 ± 230.0	3.08 ± 1.53	5.2 ± 1.0
1009	98.5 ± 1.6	103.2 ± 7.3	2.66 ± 0.33	-0.77 ± 0.19	3.01 ± 0.19	10.96 ± 3.32	265.2 ± 129.1	12.71 ± 4.50	1.0 ± 1.0
Mean	99.9 ± 1.3	102.7 ± 5.2*	2.69 ± 0.43	-1.26 ± 0.58†	2.91 ± 0.44*	6.77 ± 4.73	426.9 ± 309.8	14.31 ± 12.95*	3.9 ± 1.7
P value		<0.005		<0.001	<0.001			<0.001	

Values are means ± SD. Middle cerebral artery flow (MCAF)<sub>on</sub>\* and MCAF<sub>off</sub>\*, pre- and post-MCAF baselines (%), respectively; g<sub>f,on</sub> and g<sub>f,off</sub>, gain terms for on- and off-responses (%/Torr), respectively; g<sub>s</sub>, gain term for slow "adaptation" component (%/Torr); τ<sub>f,on</sub> and τ<sub>f,off</sub>, time constants for on- and off-responses (s), respectively; τ<sub>s</sub>, time constant for slow adaptation component (s); T<sub>d</sub>, time delay (s). \*Significantly different from on-response, P < 0.005. †Significantly different from 0, P < 0.001.

adaptation that was reported for hypercapnia from the study by Ellingsen et al. (10). Because actual PETCO<sub>2</sub> values were not reported in the study by Ellingsen et al., it is difficult to determine how well the end-tidal values were controlled. In fact, the authors did report some difficulties in controlling end-tidal values and noted that "the detailed time course of these experiments depended on how the subject aimed on the predetermined alveolar PCO<sub>2</sub> value." Although the results of our previous study were not consistent with those of Ellingsen et al. for hypercapnia, the results of our present study of an adaptation of cerebral blood flow with hypocapnia are consistent with their results for hypocapnia.

Adaptation of cerebral blood flow has been reported previously with exposures to hypocapnia of substantially longer duration than those of Ellingsen et al. (10) and of the present study. Raichle et al. (30), in unanesthetized voluntarily hyperventilating men, reported a 40% decrease in cerebral blood flow after 30 min of hypocapnia (PETCO<sub>2</sub> = 15–20 Torr), with a return of cerebral blood flow to 90% of its prehypocapnic value after 4 h of hyperventilation, and a calculated overshoot of 31% over control values when eucapnia was restored. Similar reports have appeared of longer term adaptation in total cerebral blood flow over periods of 2 and 6 h for unanesthetized piglets (12) and goats (2), respectively.

The underlying mechanism for the slow component of the cerebrovascular response to hypocapnia remains unclear. However, it is reasonably well accepted that pH is one of the main regulators of the cerebral blood flow response to CO<sub>2</sub> (22). With prolonged hypocapnia, there is an initial increase in extracellular pH, with the maximal value being reached from within 30 min (2, 26) to a few hours (5, 23, 30) after the onset of hypocapnia. Although the reported time to maximal pH differs considerably among studies, most studies agree that the initial increase is then followed by a decrease in extracellular pH toward normal values (2, 5, 23, 26, 30). It is thought that the subsequent decrease in pH is due to a progressive increase in brain lactate (2, 8, 19), although the time course over which the change in lactate occurs remains uncertain, with studies reporting times from 1 to 6 h after the onset of hypocapnia before the maximum response in lactate is observed (2,

19, 25). These variations may be related to species differences (25).

#### Sensitivity of Cerebral Blood Flow Response to Hypocapnia

The magnitude of the initial change in  $\bar{P} \cdot \bar{V}_{IWM}$  resulting from the hypocapnic stimulus is substantial and similar in all our subjects. The mean value of 2.7%/Torr for the gain of the fast component at the onset of hypocapnia falls within the range of previously published steady-state values of from 1.8 to 3.4%/Torr measured in the eucapnic-hypocapnic range by using the techniques of nitrous oxide inhalation (and tissue uptake based on the Fick principle) (20, 34), positron emission tomography (4, 31), and transcranial Doppler (10, 14, 37). However, the description of a slow adaptive

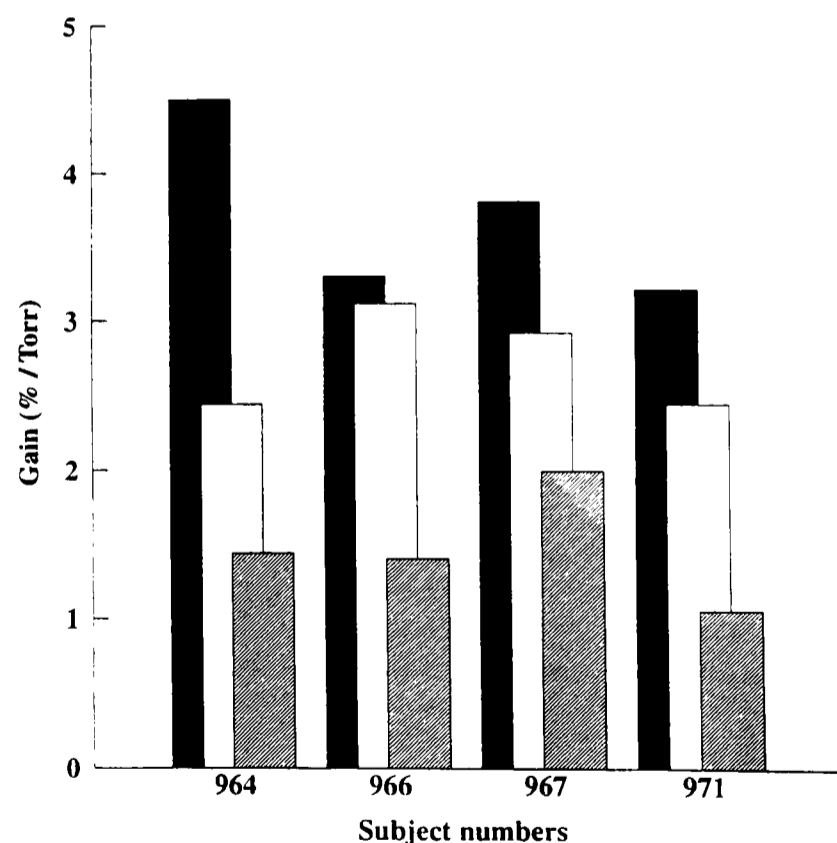


Fig. 5. Comparison of gain of cerebral blood flow response (%/Torr) to onset of hypercapnia (solid bars) with fast (g<sub>f</sub>; open bars) and fast minus slow (g<sub>f</sub> - g<sub>s</sub>; hatched bars) components of cerebral blood flow response to hypocapnia. Hypercapnic data were taken from a previous study (27).

process in our study casts a degree of uncertainty over previous measurements of "steady-state" sensitivities in the hypocapnic range. If the sensitivity were measured rapidly, then it would correspond approximately to  $g_f$  (i.e., 2.7%/Torr). If the sensitivity were measured slowly, such that the adaptive response were complete, the value would correspond to  $g_f - g_s$  (i.e., 1.4%/Torr).

The presence of an adaptive process may be one reason why there is uncertainty as to whether the cerebral blood flow sensitivity is linear, with variations in  $PET_{CO_2}$ . Some studies have been consistent with a linear response across both a hypo- and hypercapnic range (13, 14), whereas other studies have not (6, 31), with some suggesting that the relationship is better described by an exponential (18, 21, 36) or sigmoid (32) function.

One way to avoid the influence of the adaptive process on the measurement of sensitivity is to determine instead whether the gain of the fast component of the response,  $g_f$ , varies over the physiological range of  $PET_{CO_2}$ . By using our data and technique, the hypocapnic values for  $g_f$  from the present study can be compared with the hypercapnic values for  $g_f$  from Poulin et al. (27). The value for  $g_f$  in hypocapnia (2.69%/Torr) was significantly smaller (34%; unpaired *t*-test,  $P < 0.01$ ) than the value for  $g_f$  in hypercapnia (4.1%/Torr). Four of the six subjects were common to both studies, and to highlight further the differences observed between hypercapnia and hypocapnia, their gains for the fast component at the onset of hypercapnia [taken from Poulin et al. (27)] and for the fast component at the onset of hypocapnia (taken from the present study) are presented in Fig. 5. The differences on an individual basis are consistent with the statistical results for the two groups as a whole. Also shown in Fig. 5 are the values for  $g_f - g_s$  for each subject. These show that the appearance of nonlinearity will be enhanced in those studies that take longer to determine the response of cerebral blood flow to hypocapnia.

#### *Speed of Rapid Response to Onset and Offset of Hypocapnia*

The present study reports a mean value of  $6.8 \pm 4.7$  s for the time constant for the response of cerebral blood flow to a decrease in  $PET_{CO_2}$ . This value appears to be faster than the value of 20 s reported by Severinghaus and Lassen (34). However, with our technique, an important feature of the estimation procedure for the model parameters is that the actual breath-by-breath  $PET_{CO_2}$  was used as the input function, which avoids making any assumptions about the input, such as assuming that the input was a perfect step change. Additionally, our study provides a continuous beat-by-beat index of cerebral blood flow, whereas the study of Severinghaus and Lassen involved discrete sampling of arterial and jugular venous blood (at 30-s intervals over the first 2.5 min after the induction of hypocapnia). These factors may well account for the difference between our result and that of Severinghaus and Lassen.

Our study finds significant asymmetry between the response of cerebral blood flow to the onset and relief of hypocapnia. We were unable to find any related results in the literature for hypocapnia. However, the asymmetry observed in hypocapnia does show some qualitative similarities to that observed in hypercapnia (27). In both conditions, the time constant of the cerebral blood flow response to a step decrease in  $CO_2$  is less than the time constant of the cerebral blood flow response to an increase in  $CO_2$ . However, some quantitative differences are observed: the time constants for the step decreases in  $CO_2$  were similar ( $6.8 \pm 4.7$  s in hypocapnia and  $6.1 \pm 1.3$  s in hypercapnia), but the time constants for the step increases in  $CO_2$  were significantly different ( $14.3 \pm 13.0$  s in hypocapnia and  $45.3 \pm 32.9$  s in hypercapnia;  $P = 0.05$ ).

#### *Changes in Doppler Power*

This study reports only small changes in Doppler power despite large variations in cerebral blood flow. Although the regulation of cerebral blood flow is accomplished mostly by variations in pial arteriolar vessels, because they form the main resistance vessels (15), the finding of small increases in Doppler power with large decreases in cerebral blood flow during hypocapnia was not intuitively expected. Previous studies in humans (6, 29) and in baboons (9) have also provided evidence for a vasodilatation of the larger cerebral vessels at levels of hypocapnia similar to, or less than, the level used in this study (i.e.,  $PET_{CO_2} < 25$  Torr). These again suggest that a paradoxical increase in cross-sectional area of larger cerebral vessels occurs during moderate to substantial levels of hypocapnia.

We acknowledge David O'Connor for skilled technical assistance, John G. Tansley for help with data collection, and the volunteers for participation in the study.

This study was approved by the Central Oxford Research Ethics Committee and was supported by the Wellcome Trust. M. J. Poulin was supported by a Heart and Stroke Foundation of Ontario (Canada) postdoctoral research fellowship (Grant F3555).

Address for reprint requests: P. A. Robbins, Univ. Laboratory of Physiology, Parks Road, Oxford OX1 3PT, UK (E-mail: peter.robbins@physiol.ox.ac.uk).

Received 18 August 1997; accepted in final form 16 March 1998.

#### REFERENCES

1. Aaslid, R., T. Markwalder, and H. Nornes. Noninvasive transcranial Doppler ultrasound recording of flow velocity in basal cerebral arteries. *J. Neurosurg.* 57: 769-774, 1982.
2. Albrecht, R. F., D. J. Miletich, and M. Ruttle. Cerebral effects of extended hyperventilation in unanesthetized goats. *Stroke* 18: 649-655, 1987.
3. Arts, M. G. J., and J. M. J. G. Roelvros. On the instantaneous measurement of blood flow by ultrasonic means. *Med. Biol. Eng.* 10: 23-34, 1972.
4. Bednarczyk, E. M., W. F. Rutherford, G. P. Leisure, M. A. Munger, E. A. Panacek, F. D. Miraldi, and J. A. Green. Hyperventilation-induced reduction in cerebral blood flow: assessment by positron emission tomography. *DICP* 24: 456-460, 1990.
5. Christensen, M. S. Acid-base changes in cerebrospinal fluid and blood, and blood volume changes following prolonged hyperventilation in man. *Br. J. Anaesth.* 46: 348-357, 1974.
6. Clark, J. M., B. E. Skolnick, R. Gelfand, R. E. Farber, M. Stierheim, W. C. Stevens, G. Beck, and C. J. Lambertsen. Relationship of  $^{133}Xe$  cerebral blood flow to middle cerebral

- arterial flow velocity in men at rest. *J. Cereb. Blood Flow Metab.* 16: 1255-1262, 1996.
7. Corfield, D. R., M. J. Morrell, and A. Guz. The nature of breathing during hypocapnia in awake man. *Respir. Physiol.* 101: 145-159, 1995.
  8. Dager, S. R., W. L. Strauss, K. I. Marro, T. L. Richards, G. D. Metzger, and A. A. Artru. Proton magnetic resonance spectroscopy investigation of hyperventilation in subjects with panic disorder and comparison subjects. *Am. J. Psychiatry* 152: 666-672, 1995.
  9. Du Boulay, G. H., and L. Symon. The anaesthetist's effect upon the cerebral arteries. *Proc. R. Soc. Lond. B Biol. Sci.* 64: 77-80, 1971.
  10. Ellingsen, I., A. Hauge, G. Nicolaysen, M. Thoresen, and L. Walloe. Changes in human cerebral blood flow due to step changes in  $PA_{O_2}$  and  $PA_{CO_2}$ . *Acta Physiol. Scand.* 129: 157-163, 1987.
  11. Gotoh, F., J. S. Meyer, and Y. Takagi. Cerebral effects of hyperventilation in man. *Arch. Neurol.* 12: 410-423, 1965.
  12. Hansen, N. B., P. T. Nowicki, R. R. Miller, T. Malone, R. G. Bickers, and J. A. Menke. Alterations in cerebral blood flow and oxygen consumption during prolonged hypocapnia. *Pediatr. Res.* 20: 147-150, 1986.
  13. Harper, A. M., and H. I. Glass. Effect of alterations in the arterial carbon dioxide tension on the blood flow through the cerebral cortex at normal and low arterial blood pressures. *J. Neurol. Neurosurg. Psychiatry* 28: 449-452, 1965.
  14. Hauge, A., M. Thoresen, and L. Walloe. Changes in cerebral blood flow during hyperventilation and  $CO_2$ -breathing measured transcutaneously in humans by a bidirectional, pulsed, ultrasound Doppler blood velocimeter. *Acta Physiol. Scand.* 110: 167-173, 1980.
  15. Heistad, D. D., and H. A. Kontos. Cerebral circulation. In: *Handbook of Physiology. The Cardiovascular System*. Bethesda, MD: Am. Physiol. Soc., 1983, sect. 2, vol. III, p. 137-182.
  16. Howson, M. G., S. Khamnei, M. E. McIntyre, D. F. O'Connor, and P. A. Robbins. A rapid computer controlled binary gas mixing system for studies in respiratory control (Abstract). *J. Physiol. (Lond.)* 403: 103P, 1987.
  17. Howson, M. G., S. Khamnei, D. F. O'Connor, and P. A. Robbins. The properties of a turbine device for measuring respiratory volumes in man (Abstract). *J. Physiol. (Lond.)* 382: 12P, 1986.
  18. James, I. M., R. A. Millar, and M. J. Purves. Observations on the extrinsic neural control of cerebral blood flow in the baboon. *Circ. Res.* 25: 77-93, 1969.
  19. Kazemi, H., L. M. Valenca, and D. C. Shannon. Brain and cerebrospinal fluid lactate concentration in respiratory acidosis and alkalosis. *Respir. Physiol.* 6: 178-186, 1969.
  20. Kety, S. S., and C. F. Schmidt. The effects of active and passive hyperventilation on cerebral blood flow, cerebral oxygen consumption, cardiac output, and blood pressure of normal young men. *J. Clin. Invest.* 25: 107-119, 1946.
  21. Kety, S. S., and C. F. Schmidt. The effects of altered arterial tensions of carbon dioxide and oxygen on cerebral blood flow and cerebral oxygen consumption of normal young men. *J. Clin. Invest.* 27: 484-492, 1948.
  22. Kuschinsky, W. Role of hydrogen ions in regulation of cerebral blood flow and other regional flows. In: *Ionic Regulation of the Microcirculation*, edited by B. M. Altura. Basel: Karger, 1982, p. 1-19.
  23. Muizelaar, J. P., H. G. van der Poel, Z. Li, H. A. Kontos, and J. E. Levasseur. Pial arteriolar vessel diameter and  $CO_2$  reactivity during prolonged hyperventilation in the rabbit. *J. Neurosurg.* 69: 923-927, 1988.
  24. Padayachee, T. S., F. J. Kirkham, R. R. Lewis, J. Gillard, M. C. E. Hutchinson, and R. G. Gosling. Transcranial measurement of blood velocities in the basal cerebral arteries using pulsed Doppler ultrasound: a method of assessing the circle of Willis. *Ultrasound Med. Biol.* 12: 5-14, 1986.
  25. Petroff, O. A. C., J. W. Prichard, K. L. Behar, D. L. Rothman, J. R. Alger, and R. G. Shulman. Cerebral metabolism in hyper- and hypocapnia:  $^{31}P$  and  $^1H$  nuclear magnetic resonance studies. *Neurology* 35: 1681-1688, 1985.
  26. Plum, F., J. B. Posner, and W. W. Smith. Effect of hyperbaric-hyperoxic hyperventilation on blood, brain, and CSF lactate. *Am. J. Physiol.* 215: 1240-1244, 1968.
  27. Poulin, M. J., P.-J. Liang, and P. A. Robbins. Dynamics of the cerebral blood flow response to step changes in end-tidal  $PCO_2$  and  $PO_2$  in humans. *J. Appl. Physiol.* 81: 1084-1095, 1996.
  28. Poulin, M. J., and P. A. Robbins. Indexes of flow and cross-sectional area of the middle cerebral artery using Doppler ultrasound during hypoxia and hypercapnia in humans. *Stroke* 27: 2244-2250, 1996.
  29. Radu, E. W., and G. H. du Boulay. Paradoxical dilation of the large cerebral arteries in hypocapnia in man. *Stroke* 7: 569-572, 1976.
  30. Raichle, M. E., J. B. Posner, and F. Plum. Cerebral blood flow during and after hyperventilation. *Arch. Neurol.* 23: 394-403, 1970.
  31. Ramsay, S. C., K. Murphy, S. A. Shea, K. J. Friston, A. A. Lammertsma, J. C. Clark, L. Adams, A. Guz, and R. S. J. Frackowiak. Changes in global cerebral blood flow in humans: effect on regional cerebral blood flow during a neural activation task. *J. Physiol. (Lond.)* 471: 521-534, 1993.
  32. Reivich, M. Arterial  $PCO_2$  and cerebral hemodynamics. *Am. J. Physiol.* 206: 25-35, 1964.
  33. Robbins, P. A., G. D. Swanson, and M. G. Howson. A prediction correction scheme for forcing alveolar gases along certain time courses. *J. Appl. Physiol.* 52: 1353-1357, 1982.
  34. Severinghaus, J. W., and N. Lassen. Step hypocapnia to separate arterial from tissue  $PCO_2$  in the regulation of cerebral blood flow. *Circ. Res.* 20: 272-278, 1967.
  35. Shapiro, W., A. J. Wasserman, and J. L. Patterson. Mechanism and pattern of human cerebrovascular regulation after rapid changes in blood  $CO_2$  tension. *J. Clin. Invest.* 45: 913-922, 1966.
  36. Waltz, A. G. Effect of  $Pa_{CO_2}$  on blood flow and microvasculature of ischemic and nonischemic cerebral cortex. *Stroke* 1: 27-37, 1970.
  37. Young, R. S. K., and S. K. Yagel. Cerebral physiological and metabolic effects of hyperventilation in the neonatal dog. *Ann. Neurol.* 16: 337-342, 1984.

## **CHAPTER 5**

### **ASSESSMENTS OF FLOW BY TRANSCRANIAL DOPPLER ULTRASOUND IN THE MIDDLE CEREBRAL ARTERY DURING EXERCISE IN HUMANS**

Poulin, M.J., R.J. Syed and P.A. Robbins (1999)  
*J. Appl. Physiol.* **86**:1632-1637

## PREFACE

The techniques developed for the studies described in Chapters 2, 3, and 4 revealed that our method of using transcranial Doppler ultrasound allowed the detection of changes in the total reflected Doppler power signal, which should provide an index of the cross-sectional area of the middle cerebral artery. Thus, it has become possible to examine one of the fundamental assumptions (i.e. no changes in cross sectional area of the vessel under investigation) underlying the way transcranial Doppler ultrasound has been used previously in other studies. To examine this further, we sought to find appropriate physiological interventions that were likely to influence the calibre of the middle cerebral artery. Serendipitously I stumbled across results of several studies that used transcranial Doppler ultrasound (and maximal velocity) to assess changes in cerebral blood flow (CBF) during dynamic submaximal exercise. Consistently, these studies reported increases in CBF. However, while changes in cross-sectional area were sometimes speculated, no assessment had yet been made. I set out to do a few simple experiments of submaximal exercise (with subject 964 and a set-up that included the administrator's old chair in tandem with a constant load cycle ergometer). It quickly became apparent that our three indices of CBF that can be extracted from the whole Doppler spectrum provided different results. This formed the initial observations that lead to a visit at Argos on a Friday afternoon to purchase a standard exercise bench (to replace the old chair) in order to undertake the study described in this Chapter. In this Chapter, we examined the degree of consistency between three indices of cerebral blood flow during light to moderate intensity dynamic exercise. In particular, we examined one index of cross-sectional area, the total power of the reflected Doppler signal.

## DECLARATION

The work presented in this chapter was carried out over a two-year period in the University Laboratory of Physiology. The pilot work for this study was conceived and undertaken by myself. Professor Robbins and I conceived, designed, and planned the main study. The experiments were carried out by myself, with the assistance of Ms. Syed, a dissertation student who was co-supervised by Professor Robbins and me. Ms. Syed also assisted with some of the data analysis. Professor Robbins and I wrote the resulting paper. Results of this study were presented at the Experimental Biology '98 Meetings (San Francisco, USA) and published in Abstract form in *The FASEB Journal* (abstract, 12:A1116, 1998).

# Assessments of flow by transcranial Doppler ultrasound in the middle cerebral artery during exercise in humans

MARC J. POULIN, REBECCA J. SYED, AND PETER A. ROBBINS  
*University Laboratory of Physiology, University of Oxford,  
 Oxford OX1 3PT, United Kingdom*

**Poulin, Marc J., Rebecca J. Syed, and Peter A. Robbins.** Assessments of flow by transcranial Doppler ultrasound in the middle cerebral artery during exercise in humans. *J. Appl. Physiol.* 86(5): 1632–1637, 1999.—This study examined the consistency between three indexes of cerebral blood flow (CBF) obtained by using transcranial Doppler ultrasound in eight human volunteers. Each subject undertook three sessions of graded exercise, consisting of 6 min of rest, 6 min at 20% of maximal oxygen uptake ( $\dot{V}O_{2\max}$ ), 6 min at 40%  $\dot{V}O_{2\max}$ , and 6 min of recovery. Values were obtained every 10 ms for the velocity associated with the maximal frequency of the Doppler shift ( $V_P$ ), the intensity-weighted mean velocity ( $V_{IWM}$ ), and total signal power ( $P$ ). Beat-by-beat averages for three indexes ( $\bar{V}_P$ ,  $\bar{V}_{IWM}$ ,  $\bar{P} \cdot \bar{V}_{IWM}$ ) provided significantly different results for the percent changes in CBF with exercise. At 20% of  $\dot{V}O_{2\max}$ ,  $\bar{V}_P$  and  $\bar{V}_{IWM}$  showed significant ( $P < 0.05$ ) increases of 8 and 6%, respectively, whereas  $\bar{P} \cdot \bar{V}_{IWM}$  showed a nonsignificant increase of 3%. At 40% of  $\dot{V}O_{2\max}$ ,  $\bar{V}_P$  and  $\bar{V}_{IWM}$  showed significant ( $P < 0.05$ ) increases of 14 and 8%, respectively, whereas  $\bar{P} \cdot \bar{V}_{IWM}$  showed a nonsignificant increase of 4%. Our results suggest that the increase in CBF with exercise that has been reported with transcranial Doppler ultrasound needs to be treated with caution, as much of the response could arise as an artifact from the increase in amplitude and frequency of the arterial pressure waveform.

Doppler power; cerebral blood flow

MODERN IMAGING TECHNIQUES have revealed certain very localized increases in cerebral blood flow with dynamic exercise, for example, those to certain parts of the primary motor cortex (2, 24). However, there remain conflicting reports as to whether there are significant overall changes in cerebral blood flow during dynamic exercise. This lack of agreement is related, in part, to whether global (11, 12, 22, 26), cortical (6, 9, 10, 23), or larger regional changes (4, 5, 10, 13–15) in cerebral blood flow are being measured. It may also be related to the limitations associated with the various techniques used and the different intensities of exercise studied.

Techniques based on Doppler ultrasound have given fairly consistent results, suggesting modest increases of 10–42% during light-to-moderate dynamic exercise [20–60% of maximal oxygen uptake ( $\dot{V}O_{2\max}$ )] (4, 5, 9, 10, 13–15, 19). However, all of these relate to beat averages of the velocities associated with the maximal frequencies of the Doppler shift. The use of this velocity as an index of cerebral blood flow requires, first, that the maximal velocity is proportional to the mean velocity of the blood flow in the vessel, and, second, that the cross-sectional area of the blood vessel remains unchanged. During exercise, both heart rate and the pulsatility of arterial blood pressure increase markedly, and,

consequently, the characteristics of cerebral blood flow may change. In this case, it is not clear that changes in the velocities associated with the maximal frequencies of the Doppler shift necessarily reflect changes in flow.

The purpose of this study is to examine further the changes in the Doppler signal during light-to-moderate-intensity dynamic exercise, and, in particular, to examine the degree of consistency among different indexes of cerebral blood flow. Four variables obtained from the Doppler spectrum will be examined. The first is the velocity associated with the maximal frequency of the Doppler shift ( $V_P$ ). This velocity is associated with the blood that is moving fastest within the vessel. The second is the intensity-weighted mean velocity, based on the entire velocity spectrum ( $V_{IWM}$ ). This velocity represents a mean velocity averaged over the entire cross section of the blood vessel. The third variable is an index of cross-sectional area and is the total power of the reflected Doppler signal ( $P$ ), which is a measure of the total number of ultrasound scatterers causing a Doppler shift (i.e., red blood cells). The fourth variable is another flow index, which tries to account for changes in cross-sectional area and is the product of  $P$  and  $V_{IWM}$  ( $P \cdot V_{IWM}$ ).

## METHODS

### Definitions

Let the  $i$ th element of a Doppler spectrum have an amplitude  $a_i$  and a frequency shift of  $f_i$ . Let the maximum frequency shift for which an amplitude is observed be at the  $m$ th element in the spectrum and be denoted by  $f_m$ . Let  $\lambda$  be the constant of proportionality between the frequency shift,  $f_i$ , and the associated velocity,  $v_i$ , such that  $v_i = \lambda f_i$ . The following functions on the Doppler spectrum may now be defined.

### Glossary

Symbol	Expression	Description
$V_P$	$\lambda f_m$	Instantaneous <sup>1</sup> value for the velocity associated with the maximum frequency of the Doppler shift
$V_{IWM}$	$\lambda \frac{\sum_i (a_i^2 f_i)}{\sum_i a_i^2}$	Instantaneous value for the velocity associated with the intensity-weighted mean frequency of the Doppler spectrum
$P$	$\sum_i a_i^2$	Instantaneous value for the total power (arbitrary units) of the Doppler spectrum.
$P \cdot V_{IWM}$	$(P)(V_{IWM})$	Instantaneous product of $V_{IWM}$ and $P$

<sup>1</sup> The Doppler ultrasound system used in the present study produced a Doppler spectrum every 10 ms, and the term "instantaneous" refers to the value obtained for one of these spectra.

The Doppler spectra vary with blood flow throughout the cardiac cycle. Suppose there are  $n$  spectra within a cardiac cycle, and let the subscript  $j$  represent the  $j$ th Doppler spectrum within that cycle. The following mean values may be calculated for the cycle.

#### Glossary

Symbol	Expression	Description
$\bar{V}_P$	$(1/n) \sum_j V_{Pj}$	Mean for $V_P$ , averaged over the cardiac cycle
$\bar{V}_{IWM}$	$(1/n) \sum_j V_{IWMj}$	Mean for $V_{IWM}$ , averaged over the cardiac cycle
$\bar{P}$	$(1/n) \sum_j P_j$	Mean for $P$ , average over the cardiac cycle
$\overline{P \cdot V_{IWM}}$	$(1/n) \sum_j (P \cdot V_{IWM})_j$	Mean for $P \cdot V_{IWM}$ averaged over the cardiac cycle

#### Subjects

The study involved eight young adults (3 women, 5 men). The study requirements were fully explained to all participants, with each giving informed consent before participation in the study. The research was approved by the Central Oxford Research Ethics Committee. Participants were not taking any medication, all were nonsmokers, and none had any history of cardiovascular, cerebrovascular, or respiratory disease.

#### Protocols

The subjects visited the laboratory on two occasions. The first visit served as an opportunity to obtain preliminary data, and the second to perform the submaximal exercise experiments.

The first visit included a brief medical history including age, height, weight, and resting arterial blood pressure. This was followed by two cycle exercise (ramp) tests to determine for each subject the workloads that were equivalent to 20 (WLI) and 40% (WLII) of  $\dot{V}O_{2\max}$  for use in the subsequent submaximal exercise experiments. The techniques employed for measuring oxygen consumption have been described elsewhere (18). The particular percentages of  $\dot{V}O_{2\max}$  were chosen because previous studies using transcranial Doppler ultrasound have suggested that the largest increases in cerebral blood flow may occur in this intensity domain of exercise (4).

The two ramplike tests were administered 30 min apart. The exercise tests were preceded by a 6-min period at rest, during which baseline data were collected. Then, the subjects were instructed to begin pedaling (60–80 rpm), and the workload was increased automatically each minute in increments of 15–25 W to elicit a test of 8- to 12-min duration before maximum exercise capacity was reached.

The second laboratory visit was held within a few (2–7) days after the first and included three sessions of submaximal exercise on the cycle ergometer. Each submaximal exercise session lasted 24 min and con-

sisted of a 6-min period of rest, then 6 min at WLI, 6 min at WLII, and finally a 6-min period of recovery. In two of the submaximal exercise sessions, subjects breathed through a mouthpiece, whereas in the third session no mouthpiece was used and a catheter was taped to one of the subject's nostrils to sample the end-tidal  $PCO_2$  ( $P_{ETCO_2}$ ) and  $PO_2$  ( $P_{ETO_2}$ ). Each session of exercise was separated by a 30-min period of rest to ensure full recovery from the previous test.

#### Apparatus and Technique

A Mijnhardt KEM-3 electromagnetically braked cycle ergometer (CardioKinetics) set in the constant-power mode was used for the exercise testing (8). To record stable measurements from the Doppler system, it was necessary to ensure immobilization of the head and upper body during the exercise tests. Therefore, the experiments were conducted with subjects sitting behind the cycle ergometer, in a semisupine position on an exercise bench (York DB5 folding dumbbell bench) that was fastened to the cycle ergometer. This provided a firm headrest for the subject while exercising. The subjects' feet were fastened tightly to the pedals by using standard bicycle toe-clips and straps. Subjects were asked to maintain a pedaling frequency of between 60 and 80 rpm.

Heart rate was monitored from an electrocardiogram by using electrodes attached in a modified V-5 configuration. A noninvasive measurement of finger arterial pressure was taken throughout the exercise test protocols (Ohmeda 2300, Finapres). The Finapres data were sampled every 10 ms. These data, along with the occurrence of each QRS complex from the electrocardiogram, were logged to a computer and saved for later analysis.

End-tidal gases ( $P_{ETCO_2}$  and  $P_{ETO_2}$ ) were measured in all experiments. Gas was sampled at a rate of 80 ml/min and analyzed by mass spectrometry (Airspec MGA 3000) for fractional concentrations of  $O_2$ ,  $CO_2$ ,  $N_2$ , and Ar. A computer sampled the experimental variables every 20 ms.

Backscattered Doppler signals from the right middle cerebral artery were measured by using a 2-MHz pulsed Doppler ultrasound system (PCDop842, SciMed). The Doppler system was adapted by the manufacturer to make the Doppler signals (maximum and intensity-weighted mean Doppler frequency shifts and  $P$ ) available as analog signals. These were updated each time a new spectrum was calculated every 10 ms. Our data-acquisition system sampled those signals every 10 ms.

To obtain useful measurements of  $V_{IWM}$  and  $P$ , it is necessary that the whole of the vessel be insonated. The procedure for ensuring this was as follows. The middle cerebral artery was identified by an insonation pathway through the right temporal window above the zygomatic arch (1, 20). The insonation depth (the distance from the probe to the start of the Doppler-sample volume) was set initially at a depth of 5.0–5.5 cm, and then a short search procedure began (by varying the angle and position of the probe) to identify

a window that provided Doppler spectra from the middle cerebral artery. The sample depth was then increased in small increments of 0.7–0.8 mm until the quality of the Doppler spectra from the middle cerebral artery became poor (usually, at ~5.5–6.0 cm). At this point, the sample depth was decreased, in small increments (again in small steps of 0.7–0.8 mm), to a depth of 4.5 cm. At each depth, a short search was performed by making small adjustments to the angle and the position of the probe to assess the relative magnitude of  $P$ , along with the quality of the Doppler spectra. The sample was then returned to the depth at which the Doppler power signal was maximized and, at that depth, the angle and position of insonation were adjusted to provide the maximum Doppler power signal (this always was associated with the highest quality Doppler spectra). The center of this position was identified with a marker directly on the skin, the Doppler probe was removed, and a headband device (Müller and Moll Fixation, Nicolet Instruments) was strapped snugly around the subject's head. The Doppler probe was securely positioned in this headband device to maintain the optimal insonation position and angle.

### Analysis

*Visualization of profiles for  $V_p$ ,  $V_{IWM}$ , and  $P$  over the cardiac cycle.* Profiles for  $V_p$ ,  $V_{IWM}$ , and  $P$  were determined over the cardiac cycle by using data from the last minute of each of the four different 6-min periods (i.e., rest, WLI, WLII, and recovery). To achieve this, the 10-ms data for  $V_p$ ,  $V_{IWM}$ , and  $P$  for each subject for each test were ensemble averaged by using the peak value for  $V_p$  within each cardiac cycle as the central data point around which 140 other data points were aligned. Thus the averaging procedure included 70 10-ms samples before, and 70 10-ms samples after, the occurrence of each peak value for  $V_p$  within a given cardiac cycle. The results from the three repetitions of the exercise protocol in each subject were used to calculate overall averages for each subject. Finally, the averages for each subject were combined to calculate overall profiles for  $V_p$ ,  $V_{IWM}$ , and  $P$  for the entire group.

*Averaging of data for statistical analysis.* The data that related to middle cerebral artery blood flow comprise one observation for  $V_p$ ,  $V_{IWM}$ , and  $P$  every 10 ms.  $P \cdot V_{IWM}$  was calculated every 10 ms. To give averages for  $V_p$ ,  $V_{IWM}$ ,  $P$ , and  $P \cdot V_{IWM}$  over longer periods of time, the variables were first averaged over each heartbeat to give the beat-by-beat average values,  $\bar{V}_p$ ,  $\bar{V}_{IWM}$ ,  $\bar{P}$ , and  $\bar{P} \cdot \bar{V}_{IWM}$ . For the statistical analysis, these beat-by-beat data were then averaged to give a 3-min value for rest (+3 to +6 min) and 1-min values for each of WLI (+11 to +12 min), WLII (+17 to +18 min), and recovery (+23 to +24 min).

In addition to calculating absolute values, normalized beat-by-beat values were calculated for  $\bar{V}_p$ ,  $\bar{V}_{IWM}$ ,  $\bar{P}$ , and  $\bar{P} \cdot \bar{V}_{IWM}$ . The beat-by-beat data during the 3-min period immediately before the onset of exercise were used as the baseline (100%) values in this process.

*Statistics.* Changes in  $\bar{V}_p$ ,  $\bar{V}_{IWM}$ ,  $\bar{P}$ , and  $\bar{P} \cdot \bar{V}_{IWM}$  were assessed statistically by using ANOVA with period (rest, WLI, WLII, recovery) as a fixed factor and subjects as a random factor. Post hoc comparisons were made by using  $t$ -tests with the appropriate Bonferroni correction. Additionally, Student's paired  $t$ -tests were used to compare percent changes in  $\bar{V}_p$  with percent changes in  $\bar{V}_{IWM}$  during exercise. The overall level of statistical significance was taken as  $P < 0.05$ .

## RESULTS

### Preliminary Observations

The average age, height, and weight of the eight subjects were  $22.3 \pm 2.4$  (SD) yr,  $169.8 \pm 8.1$  cm, and  $63.8 \pm 8.2$  kg, respectively. All were normotensive with average values for systolic, diastolic, and mean arterial blood pressure of  $104.1 \pm 4.8$ ,  $67.4 \pm 5.1$ , and  $79.6 \pm 4.3$  mmHg, respectively. Average values determined for WLI and WLII are given in Table 1.

Average values for  $PET_{CO_2}$  and  $PET_{O_2}$  at each stage of the protocol are given in Table 1. Compared with resting values,  $PET_{CO_2}$  was significantly increased at WLI and WLII. The relationship between arterial  $PCO_2$  and  $PET_{CO_2}$  is not constant going from rest to exercise;  $PET_{CO_2}$  underestimates arterial  $PCO_2$  at rest and overestimates it during exercise. Increases in  $PET_{CO_2}$  on the order of magnitude reported in this study are broadly consistent with there being no underlying change in arterial  $PCO_2$  (21).

The average insonation depth for the subjects was  $4.92 \pm 0.26$  cm. Initial resting values for  $\bar{V}_p$  and  $\bar{V}_{IWM}$  were  $58.7 \pm 5.4$  and  $37.5 \pm 3.4$  cm/s, respectively.

### Submaximal Exercise

*General.* Table 1 shows the values for work rate, heart rate, blood pressure,  $PET_{CO_2}$ , and  $PET_{O_2}$  for control, WLI, WLII, and recovery. The 3-min period of rest

Table 1. Heart rate, blood pressure, and end-tidal values at rest, during submaximal exercise, and in the recovery after exercise

	Rest	WLI	WLII	Recovery
Work rate				
W	$0.0 \pm 0.0$	$35.0 \pm 16.9$	$80.6 \pm 13.7$	$0.0 \pm 0.0$
%Max	$0.0 \pm 0.0$	$17.4 \pm 7.8$	$39.2 \pm 5.5$	$0.0 \pm 0.0$
HR, beats/min	$69.6 \pm 6.4$	$96.6 \pm 12.6^{*\dagger}$	$120.7 \pm 11.5^{*\dagger\dagger}$	$74.4 \pm 6.6$
BP, mmHg	$75.8 \pm 12.0$	$82.4 \pm 9.4^*$	$86.7 \pm 12.3^{*\dagger}$	$78.5 \pm 12.0$
$PET_{CO_2}$ , Torr	$37.0 \pm 2.8$	$40.3 \pm 3.3^{*\dagger}$	$41.7 \pm 4.7^{*\dagger\dagger}$	$37.0 \pm 2.5$
$PET_{O_2}$ , Torr	$102.7 \pm 2.1$	$98.9 \pm 3.6^{*\dagger}$	$100.0 \pm 4.9^\dagger$	$103.9 \pm 2.8$

Values are means  $\pm$  SD;  $n = 8$  subjects. WLI, submaximal workload I; WLII, submaximal workload II; Max, maximal; HR, heart rate; BP, blood pressure;  $PET_{CO_2}$ , end-tidal  $PCO_2$ ;  $PET_{O_2}$ , end-tidal  $PO_2$ . \*Significantly different from rest,  $P < 0.05$ .  $\dagger$ Significantly different from recovery,  $P < 0.05$ .  $\dagger\dagger$ Significantly different from WLI,  $P < 0.05$ .

immediately before the start of exercise was used for obtaining control values. The responses during the two levels of exercise and the subsequent recovery period were calculated over the last minute of each stage.

**Changes in  $V_P$ ,  $V_{IWM}$ , and  $P$  profiles throughout the cardiac cycle.** Group averages for the profiles of  $V_P$ ,  $V_{IWM}$ , and  $P$  throughout the cardiac cycle, during the last minute of each of the four 6-min periods, are presented in Fig. 1. From these data two observations can be made. First, compared with rest and recovery, the data for  $V_P$  and  $V_{IWM}$  during WLI and WLII exhibit an increase in the magnitude of the variation in velocity between the systolic and diastolic parts of the cardiac cycle. Second, turning to the Doppler power signal, a reduction in  $P$  is observed during systole in each of the four conditions. This reduction in  $P$  appears markedly greater during WLI and WLII than during rest or recovery. During WLI and WLII, some individual differences were observed: although the decrease in  $P$  appeared quite large (i.e., >15%) in some subjects, it appeared much less (i.e., <5%) in others. However, in all subjects and for all conditions, the decreases in  $P$  appeared to be consistent, reproducible events.

**Beat-averaged Doppler power signal during exercise.** The group mean for the 3-min average at rest and the 1-min averages for WLI, WLII, and recovery are given in Table 2 and presented in Fig. 2. The power signal appears to decrease with increasing workload. These variations in the power signal were statistically significant (ANOVA), with the value for  $\bar{P}$  at WLII significantly below those during rest, WLI, and recovery.

**Changes in  $\bar{V}_P$ ,  $\bar{V}_{IWM}$ , and  $\bar{P} \cdot \bar{V}_{IWM}$  during exercise.** The group means for the 3-min averages at rest and the

1-min averages for WLI, WLII, and recovery are presented as absolute velocities and normalized responses in Table 2 and are illustrated in Fig. 2. The values for  $\bar{V}_P$  and  $\bar{V}_{IWM}$  appear to increase with increasing workloads, and this was confirmed by statistical analysis (ANOVA). Compared with rest,  $\bar{V}_P$  increased by 7.7 and 14.1% at WLI and WLII, respectively, whereas  $\bar{V}_{IWM}$  increased by 5.5 and 8.2% at WLI and WLII, respectively. In contrast, the changes in  $\bar{P} \cdot \bar{V}_{IWM}$  are much smaller and nonsignificant.

During WLI and WLII, the normalized values for  $\bar{V}_P$  appear to be higher than those for  $\bar{V}_{IWM}$ . When the differences between  $\bar{V}_P$  and  $\bar{V}_{IWM}$  were assessed statistically, they were found to be significant, during both WLI (difference of 2.24%, 95% confidence interval = 0.77–3.70%,  $P < 0.01$ , paired  $t$ -test) and WLII (difference of 5.97%, 95% confidence interval = 4.09–7.85%,  $P < 0.001$ , paired  $t$ -test).

## DISCUSSION

The purpose of this study was to examine the percent change in cerebral blood flow from rest to exercise by using a number of different indexes of cerebral blood flow derived from transcranial Doppler ultrasound data. Each of the indexes of cerebral blood flow provided different results for the percent change in cerebral blood flow between rest and exercise. This lack of consistency indicates that Doppler indexes of cerebral blood flow cannot necessarily be relied on as indicative of changes in cerebral blood flow when rest is compared with exercise. In particular, the modest increase in  $\bar{V}_P$  observed in this and other studies may not reflect any

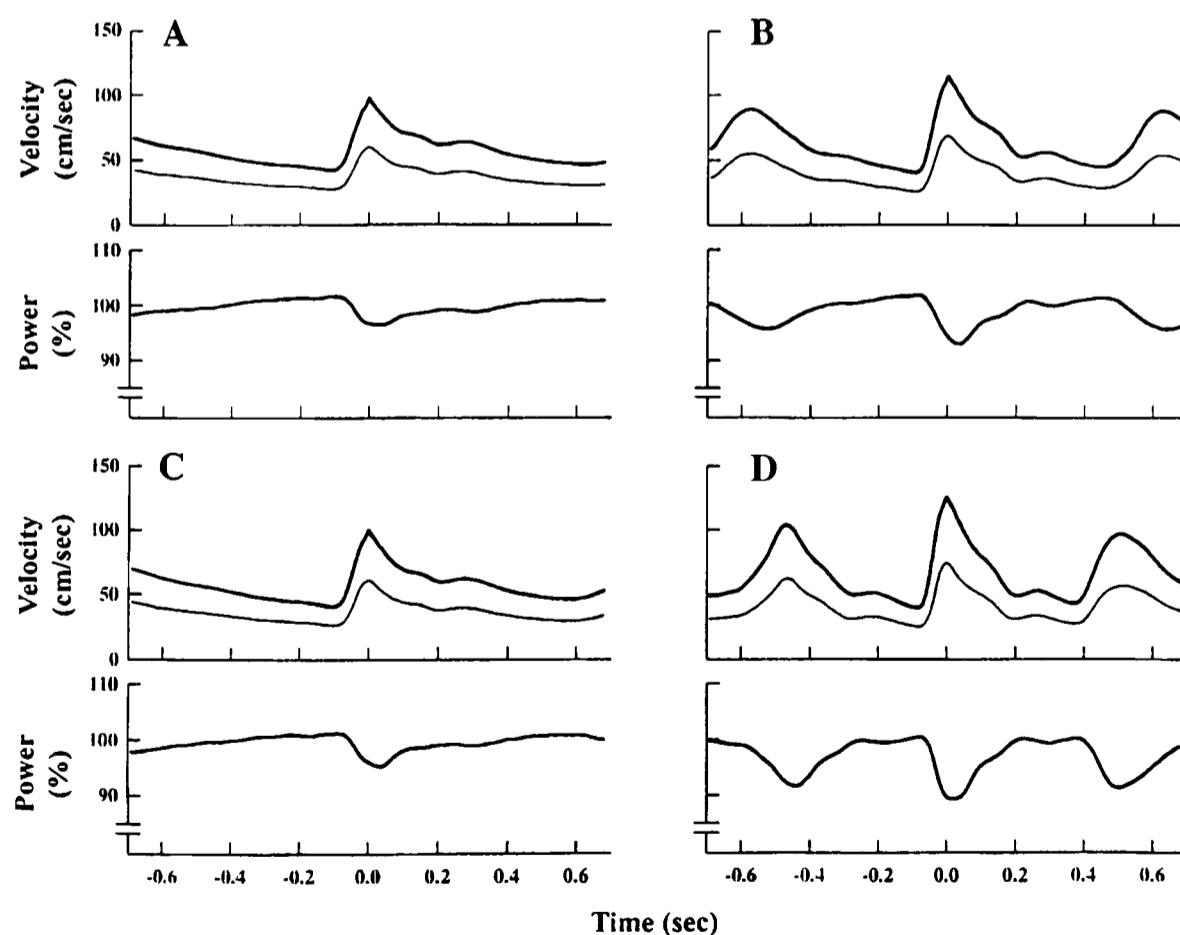


Fig. 1. Group means ( $n = 24$ ; 3 tests for each of 8 subjects) for profiles of maximum velocity ( $V_P$ ), intensity-weighted mean velocity ( $V_{IWM}$ ), and total Doppler power ( $P$ ) throughout cardiac cycle during last minute of each of 4 different periods. A: rest. B: workload I (WLI) 17% maximal  $\dot{V}O_{2\max}$ . C: recovery from exercise. D: workload II (WLII) 39%  $\dot{V}O_{2\max}$ . A-D: top and bottom: absolute values (cm/s) for  $V_P$  (heavy lines) and  $V_{IWM}$  (thin lines) and  $P$  (%change), respectively. Percent change in  $P$  was calculated for each test as deviation from normalized value of 100%, which consisted of average of 3-min period immediately before onset of exercise.

Table 2.  $\bar{V}_P$ ,  $\bar{V}_{IWM}$ ,  $\bar{P} \cdot \bar{V}_{IWM}$ , and  $\bar{P}$  at rest, during submaximal exercise, and in the recovery after exercise

	Rest	WLI (17.4%)	WLI (39.2%)	Recovery
Absolute values, cm/s				
$\bar{V}_P$	58.7 ± 5.4	63.2 ± 5.5*†	66.9 ± 7.9*††	58.4 ± 5.5
$\bar{V}_{IWM}$	37.5 ± 3.4	39.4 ± 3.9*†	40.8 ± 5.7*†	37.2 ± 3.7
Normalized values, %				
$\bar{V}_P$	100.0 ± 0.1	107.7 ± 4.3*†	114.1 ± 10.2*††	99.7 ± 3.5
$\bar{V}_{IWM}$	100.0 ± 0.1	105.5 ± 4.7*†	108.2 ± 8.7*††	99.3 ± 3.0
$\bar{P}$	100.0 ± 0.1	99.2 ± 2.0	97.2 ± 3.1*††	99.4 ± 2.2
$\bar{P} \cdot \bar{V}_{IWM}$	100.0 ± 0.1	103.4 ± 4.0	104.3 ± 9.3	98.7 ± 4.7

Values are means ± SD;  $n = 8$  subjects.  $\bar{V}_P$ , average middle cerebral blood flow velocity spectral outline;  $\bar{V}_{IWM}$ , average middle cerebral blood flow intensity-weighted mean velocity;  $\bar{P}$ , average Doppler power;  $\bar{P} \cdot \bar{V}_{IWM}$ , average middle cerebral artery flow index. \*Significantly different from rest,  $P < 0.05$ . †Significantly different from recovery,  $P < 0.05$ . ‡Significantly different from WLI,  $P < 0.05$ .

real underlying increase in cerebral blood flow with exercise.

#### Differences Between $\bar{V}_P$ and $\bar{V}_{IWM}$

The small but significant differences between the results using  $\bar{V}_P$  and  $\bar{V}_{IWM}$  suggest that the velocity flow profile within the vessel may be changing with exercise. Blood flowing in the middle cerebral artery has entered the vessel from around a bend from a branch point on the Circle of Willis. Such structures can cause quite complicated velocity profiles within the vessel. In addition, the flow within the vessel is not steady but varies because of the variation in arterial pressure throughout the cardiac cycle. In such a flow there may be both some flow reversal and/or flow separation for all or part of the cycle (16, 25). At the onset of exercise, the cardiac

cycle becomes shorter, and the magnitude of the variation in arterial pressure within the cardiac cycle becomes more extreme. These changes in pressure could certainly alter the velocity profiles within the vessel directly. In addition, because the walls of the vessel are not rigid, the variations in pressure could also affect both geometry and vessel size, and these changes could also have effects on the velocity profile. With the shortening of the cardiac cycle and the increase in pulse pressure, it is possible that the degree of any flow reversal and/or flow separation could increase. If the overall mean flow is maintained, then there may be consequential increases in velocity elsewhere in the flow profile. Under conditions where the velocity flow profile is changing,  $\bar{V}_{IWM}$ , which is derived from the entire velocity spectrum, may well provide a more accurate reflection of any change in overall flow than would  $\bar{V}_P$ .

#### Changes in Doppler Power

The fall in power observed during systole was an unexpected finding. This phenomenon became more pronounced during exercise, causing  $\bar{P}$  to fall in exercise compared with rest. Extracranial vessels increase in diameter during systole (7), and, if intracranial vessels behave similarly, an increase in power would be predicted. One possibility is that the change in power reflects a genuine decrease in vessel cross-sectional area. However, there are other possibilities. First, it is possible that systole induces some relative movement between the Doppler probe and vessel so that some of the vessel is lost. This might become worse with the increased arterial pulsation and possible head movement that accompanies exercise. However, with an ultrasound beam of ~1 cm in diameter, a sample thickness of ~1 cm, and a vessel of ~0.3 cm in diameter, it is difficult to envisage how such relative motion would occur consistently across the subjects. A second possibility is that flow reversal or flow separation occurs across some of the vessel during the increased blood flow in systole. This would reduce the number of forward-moving red cells within the sample during systole and thus lead to a reduction in signal power. The possible causes of any such flow reversal and/or flow separation have been discussed above. A third possibility is that the reduction in signal power is related to some signal-processing artifact, although we have no evidence to support this.

#### Comparisons With Previous Studies

Our results for  $\bar{V}_P$  show a modest increase with submaximal exercise that is consistent with other previous reports using transcranial Doppler ultrasound (4, 5, 9, 10, 13–15, 19). In contrast to these reports, studies measuring global changes in cerebral blood flow, using the nitrous oxide-inhalation technique (based on the Fick principle) (11, 12, 22, 26) or the  $^{133}\text{Xe}$ -inhalation technique (3), generally show no changes in cerebral blood flow during dynamic exercise. However, studies using the  $^{133}\text{Xe}$ -clearance technique

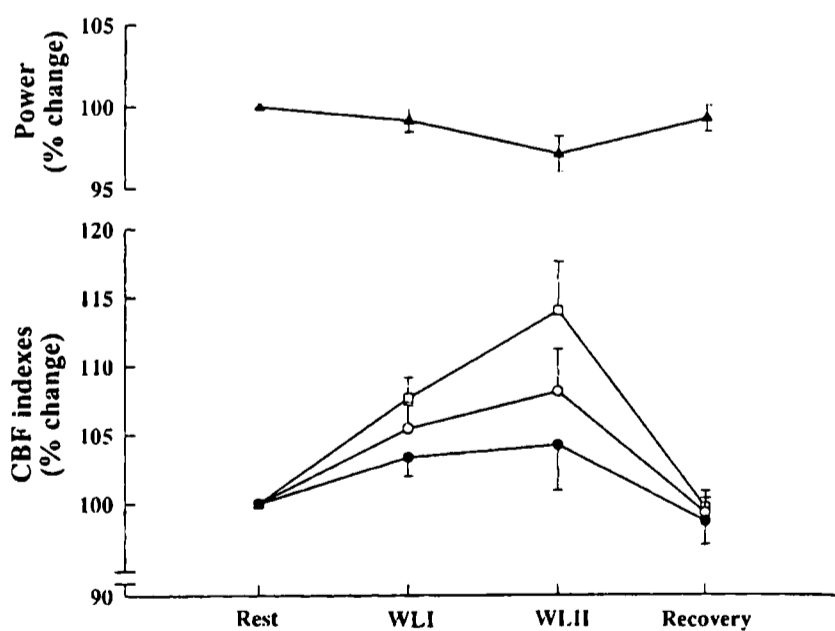


Fig. 2. Ensemble averages for group ( $n = 24$ ; 3 tests for each of 8 subjects) of changes in  $P$  and 3 indexes of cerebral blood flow (CBF) in middle cerebral artery at rest, during submaximal exercise, and during recovery. Top: average  $P$  ( $\bar{P}$ ). Bottom: normalized values for average  $V_P$  ( $\bar{V}_P$ ; □), average  $V_{IWM}$  ( $\bar{V}_{IWM}$ ; ○), and average middle cerebral artery flow index ( $\bar{P} \cdot \bar{V}_{IWM}$ ; ●). Error bars, 1 SD.

to determine larger regional (i.e., cortical) variations in cerebral blood flow have reported modest increases (i.e., 25–31%) in cerebral blood flow during dynamic exercise of light to moderate intensity (i.e., 50% of  $\dot{V}O_{2\max}$ ) (6, 9, 10, 17, 23).

Some studies have reported results of the simultaneous use of different techniques. Jørgensen et al. (10) reported similar magnitudes (i.e., 20–30%) for the changes in cerebral blood flow during moderate dynamic exercise as assessed by Doppler ultrasound and the  $^{133}\text{Xe}$ -clearance technique. However, Madsen et al. (14) reported a 22% increase in cerebral blood flow velocity by using Doppler ultrasound but found no change in global average cerebral blood flow by using  $^{133}\text{Xe}$  combined with the Kety-Schmidt technique (11). Overall, our results suggest that the observation of an increase in cerebral blood flow with exercise that has been reported with transcranial Doppler ultrasound needs to be treated with caution. One possibility is that much of the response could arise as an artifact from the increased amplitude and frequency of the arterial pressure waveform and its consequent effects on the flow profile of the arterial flow in the middle cerebral artery.

We acknowledge the assistance provided by Robert Bowyer with computing (Matlab), the skilled technical assistance from David O'Connor, and the volunteers for their participation in the study.

This study was supported by the Wellcome Trust. M. J. Poulin was supported by a Heart and Stroke Foundation of Ontario (Canada) postdoctoral research fellowship (Grant F3555).

Address for reprint requests and other correspondence: P. A. Robbins, Univ. Laboratory of Physiology, Parks Road, Oxford OX1 3PT, UK (E-mail: peter.robbins@physiol.ox.ac.uk).

Received 17 September 1997; accepted in final form 16 December 1998.

## REFERENCES

1. Aaslid, R., T. Markwalder, and H. Nornes. Noninvasive transcranial Doppler ultrasound recording of flow velocity in basal cerebral arteries. *J. Neurosurg.* 57: 769–774, 1982.
2. Fink, G. R., L. Adams, J. D. G. Watson, J. A. Innes, B. Wuyam, I. Kobayashi, D. R. Corfield, K. Murphy, T. Jones, R. S. J. Frackowiak, and A. Guz. Hyperpnoea during and immediately after exercise in man: evidence of motor cortical involvement. *J. Physiol. (Lond.)* 489: 663–675, 1995.
3. Globus, M., E. Melamed, A. Keren, D. Tzivoni, C. Granot, S. Lavy, and S. Stern. Effect of exercise on cerebral circulation. *J. Cereb. Blood Flow Metab.* 3: 287–290, 1983.
4. Hellström, G., W. Fischer-Colbrie, N. G. Wahlgren, and T. Jogestrand. Carotid artery blood flow and middle cerebral artery blood flow velocity during physical exercise. *J. Appl. Physiol.* 81: 413–418, 1996.
5. Hellström, G., and N. G. Wahlgren. Physical exercise increases middle cerebral artery blood flow velocity. *Neurosurg. Rev.* 16: 151–156, 1993.
6. Herholz, K., W. Buskies, M. Rist, G. Pawlik, W. Hollmann, and W. D. Heiss. Regional cerebral blood flow in man at rest and during exercise. *J. Neurol.* 234: 9–13, 1987.
7. Hokanson, D. E., D. J. Mozersky, D. S. Sumner, and D. E. Strandness. A phase-locked echo tracking system for recording arterial diameter changes in vivo. *J. Appl. Physiol.* 32: 728–733, 1972.
8. Howse, B. P. A., M. E. McIntyre, and P. A. Robbins. Modifications to a cycle ergometer for studying the transition from rest to exercise in man (Abstract). *J. Physiol. (Lond.)* 417: 7P, 1989.
9. Jørgensen, L. G., M. Perko, B. Hanel, T. V. Schroeder, and N. H. Secher. Middle cerebral artery flow velocity and blood flow during exercise and muscle ischemia in humans. *J. Appl. Physiol.* 72: 1123–1132, 1992.
10. Jørgensen, L. G., G. Perko, and N. H. Secher. Regional cerebral artery mean flow velocity and blood flow during dynamic exercise in humans. *J. Appl. Physiol.* 73: 1825–1830, 1992.
11. Kety, S. S., and C. F. Schmidt. The determination of cerebral blood flow in man by the use of nitrous oxide in low concentrations. *Am. J. Physiol.* 143: 53–66, 1945.
12. Kleinerman, J., and L. Sokoloff. Effects of exercise on cerebral blood flow and metabolism in man (Abstract). *Federation Proc.* 12: 77, 1953.
13. Linkis, P., L. G. Jørgensen, H. L. Olesen, P. L. Madsen, N. A. Lassen, and N. H. Secher. Dynamic exercise enhances regional cerebral artery mean flow velocity. *J. Appl. Physiol.* 78: 12–16, 1995.
14. Madsen, P. L., B. K. Sperling, T. Warming, J. F. Schmidt, N. H. Secher, G. Wildschiodtz, S. Holm, and N. A. Lassen. Middle cerebral artery blood velocity and cerebral blood flow and  $O_2$  uptake during dynamic exercise. *J. Appl. Physiol.* 74: 245–250, 1993.
15. Moraine, J. J., M. Lamotte, J. Berre, G. Niset, A. Leduc, and R. Naeije. Relationship of middle cerebral artery blood flow velocity to intensity during dynamic exercise in normal subjects. *Eur. J. Appl. Physiol.* 67: 35–38, 1993.
16. Nichols, W. W., and M. F. O'Rourke. *McDonald's Blood Flow in Arteries: Theoretical, Experimental and Clinical Principles*. London: Arnold, 1998, p. 11–53.
17. Olesen, J. Contralateral focal increase of cerebral blood flow in man during arm work. *Brain* 94: 635–646, 1971.
18. Pandit, J. J., and P. A. Robbins. Ventilation and gas exchange during sustained exercise at normal and raised  $CO_2$  in man. *Respir. Physiol.* 88: 101–112, 1992.
19. Pott, F., K. Jensen, N. J. Christensen, N. A. Lassen, and N. H. Secher. Middle cerebral artery blood velocity and plasma catecholamines during exercise. *Acta Physiol. Scand.* 158: 349–356, 1996.
20. Poulin, M. J., P. J. Liang, and P. A. Robbins. Dynamics of the cerebral blood flow response to step changes in end-tidal  $PCO_2$  and  $PO_2$  in humans. *J. Appl. Physiol.* 81: 1084–1095, 1996.
21. Robbins, P. A., J. Conway, D. A. Cunningham, S. Khamnei, and D. J. Paterson. A comparison of indirect methods for continuous estimation of arterial  $PCO_2$  in men. *J. Appl. Physiol.* 68: 1727–1731, 1990.
22. Scheinberg, P., I. Blackburn, M. Rich, and M. Saslaw. Effects of vigorous physical exercise on cerebral circulation and metabolism. *Am. J. Med.* 16: 549–554, 1953.
23. Thomas, S. N., T. Schroeder, N. H. Secher, and J. H. Mitchell. Cerebral blood flow during submaximal and maximal dynamic exercise in humans. *J. Appl. Physiol.* 67: 744–748, 1989.
24. Williamson, J. W., A. C. L. Nobrega, R. McColl, D. Mathews, P. Winchester, L. Friberg, and J. H. Mitchell. Activation of the insular cortex during dynamic exercise in humans. *J. Physiol. (Lond.)* 503: 277–283, 1997.
25. Yearwood, T. L., and K. B. Chandran. Physiological pulsatile flow experiments in a model of the human aortic arch. *J. Biomech.* 15: 683–704, 1984.
26. Zobl, E. G., F. N. Talmers, R. C. Christensen, and L. J. Baer. Effect of exercise on cerebral circulation and metabolism. *J. Appl. Physiol.* 20: 1289–1293, 1965.

## **CHAPTER 6**

### **INFLUENCE OF CEREBRAL BLOOD FLOW ON THE VENTILATORY RESPONSE TO HYPOXIA IN HUMANS**

Poulin, M.J. and P.A. Robbins (1998)  
*Experimental Physiol.*, **83**:95-106

## PREFACE

Respiratory physiologists are particularly interested in the changes that occur in cerebral blood flow with alterations in arterial gas tensions because the changes in cerebral blood flow have implications for the resulting ventilatory responses. One example is the ventilatory response to hypoxia - while it is well known that cerebral blood flow is increased by hypoxia, the role of the alterations in cerebral blood flow in the development of hypoxic ventilatory depression (HVD) remains unclear. The experiments described in Chapter 2 provided the data necessary to address this question.

Thus, this Chapter attempts to quantify the possible reduction in ventilation that could be attributed to changes in cerebral blood flow with hypoxia to determine whether it could be of sufficient magnitude to underlie HVD.

## DECLARATION

The work presented in this Chapter was carried out using the data that emerged from the experiments described in Chapters 2 and 3. This study was carried out over a one-year period in the University Laboratory of Physiology. This study was conceived, designed and planned by Professor Peter Robbins and myself. I carried out the experiments and the data analysis. Professor Robbins and I wrote the resulting paper. Results of this study were presented at The Physiological Society Meetings (Dublin, Ireland) and were published in abstract form in the *Journal of Physiology* (501P:66P, 1997).

## INFLUENCE OF CEREBRAL BLOOD FLOW ON THE VENTILATORY RESPONSE TO HYPOXIA IN HUMANS

MARC J. POULIN AND PETER A. ROBBINS\*

*University Laboratory of Physiology, Parks Road, Oxford OX1 3PT, UK*

(MANUSCRIPT RECEIVED 27 MAY 1997, ACCEPTED 11 SEPTEMBER 1997)

### SUMMARY

The purpose of this study was to quantify the possible reduction in ventilation that could be attributed to changes in cerebral blood flow (CBF) with hypoxia to determine whether it could be of sufficient magnitude to underlie hypoxic ventilatory decline (HVD). Six subjects underwent 20 min of isocapnic hypoxia (end-tidal  $P_{O_2}$ , 50 mmHg). An index of CBF was obtained using transcranial Doppler ultrasound of the middle cerebral artery. The CBF sensitivities to hypoxia and hypercapnia were obtained from the percentage changes in CBF between the last 3 min of the hypoxic or hypercapnic exposure and the 3 min period prior to the exposure. The magnitude of HVD during hypoxia was estimated by fitting a simple model of the ventilatory response to the hypoxic stimulus. The predicted fall in expiratory ventilation ( $\dot{V}_E$ ) due to a reduction in brain  $P_{CO_2}$  generated by the increase in CBF with hypoxia in all subjects was less than the measured magnitude of HVD (33%). Thus, the results from this study suggest that, in awake humans, changes in CBF during acute isocapnic hypoxia are quantitatively insufficient to underlie HVD in humans.

### INTRODUCTION

The ventilatory response to isocapnic hypoxia in humans has been well described. The response is biphasic and characterized by a fast initial increase in ventilation followed by a slower decline (hypoxic ventilatory decline, HVD) to a new value above the pre-hypoxic level (Weil & Zwillich, 1976; Easton, Slykerman & Anthonisen, 1986).

Both central and non-central mechanisms have been proposed to underlie HVD (for review see Neubauer, Melton & Edelman, 1990), and there is evidence to suggest that the mechanisms differ between conscious humans and anaesthetized animals (for review see Robbins, 1995). Among the proposed central mechanisms is the notion that an increase in cerebral blood flow (CBF) with hypoxia would increase carbon dioxide washout and thus lead to central hypocapnia (Neubauer *et al.* 1990).

While it is well known that CBF is increased by hypoxia (Kety & Schmidt, 1948; Shapiro, Wasserman & Patterson, 1966; Ellingsen, Hauge, Nicolaysen, Thoresen & Walloe, 1987; Poulin, Liang & Robbins, 1996), the role of the alterations in cerebral blood flow in the development of HVD remains unclear. In humans, Suzuki, Nishimura, Yamamoto, Miyamoto, Kishi & Kawakami (1989) examined the time course of the response of jugular venous  $P_{CO_2}$  to a step into isocapnic hypoxia. While they observed a reduction in jugular venous  $P_{CO_2}$  with hypoxia, they concluded that this reduction was too rapid to underlie HVD, which had a slower onset. On the other hand, Berkenbosch, Olievier & DeGoede (1995) concluded from studies in anaesthetized cats that 'the magnitude of ventilatory depression can be fully explained by the washout of  $CO_2$  at the site of the central chemoreceptors due to the increase in cerebral blood flow'.

\*Corresponding author: peter.robbins@physiol.ox.ac.uk

The purpose of the current study was to try to quantify the effect that an increase in CBF with hypoxia would have on ventilation in humans. In particular, we wanted to determine whether the magnitude of the effect could be sufficient to explain HVD (as concluded by Berkenbosch *et al.* 1995 for anaesthetized cats), or whether the magnitude of the expected effect was insufficient for this.

Experimental data for the response of the cerebral circulation to step changes in end-tidal  $P_{\text{CO}_2}$  and  $P_{\text{O}_2}$  ( $P_{\text{ET,CO}_2}$  and  $P_{\text{ET,O}_2}$ , respectively) have been previously reported by our laboratory (Poulin *et al.* 1996). Although not reported in this study, ventilatory data were also collected. In the current study, these data are reported and used in combination with the results for CBF in order to predict the likely effects on expiratory ventilation ( $\dot{V}_{\text{E}}$ ) of the increase in CBF. These predicted effects can be compared with the measured values for HVD.

## METHODS

### *Subjects*

Six healthy young students volunteered to take part. The study requirements were fully explained in written and verbal forms to all participants, with each giving written informed consent prior to participation in the study. The research was approved by the Central Oxford Research Ethics Committee. Participants were not on any medication and none had a history of cardiovascular, cerebrovascular or respiratory disease.

### *Protocols*

Each participant visited the laboratory, on six or seven occasions, each lasting 4–5 h. On each visit, each of four protocols (control, hypoxia, hypercapnia and combined hypoxia and hypercapnia) was performed once in a randomly assigned order, each lasting approximately 40 min. This study presents data from the hypoxic and hypercapnic (uncombined) protocols.

Each of the test protocols started with a short 6–7 min period when  $P_{\text{ET,O}_2}$  was held at 100 mmHg and  $P_{\text{ET,CO}_2}$  was held 1–2 mmHg above the subject's natural value as determined on the day. Then,  $P_{\text{ET,O}_2}$  or  $P_{\text{ET,CO}_2}$  was altered rapidly (over one or two breaths) to a new desired level, according to the protocols described below, and maintained constant for 20 min. Finally,  $P_{\text{ET,O}_2}$  or  $P_{\text{ET,CO}_2}$  was returned (again within one or two breaths) to its initial euoxic or near-eucapnic value and maintained constant for a further 10 min. For the hypoxic protocol,  $P_{\text{ET,O}_2}$  was lowered to 50 mmHg while  $P_{\text{ET,CO}_2}$  continued to be held 1–2 mmHg above the subject's normal value. For the hypercapnic protocol,  $P_{\text{ET,O}_2}$  continued to be held at 100 mmHg while  $P_{\text{ET,CO}_2}$  was elevated by 7.5 mmHg (i.e. to between 8.5 and 9.5 mmHg above the subject's normal value).

### *Experimental technique*

*Control of end-tidal gases.* Accurate control of the end-tidal gases was achieved using the technique of dynamic end-tidal forcing (Robbins, Swanson & Howson, 1982; Howson, Khamnei, McIntyre, O'Connor & Robbins, 1987). The experimental details associated with this study have been described previously (Poulin *et al.* 1996).

*Measurement of cerebral blood flow.* A 2 MHz pulsed Doppler ultrasound system was used to measure backscattered Doppler signals (maximum and intensity-weighted mean Doppler frequency shifts and total power) from the right middle cerebral artery. From these signals, an index of middle cerebral artery flow was calculated as the product of total power of the reflected Doppler signal (i.e. a measure of the total number of ultrasound scatterers) and the intensity-weighted mean velocity. This product was averaged over each cardiac cycle to give beat-by-beat values. Experimental details have been given elsewhere (Poulin *et al.* 1996).

The index of middle cerebral artery flow was expressed as a percentage of the average value over a 3 min period prior to the hypoxic or hypercapnic step. The cerebral blood flow response to hypoxia was calculated as the percentage increase in flow over the last 3 min of the hypoxic exposure compared with control (100%). The cerebral blood flow response to hypercapnia was calculated as the percentage

increase in flow over the last 3 min of the hypercapnic exposure compared with control (100%) by which time cerebral blood flow would have reached a steady state (Poulin *et al.* 1996).

*Measurement of ventilation.* During all experiments, subjects were seated in an upright position and breathed through a mouthpiece with the nostrils occluded. Respiratory volumes were measured with a turbine volume transducer (Howson, Khamnei, O'Connor & Robbins, 1986). Respiratory flows and timing information were obtained using a pneumotachograph (Hans Rudolph, Inc.) and differential pressure transducer (Validyne). The total dead space associated with the apparatus was 100 ml. Gas was sampled at the mouth at a rate of 80 ml min<sup>-1</sup> and analysed by mass spectrometry (Airspec MGA 3000) for fractional concentrations of O<sub>2</sub>, CO<sub>2</sub>, N<sub>2</sub> and Ar. A data-acquisition computer sampled the experimental variables every 20 ms and stored the data for later analysis.

#### *Model for the estimation of the magnitude of actual HVD from the ventilatory data*

In order to determine the actual magnitude of HVD, a mathematical model developed by Painter, Khamnei & Robbins (1993), with the revised parameterization of (Liang, Bascom & Robbins, 1997), was used to describe the ventilatory response to hypoxia. From this model, the magnitude of HVD was obtained. Briefly, the model of Liang *et al.* (1997) can be written in the form:

$$\dot{V}_E = \dot{V}_c + \dot{V}_p, \quad (1)$$

$$d\dot{V}_p/dt = (1/\tau_p)(g_p(1 - S(t - d_p) + k_p) - \dot{V}_p), \quad (2)$$

$$dg_p/dt = (1/\tau_h)(g_{100} - g_h(1 - S(t - d_p)) - g_p), \quad (3)$$

where  $\dot{V}_c$  and  $\dot{V}_p$  represent the central and peripheral chemoreflex contributions to ventilation, respectively. In eqn (2),  $\tau_p$  is the time constant for the rapid peripheral chemoreflex response,  $(1 - S)$  is the hypoxic stimulus where  $S$  represents the arterial oxygen saturation, approximated from the  $P_{ET,O_2}$  using the empirical relationship described by Severinghaus (1976):

$$S = 1 - 1.89 \times \exp(-0.05 \times P_{ET,O_2}), \quad (4)$$

$d_p$  is the peripheral time delay,  $k_p$  is a non-negative peripheral offset, and  $g_p$  is the peripheral chemosensitivity to hypoxia, a variable determined by a first-order dynamic process described by eqn (3). In eqn (3),  $\tau_h$  is the time constant associated with the development of HVD,  $g_{100}$  is the steady-state chemoreflex sensitivity in hyperoxia (i.e. when  $S = 1.0$ ), and  $g_h$  is the ratio of the sensitivity decrease to the decrease in the arterial oxygen saturation. Both  $g_{100}$  and  $g_h$  are constrained to be positive.

Assuming both  $S$  and  $g_p$  remain constant throughout the breath, the differential equations can be solved to provide a set of difference equations that can be written as:

$$g_{p_{n+1}} = g_{100} - g_h(1 - S(t_n - d_p)) - (g_{100} - g_h(1 - S(t_n - d_p)) - g_{p_n}) \exp(-(t_{n+1} - t_n)/\tau_h), \quad (5)$$

$$\dot{V}_{p_{n+1}} = g_{p_n}(1 - S(t_n - d_p) + k_p) - (g_{p_n}(1 - S(t_n - d_p) + k_p) - \dot{V}_{p_n}) \exp(-(t_{n+1} - t_n)/\tau_p), \quad (6)$$

$$\dot{V}_{E_n} = \dot{V}_{c_n} + \dot{V}_{p_n}, \quad (7)$$

where  $t_n$  is the time of the  $n$ th breath.

#### *Parameter estimation*

The data from all repetitions of each protocol for each subject were fitted simultaneously so that one set of parameter values was obtained for each protocol and for each subject. The data fitted to the model included a 2 min pre-hypoxic period, the 20 min hypoxic period, and the 10 min recovery period.

All the parameters except the time delay were estimated using a routine for minimizing a sum of squares. The time delay was determined on a 'grid search' basis by minimizing the sum of squares for the other parameters over a range of fixed pure delays of between 0 and 20 s (in steps of 1 s), and choosing the pure delay associated with the lowest minimum found.

The particular routine employed for the minimization was taken from the NAG (Numerical Algorithms Group, Oxford UK) FORTRAN library, subroutine E04FDF. This routine is designed to minimize a non-linear function of a number of variables when that function takes the special form of a sum of squares. All parameters in the cost function were constrained to be positive. The routine required initial guesses to be made for the parameters of the model. The guesses were based on visual inspection of the data combined

with a knowledge of the range of likely values based on known physiology. A number of such starting points was employed in each case in order to try to determine whether there were multiple minima. In every case, only a single minimum was detected.

*Estimation of ventilation during eucapnia and hypercapnia*

These data are required in the process of predicting the magnitude of the reduction in  $\dot{V}_E$  generated through the increases in cerebral blood flow with hypoxia (see below). For each repetition of the hypercapnic protocol, the breath-by-breath data for  $\dot{V}_E$  during the 3 min period before the start of the hypercapnic step were averaged to obtain steady-state eucapnic mean values. Similarly, the data for  $\dot{V}_E$  during the last 3 min period of the hypercapnic step were averaged to obtain steady-state hypercapnic mean values. Average values for each subject are reported (Table 1).

*Prediction of the reduction in  $\dot{V}_E$  expected through the increase in CBF with hypoxia*

*Calculation of change in brain tissue  $P_{CO_2}$  ( $P_{b,CO_2}$ ) for a given change in arterial  $P_{CO_2}$  ( $P_{a,CO_2}$ ).* Assuming that  $P_{b,CO_2}$  is fully equilibrated with venous  $P_{CO_2}$ , using the Fick equation we may write:

$$\dot{V}_{b,CO_2}(1) = \dot{Q}_b(1)\beta(P_{b,CO_2}(1) - P_{a,CO_2}(1)), \quad (8)$$

and

$$\dot{V}_{b,CO_2}(2) = \dot{Q}_b(2)\beta(P_{b,CO_2}(2) - P_{a,CO_2}(2)), \quad (9)$$

where  $\dot{V}_{b,CO_2}$  is the metabolic production of  $CO_2$  in the brain,  $\dot{Q}_b$  the blood flow,  $\beta$  the 'solubility' of  $CO_2$  in blood, and the indices (1) and (2) refer to the two conditions of euoxic eucapnia and euoxic hypercapnia, respectively. Assuming that  $\dot{V}_{b,CO_2}$  is unchanged in the two conditions, the right-hand sides of the two equations may be equated:

$$\dot{Q}_b(1)\beta(P_{b,CO_2}(1) - P_{a,CO_2}(1)) = \dot{Q}_b(2)\beta(P_{b,CO_2}(2) - P_{a,CO_2}(2)). \quad (10)$$

This may be re-arranged to yield:

$$(P_{b,CO_2}(2) - P_{b,CO_2}(1)) = (P_{a,CO_2}(2) - P_{a,CO_2}(1)) - (1 - \dot{Q}_b(1)/\dot{Q}_b(2))(P_{b,CO_2}(1) - P_{a,CO_2}(1)). \quad (11)$$

Equation (11) essentially describes the change in brain tissue  $P_{CO_2}$  as equal to the change in arterial  $P_{CO_2}$ , but with a correction relating to the change in blood flow with hypercapnia.  $\dot{Q}_b(1)/\dot{Q}_b(2)$  was obtained from the Doppler data, and an assumed value of 8.7 mmHg for  $(P_{b,CO_2}(1) - P_{a,CO_2}(1))$  was used (Suzuki *et al.* 1989) (see Discussion).

*Calculation of ventilatory sensitivity to changes in  $P_{b,CO_2}$ .* The ventilatory sensitivity for a change in  $P_{b,CO_2}$  is given by:

$$\frac{\Delta\dot{V}_E}{\Delta P_{b,CO_2}} = \frac{\dot{V}_E(2) - \dot{V}_E(1)}{(P_{b,CO_2}(2) - P_{b,CO_2}(1))}, \quad (12)$$

where,  $\dot{V}_E(1)$  and  $\dot{V}_E(2)$  are the values for expiratory ventilation during eucapnia and hypercapnia, respectively, and  $(P_{b,CO_2}(2) - P_{b,CO_2}(1))$  is the difference in brain tissue  $P_{CO_2}$  between hypercapnia and eucapnia, as calculated from eqn (11).

*Calculation of change in  $P_{b,CO_2}$  for a given change in  $P_{O_2}$ .* Assuming that  $P_{b,CO_2}$  is fully equilibrated with venous  $P_{CO_2}$ , using the Fick equation we may write:

$$\dot{V}_{b,CO_2}(1) = \dot{Q}_b(1)\beta(P_{b,CO_2}(1) - P_{a,CO_2}(1)), \quad (13)$$

and

$$\dot{V}_{b,CO_2}(3) = \dot{Q}_b(3)\beta(P_{b,CO_2}(3) - P_{a,CO_2}(3)), \quad (14)$$

where the indices (1) and (3) refer to the conditions of eucapnic euoxia and eucapnic hypoxia, respectively. Again, assuming that  $\dot{V}_{b,CO_2}$  is unchanged in the two conditions, the right-hand side of the two equations may be equated:

$$\dot{Q}_b(1)\beta(P_{b,CO_2}(1) - P_{a,CO_2}(1)) = \dot{Q}_b(3)\beta(P_{b,CO_2}(3) - P_{a,CO_2}(3)). \quad (15)$$

Table 1. *Ventilatory and cerebral blood flow responses to hypoxia and hypercapnia*

SIN	Hypoxia								Hypercapnia							
	$P_{ET,CO_2}$ (mmHg)		$P_{ET,O_2}$ (mmHg)		$\dot{V}_E$ (l min <sup>-1</sup> )		MCAF (%)		$P_{ET,CO_2}$ (mmHg)		$P_{ET,O_2}$ (mmHg)		$\dot{V}_E$ (l min <sup>-1</sup> )		MCAF (%)	
	A	B	A	B	A*	B*	A	B	A	B	A	B	A	B	A	B
940	41.0	41.0	99.6	49.8	43.8	24.5	100.0	112.3	41.3	48.8	99.3	100.0	14.6	49.9	100.1	132.2
959	39.7	39.9	99.7	50.7	23.1	16.5	100.0	112.2	40.3	47.6	99.2	100.0	12.1	30.6	100.0	142.4
964	42.1	42.4	100.0	49.8	16.8	11.2	99.9	109.7	42.3	49.7	100.0	100.0	10.7	25.6	100.0	137.6
966	40.7	40.8	100.1	49.8	25.1	15.3	100.1	105.5	41.0	48.4	99.8	100.0	11.6	30.2	100.0	126.9
967	39.7	39.7	100.2	50.1	25.8	20.2	100.0	106.9	39.4	47.0	100.1	100.0	17.1	30.0	100.1	127.0
971	38.0	38.3	99.7	49.8	20.1	15.9	100.0	105.9	38.0	45.4	99.4	100.0	9.9	31.7	100.1	116.5
Mean	40.2	40.4	99.9	50.0	25.8	17.3	100.0	108.7	40.4	47.8	99.7	100.0	12.7	33.0	100.0	130.1
s.d.	1.4	1.4	0.6	0.6	9.4	4.6	0.1	3.1	1.5	1.5	0.7	0.1	2.7	8.6	0.0	9.1

SIN, subject identification number; A, mean value over a 3 min period prior to the hypoxic or hypercapnic step; B, mean value over the last 3 min of the hypoxic or hypercapnic exposure; A\*, peak ventilatory response on initiation of hypoxia, from the model output; B\*, ventilatory response at the end of the 20 min hypoxic exposure, from the model output. MCAF, middle cerebral artery flow.  $n = 6$  for all subjects except subject 959 for whom  $n = 5$ .

Under eucapnic conditions,  $P_{a,CO_2}(1) = P_{a,CO_2}(3)$ , so the equation may be re-arranged to yield:

$$(P_{b,CO_2}(1) - P_{b,CO_2}(3)) = (1 - \dot{Q}_b(1)/\dot{Q}_b(3))(P_{b,CO_2}(1) - P_{a,CO_2}(1)). \quad (16)$$

Equation (16) gives the change in  $P_{b,CO_2}$  with hypoxia as a function of the ratio of blood flow in the euoxic and hypoxic conditions (obtained from the Doppler data) and the difference in  $P_{CO_2}$  between brain tissue and arterial blood in euoxic eucapnia for which a value of 8.7 is assumed (Suzuki *et al.* 1989) (again, see Discussion).

*Predicted fall in  $\dot{V}_E$  through changes in cerebral blood flow.* The predicted magnitude of the fall in  $\dot{V}_E$  arising through changes in cerebral blood flow, is given by:

$$\delta\dot{V}_{E,pred} = (P_{b,CO_2}(1) - P_{b,CO_2}(3))(\Delta\dot{V}_E/\Delta P_{b,CO_2}), \quad (17)$$

where  $(P_{b,CO_2}(1) - P_{b,CO_2}(3))$  is obtained from eqn (16) and  $(\Delta\dot{V}_E/\Delta P_{b,CO_2})$  is obtained from eqn (12).

## RESULTS

### General

The six subjects who undertook the study had an average age of  $20.8 \pm 1.7$  years (mean  $\pm$  s.d.), an average height of  $183.3 \pm 5.0$  cm and an average weight of  $74.2 \pm 10.0$  kg. None had a history of cardiovascular or respiratory disease and all had normal resting systolic ( $116.3 \pm 6.3$  mmHg) and diastolic ( $79.0 \pm 4.0$  mmHg) blood pressure. Each subject attended the laboratory on at least six occasions apart from one subject (959) who was only able to attend on five occasions.

### Cerebral blood flow responses to hypoxia and hypercapnia

The cerebral blood flow responses to hypoxia and hypercapnia are shown in Table 1. On average, in the hypoxic protocol, middle cerebral artery flow increased by  $8.7 \pm 3.1$  % while in the hypercapnic protocol, middle cerebral artery flow increased by  $30.1 \pm 9.1$  %.

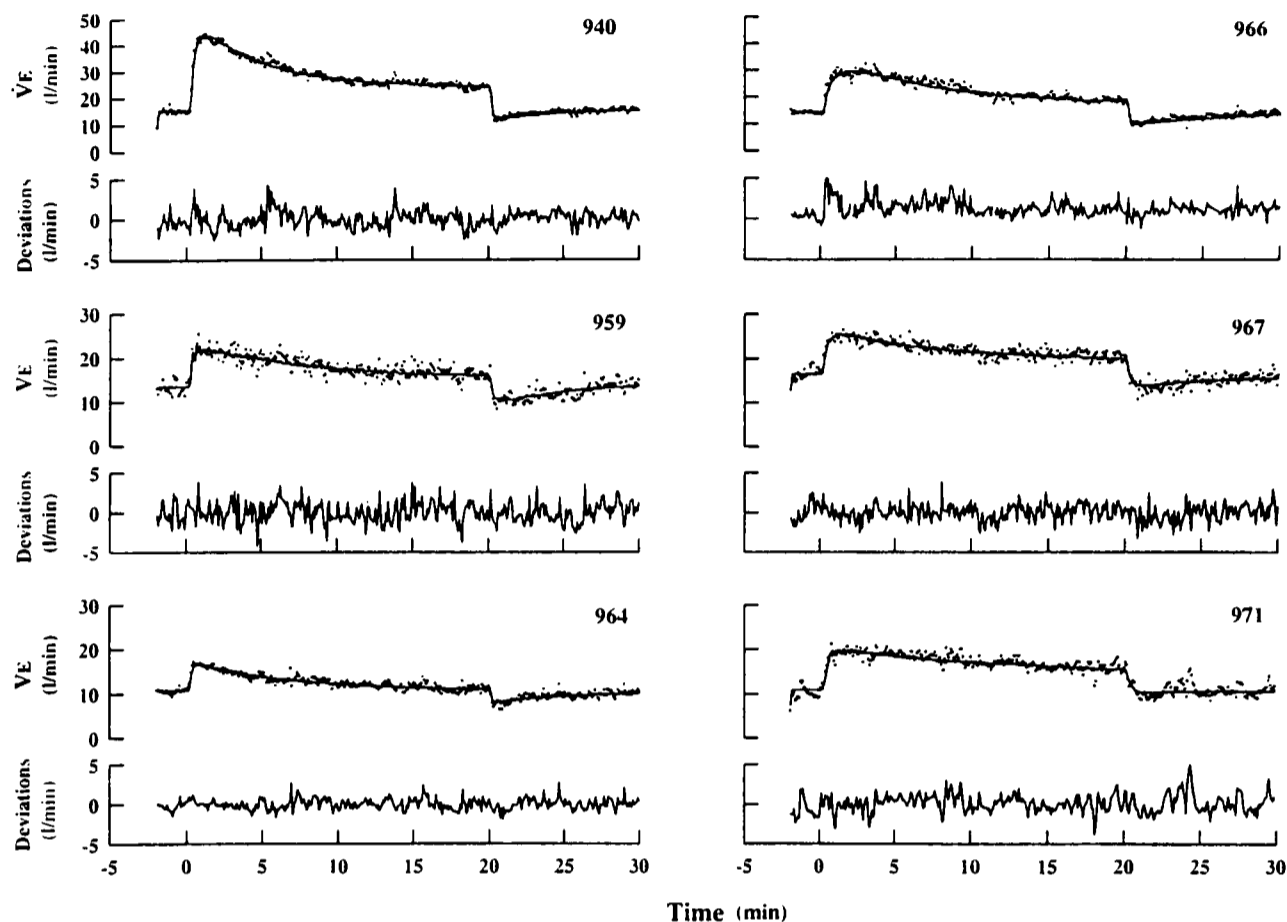


Fig. 1. Paired data sets for each subject: ventilatory responses to hypoxia (●) with the model output (continuous curve) (upper records) and the deviations between the averaged data and the model output (lower records). Each data set represents an ensemble-average of the data from all repetitions for each subject. The breath-by-breath data are interpolated over 1 s intervals.

### Ventilatory responses

*Ventilatory response to hypoxia.* The fitted model output along with the averaged experimental data and the deviations between the averaged data and the model output are shown for each subject in Fig. 1. The results of model fitting show a good fit of the model to the data. The individual values and group means for the estimated model parameters, including the pure delay, the time constant for the rapid peripheral chemoreflex response for the on-transient, the time constant for the rapid peripheral chemoreflex response for the off-transient, and the gain term for the magnitude for HVD are given in Table 2.

*Ventilatory response to hypercapnia.* The steady-state ventilatory responses to hypercapnia are shown in Table 1. The data represent average values for each subject, and were obtained by first determining the mean value of each repetition in a single subject over the 3 min periods and then averaging the responses of each subject.

### The magnitude of the expected fall in $\dot{V}_E$ through changes in cerebral blood flow

The data for the calculated change in brain tissue  $P_{CO_2}$  for a given change in arterial  $P_{CO_2}$  are presented in Table 3. The data assume a standard value of 8.7 mmHg for the difference between brain and arterial  $P_{CO_2}$  under normal air-breathing conditions (Suzuki *et al.* 1989). These data were used to calculate the ventilatory sensitivity to changes in brain tissue  $P_{CO_2}$ .

Table 2. Values for the estimated model parameters of the ventilatory response to hypoxia

<i>n</i>	SIN	$g_h$ (l min <sup>-1</sup> )	$g_{100}$ (l min <sup>-1</sup> )	$k_p$ (l min <sup>-1</sup> )	$\tau_{p1}$ (s)	$\tau_{p2}$ (s)	$\tau_h$ (s)	$\dot{V}_c$ (l min <sup>-1</sup> )	$d_p$ (s)
6	940	1032.4	244.8	0.01	18.0	0.1	279.5	10.2	0.0
5	959	156.8	64.5	0.19	4.5	4.7	463.6	2.0	3.0
6	964	168.9	45.1	0.10	0.8	1.9	412.3	6.0	4.0
6	966	436.3	105.7	0.06	29.4	5.3	450.3	6.1	0.0
5	967	177.7	73.2	0.11	9.3	11.0	370.1	7.9	1.0
5	971	264.6	71.7	0.01	14.8	14.1	264.6	9.5	0.0
	Mean	372.8	100.8	0.08	12.8	6.2	373.4	6.9	1.3
	S.D.	138.7	29.9	0.03	4.2	2.2	34.8	1.2	0.7

Definition of terms:  $g_h$ , the ratio of the sensitivity decrease to the decrease in the arterial fractional oxygen saturation;  $g_{100}$ , the steady-state chemoreflex sensitivity to hypoxia when oxygen saturation has been sustained at 100%;  $k_p$ , offset so that peripheral ventilation can take a non-zero value when saturation is 100%;  $\tau_{p1}$ , the time constant for the rapid peripheral chemoreflex response for the on-transient;  $\tau_{p2}$ , the time constant for the rapid peripheral chemoreflex response for the off-transient;  $\tau_h$ , the time constant associated with the development of hypoxic ventilatory decline;  $\dot{V}_c$ , the central chemoreflex contribution to ventilation;  $d_p$ , the peripheral time delay.

Table 3. Changes in arterial and brain  $P_{CO_2}$  in response to hypercapnia and hypoxia, together with calculated ventilatory sensitivities to brain hypercapnia, the predicted fall in  $\dot{V}_E$  with the increase in CBF, and the values for HVD

<i>n</i>	SIN	Hypercapnia			Hypoxia		
		$\Delta P_{a,CO_2}$ (mmHg)	$\Delta P_{b,CO_2}$ (mmHg)	$\Delta \dot{V}_E / \Delta P_{b,CO_2}$ (l min <sup>-1</sup> mmHg <sup>-1</sup> )	$\Delta P_{b,CO_2}$ (mmHg)	$\delta \dot{V}_{E, pred}$ (l min <sup>-1</sup> )	HVD (l min <sup>-1</sup> )
6	940	7.49	5.38	6.57	0.95	6.25	19.26
5	959	7.27	4.68	3.95	0.95	3.76	6.64
6	964	7.49	5.12	2.90	0.77	2.24	5.65
6	966	7.41	5.57	3.33	0.45	1.50	9.73
5	967	7.59	5.75	2.23	0.56	1.25	5.66
5	971	7.49	6.26	3.48	0.49	1.69	4.18
	Mean	7.46	5.46	3.74	0.70	2.78	8.52
	S.D.	0.11	0.54	1.50	0.23	1.92	5.58

For hypercapnia: the change in brain tissue  $P_{CO_2}$  ( $\Delta P_{b,CO_2}$ ) for a given change in arterial  $P_{CO_2}$  ( $\Delta P_{a,CO_2}$ ) is calculated from eqn (11); the ventilatory sensitivity to changes in brain tissue  $P_{CO_2}$  ( $\Delta \dot{V}_E / \Delta P_{b,CO_2}$ ) is calculated from eqn (12). For hypoxia:  $\Delta P_{b,CO_2}$  for a given change in cerebral blood flow is calculated from eqn 16;  $\delta \dot{V}_{E, pred}$  is calculated from eqn (17); HVD is obtained from the data in Table 1.

( $\Delta \dot{V}_E / \Delta P_{b,CO_2}$ ). Also presented in Table 3 are the data showing the calculated change in brain tissue  $P_{CO_2}$  with hypoxia, related to the change in MCAF, also assuming a difference of 8.7 mmHg in  $P_{CO_2}$  between brain tissue and arterial blood in euoxic eucapnia (Suzuki *et al.* 1989).

Table 3 also shows the predicted fall in  $\dot{V}_E$  through changes in cerebral blood flow and the actual measured values for HVD. The relationship between these is shown in Fig. 2. In all cases, the values for the predicted fall in  $\dot{V}_E$  from changes in cerebral blood flow are substantially smaller than the measured values for HVD. This finding is significant on the basis of a significant test (Student's paired *t* test;  $P < 0.05$ ). However, the relationship between the two variables does show a positive and significant correlation (correlation coefficient,  $r = 0.83$ ;  $P < 0.05$ ).

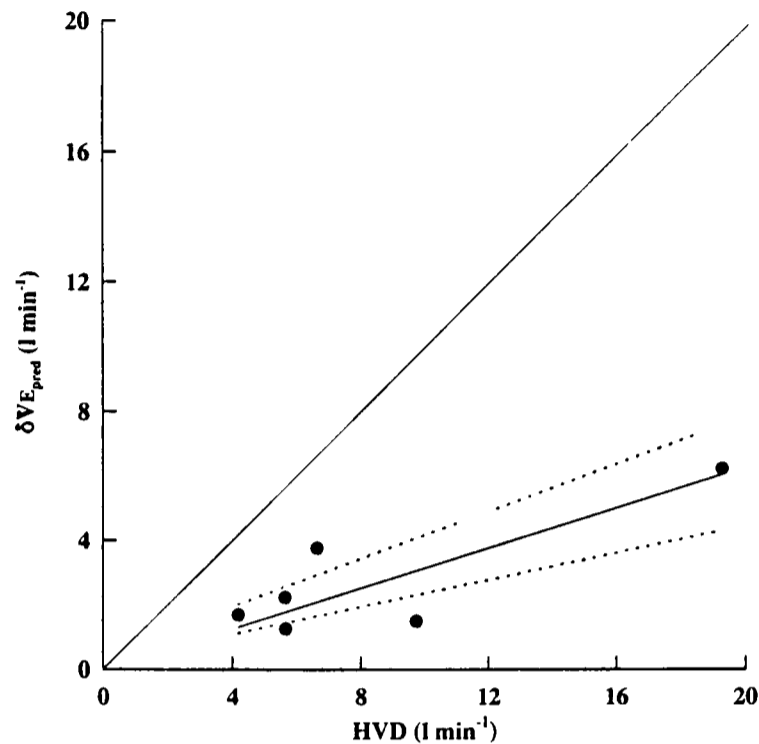


Fig. 2. Comparison of the measured hypoxic ventilatory depression (HVD) with the predicted fall in  $\dot{V}_E$  ( $\delta\dot{V}_{E,\text{pred}}$ ) calculated from the changes in cerebral blood flow. The values for  $\delta\dot{V}_{E,\text{pred}}$  were calculated by assuming a value of 8.7 mmHg for the difference in  $P_{\text{CO}_2}$  between brain tissue and arterial blood in euoxic eucapnia (Suzuki *et al.* 1989). The continuous line through the filled circles represents the least-squares linear regression. The upper and lower dashed lines represent the least-squares linear regressions that were determined by assuming values for the difference in  $P_{\text{CO}_2}$  between brain tissue and arterial blood that are 20% higher and lower than the assumed value of 8.7 mmHg.

## DISCUSSION

### Major findings

This study assessed the relationship between cerebral blood flow and HVD during sustained isocapnic hypoxia in humans. The major finding of this study is that, with sustained hypoxia over 20 min, the predicted magnitude of the reduction in  $\dot{V}_E$  arising through changes in cerebral blood flow is much less than the measured magnitude of HVD. These findings for conscious humans differ from those for the anaesthetized cat, where Berkenbosch *et al.* (1995) concluded that the magnitude of HVD could be fully explained by the washout of  $\text{CO}_2$  arising from the increase in CBF.

### Assumptions of this study

One assumption used in the derivation of the eqns (10) and (15) is that the metabolic rate of the brain remains constant during the variations in  $\text{CO}_2$ . There is some evidence that overall oxygen consumption may vary with  $P_{\text{CO}_2}$ , with a decrease in  $\text{CO}_2$  resulting in an increase in oxygen consumption (Karetzky & Cain, 1970). However, the overall effect is small (ca. 0.8% change in oxygen consumption per mmHg  $P_{\text{CO}_2}$ ) compared with the effect of  $P_{\text{CO}_2}$  on brain blood flow (ca. 4.0% per mmHg  $P_{\text{CO}_2}$ ). Since the percentage changes in brain blood flow and metabolic rate have similar effects in the equations, it seems reasonable to neglect this phenomenon.

In this study, the changes in middle cerebral artery blood flow with hypoxia and hypercapnia have been assumed to represent the changes in local blood flow to the chemosensitive areas of the medulla. In humans, there is evidence available to suggest that the cerebral blood flow response to hypercapnia appears to be similar in the arterial vessels supplying the ventral medullary (i.e. putative central chemoreceptors) and cortical areas (Hida, Kikuchi, Okabe, Miki, Kurosawa & Shirato, 1996). In anaesthetized cats, studies using the hydrogen clearance technique (Feustel, Stafford, Allen & Severinghaus, 1984) have shown that the relative responses to hypoxia and hypercapnia at the ventrolateral medullary surface are similar to those reported for the cortex (Marcus, Heistad, Ehrhardt & Abboud, 1976). This is supported by other studies in lightly anaesthetized rats using microelectrodes (Macmillan, Salford & Siesjo, 1974) and in anaesthetized and ventilated dogs using microspheres (Heistad, Marcus, Ehrhardt & Abboud, 1976), where again no regional differences were detected. However, there is one report (Neubauer & Edelman, 1984) which suggests that, in unanaesthetized cats, the medullary regions may be more sensitive to hypoxia than cortical regions, and if this were the case in conscious humans, then our calculations could underestimate the effects of cerebral blood flow.

A third assumption of this study is that the global jugular venous to arterial  $P_{b,CO_2} - P_{a,CO_2}$  difference represents the local venous to arterial  $P_{CO_2}$  difference at the sites of respiratory chemosensitivity. There is evidence in conscious humans to suggest that jugular venous  $P_{CO_2}$  does reflect the  $P_{CO_2}$  in the lumbar cerebro-spinal fluid (Bradley & Semple, 1962) and there is good agreement between lumbar and cisternal magna cerebro-spinal  $P_{CO_2}$ , which presumably should be more representative of medullary  $P_{CO_2}$  (Bradley & Semple, 1962). This assumption is supported by evidence in anaesthetized and unanaesthetized decerebrate cats showing that extracellular pH measured on the ventral surface of the medulla reflects the respiratory drive arising from the central chemosensitive areas (Ahmad & Loeschcke, 1982).

A fourth assumption of this study is that the level of hypoxia used was not sufficient to stimulate lactate production and thus alter ventilation in this manner. Allen, Busza, Crockard & Gadian (1992) have studied lactate production by the brain in the gerbil using  $^1H$ -NMR spectroscopy and found little effect of hypoxia down to a level of 50 mmHg, although lactate concentrations rose at values of  $P_{a,O_2}$  below this. If there were an increase in brain lactate, then it might be expected to accumulate over several minutes, and this should result in a slow adaptation of cerebral blood flow with the change in pH. No such change was observed (Poulin *et al.* 1996). Overall, it seems relatively unlikely that changes in lactate production would be affecting our results to any great extent.

*Factors affecting the magnitude of the predicted fall in  $\dot{V}_E$  associated with the increase in cerebral blood flow with hypoxia*

The magnitudes of the predicted fall in  $\dot{V}_E$  reported in this study depend first on the calculated falls in brain  $P_{CO_2}$  with hypoxia, which in turn depend on the initial arterio-venous differences and the increases in cerebral blood flow with hypoxia, and secondly on the ventilatory sensitivities to the change in  $P_{CO_2}$ .

The average calculated reduction in arterio-venous  $P_{CO_2}$  differences in our study is 0.7 mmHg after induction of hypoxia at 50 mmHg. This can be compared with a measured reduction in arterio-venous difference of 2.3 mmHg after induction of hypoxia at 44 mmHg (Suzuki *et al.* 1989). In part, our lower value for the reduction in arterio-venous  $P_{CO_2}$  difference is likely to be

due to the more moderate level of hypoxia in our study. However, it may also be due to the relatively small changes in cerebral blood flow observed in our subjects when compared with other studies (Kety & Schmidt, 1948; Cohen, Alexander, Smith, Reivich & Wollman, 1967; Shapiro, Wasserman, Baker & Patterson, 1970; Ellingsen *et al.* 1987; Poulin *et al.* 1996).

It is interesting to note that, while our subjects may have a rather small increase in CBF compared with other studies, they do not appear to have any associated reduction in HVD which is broadly in line with other studies (Khamnei & Robbins, 1990; Bascom, Pandit, Clement & Robbins, 1992).

In our study we assumed a difference of 8.7 mmHg in  $P_{\text{CO}_2}$  between brain tissue and arterial blood in euoxic eucapnia (Suzuki *et al.* 1989). Variations in this assumed difference will cause variations in the magnitude of the predicted fall in  $\dot{V}_{\text{E}}$  with increases in CBF. In order to examine this quantitatively, predicted values for the fall in  $\dot{V}_{\text{E}}$  were calculated using variations of  $\pm 20\%$  in the standard value of 8.7 mmHg (i.e. values of 10.44 and 6.96 mmHg) for the  $P_{\text{b,CO}_2} - P_{\text{a,CO}_2}$  difference. Even with such deviations in the brain tissue difference for  $P_{\text{CO}_2}$ , the predicted values for the fall in  $\dot{V}_{\text{E}}$  remain much smaller than measured values for HVD. The effect of this on the relationship between the two variables is shown in Fig. 2.

#### *Do changes in cerebral blood flow with hypoxia play a role in HVD?*

The study of Suzuki *et al.* (1989) found that there was no progressive fall in jugular venous  $P_{\text{CO}_2}$  associated with the development of HVD, a finding which is consistent with work from our own laboratory in awake humans showing that there is no adaptation or progressive increase in the cerebral blood flow response to moderate hypoxia after the initial transient (Poulin *et al.* 1996). The current study demonstrates that the calculated reduction in  $\dot{V}_{\text{E}}$  associated with an increase in CBF with hypoxia would seem to be quantitatively insufficient to account for HVD. Taken together, these findings suggest there is no major role for changes in CBF in generating HVD in humans.

There remains the possibility that a minor contribution to HVD from changes in CBF could be present. One prediction that might be made is that, if HVD were generated through changes in cerebral blood flow, then the magnitude of HVD would show a correlation with central ventilatory sensitivity to hypercapnia. We are unaware of any results which pertain to this. However, it is interesting to note that from our current study we do find a correlation between this sensitivity and the measured value for HVD ( $r = 0.89$ ;  $P < 0.05$ ) although many factors other than a causal relationship between cerebral blood flow and HVD could account for this.

Another suggestion that CBF might give rise to a contribution to HVD in some subjects comes from the study of Liang *et al.* (1997). They found that in some subjects, but not all, that HVD could be broken down into two components, one acting via a modulation of peripheral chemoreflex sensitivity and the other, more minor, contribution independent of peripheral chemoreflex sensitivity. They suggest one possible origin for this second component could be the changes in CBF.

This study was supported by The Wellcome Trust. M. J. Poulin was supported by postdoctoral fellowships from the MRC of Canada (1993–1996) and the Heart and Stroke Foundation of Ontario (1996–1997). We wish to acknowledge the computer programming assistance provided by Dr Pei-Ji Liang, the skilled technical assistance from Mr David O'Connor and the volunteers for their participation in the study.

## REFERENCES

- AHMAD, H. R. & LOESCHCKE, H. H. (1982). Transient and steady state responses of pulmonary ventilation to the medullary extracellular pH after approximately rectangular changes in alveolar  $P_{CO_2}$ . *Pflügers Archiv* **395**, 285–292.
- ALLEN, K., BUSZA, A. L., CROCKARD, H. A. & GADIAN, D. G. (1992). Brain metabolism and blood flow in acute cerebral hypoxia studied by NMR spectroscopy and hydrogen clearance. *NMR in Biomedicine* **5**, 48–52.
- BASCOM, D. A., PANDIT, J. J., CLEMENT, I. D. & ROBBINS, P. A. (1992). Effects of different levels of end-tidal  $P_{O_2}$  on ventilation during isocapnia in humans. *Respiration Physiology* **88**, 299–311.
- BERKENBOSCH, A., OLIEVIER, C. N. & DEGOEDE, J. (1995). Respiratory responses to hypoxia: peripheral and central effects. In *Modelling and Control of Ventilation*, ed. SEMPLE, S. J. G., ADAMS, L. & WHIPP, B. J., pp. 251–256. Plenum Press, New York.
- BRADLEY, R. D. & SEMPLE, S. J. G. (1962). A comparison of certain acid–base characteristics of arterial blood, jugular venous blood and cerebrospinal fluid in man, and the effect on them of some acute and chronic acid–base disturbances. *Journal of Physiology* **160**, 381–391.
- COHEN, P. J., ALEXANDER, S. C., SMITH, T. C., REIVICH, M. & WOLLMAN, H. (1967). Effects of hypoxia and normocarbica on cerebral blood flow and metabolism in conscious man. *Journal of Applied Physiology* **23**, 183–189.
- EASTON, P. A., SLYKERMAN, L. J. & ANTHONISEN, N. R. (1986). Ventilatory response to sustained hypoxia in normal adults. *Journal of Applied Physiology* **61**, 906–911.
- ELLINGSEN, I., HAUGE, A., NICOLAYSEN, G., THORESEN, M. & WALLOE, L. (1987). Changes in human cerebral blood flow due to step changes in  $P_{A}O_2$  and  $P_{A}CO_2$ . *Acta Physiologica Scandinavica* **129**, 157–163.
- FEUSTEL, P. J., STAFFORD, M. J., ALLEN, J. S. & SEVERINGHAUS, J. W. (1984). Ventrolateral medullary surface blood flow determined by hydrogen clearance. *Journal of Applied Physiology* **56**, 150–154.
- HEISTAD, D. D., MARCUS, M. L., EHRHARDT, J. C. & ABBOUD, F. M. (1976). Effect of stimulation of carotid chemoreceptors on total and regional cerebral blood flow. *Circulation Research* **38**, 20–25.
- HIDA, W., KIKUCHI, Y., OKABE, S., MIKI, H., KUROSAWA, H. & SHIRATO, K. (1996).  $CO_2$  response for the brain stem artery blood flow velocity in man. *Respiration Physiology* **104**, 71–75.
- HOWSON, M. G., KHAMNEI, S., MCINTYRE, M. E., O'CONNOR, D. F. & ROBBINS, P. A. (1987). A rapid computer controlled binary gas mixing system for studies in respiratory control. *Journal of Physiology* **403**, 103P.
- HOWSON, M. G., KHAMNEI, S., O'CONNOR, D. F. & ROBBINS, P. A. (1986). The properties of a turbine device for measuring respiratory volumes in man. *Journal of Physiology* **382**, 12P.
- KARETZKY, M. S. & CAIN, S. M. (1970). Effect of carbon dioxide on oxygen uptake during hyperventilation in normal man. *Journal of Applied Physiology* **28**, 8–12.
- KETY, S. S. & SCHMIDT, C. F. (1948). The effects of altered arterial tensions of carbon dioxide and oxygen on cerebral blood flow and cerebral oxygen consumption of normal young men. *Journal of Clinical Investigation* **27**, 484–492.
- KHAMNEI, S. & ROBBINS, P. A. (1990). Hypoxic depression of ventilation in humans: alternative models for the chemoreflexes. *Respiration Physiology* **81**, 117–134.
- LIANG, P.-J., BASCOM, D. A. & ROBBINS, P. A. (1997). Extended models of the ventilatory response to sustained isocapnic hypoxia in humans. *Journal of Applied Physiology* **82**, 667–677.
- MACMILLAN, V., SALFORD, L. G. & SIESJO, B. K. (1974). Metabolic state and blood flow in rat cerebral cortex, cerebellum and brainstem in hypoxic hypoxia. *Acta Physiologica Scandinavica* **92**, 103–113.
- MARCUS, M. L., HEISTAD, D. D., EHRHARDT, J. C. & ABBOUD, F. M. (1976). Total and regional cerebral blood flow measurement with 7-, 10-, 15-, 25-, and 50-micrometer microspheres. *Journal of Applied Physiology* **40**, 501–507.
- NEUBAUER, J. A. & EDELMAN, N. H. (1984). Nonuniform brain blood flow response to hypoxia in unanesthetized cats. *Journal of Applied Physiology* **57**, 1803–1808.
- NEUBAUER, J. A., MELTON, J. E. & EDELMAN, N. H. (1990). Modulation of respiration during brain hypoxia. *Journal of Applied Physiology* **68**, 441–451.

- PAINTER, R., KHAMNEI, S. & ROBBINS, P. A. (1993). A mathematical model of the human ventilatory response to isocapnic hypoxia. *Journal of Applied Physiology* **74**, 2007–2015.
- POULIN, M. J., LIANG, P.-J. & ROBBINS, P. A. (1996). Dynamics of the cerebral blood flow response to step changes in end-tidal  $P_{\text{CO}_2}$  and  $P_{\text{O}_2}$  in humans. *Journal of Applied Physiology* **81**, 1084–1095.
- ROBBINS, P. A. (1995). Hypoxic ventilatory decline: site of action. *Journal of Applied Physiology* **79**, 373–374.
- ROBBINS, P. A., SWANSON, G. D. & HOWSON, M. G. (1982). A prediction correction scheme for forcing alveolar gases along certain time courses. *Journal of Applied Physiology* **52**, 1353–1357.
- SEVERINGHAUS, J. W. (1976). Proposed standard determination of ventilatory responses to hypoxia and hypercapnia in man. *Chest* **1**, suppl., 129–131.
- SHAPIRO, W., WASSERMAN, A. J., BAKER, J. P. & PATTERSON, J. L. (1970). Cerebrovascular response to acute hypocapnic and eucapnic hypoxia in man. *Journal of Clinical Investigation* **49**, 2362–2368.
- SHAPIRO, W., WASSERMAN, A. J. & PATTERSON, J. L. (1966). Human cerebrovascular response to combined hypoxia and hypercapnia. *Circulation Research* **19**, 903–910.
- SUZUKI, A., NISHIMURA, M., YAMAMOTO, H., MIYAMOTO, K., KISHI, F. & KAWAKAMI, Y. (1989). No effect of brain blood flow on ventilatory depression during sustained hypoxia. *Journal of Applied Physiology* **66**, 1674–1678.
- WEIL, J. V. & ZWILLICH, C. (1976). Assessment of ventilatory response to hypoxia. *Chest* **1**, 124–128.

## **CHAPTER 7**

### **GENERAL DISCUSSION**

## **7 GENERAL DISCUSSION**

### **7.1 MAJOR FINDINGS**

The studies presented in this Thesis examined aspects of cerebral blood flow in humans, at rest and during exercise. Two novel techniques were combined, thus making it possible to by-pass many of the difficulties encountered in previous studies of cerebral blood flow in humans. The first technique, transcranial Doppler ultrasound, was used to assess changes in middle cerebral artery flow. The second technique, dynamic end-tidal forcing, was used to gain accurate control over arterial (end-tidal) PCO<sub>2</sub> and PO<sub>2</sub>.

In a first series of studies, we examined the cerebral blood flow response to step changes of hypoxia and carbon dioxide, and determined the degree of consistency between three indices of flow, along with an index of cross-sectional area in response to those stimuli (Chapters 2,4). In Chapters 3 and 4, the dynamic components of the response to each stimulus was also determined. The next study examined the changes in cerebral blood flow during submaximal exercise. In particular, three indices of flow were compared and one index of changes in cross-sectional area was evaluated (Chapter 5). Finally, an attempt was made to quantify the role of changes in cerebral blood flow in contributing to the magnitude of hypoxic ventilatory depression in humans (Chapter 6). This Chapter presents a brief summary of the major findings along with a brief discussion of ideas for future directions.

#### **7.1.1 Doppler Power**

In Chapters 2 and 5, it was shown that transcranial Doppler ultrasound can be used to detect changes in total Doppler power, which is proportional to changes in cross-sectional area of the vessel under investigation (5,89). At rest, with either hypoxia or hypercapnia

alone, the changes in Doppler power were not significant. However, with combined hypoxia and hypercapnia a significant increase (~4%) in the Doppler signal power was observed, at the relief of the stimuli when there was a very large and rapid decrease in cerebral blood flow (Fig. 2 and Table 2, Chapter 2). Significant changes in Doppler power were also observed during submaximal exercise (~40% of  $\dot{V}O_{2\max}$ ), where a small decrease (~4%) in power was observed (Table 2 and Fig. 2, Chapter 5).

Results from the exercise study showed a decrease in power predominantly during systole (Fig. 1, Chapter 5). Exercise represents one situation when blood flow in the middle cerebral artery might be under considerable influence from the concomitant changes in heart rate and blood pressure during exercise. In vessels with curvatures such as the middle cerebral artery the velocity profile within the vessel can become quite complicated. In addition, the flow within the vessel is not steady but pulsatile. In such a flow there may be both some flow reversal and/or flow separation for all or part of the cycle (71,121). Westerhof *et al.* (115) referred to arterial pulsatile flow as a series of forward and backward waveforms, with flow at bifurcations being susceptible to a significant backward component. Thus, although the changes in Doppler power normally reflect genuine changes in vessel cross-sectional area, there are situations (i.e. exercise) when the Doppler power might be greatly influenced by factors such as flow reversal or flow separation, hematocrit, shear rate and turbulence (25,29,97,98).

One clinical situation that might offer some insights into the issue of flow reversal and/or flow separation is cardiopulmonary bypass surgery (CPB). During CPB, cerebral perfusion is maintained by way of an extracorporeal circuit. Usually, but not always, a steady-state non-pulsatile flow is delivered to the brain. However, the appropriateness of

steady-state vs pulsatile flow remains unsettled. Furthermore, although previous studies have monitored cerebral blood flow during CPB, conflicting findings are reported vis-a-vis CO<sub>2</sub> reactivity (27,59-61) and the issue of changes in cross-sectional area has not been dealt with. Thus, other than addressing the issue of flow complexities, such *in vivo* studies might be of clinical merit, especially since patients are at increased risk of stroke and other cerebrovascular events during, and immediately after, CPB.

The issue of changes in Doppler power and vessel cross-sectional area could be further addressed by using various pharmacological interventions that are thought to vasodilate or vasoconstrict the larger cerebral vessels. Some interventions that hold particular clinical interest include administration of acetazolamide (i.e. Diamox), nitroglycerine, calcium antagonists and nitric oxide synthase inhibitors. Despite the widespread use of drugs such as Diamox (in altitude medicine) and nitroglycerine (in clinical practice), the cerebral hemodynamic effects of these and other drugs, and how they might modify cerebral blood flow and cerebral reactivity to carbon dioxide, remain unclear (16,33,111,116,117). Results from such studies could provide valuable insights into the mechanisms of regulation of cerebral blood flow.

### **7.1.2 Indices of Cerebral Blood Flow**

In Chapters 2 and 5, three indices of cerebral blood flow were compared. At rest, with either hypoxia or hypercapnia alone, changes in the three indices of cerebral blood flow were all very similar (Fig. 2 and Table 3, Chapter 2). However, with combined hypoxia and hypercapnia, the changes in the velocities significantly under-estimated the change in the flow index (Fig. 2 and Table 3, Chapter 2). With exercise, each of the three indices of cerebral blood flow provided different results for the changes in cerebral blood flow.

The difference between the indices was greatest at the highest level of exercise (~40% of  $\dot{V}O_2\text{max}$ ) (Table 2 and Fig. 2, Chapter 5). Collectively, these results show that while there are situations when either of the three indices can be used to assess cerebral blood flow, there are other situations (for example, exercise) when the use of a flow index might be preferable over the use of velocities.

### **7.1.3 Dynamic Aspects**

In Chapters 3 and 4, the dynamic components of the cerebral blood flow response to step changes of hypoxia, hypercapnia, and hypocapnia were described. With sustained hypoxia or hypercapnia there was no adaptation or progressive increase in middle cerebral artery flow (Figs.5,6 and Table 2, Chapter 3). In contrast, the response to hypocapnia was characterised by a slow progressive adaptation in flow which persisted for the entire period of hypocapnia (Table 3 and Fig. 4, Chapter 4).

It is possible that an increase in lactate may form part of the mechanism underlying the slow progressive increase in cerebral blood flow with sustained euoxic hypocapnia (3,14,41,49,58,77-79,81,108,109,122). One way to further address this issue is to use the technique of proton magnetic resonance spectroscopy ( $^1\text{H-MRS}$ ) to determine whether the time course of change in brain lactate matches the time course of change in cerebral blood flow. This has been the focus of a collaborative study with members of the spectroscopy Unit at the John Radcliffe Hospital. Preliminary studies are so far inconclusive.

One of the striking findings in this Thesis is that the cerebral blood flow response to hypoxia, hypercapnia, and hypocapnia in humans was shown to be much faster than has

been previously reported. Along with this is the finding of a significant asymmetry in the cerebral blood flow response to carbon dioxide. The asymmetry in hypercapnia (Table 2, Chapter 3) did show some qualitative similarities to that observed in hypocapnia (Table 3, Chapter 4). In both conditions, the time constant of the cerebral blood flow response to a step decrease in CO<sub>2</sub> was less than the time constant of the cerebral blood flow response to an increase in CO<sub>2</sub>. However, some quantitative differences were observed. The time constants for the step decreases in CO<sub>2</sub> were similar (~7 s in hypocapnia and ~6 s in hypercapnia) but the time constants for the step increases in CO<sub>2</sub> were significantly different (~14 s in hypocapnia and ~45 s in hypercapnia). The reason for these differences remains unclear. It is possible that the asymmetry between the on- and off- transients represents different vasodilatory and vasoconstrictive mechanisms inherent to the cerebral vasculature. On the other hand, the differences in the time constants for the step increases in CO<sub>2</sub> between hypercapnia and hypocapnia may not be quite as straightforward. Although it is possible that intrinsic mechanisms underlie these differences, changes in ventilation might also play a role. In the hypercapnic experiment, ventilation was left uncontrolled and this resulted in a large increase in ventilation (13 to 33 l/min, ~160% increase) with hypercapnia (see Table 1, Chapter 6). In the hypocapnic experiment, a controlled voluntary hyperventilation was maintained throughout and this resulted in a level of ventilation that remained pretty much constant (~35 l/min). The underlying reason for these differences remains to be investigated. Future studies using protocols which ventilation is controlled mechanically (13) might prove useful.

We failed to report a significant asymmetry with hypoxia (Table 2, Chapter 3). However, this may have been due to a low hypoxic cerebral blood flow sensitivity in our volunteers.

This may also be explained by the moderate level of hypoxia that was used ( $P_{ET_{O_2}}=50\text{mmHg}$ ) as this coincides with a “threshold” phenomenon that occurs when arterial  $P_{O_2}$  falls to about 50-60 mmHg (50). This phenomenon was illustrated for humans in Chapter 1 of this Thesis (Fig. 1.2), and has been reported elsewhere in other species (18,65).

#### 7.1.4 Aspects of Hypoxia

In general, studies of the cerebral blood flow response to acute hypoxia in humans have experienced varying degrees of success in separating the effects of hypoxia from those of  $CO_2$  (11,12,19,37,43,55,95,113). While some studies have attempted to control the background level of carbon dioxide at normal (eucapnic) levels, others have not, and this has contributed to a large variability of responses. As discussed in the opening Chapter (see section 1.5 and Fig. 1.2), the effect of hypocapnia, secondary to the ventilatory response to hypoxia, is a blunting of the cerebral blood flow response to hypoxia. Evidence of this effect is found in the recent study by Clar *et al.* (11), who examined the cerebral blood flow response to hypoxia in humans after twenty minutes and eight hours of either isocapnic and poikilocapnic hypoxia. In that study, a greater hypoxic sensitivity was observed with in eucapnic hypoxia (61%/unit desaturation) than with poikilocapnic hypoxia (36%/unit desaturation) although this difference was not significant.

Several mechanisms of action have been advanced to explain the regulation of cerebral blood flow during hypoxia. The most likely mechanisms include a direct effect of a low  $P_{O_2}$  on the smooth muscle of the pial arterioles (62), an indirect affect from the release of vasodilators from the endothelium or from the release of vasodilator metabolites (i.e. adenosine) from the surrounding tissue (83,118), shear stress and the production of nitric

oxide (34,52,83), the activation of ATP-sensitive (22,46,80,83,84,104) and/or calcium-dependant (22) potassium channels, lactate (4,76), and a neurogenic component initiated in the medulla (26). In addition, a mechanism more closely linked to arterial oxygen content has recently been proposed (10,69,102). Support for this latter mechanism comes from experiments involving carbon monoxide and hemodilution (31,39,75). The way by which changes in oxygen content serve as the signal for regulating blood flow remains unclear. However, a theory has been advanced which proposes that deoxygenation promotes an allosteric transition in hemoglobin, thereby favouring the release of nitric oxide which serves to relax blood vessels and increase blood flow (102).

A simple experimental approach using the techniques described in this Thesis, combined with protocols involving hypoxia, carbon monoxide and hemodilution, could prove useful in helping to separate the effects of a reduction in the oxygen binding capacity of the blood (i.e. oxygen content) from those of hypoxia (i.e. low  $P_{O_2}$ ).

Although the cerebral blood flow response to acute (~20 min) and short term hypoxia (~8 hours) has been fairly well established, the effect of longer periods of hypoxia on cerebral blood flow remains to be elucidated. This has been the focus of a study in the Oxford laboratory, where the period of hypoxia (under both isocapnic and poikilocapnic exposures in a purpose-built chamber (32)) has been extended to 48 hours. This period may allow the possibility of examining the cerebral blood flow response over the time that is associated with the onset of acute mountain sickness (AMS). It is hoped that these data, along with the recently published ventilatory data (105), may help clarify the role of cerebral blood flow in AMS, where both the etiology and the underlying cause remain obscure (6,33,38,63,73,86).

### 7.1.5 Transcranial Doppler Ultrasound: Advantages and Limitations

In previous studies of transcranial Doppler ultrasound, the most commonly used index of cerebral blood flow has been  $\bar{V}_P$ . Under conditions of laminar flow in a rigid tube, axial flow velocity (i.e.  $\bar{V}_P$ ) is proportional to true flow. However, if the flow is complex, then the possibility exists that the relationship between  $\bar{V}_P$  and true flow may not be linear. The studies presented in Chapters 2 to 6 of this Thesis have presented two additional indices of flow ( $\bar{V}_{IWM}$  and  $\bar{P} \cdot \bar{V}_{IWM}$ ) and one index of changes in cross-sectional area ( $\bar{P}$ ) that can be extracted from the whole Doppler spectrum. As a result, this Thesis provides useful comparative data for future studies electing to use any of these indices, at rest and during exercise, and in response to hypoxia, hypercapnia and hypocapnia.

The results from the studies in Chapters 2 to 6 indicate that, generally, there is very little difference among the three indices when assessing cerebral blood flow responses to modest stimuli. Thus, in situations when the three indices provide similar results, the use of either  $\bar{V}_P$  or  $\bar{V}_{IWM}$  has considerable advantages over  $\bar{P} \cdot \bar{V}_{IWM}$  (see Chapter 2, page 2249). However, despite the particular difficulties and time requirements involved with measuring  $\bar{P} \cdot \bar{V}_{IWM}$  (i.e. considerable patience, practice and skill needed to optimize and maximize the reflected Doppler power signal), this Thesis has shown that the measurement of power can provide a useful check on whether there are changes in cross-sectional area in situations in which this might be suspected. In such conditions, the use of  $\bar{P} \cdot \bar{V}_{IWM}$  is preferable because this index is proportional to overall flow regardless of the complexity of the flow pattern and should result in a constant estimation of flow.

Transcranial Doppler ultrasound provides a technique for the assessment of cerebral

blood flow that is noninvasive, safe, repeatable, and portable. This thesis has demonstrated the suitability of this technique to assess dynamic changes in cerebral blood flow in response to hypoxia, hypercapnia and hypocapnia. It should now be possible to use this technique with various pharmacological interventions (see section 7.2.6), along with the technique of dynamic end-tidal forcing, to help elucidate the mechanisms of action underlying the cerebral blood flow response to hypoxia, hypercapnia and hypocapnia.

Despite the clear advantages of transcranial Doppler ultrasound, a few words of caution are warranted. In situations where the characteristics of cerebral blood flow may change (for example, during exercise - see Chapter 5) it is not clear that changes in  $\bar{V}_P$  necessarily reflect changes in underlying flow. In such situations,  $\bar{V}_{IWM}$ ,  $\bar{P} \cdot \bar{V}_{IWM}$  and  $\bar{P}$  should also be measured. An additional concern is that blood flowing in vessels with bends and curves (such as in the MCA) may become complex (i.e. flow reversal and/or flow separation for all or part of the cardiac cycle). In this situation,  $\bar{P} \cdot \bar{V}_{IWM}$  may provide a more accurate reflection of any changes in overall flow than  $\bar{V}_P$  or  $\bar{V}_{IWM}$ . Finally, it should be kept in mind that the reflected Doppler power signal might be influenced by factors such as hematocrit, shear rate, and turbulence. Clearly, further studies using flow phantoms may be useful to further validate the use of Doppler power as an index of changes in cross-sectional area of cerebral vessels.

## 7.2 FUTURE DIRECTIONS

### 7.2.1 Antioxidant Vitamins

In recent years, antioxidant vitamins have been the focus of an increasing number of scientific studies. In a study using a model of cerebral infarction in rats, van der Worp *et*

*al.* (107) showed that a diet rich in vitamin E resulted in a 50% reduction in the size of infarctions after middle cerebral artery occlusion. They postulated that free radical formation and lipid peroxidation were involved in the pathogenesis of ischemia and that vitamin E provided some protection against oxidative damage. In mice, a vitamin E-enriched diet has been shown to have a protective effect on the endothelium of pial vessels from damage impairing the acetylcholine-mediated EDRF response (88). In humans, studies in young and aged subjects have shown that antioxidant vitamins (E, C, and beta-carotene) play a beneficial role in lowering the levels of lipid peroxidation (and thereby reducing oxidative stress) at rest and during exercise (40,66). The effects of antioxidants on the cerebral reactivity to hypoxia and carbon dioxide remain unknown. Since atherosclerosis is an age-related problem that also appears to be associated with an attenuation of endothelium-dependent relaxation (possibly through oxygen radical mechanisms) (101), further studies in animal models and humans might prove worthwhile.

### **7.2.2 Ageing**

Of the many potential areas of future investigation, the cerebrovascular physiology of ageing is very relevant, especially since the proportion of people aged 65 years and over is projected to increase dramatically in the early part of the next millennium. Almost one third of all cardiovascular deaths worldwide are due to stroke, a disease directly related to age, with the largest number among persons 60 years of age and over (9). Stroke imposes an enormous cost both as a burden to the health care system (99) and to the patient in terms of disability and decrease in the quality of life. Despite this, the effects of *age-alone* on cerebral hemodynamics and reactivity remain poorly understood. Clearly, a better understanding of the alterations that occur in the responsiveness of the

cerebral circulation with ageing is important.

Findings of studies on age-related alterations in cerebral blood flow are equivocal (1,15,35,42,56,82,100,120). Of the studies showing an age-related decrease in cerebral blood flow, a rate of decline 0.5% per year is suggested (57) and this is enhanced by risk factors (70). Studies using various techniques (57,70,74,112) have reported regional differences in flow with advancing age with the most evident decreases in cerebral blood flow observed in gray matter, and in the regions supplied by the middle cerebral artery (MCA). Although it is unclear why the regions supplied by the MCA are most affected, it is interesting to note that the MCA has many sites of curvatures and, because these are often sites of atherosclerotic plaque formation, it is possible that fluid-dynamic phenomena may be a causative factor in atherogenesis (7) which can lead to stroke.

Findings from recent studies suggest that regular physical activity may play an important role in minimizing the age-related declines in cardiovascular function and in maintaining cerebral blood flow and cognitive function (87,96). Despite some study shortcomings, the findings of Rogers *et al.* (87), together with evidence that age-related declines in cerebral blood flow become accelerated in subjects with risk factors for stroke (67), suggest that physical activity may play an important role in preventing or delaying the risk of stroke in retirement. There is some suggestion that a reduction in cerebral blood flow is measurable for at least two years prior to the onset of various cerebrovascular diseases (67). Thus, those at risk may have the most to gain from structured physical activity programmes. Clearly, defining the effects of *age alone* on cerebral blood flow, along with any potential benefits of physical activity, seems worthwhile.

### 7.2.3 Nonlinear Analyses

Recent studies have used a different approach to examine Doppler-derived data. The techniques of dynamical chaos, nonlinear time series analysis, and frequency domain analysis have been applied to extract details from the blood flow velocity waveform in the middle cerebral artery measured with transcranial Doppler ultrasound (44,45,53,110). In a study by Keunen *et al.* (44), nonlinear time series analysis techniques were applied to the maximum velocity waveform of the transcranial Doppler shift in order to study age-related changes in the complexity of the arterial blood flow. From their analysis, they inferred age-related changes (range 19-86 years) in the gain of the baroreceptor reflex and an increase in the vessel wall stiffness of the middle cerebral artery. If the technique proposed by Keunen *et al.* (44) proves valid, it is tempting to speculate on whether the complexity of the velocity waveform in aged individuals could be modified (i.e. become more like young) with a structured exercise programme of cardiovascular endurance training. This remains to be studied.

In another study, Kuo *et al.* (53) applied frequency domain and spectral analysis to extract several components from the blood flow velocity waveform in the middle cerebral artery and compared the waveform with the arterial blood pressure waveform (using a Finapres). They concluded that some of the mechanisms underlying cerebral blood flow velocity variability originated from fluctuations in blood pressure. This novel noninvasive approach of extracting physiological signals from the velocity waveform needs to be further explored, as it might prove useful in clinical medicine.

There are two obvious shortcomings in the studies described above. First, only peak velocity was used as the index of cerebral blood flow. Second, no attempts were made

to control the arterial  $\text{PCO}_2$ . This latter shortcoming is particularly worrisome since in the eucapnic range, cerebral blood flow is likely to vary by approximately 4%/Torr change in arterial  $\text{PCO}_2$ . The techniques described in this thesis could address these two issues.

#### **7.2.4 Functional Magnetic Resonance Imaging**

The advent of techniques such as functional magnetic resonance imaging (fMRI) have been well received as noninvasive techniques to study human cerebral circulation. Currently, however, there are still some struggles in dealing with fluctuations in physiological signals, for example those of cardiac and respiratory origins (72). Fluctuations in a third signal, variations in arterial  $\text{PCO}_2$ , are perhaps not yet fully appreciated as potential source of noise in fMRI signals. However this issue could be easily addressed by combining the techniques of dynamic end-tidal forcing with fMRI.

#### **7.2.5 Neural Control**

In the Introduction (see section 1.2.1), the innervation of the cerebral vasculature was discussed briefly and it was shown that the physiological significance of neural control of cerebral blood flow remains unclear (17). Insofar as the chemical regulation of the cerebral circulation is concerned, it is generally thought that neural mechanisms play perhaps only a minor role (8). Of interest are the results of a recent study in which transcranial Doppler ultrasound was used to assess changes in middle cerebral artery blood flow velocity in response to a cold pressor test (CPT) as a model of sympathetic activation (68). The authors reported a large decrease in blood flow velocity (range 20-35%) in response to the CPT and attributed this to a central noradrenergic activation of cerebral vessels. However, Doppler power was not measured and it is not possible to conclude whether the decrease in velocity was caused by a vasodilation of the middle

cerebral artery or by a decrease in blood flow. Further studies using Doppler power as an index of changes in cross-sectional area might provide a simple noninvasive and non-pharmacological method of clarifying the role of neural mechanisms in the control of larger cerebral vessels.

### 7.2.6 Pharmacological Interventions

From the many studies that have been published on the proposed mechanisms of regulation for cerebral blood flow (see section 1.2 for review), a considerable amount of evidence has emerged pointing in the direction of nitric oxide and potassium channels as likely candidates in the control of cerebral blood flow. This stems largely from studies using various animal models or *in vitro* preparations. So far, few *in vivo* studies in humans have been completed. Clearly, the techniques described in this Thesis could be used to explore several areas of future investigation.

Nitric oxide has been implicated in the control of basal levels of cerebral blood flow as well as mediating, at least in part, the cerebral blood flow response to hypercapnia (21,85,117). Its role in hypocapnia remains unclear. The use of nitric synthase inhibitors has recently been established in human cerebral blood flow studies (117). However, several important questions remain unresolved. For example, results from the study by White et al. (117) suggest a dilatation of the middle cerebral artery with nitric oxide inhibition. However, this has not been quantified or verified. Studies of dynamic aspects of the cerebral blood flow response to step changes in carbon dioxide could help clarify the role and source of nitric oxide, along with its effect on the cross-sectional area of large cerebral vessels such as the middle cerebral artery. Since endothelium-dependent relaxation of cerebral vessels appears to be impaired in several conditions including

hypertension, diabetes and ageing (21), there may be some clinical merits of these studies for these populations.

A role for ATP-sensitive and calcium-activated potassium channels has been shown in the dilatation of cerebral vessels in response to hypoxia (104) and hypercapnia (20). However, in diseases such as hypertension, diabetes, and atherosclerosis, these channels appear to be altered (22,46). Glibenclamide, a sulfenylurea, is of particular interest; it is a selective inhibitor of ATP-sensitive potassium channels in blood vessels (20,104) and commonly used in the treatment of diabetes (46). Yet, young diabetic patients, who show no clinical evidence of complications, appear to have an impaired cerebral blood flow response to hypercapnia (28). Future studies involving the administration of glibenclamide in young healthy volunteers could help elucidate the role of ATP-sensitive potassium channels in the chemical control of cerebral blood flow in humans.

The use of calcium antagonists in research settings with humans may help unravel some of the underlying mechanisms of cerebral blood flow regulation involving calcium channels. Changes in extracellular pH have been shown to affect different types of calcium channels in the smooth muscle from the rat aorta (36,119) and in isolated smooth muscle cells from the guinea pig basilar artery (114). A role for calcium-dependent potassium channels has been postulated, in the regulation of arterial diameter and myogenic tone in isolated rat cerebral arteries (47,48).

Calcium antagonists effect the excitation-contraction coupling within the cell via various mechanisms (18). Of the several families of calcium antagonists, each has different potency and selectivity properties (for reviews of calcium antagonists see

(18,24,94,103)). For studies of cerebral circulation, nimodipine appears to be preferred, as it is a potent selective cerebrovascular vasodilator (24). In baboons, low doses of nimodipine increase basal cerebral blood flow (~18%) and impair CO<sub>2</sub> reactivity but do not alter cerebral oxidative metabolism or blood pressure (64). In anesthetized cats, nimodipine was found to inhibit the vasoconstrictor response of pial arteries to hypocapnia (30). In humans, clinical doses of nimodipine were found to reduce blood pressure and impair CO<sub>2</sub> reactivity (90,91). However, the effects of nimodipine on baseline cerebral blood flow and cerebral oxidative metabolism remain unclear, with some studies showing increases (90) or no changes (91) cerebral blood flow.

To date, the effects of calcium antagonists on the dynamic response of the cerebral vasculature to alterations in carbon dioxide, and/or their effects on the vessel caliber of large cerebral vessels such as the middle cerebral artery, have not been determined. This could prove useful, especially since calcium antagonists are used widely in clinical situations involving subarachnoid hemorrhage, migraine, stroke, head injuries and ischaemia, and ageing. Yet, there appears to be a large variability of therapeutic effects of calcium antagonists in those populations (2).

The intricate control of the cerebral circulation, along with the array of proposed mechanisms, suggest the existence of several parallel (and possibly permissive and/or redundant) mechanisms. Thus, caution is required in the interpretation of *in vitro* and *in vivo* studies, in comparing different species, and in assessing the pharmacological interventions and dosages used.

### 7.3 CONCLUDING COMMENTS

In a recent editorial the experimental setup used in this Thesis was described as “a current day ‘hard point’, an engineering term denoting a point of reinforcement in cerebrovascular and respiratory physiology” (54). With new technological advances such as the ones described in this Thesis and elsewhere (23,106), the door is open for new opportunities to investigate further and define the mechanisms controlling cerebral blood flow in humans, in health and in disease.

Finally, it seems appropriate to conclude with a few words on the power of ideas in scientific research. In 1946, August Krogh gave a lecture to the Harvard medical students (51) (accounts of the work and life of August Krogh are also found elsewhere (92,93)). In his talk, Krogh shared with the students the events that unfolded on the day when he came up with the idea that led to his work on the regulation of capillary circulation, for which he was awarded the 1920 Nobel Prize in Physiology or Medicine. He recounts how on that day, he was struck with an idea while reflecting in the University library. Later in the evening he discussed his idea with Marie, his wife (“who was always my nearest colleague”(51)), he illustrated his idea to her on paper, and then thought it was worth testing his idea experimentally:

“...At this stage allow me a few words on the role of ideas. An idea or an hypothesis is a very insignificant, but very essential, part of an investigation. Most ideas are wrong and almost all are faulty: but even so experiments have to be planned so as to give an answer: right or wrong. Most ideas are quite vague. Nothing short of experimentation helps more to clarify them and bring them to the testing stage than discussion with a sympathetic and critical colleague.” (51)

## 7.3 REFERENCES (CHAPTER 7)

1. **Ackerstaff, R. G. A., R. W. M. Keunen, W. van Pelt, A. D. M. van Swijndregt, and T. Stijnen.** Influence of biological factors on changes in mean cerebral blood flow velocity in normal ageing: a transcranial Doppler study. *Neurol. Res.* 12:187-191, 1990.
2. **Akopov, S. S., G. S. Grigorian, and E. S. Gabrielian.** Dynamic component of internal carotid artery stenosis in patients with cerebrovascular disease: effects of nifedipine. *Int. J. Clin. Pharmacol. Ther.* 32:219-222, 1994.
3. **Albrecht, R. F., D. J. Miletich, and M. Ruttle.** Cerebral effects of extended hyperventilation in unanesthetized goats. *Stroke* 18:649-655, 1987.
4. **Allen, K., A. L. Busza, H. A. Crockard, and D. G. Gadian.** Brain metabolism and blood flow in acute cerebral hypoxia studied by NMR spectroscopy and hydrogen clearance. *NRM in Biomedicine* 5:48-52, 1992.
5. **Arts, M. G. J. and J. M. J. G. Roevros.** On the instantaneous measurement of blood flow by ultrasonic means. *Med. Biol. Eng.* 10:23-34, 1972.
6. **Baumgartner, R. W., P. Bartsch, M. Maggiorini, A. Thomi, and O. Oelz.** The role of cerebral blood flow in acute mountain sickness. In: *Hypoxia and Mountain Sickness*. Edited by: J. R. Sutton, G. Coates, and C. S. Houston. Oxford: Pergamon Press, 1992, p. 252-259.
7. **Berger, S. A., L. Talbot, and L.-S. Yao.** Flow in curved pipes. *Ann. Rev. Fluid Mech.* 15:461-512, 1983.
8. **Bevan, J. A. and R. D. Bevan.** Is innervation a prime regulator of cerebral blood flow? *NIPS* 8:149-153, 1993.
9. **Bonita, R., R. Beaglehole, and K. Asplund.** The worldwide problem of stroke. *Current Opinion in Neurology* 7:5-10, 1994.
10. **Brown, M. M., J. P. H. Wade, and J. Marshall.** Fundamental importance of arterial oxygen content in the regulation of cerebral blood flow in man. *Brain* 108:81-93, 1985.
11. **Clar, C., M. Pedersen, M. J. Poulin, J. G. Tansley, and P. A. Robbins.** Effects of 8 h of eucapnic and poikilocapnic hypoxia on middle cerebral artery velocity and heart rate in humans. *Experim. Physiol.* 82:791-802, 1997.
12. **Cohen, P. J., S. C. Alexander, T. C. Smith, M. Reivich, and H. Wollman.** Effects of hypoxia and normocarbica on cerebral blood flow and metabolism in conscious man. *J. Appl. Physiol.* 23:183-189, 1967.
13. **Corfield, D. R., M. J. Morrell, and A. Guz.** The nature of breathing during hypocapnia in awake man. *Respir. Physiol.* 101:145-159, 1995.
14. **Dager, S. R., W. L. Strauss, K. I. Marro, T. L. Richards, G. D. Metzger, and A. A. Artru.** Proton magnetic resonance spectroscopy investigation of hyperventilation in subjects with panic disorder and comparison subjects. *Am. J. Psychiatry* 152:666-672, 1995.
15. **Davis, S. M., R. H. Ackerman, J. A. Correia, N. M. Alpert, J. Chang, F. Buonanno, R. E. Kelley, B. Rosner, and J. M. Taveras.** Cerebral blood flow and cerebrovascular CO<sub>2</sub> reactivity in stroke-age normal controls. *Neurology* 33:391-399, 1983.
16. **Demolis, P., S. Chalon, and J. F. Giudicelli.** Acetazolamide-induced vasodilation in the carotid vascular bed in healthy volunteers. *J. Cardiovasc. Pharmacol.* 26:841-844, 1995.
17. **Edvinsson, L.** Sympathetic control of cerebral circulation. *TINS* 5:425-429, 1982.

18. Edvinsson, L, MacKenzie, E.T., and J. McCulloch. *Cerebral Blood Flow and Metabolism*. New York: Raven Press, Ltd, 1993.
19. Ellingsen, I., A. Hauge, G. Nicolaysen, M. Thoresen, and L. Walloe. Changes in human cerebral blood flow due to step changes in  $PAO_2$  and  $PACO_2$ . *Acta Physiol. Scand.* 129: 157-163, 1987.
20. Faraci, F. M., K. R. Breese, and D. D. Heistad. Cerebral vasodilation during hypercapnia. Role of glibenclamide-sensitive potassium channels and nitric oxide. *Stroke* 25:1679-1683, 1994.
21. Faraci, F. M. and J. E. J. Brian. Nitric oxide and the cerebral circulation. *Stroke* 25:692-703, 1994.
22. Faraci, F. M. and D. D. Heistad. Regulation of cerebral circulation: role of endothelium and potassium channels. *Physiol. Rev.* 78:53-97, 1998.
23. Frackowiak, R.S.J., Friston, K.J., Frith, C.D., Dolan, R.J., and J.C. Mazziotta. *Human Brain Function*. San Diego: Academic Press, 1997.
24. Freedman, D. D. and D. D. Waters. 'Second generation' dihydropyridine calcium antagonists. *Drugs* 34:578-598, 1987.
25. Gill, R. W. Measurement of blood flow by ultrasound: accuracy and sources of error. *Ultrasound Med. Biol.* 11:625-641, 1985.
26. Golanov, E. V. and D. J. Reis. Contribution of oxygen-sensitive neurons of the rostral ventrolateral medulla to hypoxic cerebral vasodilation in the rat. *J. Physiol. (Lond.)* 495:201-216, 1996.
27. Govier, A. V., J. G. Reves, R. D. McKay, R. B. Karp, G. L. Zorn, R. B. Morawetz, L. R. Smith, M. Adams, and A. M. Freeman. Factors and their influence on regional cerebral blood flow during nonpulsatile cardiopulmonary bypass. *Ann. Thorac. Surg.* 38:592-600, 1984.
28. Griffith, D. N., S. Saimbi, C. Lewis, S. Tolfree, and D. J. Betteridge. Abnormal cerebrovascular carbon dioxide reactivity in people with diabetes. *Diabet. Med.* 4:217-20, 1987.
29. Hatab, M. R., C. A. Giller, and G. D. Clarke. Evaluation of cerebral arterial flow with transcranial Doppler ultrasound: theoretical development and phantom studies. *Ultrasound Med. Biol.* 23:1025-1031, 1997.
30. Haws, C. W. and D. D. Heistad. Effects of nimodipine on cerebral vasoconstrictor responses. *Am. J. Physiol.* 247:H170-H176, 1984.
31. Henriksen, L., O. B. Paulson, and R. J. Smith. Cerebral blood flow following normovolemic hemodilution in patients with high hematocrit. *Ann. Neurol.* 9:454-457, 1981.
32. Howard, L. S. G. E., R. A. Barson, B. P. A. Howse, T. R. McGill, M. E. McIntyre, D. F. O'Connor, and P. A. Robbins. Chamber for controlling end-tidal gas tensions over sustained periods in humans. *J. Appl. Physiol.* 78:1088-1091, 1995.
33. Huang, S. Y., R. G. McCullough, A. J. Micco, M. Manco-Johnson, J. V. Weil, and J. T. Reeves. Usual clinical dose of acetazolamide does not alter cerebral blood flow velocity. *Respir. Physiol.* 72:315-326, 1988.
34. Iadecola, C., D. A. Pelligrino, M. A. Moskowitz, and N. A. Lassen. Nitric oxide synthase inhibition and cerebrovascular regulation. *J. Cereb. Blood Flow Metab.* 14:175-192, 1994.
35. Itoh, M., J. Hatazawa, H. Miyazawa, H. Matsui, K. Meguro, K. Yanai, K. Kubota, S. Watanuki, T. Ido, and T. Matsuzawa. Stability of cerebral blood flow and oxygen metabolism during normal aging. *Gerontology* 36:43-48, 1990.

36. Iwasawa, K., T. Nakajima, H. Hazama, A. Goto, W. S. Shin, T. Toyo-oka, and M. Omata. Effects of extracellular pH on receptor-mediated  $\text{Ca}^{2+}$  influx in A7r5 rat smooth muscle cells: involvement of two different types of channel. *J. Physiol. (Lond.)* 503:237-251, 1997.
37. Jensen, J. B., B. Sperling, J. W. Severinghaus, and N. A. Lassen. Augmented hypoxic cerebral vasodilation in men during 5 days at 3,810 m altitude. *J. Appl. Physiol.* 80:1214-1218, 1996.
38. Jensen, J. B., A. D. Wright, N. A. Lassen, T. C. Harvey, M. H. Winterborn, M. E. Raichle, and A. R. Bradwell. Cerebral blood flow in acute mountain sickness. *J. Appl. Physiol.* 69:430-433, 1990.
39. Jones, M. D., R. J. Traystman, M. A. Simmons, and R. A. Molteni. Effects of changes in arterial  $\text{O}_2$  content on cerebral blood flow in the lamb. *Am. J. Physiol.* 240:H209-H215, 1981.
40. Kanter, M. M., L. A. Nolte, and J. O. Holloszy. Effects of an antioxidant vitamin mixture on lipid peroxidation at rest and postexercise. *J. App. Physiol.* 74:965-969, 1993.
41. Kazemi, H., L. M. Valenca, and D. C. Shannon. Brain and cerebrospinal fluid lactate concentration in respiratory acidosis and alkalosis. *Respir. Physiol.* 6:178-186, 1969.
42. Kety, S. S. Human Cerebral Blood Flow and Oxygen Consumption as Related to Aging. In: *The Neurologic and Psychiatric Aspects of the Disorders of Aging*. Edited by: J. E. Moore, H. H. Merritt, and R. J. Masselink. Baltimore: The Williams & Wilkins Company, 1956, p. 31-45.
43. Kety, S. S. and C. F. Schmidt. The effects of altered arterial tensions of carbon dioxide and oxygen on cerebral blood flow and cerebral oxygen consumption of normal young men. *J. Clin. Invest.* 27:484-492, 1948.
44. Keunen, R. W. M., J. H. R. Vliegen, C. J. Stam, and D. L. J. Tavy. Nonlinear transcranial Doppler analysis demonstrates age-related changes of cerebral hemodynamics. *Ultrasound Med. Biol.* 22:383-390, 1996.
45. Keunen, W. M., H. C. Pijlman, H. F. Visee, J. H. R. Vliegen, D. L. J. Tavy, and K. J. Stam. Dynamical chaos determines the variability of transcranial Doppler signals. *Neurol. Res.* 16:353-358, 1994.
46. Kitazono, T., F. M. Faraci, H. Taguchi, and D. D. Heistad. Role of potassium channels in cerebral blood vessels. *Stroke* 26:1713-1723, 1995.
47. Knot, H. J. and M. T. Nelson. Regulation of arterial diameter and wall  $[\text{Ca}^{2+}]$  in cerebral arteries of rat by membrane potential and intravascular pressure. *J. Physiol. (Lond.)* 508:199-209, 1998.
48. Knot, H. J., N. B. Standen, and M. T. Nelson. Ryanodine receptors regulate arterial diameter and wall  $[\text{Ca}^{2+}]$  in cerebral arteries of rat  $\text{Ca}^{2+}$ -dependent  $\text{K}^+$  channels. *J. Physiol. (Lond.)* 508:211-221, 1998.
49. Kogure, K., R. Busto, A. Matsumoto, P. Scheinberg, and O. M. Reinmuth. Effect of hyperventilation on dynamics of cerebral energy metabolism. *Am. J. Physiol.* 228:1862-1867, 1975.
50. Kogure, K., P. Scheinberg, O. M. Reinmuth, M. Fujishima, and R. Busto. Mechanism of cerebral vasodilation in hypoxia. *J. Appl. Physiol.* 29:223-229, 1970.
51. Krogh, A. Reminiscences of work on capillary circulation. *ISIS - Official Quarterly Journal of the History of Science Society* 41:14-20, 1950.
52. Kuo, L., M. J. Davis, and W. M. Chilian. Endothelial modulation of arterial tone. *NIPS* 7:5-10, 1992.
53. Kuo, T. B. J., C. M. Chern, W. Y. Sheng, W. J. Wong, and H. H. Hu. Frequency domain analysis of cerebral blood flow velocity and its correlation with arterial blood pressure. *J. Cereb. Blood Flow Metab.* 18:311-318, 1998.

54. **Lambertsen, C. J.** Invited Editorial on "Fast and slow components of cerebral blood flow response to step decreases in end-tidal PCO<sub>2</sub> in humans". *J. Appl. Physiol.* 88:386-387, 1998.
55. **Lambertsen, C. J., R. H. Kough, D. Y. Cooper, G. L. Emmel, H. H. Loeschcke, and C. F. Schmidt.** Oxygen toxicity. Effects in man of oxygen inhalation at 1 and 3.5 atmospheres upon blood gas transport, cerebral circulation and cerebral metabolism. *J. Appl. Physiol.* 5:471-486, 1953.
56. **Lassen, N. A.** Control of cerebral circulation in health and disease. *Circ. Res.* 34:749-760, 1974.
57. **Leenders, K. L., D. Perani, A. A. Lammertsma, J. D. Heather, P. Buckingham, M. J. R. Healy, J. M. Gibbs, R. J. S. Wise, J. Hatazawa, S. Herold, R. P. Beaney, D. J. Brooks, T. Spinks, C. Rhodes, R. S. J. Frackowiak, and T. Jones.** Cerebral blood flow, blood volume and oxygen utilization: Normal values and effect of age. *Brain* 113:27-47, 1990.
58. **Leusen, I. and G. Demeester.** Lactate and pyruvate in the brain of rats during hyperventilation. *Archives Internationales de Physiologie et de Biochimie* 74:25-34, 1966.
59. **Lundar, T., K. F. Lindegaard, T. Froysaker, R. Aaslid, A. Grip, and H. Nornes.** Dissociation between cerebral autoregulation and carbon dioxide reactivity during nonpulsatile cardiopulmonary bypass. *Ann. Thorac. Surg.* 40:582-587, 1985.
60. **Lundar, T., K. F. Lindegaard, T. Froysaker, R. Aaslid, J. Wiberg, and H. Nornes.** Cerebral perfusion during nonpulsatile cardiopulmonary bypass. *Ann. Thorac. Surg.* 40:144-150, 1985.
61. **Lundar, T., K. F. Lindegaard, T. Froysaker, A. Grip, M. Bergman, E. Am-Holen, and H. Nornes.** Cerebral carbon dioxide reactivity during nonpulsatile cardiopulmonary bypass. *Ann. Thorac. Surg.* 41:525-530, 1986.
62. **Madden, J. A., M. S. Vadula, and V. P. Kurup.** Effects of hypoxia and other vasoactive agents on pulmonary and cerebral artery smooth muscle cells. *Am. J. Physiol.* 263:L384-L393, 1992.
63. **Maher, J. T., A. Cymerman, J. T. Reeves, J. C. Cruz, J. C. Denniston, and R. F. Grover.** Acute mountain sickness: increased severity in eucapnic hypoxia. *Aviat. Space Environ. Med.* 46:826-829, 1975.
64. **McCalden, T. A., R. G. Nath, and K. Thiele.** The effects of a calcium antagonist (nimodipine) on basal cerebral blood flow and reactivity to various agonists. *Stroke* 15:527-530, 1984.
65. **McDowall, D. G.** Interrelationships between blood oxygen tension and cerebral blood flow. In: *Oxygen Measurements in Blood and Tissues*. Edited by: J. P. Payne and D. W. Hill. London: Churchill, 1966, p. 205-214.
66. **Meydani, M., W. J. Evans, G. Handelman, L. Biddle, R. A. Fielding, S. N. Meydani, J. Burrill, M. A. Fiatarone, J. B. Blumberg, and J. G. Cannon.** Protective effect of vitamin E on exercise-induced oxidative damage in young and older adults. *Am. J. Physiol.* 264:R992-R998, 1993.
67. **Meyer, J. S., Y. Terayama, and S. Takashima.** Cerebral circulation in the elderly. *Cerebrovasc Brain Metab Rev* 5:122-146, 1993.
68. **Micieli, G., C. Tassorelli, D. Bosone, A. Cavallini, E. Viotti, and G. Nappi.** Intracerebral vascular changes induced by cold pressor test: a model of sympathetic activation. *Neurol. Res.* 16:163-167, 1994.
69. **Muizelaar, J. P., G. J. Bouma, J. E. Lvasseur, and H. A. Kontos.** Effect of hematocrit variations on cerebral blood flow and basilar artery diameter in vivo. *Am. J. Physiol.* 262:H949-H954, 1992.
70. **Naritomi, H., J. S. Meyer, F. Sakai, F. Yamaguchi, and T. Shaw.** Effects of advancing age on regional cerebral blood flow. Studies in normal subjects and subjects with risk factors for atherothrombotic stroke. *Arch. Neurol.* 36:410-416, 1979.

71. **Nichols WW and M.F. O'Rourke.** *McDonald's Blood Flow in Arteries: Theoretical, Experimental and Clinical Principles.* London: Arnold Publishers, 1998.
72. **Ogawa, S., R. S. Menon, S.-G. Kim, and K. Ugurbil.** On the characteristics of functional magnetic resonance imaging of the brain. *Ann. Rev. Biophys. Biomol. Struct.* 27:447-474, 1998.
73. **Otis, S. M., M. E. Rossman, P. A. Schneider, M. P. Rush, and E. B. Ringelstein.** Relationship of cerebral blood flow regulation to acute mountain sickness. *J. Ultrasound Med.* 8:143-148, 1989.
74. **Pantano, P., J. C. Baron, P. Lebrun-Grandie, N. Duquesnoy, M. G. Bousser, and D. Comar.** Regional cerebral blood flow and oxygen consumption in human aging. *Stroke* 15:635-641, 1984.
75. **Paulson, O. B., H.-H. Parving, J. Olesen, and E. Skinhoj.** Influence of carbon monoxide and of hemodilution on cerebral blood flow and blood gases in man. *J. Appl. Physiol.* 35:111-116, 1973.
76. **Payen, J. F., E. LeBars, B. Wuyam, B. Tropini, J. L. Pepin, P. Levy, and M. Decorps.** Lactate accumulation during moderate hypoxic hypoxia in neocortical rat brain. *J. Cereb. Blood Flow Metab.* 16:1345-1352, 1996.
77. **Petroff, O. A. C., J. W. Prichard, K. L. Behar, D. L. Rothman, J. R. Alger, and R. G. Shulman.** Cerebral metabolism in hyper- and hypocapnia:  $^{31}\text{P}$  and  $^1\text{H}$  nuclear magnetic resonance studies. *Neurology* 35:1681-1688, 1985.
78. **Plum, F. and J. B. Posner.** Selective CNS lactic acidosis in response to hypocapnia. *J. Clin. Invest.* 45:1057, 1966.
79. **Plum, F. and J. B. Posner.** Blood and cerebrospinal fluid lactate during hyperventilation. *Am. J. Physiol.* 212:864-870, 1967.
80. **Quayle, J. M., M. T. Nelson, and N. B. Standen.** ATP-sensitive and inwardly rectifying potassium channels in smooth muscle. *Physiol. Rev.* 77: 1165-1232, 1997.
81. **Raichle, M. E., J. B. Posner, and F. Plum.** Cerebral blood flow during and after hyperventilation. *Arch. Neurol.* 23:394-403, 1970.
82. **Reich, T. and H. Rusinek.** Cerebral cortical and white matter reactivity to carbon dioxide. *Stroke* 20:453-457, 1989.
83. **Reid, J. M., A. G. Davies, F. M. Ashcroft, and D. J. Paterson.** Effect of L-NMMA, cromakalim, and glibenclamide on cerebral blood flow in hypercapnia and hypoxia. *Am. J. Physiol.* 269:H916-H922, 1995.
84. **Reid, J. M., D. J. Paterson, F. M. Ashcroft, and D. H. Bergel.** The effect of tolbutamide on cerebral blood flow during hypoxia and hypercapnia in the anaesthetized rat. *Eur. J. Physiol.* 425:362-364, 1993.
85. **Reutens, D. C., M. D. McHugh, P.-J. Toussaint, A. C. Evans, A. Gjedde, E. Meyer, and D. J. Stewart.** L-arginine infusion increases basal but not activated cerebral blood flow in humans. *J. Cereb. Blood Flow Metab.* 17:309-315, 1997.
86. **Roach, R. C., J. A. Loeppky, and M. V. Icenogle.** Acute mountain sickness: increased severity during simulated altitude compared with normobaric hypoxia. *J. Appl. Physiol.* 81:1908-1910, 1996.
87. **Rogers, R. L., J. S. Meyer, and K. F. Mortel.** After reaching retirement age physical activity sustains cerebral perfusion in normal aging. *J. Am. Geriatric Soc.* 38:123-128, 1990.
88. **Rosenblum, W. I., G. H. Nelson, R. Bey, R. B. Brandt, and W. Chan.** Vitamin E ameliorates adverse effects of endothelial injury in brain arterioles. *Am. J. Physiol.* 271:H637-H642, 1996.
89. **Saini, V. D., D. Maulik, N. C. Nanda, and M. S. Rosenzweig.** Computerized evaluation of blood flow measurement indices using Doppler ultrasound. *Ultrasound Med. Biol.* 9:657-660, 1983.

90. **Schmidt, J. F. and G. Waldemar.** Effect of nimodipine on cerebral blood flow in human volunteers. *J. Cardiovasc. Pharmacol.* 16:568-571, 1990.
91. **Schmidt, J. F., G. Waldemar, and O. B. Paulson.** The acute effect of nimodipine on cerebral blood flow, its CO<sub>2</sub> reactivity, and cerebral oxygen metabolism in human volunteers. *Acta Neurochir. Wien* 111:49-53, 1991.
92. **Schmidt-Nielsen, B.** August and Marie Krogh and respiratory physiology. *J. Appl. Physiol.* 57:293-303, 1984.
93. **Schmidt-Nielsen, B.** *August and Marie Krogh: Lives in Science.* New York: American Physiological Society, 1995.
94. **Scriabine, A. and W. van den Kerckhoff.** Pharmacology of Nimodipine. *Ann. NY. Acad. Sci.* 522:698-706, 1988.
95. **Shapiro, W., A. J. Wasserman, J. P. Baker, and J. L. Patterson.** Cerebrovascular response to acute hypocapnic and eucapnic hypoxia in man. *J. Clin. Invest.* 49:2362-2368, 1970.
96. **Shinton, R. and G. Sagar.** Lifelong exercise and stroke. *Br. Med. J.* 307:231-234, 1993.
97. **Shung, K. K.** On the ultrasound scattering from blood as a function of hematocrit. *IEEE Transactions on Sonics and Ultrasonics* SU-29:327-331, 1982.
98. **Shung, K. K., G. Cloutier, and C. C. Lim.** The effects of hematocrit, shear rate, and turbulence on ultrasonic Doppler spectrum from blood. *IEEE Trans. Biomed. Eng.* 39:462-469, 1992.
99. **Smurawska, L. T., A. V. Alexandrov, C. F. Bladin, and J. W. Norris.** Cost of acute stroke care in Toronto, Canada. *Stroke* 25:1628-1631, 1994.
100. **Sokoloff, L.** Cerebral Circulatory and Metabolic Changes Associated with Aging. *Res. Publ. Assoc. Res. Nerv. Ment. Dis.* 41:237-254, 1966.
101. **Stamler, J. S.** A radical vascular connection. *Nature* 380: 108-111, 1996.
102. **Stamler, J. S., L. Jia, J. P. Eu, T. J. McMahon, I. T. Demchenko, J. Bonaventura, K. Gernert, and C. A. Piantadosi.** Blood flow regulation by S-Nitrosohemoglobin in the physiological oxygen gradient. *Science* 276:2034-2037, 1997.
103. **Struyker-Boudier, H. A., J. F. Smits, and J. G. De May.** The pharmacology of calcium antagonists: a review. *J. Cardiovasc. Pharmacol.* 15 (Suppl.4):S1-S10, 1990.
104. **Taguchi, H., D. D. Heistad, T. Kitazono, and F. M. Faraci.** ATP-sensitive K<sup>+</sup> channels mediate dilatation of cerebral arterioles during hypoxia. *Circ. Res.* 74:1005-1008, 1994.
105. **Tansley, J. G., M. Fatemian, L. S. G. E. Howard, M. J. Poulin, and P. A. Robbins.** Changes in respiratory control during and after 48 h of isocapnic and poikilocapnic hypoxia in humans. *J. Appl. Physiol.* (in press).
106. **Tegeler, C. H., Babikian, V.L., and C.R. Gomez.** *Neurosonology.* St. Louis: Mosby, 1996.
107. **van der Worp, H. B., P. R. Bar, L. J. Kappelle, and D. J. de Wildt.** Dietary vitamin E levels affect outcome of permanent focal cerebral ischemia in rats. *Stroke* 29:1002-1006, 1998.
108. **van Rijen, P. C., P. R. Luyten, J. W. Berkelbach van der Sprenkel, V. Kraaier, A. C. van Huffelen, C. A. F. Tulleken, and J. A. den Hollander.** <sup>1</sup>H and <sup>31</sup>P NMR measurement of cerebral lactate, high energy phosphate levels, and pH in humans during voluntary hyperventilation: associated EEG, capnographic, and Doppler findings. *Magn. Reson. Med.* 10:182-193, 1989.

109. **van Vaerenbergh, P. J. J., E. Lacroix, G. Demeester, and I. Leusen.** Lactate in cerebrospinal fluid during muscular exercise. *Archives Internationales de Physiology et de Biochimie* 73:729-737, 1965.
110. **Visee, H. F., W. M. Keunen, H. C. Pijlman, J. H. R. Vliegen, D. L. J. Tavy, K. J. Stam, and C. A. Giller.** The physiological and clinical significance of nonlinear TCD waveform analysis in occlusive cerebrovascular disease. *Neurol. Res.* 17:384-388, 1995.
111. **Vorstrup, S., K. E. Jensen, C. Thomsen, O. Henriksen, N. A. Lassen, and O. B. Paulson.** Neuronal pH regulation: constant normal intracellular pH is maintained in brain during low extracellular pH induced by acetazolamide - <sup>31</sup>P NMR study. *J. Cereb. Blood Flow Metab.* 9:417-421, 1989.
112. **Wahlund, L. O., O. Almkvist, H. Basun, and P. Julin.** MRI in successful aging, a 5-year follow-up study from the eighth to ninth decade of life. *Magn. Reson. Imaging* 14:601-608, 1996.
113. **Wasserman, A. J., W. Shapiro, and J. L. Patterson.** Human cerebrovascular effects of graded hypoxemia. *Circulation* 30:III-175, 1964.
114. **West, G. A., D. C. Leppla, and J. M. Simard.** Effects of external pH on ionic currents in smooth muscle cells from the basilar artery of the guinea pig. *Circ. Res.* 71:201-209, 1992.
115. **Westerhof, N., P. Sipkema, G. C. Van Den Bos, and G. Elzinga.** Forward and backward waves in the arterial system. *Cardiovasc. Res.* 6:648-656, 1972.
116. **Weyland, A., F. Grune, W. Buhre, S. Kazmaier, H. Stephan, and H. Sonntag.** The effect of nitroglycerin on cerebrovascular circulation, cerebrovascular CO<sub>2</sub> reactivity and blood flow rate in basal cerebral arteries. *Anaesthetist* 45:1037-1044, 1996.
117. **White, R. P., C. Deane, P. Vallance, and H. S. Markus.** Nitric oxide synthase inhibition in humans reduces cerebral blood flow but not the hyperemic response to hypercapnia. *Stroke* 29:467-472, 1998.
118. **Winn, H. R., R. Rubio, and R. M. Berne.** Brain adenosine concentration during hypoxia in rats. *Am. J. Physiol.* 241:H235-H242, 1981.
119. **Wray, S.** The outside-in story of pH, Ca<sup>2+</sup> and vascular tone. *J. Physiol. (Lond.)* 503:235, 1997.
120. **Yamaguchi, F., J. S. Meyer, F. Sakai, and M. Yamamoto.** Normal human aging and cerebral vasoconstrictive responses to hypocapnia. *J. Neurol. Sci.* 44:87-94, 1979.
121. **Yearwood, T. L. and K. B. Chandran.** Physiological pulsatile flow experiments in a model of the human aortic arch. *J. Biomechanics* 15:683-704, 1984.
122. **Young, R. S. K. and S. K. Yagel.** Cerebral physiological and metabolic effects of hyperventilation in the neonatal dog. *Ann. Neurol.* 16:337-342, 1984.